
Arnold Schwarzenegger
*Governor*

# AIR QUALITY IMPACTS OF DISTRIBUTED GENERATION IN THE SOUTH COAST AIR BASIN AND THE SAN JOAQUIN VALLEY

PIER FINAL PROJECT REPORT

*Prepared For:*
**California Energy Commission**
Public Interest Energy Research Program

*Prepared By:*
Scott Samuelsen, Donald Dabdub, Jacob Brouwer, Marc Carreras-Sospedra, Satish Vutukuru
University of California, Irvine

April 2010
CEC-500-2009-070


***Prepared By:***
Professor Scott Samuelsen
Professor Donald Dabdub
Dr. Jacob Brouwer
Dr. Marc Carreras-Sospedra
Dr. Satish Vutukuru
University of California, Irvine
221 Engineering Laboratory Facility
Irvine, California 92679-3550
Commission Contract No. 500-02-004
Commission Work Authorization No. MR-026

***Prepared For:***
Public Interest Energy Research (PIER)
**California Energy Commission**

Beth Chambers
***Contract Manager***

Marla Mueller
***Project Manager***

Linda Spiegel
***Program Area Lead***
***Energy-Related Environmental Research***

Kenneth Koyama
***Office Manager***
***Energy Systems Research***

Thom Kelly
***Deputy Director***
***ENERGY RESEARCH & DEVELOPMENT DIVISION***

Melissa Jones
***Executive Director***

# Acknowledgments

The authors graciously acknowledge the financial support of the California Energy Commission, which sponsored this work.

The authors thank the California Air Resources Board, South Coast Air Quality Management District, and San Joaquin Valley Air Pollution Control District for their provision of air quality modeling inputs and invaluable support and guidance in this effort. The regular attendance, participation, and guidance provided by Marty Kay, Ajith Kaduwela, David Mehl, and David Nunez, was invaluable to the successful completion of this effort. Others that supported this effort include: Joseph Cassmassi, Grant Chin, Mark Rawson, Linda Kelly, Paul Livingstone, and John DaMassa.

The authors thank the Southern California Area Governments (SCAG) for its generous donation of the geographic information system (GIS) land-use data.

The authors thank the University of California, Irvine (UCI) Network and Computing Services of UCI; especially Joseph Farran for his technical support of the authors' computing infrastructure, and Tony Soeller for his assistance in processing GIS data.

Please cite this report as follows:

Samuelsen, Scott, Donald Dabdub, Jacob Brouwer, Marc Carreras-Sospedra, Satish Vutukuru. 2009. *Air Quality Impacts of Distributed Generation in the South Coast Air Basin and the San Joaquin Valley.* California Energy Commission, PIER Energy-Related Environmental Research Program. CEC-500-2009-070.

# Preface

The California Energy Commission's Public Interest Energy Research (PIER) Program supports public interest energy research and development that will help improve the quality of life in California by bringing environmentally safe, affordable, and reliable energy services and products to the marketplace.

The PIER Program conducts public interest research, development, and demonstration (RD&D) projects to benefit California.

The PIER Program strives to conduct the most promising public interest energy research by partnering with RD&D entities, including individuals, businesses, utilities, and public or private research institutions.

PIER funding efforts are focused on the following RD&D program areas:

- Buildings End-Use Energy Efficiency
- Energy Innovations Small Grants
- Energy-Related Environmental Research
- Energy Systems Integration
- Environmentally Preferred Advanced Generation
- Industrial/Agricultural/Water End-Use Energy Efficiency
- Renewable Energy Technologies
- Transportation

*Air Quality Impacts of Distributed Generation in the South Coast Air Basin and the San Joaquin Valley* is the final report for the Air Quality Impacts of Distributed Generation in the South Coast Air Basin and the San Joaquin Valley project (Contract Number 500-02-004, WA No. MR-026) conducted by the University of California, Irvine. The information from this project contributes to PIER's Energy-Related Environmental Research Program.

For more information about the PIER Program, please visit the Energy Commission's website at www.energy.ca.gov/pier or contact the Energy Commission at (916) 654-4878.

# Table of Contents

# List of Figures

## List of Tables

# Abstract

A systematic approach based on land-use geographical information systems data was applied to characterize installation of distributed generation in the South Coast and San Joaquin Valley air basins and simulate potential air quality impacts using state-of-the-art, three-dimensional computer models. Potential distributed generation market penetration focused on 2023 and beyond. Distributed generation is expected to meet 7 to 18 percent of new installed capacity between 2007 and 2023—up to 1789 megawatts and 373 megawatts of capacity in the South Coast and San Joaquin Valley, respectively. Air quality impacts were found to be small due to the use of combined heating and power and application of restrictive 2007 California Air Resources Board air emission standards to all distributed generation units. Net carbon dioxide emissions from distributed generation (including heating emissions displacement) are approximately 9 percent lower than average California grid emissions. If distributed generation units were allowed to emit at levels higher than the 2007 Air Resources Board standards, air quality impacts could compromise compliance with the federal 8-hour average ozone standard in the South Coast. The San Joaquin Valley can potentially install 584 megawatts of biomass distributed generation capacity. Modeled results show small air quality impacts from such installations.

**Keywords:** Distributed generation, DG, distributed energy resources, DER, air quality, air quality impacts, scenarios, air quality model, land-use GIS data, South Coast Air Basin, San Joaquin Valley

# Executive Summary

## Introduction

Power generation in California contributes 1 to 2 percent of the total in-state emissions of nitrogen oxides and fine particulate matter. California power demand is expected to grow in the following decades by an average of 1.5 percent per year. On the other hand, some specific regions in the state, such as the South Coast Air Basin and the San Joaquin Valley, are among the areas with the poorest air quality in the United States. Consequently, the state must ensure that air quality continues to improve at the same time that electricity production continues to grow to meet the state's needs.

Distributed generation—electricity generation that is produced by many small stationary power generators distributed throughout an urban air basin—has the potential to supply a significant portion of electricity in future years. As a result, distributed generation may lead to increased pollutant emissions within an urban air basin, which could adversely affect air quality. However, the use of combined heating and power with distributed generation may reduce the energy consumption for space heating and air conditioning, resulting in a net decrease of pollutant emissions. The use of biomass as a distributed generation fuel could contribute to the renewable electricity generation portfolio and potentially reduce carbon dioxide, although it could also increase criteria pollutant emissions.

A previous effort by the Advanced Power and Energy Program at the University of California, Irvine, assessed the regional air quality impacts of distributed generation in the South Coast Air Basin in 2010. That study first developed a detailed method for characterizing the spatial, temporal, and compositional variations in distributed generation emissions in the South Coast Air Basin.

## Purpose

This effort continues the previous study on regional air quality impacts of distributed generation in the South Coast Air Basin. In particular, this project had two main goals: (1) evaluate the air quality impacts of distributed generation in the South Coast Air Basin in years beyond 2010 (the year of study in the preceding project), and (2) evaluate the future air quality impacts of distributed generation in the San Joaquin Valley Air Basin—an area where electricity demand is growing more rapidly than the California average and where distributed generation could provide a significant portion of that electricity.

## Project Objectives

The method employed during the preceding project to estimate distributed generation penetration was updated using new market studies. In addition, this method, which was originally developed for the South Coast Air Basin, was adapted for use in the San Joaquin

Valley Air Basin. New air quality models were acquired to simulate air quality in the San Joaquin Valley Air Basin.

The team developed (1) a set of scenarios that tried to reflect a likely distributed generation adoption by the year of interest (named "realistic" scenarios), and (2) a set of scenarios that could reflect unexpected outcomes in distributed generation implementation or that expanded the possibilities of distributed generation adoption for scientific completeness (named "spanning" scenarios).

**Project Outcomes**

*Implementation of Distributed Generation in the South Coast Air Basin*

A series of scenarios was investigated to determine the potential regional air quality impacts of distributed generation in the South Coast Air Basin. According to market studies, distributed generation market penetration could supply more than 2 gigawatts of power capacity by 2030 in the South Coast Air Basin. Such penetration, considered for the realistic scenarios, would introduce new spatial and temporal distributions of emissions throughout the South Coast Air Basin. Assuming that all distributed generation units (even those permitted by the South Coast Air Quality Management District) would comply with the California Air Resources Board's 2007 standards as early as 2023, the distributed generation emissions would contribute less than 1 percent to total basinwide emissions. In addition, the use of combined heating and power technologies in distributed generation systems has the potential to reduce net nitrogen oxide emissions.

The changes in emissions due to distributed generation implementation were evaluated using the University of California, Irvine-California Institute of Technology Airshed model. Baseline emissions inventories were generated for 2023 and 2030. The resulting regional air quality impacts of realistic distributed generation scenarios were found to be very small. In particular, peak ozone and 24-hour average fine particulate would increase by less than 1 part per billion and 1.1 microgram per cubic meter, respectively, due to the addition of emissions from distributed generation.

To investigate some of the parameters that define a distributed generation implementation scenario, a set of spanning scenarios was developed and simulated to analyze the potential effects of distributed generation on air quality. The parameters studied include the spatial distribution of distributed generation, the duty cycle of distributed generation operation, the technology mix of distributed generation, the potential for emissions displacement, the distributed generation market penetration, and the emission factors for distributed generation.

The application of the 2007 California Air Resources Board emissions standards for all distributed generation units represented in the modeling reduced the impacts of distributed generation significantly. Even assuming high distributed generation penetration of up to five gigawatts, emissions from distributed generation technologies were shown to increase peak ozone concentration and 24-hour average fine particulate concentrations by only one part per

billion and one microgram per cubic meter, respectively, if the California Air Resources Board's 2007 limits are applied.

On the contrary, installation of a large fraction of internal combustion engines permitted under the Best Available Control Technology standards effective in 2007 could significantly increase the air quality impacts of distributed generation, and this would strongly hinder the efforts to reduce ozone concentrations to achieve compliance with ozone air quality standards.

*Implementation of Distributed Generation in the San Joaquin Valley Air Basin*

A series of scenarios was investigated to determine the potential regional air quality impacts of distributed generation in the San Joaquin Valley Air Basin for 2023. Baseline emissions for 2023 were developed based on emissions estimates presented in the 8-hour ozone attainment plan by the San Joaquin Valley Air Pollution Control District. The results from the distributed generation implementation scenarios development show that realistic scenarios do not add significant amounts of emissions to the basin. This is mainly true because the distributed generation technologies considered in the current analyses have relatively low pollutant emissions rates, limited by the California Air Resources Board 2007 emission standards (even distributed generation permitted by the San Joaquin Valley Air Pollution Control District). In addition, the application of combined heating and power results in displaced boiler emissions in the San Joaquin Valley, although combined heating and power does not completely offset direct distributed generation nitrogen oxide emissions.

Air quality impacts from distributed generation scenarios were calculated using two regional air quality models: the Comprehensive Air Quality Model with extensions and the Community Multiscale Air Quality modeling system. The Comprehensive Air Quality Model with extensions was used to simulate a summer ozone episode, and the Community Multiscale Air Quality modeling system was used to simulate a winter particulate matter episode.

Simulation results showed that realistic scenarios would have no significant impacts on the regional air quality in the San Joaquin Valley. There was no significant change in maximum 1-hour average ground-level ozone concentrations. On the other hand, 24-hour average ground-level particulate matter concentrations could increase by as much as 0.3 microgram per cubic meter at certain locations for the realistic scenarios. Some spanning scenarios showed higher impacts when a high level of distributed generation deployment was considered or when less stringent emission standards or non-compliance with standards was considered.

For instance, if internal combustion engines were allowed to emit in the San Joaquin Valley at the levels permitted in 2007 by Best Available Control Technology emissions standards, air quality impacts of internal combustion engines on maximum ozone and 24-hour average particulate matter concentrations would be significantly higher than the ones predicted for distributed generation emitting at 2007 California Air Resources Board emissions standards. Similarly, assuming an extra-high penetration of distributed generation would produce more significant overall impacts.

The potential in the San Joaquin Valley Air Basin to use distributed generation technologies fueled by biomass resources is high. The current study analyzed the potential use of several biomass fuel sources including agricultural residue, forestry waste, animal manure, and municipal waste. Two types of biomass conversion technologies were considered: (1) fuel cell operation on anaerobic digestion gas from animal manure, and (2) fluidized bed combustion of the other biomass resources to raise steam to produce power in a steam turbine. (Fluidized bed combustion technology suspends solid fuels on air jets to optimize fuel combustion.) Modeling regional air quality impacts from biomass scenarios that included fluidized bed combustion showed increases in maximum 1-hour ozone by 0.1 part per billion and fine particulate by 0.2 microgram per cubic meter. These increases were due to the installation of between 326 and 386 megawatts (MW) of the biomass combustion technology. The current Best Available Control Technology emissions rate for nitrogen oxides associated with this technology is 0.1 pounds per megawatt-hour (lb/MWh). In contrast to distributed generation scenarios, the application of combined heating and power would not completely offset nitrogen oxide emissions from the biomass generation scenarios that included the biomass combustion approach.

On the other hand, anaerobic digestion of animal manure can effectively reduce volatile organic compounds and greenhouse gas emissions while producing a high methane content gas that can be processed to remove contaminants and water for use as a fuel. The processed fuel can be converted to electricity in a fuel cell, resulting in relatively low nitrogen oxide emissions of 0.017 lb/MWh. Modeling results showed that the use of fuel cells operated on anaerobic digestion of animal waste streams reduced the air quality impacts of biomass scenarios. The California Energy Commission estimates that approximately 500 megawatts of electricity could be generated from animal manure, while about 1100, 1900, and 2800 megawatts could be generated from agricultural residue, municipal waste, and forestry waste, respectively. Thus, if conversion technology for producing a fuel stream amenable to use in fuel cell power generation could be significantly advanced in future years, then use of this biomass resource would be encouraging from an air quality and greenhouse gas emissions perspective.

*Contribution of Distributed Generation to Greenhouse Gas Emissions*

Direct carbon dioxide emissions from distributed generation technologies were found to be higher than average grid emissions (1014 pounds per megawatt-hour, lb/MWh) for all realistic scenarios, due to a relatively high penetration of gas turbines. However, combined heating and power has the potential to offset a fraction of distributed generation carbon dioxide emissions. Assuming an overall combined heating and power usage of 50 percent and heat recovery factor of 60 percent, to account for losses and mismatch with the heat demand, net emissions from distributed generation with some combined heating and power are less than 920 lb/MWh—approximately 9 percent lower than average California grid emissions. Average distributed generation greenhouse gas emissions in the realistic scenarios for the San Joaquin Valley are slightly lower than those in the South Coast Air Basin because the distributed generation technology mix estimated for the San Joaquin Valley includes a higher percentage of natural gas internal combustion engines and a lower percentage of gas turbines, compared to the realistic scenarios for South Coast Air Basin. As mentioned above, internal combustion engines could be

preferred over gas turbines if only carbon dioxide emissions were considered. However, criteria pollutant emissions from internal combustion engines are significantly higher than from gas turbines, which could offset the benefits of reducing carbon dioxide emissions. Scenarios with high deployment of high-temperature fuel cells that include a reasonable fraction (30 percent) of effective heat usage (fuel cells with combined heat and power systems) were found to most significantly reduce carbon dioxide emissions compared to California electric grid and boiler emissions standards. High deployment of high temperature fuel cells in this manner could lead to decreases in carbon dioxide emissions of 11.2 percent in the South Coast Air Basin and 12.0 percent in the San Joaquin Valley. These findings are consistent with actual heat recovery metered data obtained by the California Public Utilities Commission, which suggest that fuel cells have the highest potential for overall carbon dioxide emission reductions with respect to current California grid emissions.

*Model Sensitivity Analysis*

Evaluation of model sensitivity to key parameters that may affect regional air quality impacts of distributed generation was conducted for the South Coast Air Basin and the San Joaquin Valley. Changes in baseline emissions proposed in the air quality management plan for the South Coast Air Basin and in the attainment plan for the San Joaquin Valley were evaluated using air quality models for those two particular areas. The air quality impacts of distributed generation in the South Coast Air Basin were sensitive to changes in future emissions, mainly because the updated air quality management plan reduced nitrogen oxide emissions so substantially that ozone production changed from volatile organic compound-limited to nitrogen oxide-limited conditions. On the contrary, the modeled changes in baseline emissions in the San Joaquin Valley Air Basin did not strongly affect air quality impacts of distributed generation. Finally, analysis of central electricity generation shows that air quality impacts from central plants are higher in magnitude than those from the use of distributed generation technologies because for the same amount of electricity produced, emissions are more dispersed for distributed generation. The air quality impacts attributable to central plants are more localized and concentrated downwind of the central plants considered.

**Conclusions**

This project investigated realistic scenarios that considered a market-based mix of distributed generation technologies, including primarily internal combustion engine and gas turbine technologies with a small amount (less than 10 percent) of fuel cell technology. The results suggest that adding distributed generation technologies would have small impacts on ozone and fine particulate concentrations in the South Coast Air Basin and San Joaquin Valley. Only scenarios that allowed for less-restrictive emission standards for distributed generation technologies (for example, at 2007 permitted levels), or scenarios that assumed a high percentage of non-compliant distributed generators, had significant effects on ozone and particulate matter concentrations. The use of combined heating and power in conjunction with distributed generation has the potential to reduce greenhouse gases emissions with respect to the existing electricity generation mix. In particular, high-efficiency and low-emitting

technologies, such as fuel cells, can provide electricity while minimizing air quality impacts and reducing overall greenhouse gas emissions from electricity generation.

**Recommendations**

The present effort has produced the following recommendations regarding the implementation of distributed generation in California:

- Low-emitting technologies, such as fuel cells and solar power, should be encouraged and widely implemented to minimize the effects of electricity generation on air quality. In addition, these technologies would help reduce emissions of greenhouse gases in comparison to other distributed generation technologies, such as gas turbines and internal combustion engines.
- Emission standards similar to the current 2007 ARB standards should be enforced for all distributed technologies.
- Combined heating and power applications should be encouraged to reduce air quality impacts and reduce greenhouse gas emissions.
- The combined heat and power emission credits currently allowed by the 2007 ARB air emission standards should be reduced to promote cleaner distributed generation technologies and maximize the benefits of cogeneration of heat and power.
- More active emissions monitoring, such as continuous monitoring or more frequent compliance testing, should be implemented to minimize the impacts of non-compliant equipment.
- There is high uncertainty in how widespread deployment of biomass technologies could affect air quality and net greenhouse gases emissions. This study recommends further research on how to integrate systems of biomass collection, transport, and use.
- From a regional air quality perspective, emissions from electricity generation should be spatially and temporally dispersed as much as possible. Hence, distributed generation is preferred over in-basin central generation with regard to air quality impacts.
- The current method and tools are useful for assessing regional air quality impacts. Regional air quality impact assessments require the use of all elements of the current approach (that is, spatially and temporally resolved emissions fields for emerging and future energy and power technologies, followed by a detailed solution of atmospheric chemistry and transport in air basins of interest).
- Additional research is required to determine the near-field impacts of emissions from distributed generation.

**Benefits to California**

California leads the nation in reducing emissions of greenhouse gases, and the electrical sector is a key area in which emission reductions can be achieved. Distributed generation has the

potential to help reduce greenhouse gas emissions from electricity production, especially when combined heating cooling and power technologies are used. However, use of distributed generation could increase in-basin emissions of pollutants compared to out-of-basin central generation, which could have adverse effects on regional air quality. This report provides a scientific basis for policy makers to assess the potential benefits and/or drawbacks of alternatives to conventional electricity generation in two important areas of the state: the South Coast Air Basin and the San Joaquin Valley. Policies that are established with knowledge of the current project results will be better equipped to encourage introduction of new technologies that improve air quality and reduce greenhouse gas emissions. Distributed generation technologies that are developed and implemented as a result of the current project findings will provide California ratepayers with high efficiency and low emissions power that also contributes to improved air quality.

Note: Unless otherwise noted, all tables and graphics within this report were prepared by the authors for this study.

# 1.0 Introduction

Power generation in California contributes 1%–2% of the total in-state emissions of nitrogen oxides ($NO_X$) and fine particulate matter ($PM_{2.5}$) (ARB 2007a). As one of the largest economies in the world, California power demand is expected to grow in the following decades by an average of 1.5% per year (EIA 2006). On the other hand, some specific regions in the state, such as the South Coast Air Basin of California (SoCAB) and the San Joaquin Valley Air Basin (SJVAB), are amongst the areas with the poorest air quality in the United States. Consequently, the state must continue to ensure that air quality improves as electricity supplies grow to meet California's burgeoning needs.

Distributed generation entails the use of power generation technologies (such as gas turbines, internal combustion engines and fuel cells) to produce electricity and thermal energy for local use. Emissions from DG units are characterized by many small point sources allocated throughout an urban air basin. In contrast, central-generation sources are concentrated in locations that oftentimes are located outside that air basin. Distributed Generation (DG) has the potential to supply a significant portion of the increasing power demand (California Energy Commission 1999). Gellins and Yeager (2004) considered DG to be one of the emerging technology types that will transform the electric infrastructure into a smart power system capable of supporting the needs of the digital society of the twenty-first century.

If installed correctly, DG technologies can fulfill the energy needs of numerous customers and provide overall emissions reduction, energy efficiency, and cost savings in multiple applications. For instance, DG units can deliver critical customer loads with emergency stand-by power; support available capacity to meet peak power demands; improve user power quality; and provide low-cost total energy in combined cooling, heating and power (CHP) applications.

In these past years, California has been reorganizing its electric power industry. In 2002 more than 2000 megawatts (MW) of electricity generation equipment was classified as DG according to the DG strategic plan developed by the California Energy Commission (Energy Commission) (Tomashefsky and Marks 2002). Due to grid constraints, growing power demands and high-cost power, California is one of the first places where DG adoption may become widespread.

Distributed generation technology is currently approved for installation and regular use in California by two separate procedures, depending upon the size of the DG unit and/or the DG technology. In general, DG units must be permitted by local air quality management districts and are required to meet the Best Available Control Technology (BACT) emissions limits. However, fuel cells of any size, reciprocating engines smaller than 37 kilowatts (kW) (50 horsepower, hp) and gas turbines smaller than 220 kW (corresponding to 2.975 million British thermal units per hour [MMBTU/hr] of heat input rate) are exempt from air district permitting and require emissions certification from the California Air Resources Board (ARB).

Currently diesel generators cannot meet the emissions standards for continuous operation under either the ARB certification or districts permitting processes. Diesel generators can only meet emissions limits for use as backup generators. However, it should be noted that there are

some exceptions for diesel generators in the SoCAB and the San Joaquin Valley. In the SoCAB, diesel generators are permitted for continuous operation in remote areas of the basin such as San Clemente and Santa Catalina islands. In SJV, diesel engines may be used for agricultural water pumping. Since diesel generators are installed on exception basis, these engines are not considered in the current study as distributed generators. In other areas, emissions standards may be sufficiently less stringent that diesel generators may need to be considered in the mix of DG technologies.

The shift from central to distributed power generation may increase basin pollutant emissions and lead to higher levels of ambient ozone and particulate matter concentrations. Researchers have examined some air quality impacts due to DG emissions (Allison and Lents 2002; Ianucci et al. 2000). However, these studies are limited to the evaluation of total emissions only. Furthermore, Heath et al. (2006) considered the potential for increased human inhalation exposure to air pollutants when power plants are replaced by DG units. Yet, Heath et al. (2006) limited their work to pollutants emitted directly into the atmosphere using a simplified mass transport approach. Determination of potential air quality impacts of DG requires understanding of the spatial and temporal emission profiles and subsequent analysis of DG emissions impacts using a detailed atmospheric chemistry transport model.

The installation of DG units in urban air basins raises numerous concerns that must be addressed before any public policy decisions are made to allow, support, or regulate DG implementation. Namely, how will DG be likely adopted in California? Will increased emissions from DG units affect the levels of ambient ozone with respect to the 8-hour ozone standard? Could any increase in $NO_x$ emissions enhance secondary particulate matter formation? What DG implementation scenarios could reduce overall environmental impacts?

A previous effort by the University of California, Irvine (UCI) Advanced Power and Energy Program (APEP) assessed the air quality impacts of DG in the SoCAB in the year 2010 (Samuelsen et al. 2005). This study first developed a detailed methodology for characterizing the spatial, temporal, and compositional variations in DG emissions in the SoCAB. Using this methodology the group developed (1) a set of scenarios that tried to reflect a likely DG adoption by the year of interest—named "realistic" scenarios—and (2) a set of scenarios that could reflect unexpected outcomes in DG implementation or that expanded the possibilities of DG adoption for scientific completeness—named "spanning" scenarios. Realistic scenarios showed small impacts on ozone and $PM_{2.5}$ concentrations; whereas spanning scenarios showed more significant air quality impacts, due mainly to a DG penetration higher than those assumed for the realistic scenarios. These results suggested that DG could affect air quality in years beyond 2010, where a significantly higher penetration of DG is expected.

The present effort, funded by the Energy Commission under the Public Interest Energy Research (PIER) Program, is a continuation of the previous study on air quality impacts of DG in the SoCAB. In particular, this project has two main goals: (1) evaluate the air quality impacts of DG in the SoCAB in years beyond 2010, which was the year of study in the preceding project, and (2) evaluate the future air quality impacts of DG in the San Joaquin Valley, which is an area where electricity demand is growing more rapidly than the average California rate, and thus,

DG could provide a significant portion of the electricity generation in the SJV. The methodology employed during the preceding project to estimate DG penetration has been updated using new market studies. In addition, this methodology, which was originally developed for the SoCAB, has been adapted for its use in the SJV, and new air quality models have been acquired to simulate air quality in the San Joaquin Valley. Finally, this report includes sensitivity analyses of model predictions for the SoCAB and for the SJV. The analyses are designed to reflect the uncertainties that DG implementation scenarios introduce in air quality simulations. During the preceding study by Samuelsen et al. (2005), a detailed sensitivity analysis was conducted for the air quality model for the SoCAB. The analyses presented in the present report complement the findings acquired in the preceding study.

## 1.1. Overview of the South Coast Air Basin

The South Coast Air Basin of California includes the entire Orange County, Los Angeles (except the portion of Antelope Valley) and parts of San Bernardino and Riverside counties (see Figure 1). The current population in the SoCAB is over 16.4 million people and is expected to grow to 18.6 million by 2020.

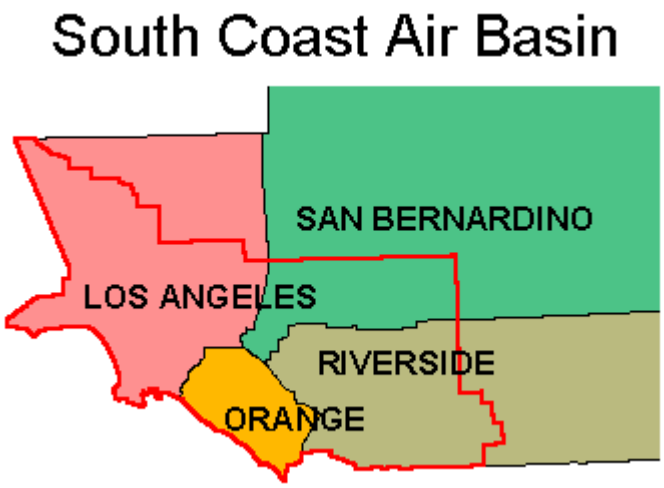


**Figure 1. South Coast Air Basin of California**
Source: www.arb.ca.gov/ei/maps/basins/absc.nvm

### *1.1.1. Geography and Topography*

The State of California is divided into regional air basins based on topographical air transport features. The South Coast Air Basin encompasses most of the greater Los Angeles area and stretches nearly 300 kilometers (km) from west to east and 150 km from south to north. The basin is delimited by the Pacific Ocean on the south and west, by the San Gabriel and San Bernardino Mountains on the north, and by the San Jacinto Mountains on the east. Typical summer meteorological conditions consist of an onshore sea breeze that pushes pollutants to inland areas. The presence of mountain ranges on the north and east stops the transport farther

inland and accumulates pollutants in regions around Riverside and San Bernardino, where the highest ozone concentrations typically occur.

### *1.1.2. Air Quality in the SoCAB Region*

Criteria pollutants such as ozone and particulate matter are formed from atmospheric transformation of both biogenic and anthropogenic emissions that come from a variety of sources. The National Ambient Air Quality Standards (NAAQS) and the State of California air quality standards regulate ambient levels of pollutants such as ozone ($O_3$), $NO_x$, sulfur oxides ($SO_x$), PM, and carbon monoxide (CO) in order to protect public health. Ambient concentrations of criteria pollutants are constantly monitored and should be below the maximum concentrations defined by state and federal air quality standards.

Figure 2 presents the evolution of maximum 1-hour and 8-hour average ozone concentration in the SoCAB for the past three decades, and Figure 3 presents the number of days a year that the California 1-hour and the federal 1-hour and 8-hour ozone standards are exceeded. Although there has been a significant improvement in air quality since the mid seventies, ozone concentration still exceeds the federal 1-hour ozone air quality standard over 30 days a year. In addition, the recently approved 8-hour average ozone standard is violated over 80 days a year. Based on the poor air quality in the SoCAB, the U.S. Environmental Protection Agency (U.S. EPA) classified this area as a "Severe-17" non-attainment region for the purposes of compliance with the federal 8-hour ozone standard, and the SoCAB is required to develop a plan that shows attainment of standards by the year 2023.

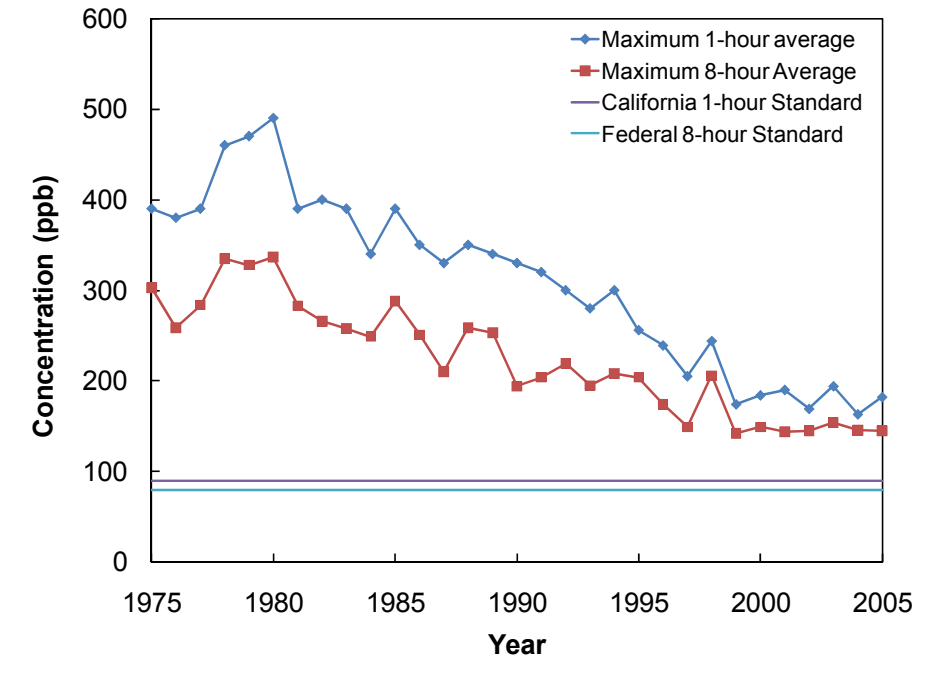


**Figure 2. SoCAB basinwide maximum concentrations with reference to state and federal standards**

Source: ARB 2006b

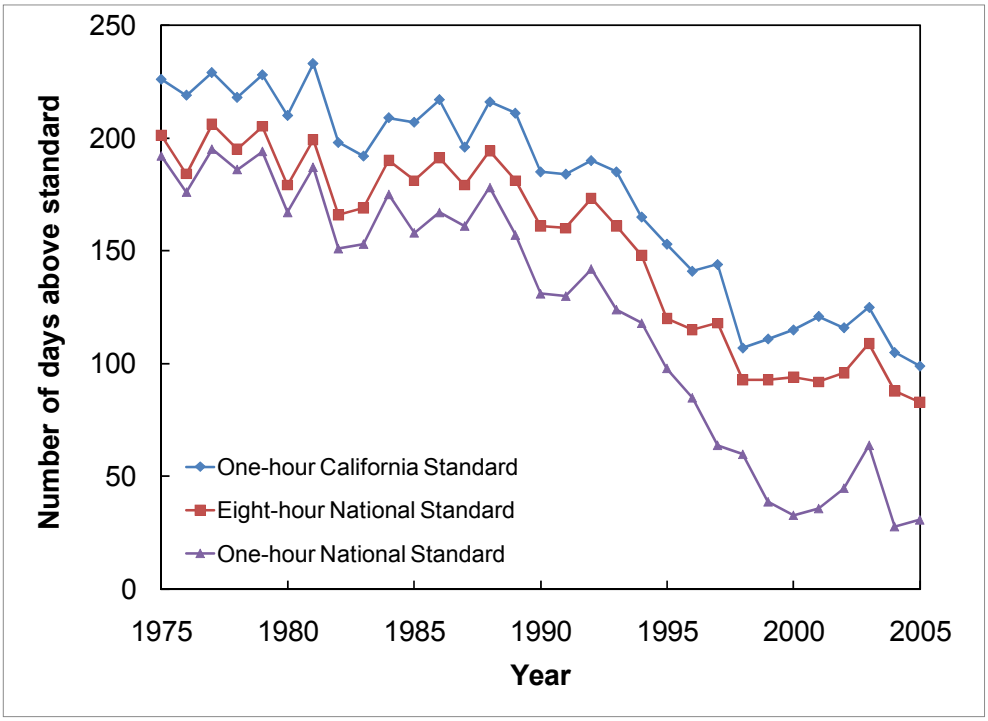


**Figure 3. Number of days the SoCAB is out of compliance with the state and federal standards**

Source: ARB 2006b

## 1.2. Overview of San Joaquin Valley Region

The San Joaquin Valley (SJV) air basin consists of eight counties: Fresno, Kern (western and central), Kings, Madera, Merced, San Joaquin, Stanislaus, and Tulare. Figure 4 shows the SJV air basin and other air basins in California. The current population of the SJV region is about 3.2 million and is expected to grow to 4.9 million by 2020. The SJV is one of the most fertile regions in the world. Consequently, SJV is a major contributor to the United States agricultural production.

### *1.2.1. Geography and Topography*

The SJV region is the second largest air basin in terms of land area in California. The SJV is approximately 400 km long, averaging 130 km wide, and is flanked by the coastal mountain range on the western edge and the Sierra Nevada range on the eastern side. The Tehachapi Mountains form the southern boundary of the valley. The valley floor is open only to the north. These unique geographic features of the valley have significant bearing on air movement in the valley.

The mountain ranges on the west, south, and east edges of the valley restrict the air movement, leading to stagnation and poor air flow in the valley. Furthermore, during the nighttime the airflow in the south is restricted, due to cooler drainage winds from the mountains in the Tehachapi range. This additional barrier leads to a circular flow pattern of winds in the night that is commonly known as the "Fresno eddy." The Fresno eddy transports pollutants back to the urban areas, adding to the following day's emissions.


**Figure 4. San Joaquin Valley air basin**
Source: SJVAPCD

### *1.2.2. Air Quality in the SJV Region*

The SJV region has a high number of days during which violation of the standards for criteria pollutants occurs (ARB 2006b). Figure 5 shows the basinwide maximum concentrations of ozone, averaged over one hour and eight hours, for the years 1975–2005. Although there has been a steady decrease of maximum basinwide ozone concentrations, current measurements are significantly higher than the maximum levels mandated by the state and federal standards. Figure 6 shows the number of days per year that the ambient ozone concentrations in the SJV region exceed the state and federal standards during the same period. Based on ARB-reported data, the NAAQS is continuously exceeded over 80 days per year. The U.S. EPA classified the SJVAB as a serious non-attainment region for the purposes of compliance with the federal 8-hour ozone standard, and the San Joaquin Valley Air Pollution Control District (SJVAPCD) is required to develop a plan that shows attainment of standards by June 15, 2013.

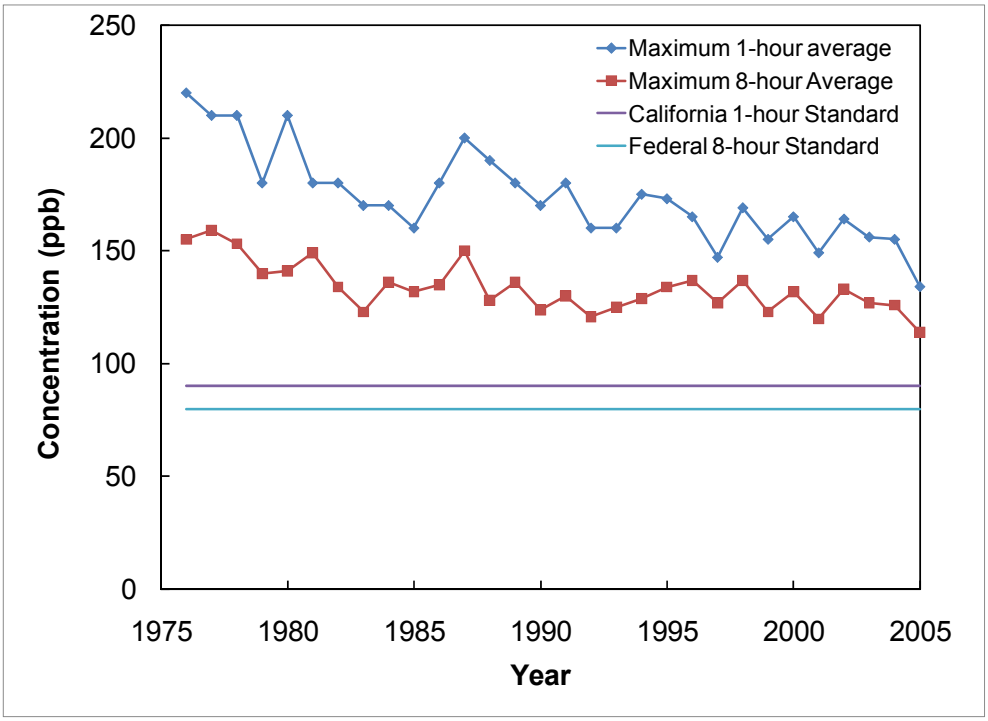


**Figure 5. SJV basinwide maximum concentrations with reference to state and federal standards**

Source: ARB 2006b

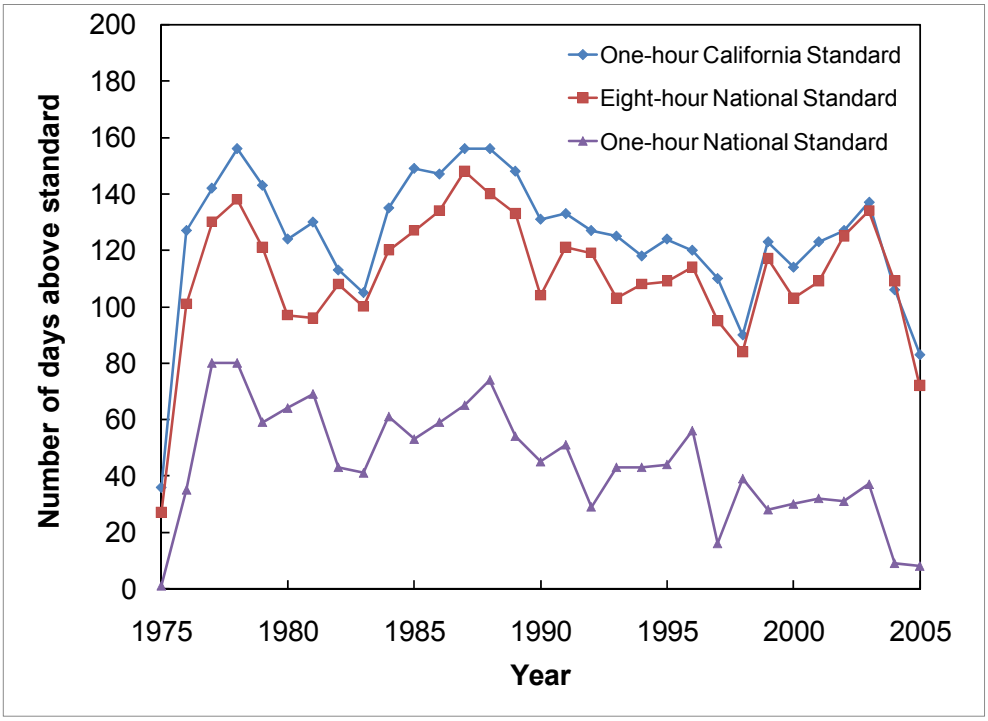


**Figure 6. Number of days the SJV is out of compliance with the state and federal standards**

Source: ARB 2006b

The San Joaquin Valley presents unique air quality simulation and pollutant control challenges due to the seasonality of air pollution episodes. High ozone concentrations are observed during summer months. However, high particulate matter episodes occur during the winter. In the Integrated Monitoring Study (IMS95) conducted in 1995, wintertime $PM_{10}$ is dominated by ammonium nitrate (50%), mobile sources (20%), and vegetative burning (15%), with approximately 70%–80% of the $PM_{10}$ present as $PM_{2.5}$ (Magliano et al. 1999).[1] Many studies have shown that ammonia emissions from agricultural activities contribute to PM episodes in the winter. A large fraction of observed PM is ammonium nitrate that is formed when the air masses from urban areas with high $NO_X$ concentrations mix with downwind ammonia emissions.

## 1.3. Years of Study

The previous study by Samuelsen et al. (2005), which started in 2002, analyzed the potential impacts of DG in the year 2010. Hence, the study assessed the implementation of DG during a period of eight years. By the year 2010, a moderate DG penetration was expected, and results of the study showed low air quality impacts due to DG implementation. One of the conclusions of that study was that higher DG penetration in years beyond 2010 could lead to more significant air quality impacts. The present study focuses on additional future years that represent a longer-term reference for DG implementation. Part of the motivation for choosing 2010 was that it was the deadline for attainment of the federal 1-hour standard for ozone concentration. On June 15, 2005 the 1-hour ozone standard was revoked for all areas except the 8-hour ozone non-attainment Early Action Compact Areas (EAC) areas (those that do not yet have an effective date for their 8-hour designations). Recently, the SoCAB and the SJVAPCD have been designated as extreme non-attainment areas with respect to the new 8-hour average ozone standard.[2] This reclassification extends the deadline for attainment with the 8-hour average ozone standard to 2024, and the South Coast Air Quality Management District (SCAQMD) and the SJVAPCD are required to design a new emissions inventory for the year 2023. This new date is significantly farther into the future than 2010, (used in the preceding report), and a significant increase in DG implementation may be expected between 2010 and 2023. Therefore, the year 2023 is selected in this new project as the first reference date for the assessment of air quality impacts due to DG implementation.

Emissions inventories for the year 2023 have been developed for the 2007 Air Quality Management Plan (AQMP) by the SCAQMD and for the 2007 Ozone Plan by the SJVAPCD. These two approved plans are available, and they include long-term emission controls that lead

[1] $PM_{10}$ is particulate matter 10 microns or smaller in diameter; $PM_{2.5}$ is particulate matter 2.5 microns or smaller in diameter.

[2] To attain this standard, the three-year average of the fourth-highest daily maximum 8-hour average ozone concentrations measured at each monitor within an area over each year must not exceed 75 parts per billion, effective May 27, 2008. The previous standard used in the 2007 Air Quality Management Plan of the South Coast Air Basin and in the 2007 Ozone Plan for the San Joaquin Valley was set to 80 parts per billion.

to significant reductions of $NO_x$ and volatile organic compounds (VOC) with respect to the 2003 AQMP. However, gridded emissions for the year 2023 are not still available. Hence, this project uses previously released emissions inventories developed for the SoCAB and the SJV, and it applies emissions reductions as described in the approved AQMP and Ozone Plan to obtain the baseline emissions inventory for the year 2023.

Moreover, the SCAQMD has recently developed an additional future inventory that shows that attainment of the ozone standard can be maintained in years beyond 2023. The year that has been selected for demonstrating continued attainment of the ozone 8-hour standard in the SoCAB is 2030, and it has been included in the 2007 AQMP. This study uses 2030 as another reference year to investigate the impacts of DG on air quality in the SoCAB. This 2030 scenario will allow investigation of more significant DG penetration in a specific future year of interest.

Finally, the current project investigates an additional future year beyond 2030 for the SoCAB. This future year will remain undesignated since it is nearly impossible to predict the year or even the decade in which some of the scientifically important changes that could impact air quality may occur in the distant future. These very significant and important changes could be due to a number of paradigm and/or technology shifts that could affect both baseline emissions and DG emissions in the future.

The magnitude of the air quality impacts of DG depend, to some extent, on the baseline emissions for the year of study. In June 2005, Governor Schwarzenegger signed an executive order to drastically reduce California's greenhouse gas (GHG) emissions by the year 2050. This plan will require implementation of new technologies that enhance efficiency of fossil fuel technologies, in addition to new alternative technologies that do not directly emit GHG, such as hydrogen-based technologies and renewable energy technologies. Hence, long term scenarios must consider the possibility of paradigm changes in energy conversion for electricity production and/or for transportation that would lead to significant reductions in baseline emissions. One potential paradigmatic change is the widespread commercialization of electric vehicles, either with some level of hybridization with combustion engines or fuel cells, or as pure electric vehicles. This scenario requires a drastic increase in electricity generation to fuel automobiles. The additional need for electricity could be supplied by conventional power generation, (i.e., central power plants) or by distributed generation. As a result, emissions from mobile sources would decrease significantly; whereas emissions from power generation could increase substantially, depending on the prevailing technology used for supplying the additional needs for power.

Emissions estimates for such a futuristic (long-term) scenario are not available, and no agency ventures to produce them due to the high uncertainty inherent in developing such scenarios. On the other hand, SCAQMD developed the 2007 Air Quality Management Plan that includes emissions inventories for year 2023 and 2030 to demonstrate continued attainment of the 8-hour ozone standard. Once ozone standards are attained there will be no federal pressure to reduce criteria pollutant emissions, and if air quality is significantly improved and maintained there may also be no local or state pressure to reduce emissions. This study uses the latest attainment inventory for the study of futuristic scenarios in the hypothetical year 20XX. This year

represents a year beyond 2030, but before 2100, that cannot be clearly identified, and thus it is labeled as "20XX." In this timeframe it is anticipated that the need for reducing GHG emissions could force additional reductions of ozone precursor emissions as well. On the other hand, population and industrial growth as well as paradigm and technology shifts that are possible in the 20XX timeframe could lead to increased emissions that affect air quality. These possibilities will be reflected in both the baseline emissions and DG technology emissions for the long-term scenario of 20XX.

### *1.3.1. Baseline Power Demand in Years of Study*

The Energy Information Administration (EIA 2006) predicts a nationwide annual increase in electricity demand of 1.51% during the period 2003–2030. During the period 2003–2020 the predicted annual increase is 1.56%. According to an Energy Commission report (CERTS 2003), the statewide peak power demand in California in 2003 was 53.4 gigawatts (GW). Based upon electricity consumption, 46% of that demand corresponds to the electricity demand in the SoCAB and 12% corresponds to the SJV. Assuming the nationwide growth in electricity demand, the increased demand estimated for the year 2023 in the SoCAB and the SJV is 7.8 GW and 2.0 GW, respectively. Additionally, the increased demand estimated for the year 2030 in the SoCAB is 11.4 GW.

According to the CERTS report (CERTS 2003), if all fossil-based power plants are retired after 50 years of operation and the state's three nuclear plants (San Onofre, Diablo Canyon, and Palo Verde) are retired after their first relicensing and will not be operating by 2030, then only 32.1 GW of the power plants out of 60.6 GW in operation in 2003 will remain operational in 2030. This implies that 28.5 GW of capacity must be installed in California by 2030, in addition to the expected increase in power demand of 30 GW in the period 2003–2030. The installation of new capacity that has to substitute for retired power plants in the future could be accomplished partly by installing DG. This possibility is explored in the spanning scenarios, as proposed in Section 2.1.6 of this report.

## 1.4. Summary of Characterization of DG Scenarios

The approach that is followed in the current work is based upon a detailed methodology for developing DG scenarios that was developed over a period of four years in a previous study (Samuelsen et al. 2005). However, new information on DG market studies and updated information on DG technology types is used to reestimate how DG will be distributed in California. To fully characterize how DG resources may be implemented, one must describe in detail a set of parameters that define the operating characteristics of the DG units, their spatial and temporal distribution throughout the basin, and other characteristics of the particular instance of DG use in the basin. A compilation of parameters that are required to fully describe all of the DG characteristics as installed in the SoCAB and the SJVAB is called a "DG Scenario."

The Advanced Power and Energy Program (APEP) team at the University of California, Irvine, determined in the previous effort the process to characterize a specific DG scenario. This process was designed following recommendations and feedback received in two stakeholder meetings, held at the National Fuel Cell Research Center during the preceding study for the

SoCAB. For the present study, an additional workshop was held at the SJVAPCD offices in Fresno, to adapt the methodology for the study of DG penetration in the San Joaquin Valley Air Basin. The space required to fully define a DG Scenario was characterized by a set of seven parameters and various factors that are subsets of these parameters. The seven parameters were identified to fully characterize a DG scenario are presented schematically in Figure 7. The seven parameters of Figure 7 include: (1) the total fraction of energy needs in a given region that are met by DG in the scenario, (2) the allocation of DG resources to meet that need, (3) the emissions associated with each DG unit type, (4) the spatial distribution of the DG in the area of interest, (5) the operational duty cycle of each DG, (6) the accounting for any emissions that are displaced by installation of the DG, and (7) other estimates that are required to account for the DG and relate the emissions to requirements of the air quality model (AQM). Each of the parameters may have several factors that are varied within the parameter space.

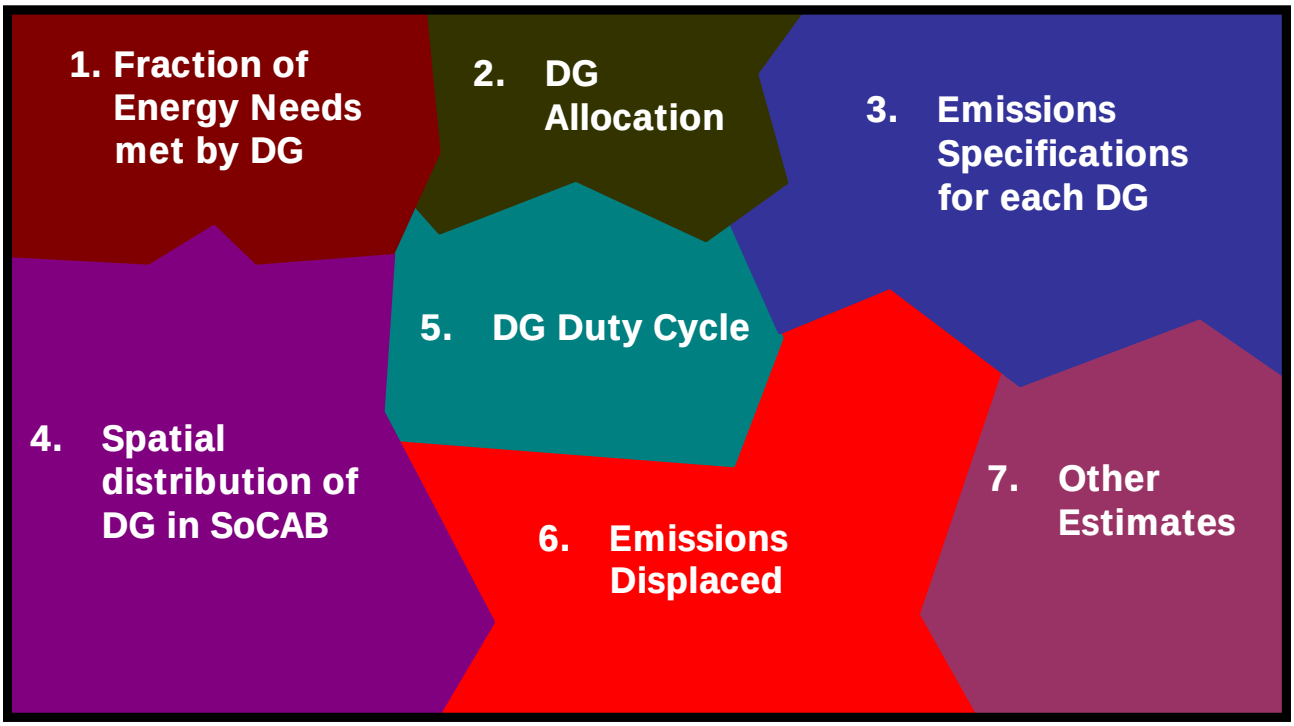


**Figure 7. Schematic of the DG scenario parameter space**

Table 1 presents more details of the parameter space and all of the factors that are considered in the development of the DG scenarios. Note that some of the parameters are fully characterized by variations in primary factors; whereas other parameters require characterizations and variation of primary and secondary factors in their definition. These factors are described in Section 2.1.

**Table 1. List of parameters and factors that are required to be characterized to represent a full distributed generation scenario**

| Main DG Parameter | Primary Factors | Secondary Factors |
|---|---|---|
| **1. Fraction of energy needs met by DG** | 1.1. Limited (7% of increase) | |
| | 1.2. Medium (12% of increase) | |
| | 1.3. High (18% of increase) | |
| | | |
| **2. DG allocation** | 2.1. Types of DG units | 2.1.1. All NG GT-DG (<50 MW) |
| | | 2.1.2. Fuel Cell Only |
| | | 2.1.3. Renewables – yes, no |
| | | 2.1.4. Mix of DG (MTG, FC, NG-ICE, Stirling, hybrid, …) |
| | | 2.1.5. Mix of DG and large GT-DG (50 MW) |
| | | 2.1.6. Diesel included – yes or no |
| | 2.2. Number of DG units of each type | 2.2.1. Large DG unit size vs. small DG unit size |
| | | 2.2.2. Technology Mix Factors<br>- High penetration of low emissions technologies (strong regulation/policy drivers)<br>- Low penetration of low emissions technologies (either modest regulation or lack of technology advancement)<br>- Zoning or land-use<br>- Economic factors |
| | | |
| **3. Emissions specification for each DG** | 3.1. Current emissions factors | 3.1.1. Known emissions factors – literature, data |
| | | 3.1.2. Estimated emissions factors |
| | 3.2. Future advancements to meet regulatory requirements | 3.2.1. Fraction that meets 2007 ARB emissions standards |
| | | |
| **4. Spatial distribution of DG in the SoCAB** | 4.1. Population growth weighted | |
| | 4.2. Land-use weighted | 4.2.1. Classify Land-use |
| | | 4.2.2. Land-use energy adoption rate factors |
| | | 4.2.3. Land-use weighted technology adoption factors |
| | | |
| **5. DG duty cycle** | 5.1. Baseloaded | |
| | 5.2. Peaking | |
| | | |
| **6. Emissions displaced** | 6.1. CHP | 6.1.1. Percentage of CHP utilization |
| | | 6.1.2. Percentage of CHP heat recovered |
| | 6.2. In-Basin electricity emissions displaced | |

**Table 1. (continued)**

| | | |
|---|---|---|
| **7. Other estimates** | 7.1. Emissions assumptions | 7.1.1. Speciation of total hydrocarbons into specific hydrocarbon compounds and particulate matter (PM) into 8 size classes and 19 species of PM |
| | 7.2. Performance degradation (yes or no) | |
| | 7.3. Geometrical features (elevated emissions – yes or no) | |
| | 7.4. DG Commercial Adoption Rate | |

Once all of the parameters and factors of Table 1 are specified, the DG scenario is fully characterized and the corresponding DG emissions inventory for each of the discrete cells in the computational air quality model can be developed for each instance in time. The air quality model calculates the physical and chemical processes that affect the concentration of all the species within the basin on an hourly averaged basis. As a result, DG emissions rates must be specified for as listed in Table 1 for each cell and for each of the 24 hours of each day of the simulation. This DG emissions inventory is then formatted as a model input file and added to the baseline emissions inventory for use in the model to assess the air quality impacts of the DG emissions.

Note that two types of DG Scenarios are developed in the current effort as follows:

- "Realistic" DG Implementation Scenarios.
- "Spanning" DG Implementation Scenarios.

These two categories segregate the DG Scenarios on the basis of the "likelihood" of the scenario. This differentiation was established during the previous effort conducted by Samuelsen et al. (2005), after presenting it to stakeholders who participated in two workshops held at UCI on September 19, 2002, and May 20, 2003. "Realistic" implementation scenarios are likely instances of DG installation in the SoCAB. However, for scientific completeness, for sensitivity analyses, and for determination of potential impacts for unexpected outcomes, "Spanning" scenarios are required. These spanning scenarios must not be considered realistic or probable. The spanning DG scenarios are not expected and are only used for purposes of garnering insights that may be useful. This approach was reviewed again during the present study in a workshop held in Fresno, in April 24, 2007.

## 1.5. DG Scenario Screening Criteria

If one decided to investigate all possible permutations of the parameters and factors identified above, one would need to simulate $1.09 \times 10^{28}$ (= 27!) scenarios. To accomplish the simulation of air quality impacts of DG for such a large number of cases is not feasible. Hence, this study focuses on limited number of scenarios based on a systematic screening that incorporates appropriate parameters and factors of concern.

The APEP group developed the criteria and presented them to experts in the air quality modeling and DG stakeholders (in three public workshops and in coordination meetings with the SCAQMD, SJVAPCD, ARB, and the Energy Commission). Table 2 presents the final screening criteria for selecting a limited number of DG Scenarios from the list of possible scenarios that could be comprised of variations in all of the parameters and factors, as well as a description of the seven primary screening criteria. The description of each criterion is stated in the affirmative. As a result, sets of parameter variations that positively meet any one of the Table 2 screening criteria have been retained in the current study.

**Table 2. Final screening criteria**

| Criterion Number | Criterion | Description |
|---|---|---|
| 1 | Likelihood of implementation | Are the variations in the parameters and factors considered realistic or not realistic based upon team and stakeholder input? If they are realistic or possible, then the variation is included in the current study. |
| 2 | Variety of implementation | Are the variations in the parameters and factors required to span the spectrum of possible implementations and/or technologies of interest? If yes, then the scenario should be included in the current study. |
| 3 | Potential for socio-political forcing | Is there a potential for social demand, regulatory requirements, energy crises, or other socio-political forcing functions to support the variations in the parameters and factors considered for a specific DG Scenario? If yes, then the scenario should be included in the current study. |
| 4 | Fundamental understanding | Does inclusion of the DG Scenario provide insight into any specific aspect of the air quality results or model itself (e.g., atmospheric chemistry, mass transport, DG emissions)? If yes, then the scenario should be included in the current study. |
| 5 | Data acquisition or additional funding required | Is the inclusion of the scenario consistent with the current contract, the funding level provided, and is sufficient information to characterize the scenario already available? If yes, then the scenario should be included in the current study. If additional funding or data acquisition is required to develop or include the scenario, then the scenario is rejected. |
| 6 | Availability of resources | Are sufficient resources such as published results, stakeholder insights, Energy Commission studies, or APEP measurements and expertise available to develop and support the validity of the variations in the parameters and factors considered for a specific DG Scenario? If yes, then the scenario should be included in the current study. |
| 7 | Required for determining specific sensitivity of the model | Is the specific DG Scenario required to conduct an appropriate sensitivity analysis or to provide insight regarding model sensitivity to simulation parameters? If yes, then the scenario should be included in the current study. |

The criteria of Table 2 were applied to the parameter and factor space outlined above and their application resulted in the selection of about 100 DG Scenarios. This number of scenarios is still too large to reasonably address in the current effort. As a result, and with feedback and encouragement from the industry stakeholder workshop participants, APEP was able to develop two additional criteria that were further used to screen the scenarios. These two criteria were used to cast a deciding vote on whether or not a scenario is included in this study. These criteria are presented in Table 3. Note that the criteria A and B are subjective, however, these criteria are applied and based upon all the literature reviewed to date, all of the expertise of the APEP team, and insights garnered from ARB, SCAQMD, SJVAPCD, and industrial participants in the stakeholder workshops. This process is briefly described in the descriptions of each criterion in Table 3.

**Table 3. Additional screening criteria**

| Criterion Letter | Criterion | Description |
|---|---|---|
| A | **Is the DG scenario realistic?** | A subjective determination is made regarding whether or not a DG scenario is realistic. This determination is made on the basis of literature review, APEP expertise, and industry and other stakeholder insights. If the scenario is deemed to be realistic or probable, then the scenario is included in the current study. |
| B | **Does the investigation of the DG scenario contribute to increased understanding?** | An assessment is made of the value of including the DG scenario, even if Criterion A is not met. The assessment is based upon whether or not the team believes increased understanding of DG air quality impacts may be garnered by inclusion of the scenario. If the scenario is deemed to have merit in this regard, then it is included in the current study. |

# 2.0 Methodology for DG Scenario Development

## 2.1. Parameters for DG Scenario Development

### *2.1.1. Fraction of Energy Met by DG*

The "Fraction of Energy Met by DG" parameter has a strong influence in the final air quality impact that a DG scenario exhibits. A high penetration scenario implies that DG units throughout the area of interest meet a considerable portion of the total energy needs. In this case, DG emissions significantly contribute to the total pollutant emissions in a given air basin. However, for the same level of emissions, air quality impacts might be very different depending on other DG scenario characterization parameters, such as spatial distribution of the DG power or duty cycle. In addition, these impacts are not easy to predict without a detailed and comprehensive model due to the highly non-linear processes that govern the coupled transport and atmospheric chemistry of an air basin.

According to the California Energy Commission's strategic plan for DG (Tomashefsky and Marks 2002), the forecasted adoption of DG in California for the year 2020 could be as high as 20% of the electricity load growth. Newer estimates by the Electric Power Research Institute (EPRI 2005) suggest that the 2005–2020 cumulative market potential for DG units with CHP in California is 1,966 MW with the existing incentive programs. This market potential corresponds to a 12% of the increase in electricity demand in California during that same period. In addition, the EPRI report identifies alternative scenarios with high level of incentives, research and development (R&D), and customer satisfaction. The highest penetration that DG could meet without electricity exports is nearly 3,000 MW, which represents 18% of the increased power demand in California. Moreover, aggressive market penetration, which includes credits for carbon dioxide ($CO_2$) emissions and favor wholesale electricity export, could lead to a cumulative market penetration of 7,340 MW, which corresponds to nearly 45% of the increased demand of electricity in the period 2005–2023. In the present study, baseline DG penetration for realistic scenarios is 12% of the increased power demand for both the SoCAB and the San Joaquin Valley Air Basin. A distributed generation penetration of 18% is considered for a realistic scenario with high penetration. Since the fraction of energy met by DG is quite uncertain, a wide variety of DG penetration levels is investigated in the DG scenarios to span the spectrum of possible air quality impacts. One spanning scenario considers a DG penetration of 45% of the increased demand between 2005 and 2030, to determine the sensitivity of air quality predictions to this DG scenario parameter.

### *2.1.2. DG Allocation*

Following the approach used in the preceding study on air quality impacts of DG (Samuelsen et al. 2005), which was based upon input from the first industry stakeholders workshop held in September 2002, the current study includes distributed generators with power capacities that range from a few kilowatts (kW) up to 50 megawatts. The 50 MW limit on DG is selected due to the permitting construct in California. The DG technologies that are likely to be implemented in California include commercial technologies (natural gas-fired combustion turbines [up to 50 MW] and natural gas-fired reciprocating internal combustion engines [ICE]), as well as

emerging technologies such as solar photovoltaics (PV), fuel cells (polymer electrolyte membrane [PEMFC], molten carbonate [MCFC], and solid oxide [SOFC]), gas turbine fuel cell hybrids, and natural gas fired micro-turbine generators (MTGs). In addition, biomass technologies are also considered for the San Joaquin Valley. In the previous effort, external combustion Stirling engines were also included in the DG mix. However, current forecasts do not include this technology to any significant extent.

The technology mix is dependent on the number and type of energy customers, as well as a host of other economic and regulatory variables (e.g., electricity prices, gas prices, DG incentives, transmission constraints, emissions standards) that exist in a given region. Every market segment can be preferentially associated with specific DG technologies that are likely to be predominant, mainly because their capacity and features are best suited to the energy demands of that segment. For example, residential applications in the range 1–5 kW will likely favor fuel cells and photovoltaics; commercial and small industrial sectors, with capacities ranges of 25–500 kW are more suited for PV, MTGs, small ICEs, and FCs; large commercial and institutional sectors, in the range of 500 kW–2 MW, will likely favor natural gas reciprocating engines and gas turbines; and finally the large institutional and industrial sectors with 2–50 MW capacity will be served mainly by gas turbines. This relationship between DG type and market sector is used in conjunction with land use information to obtain the spatial distribution of DG emissions. Information on duty cycle in each individual sector is used to determine the temporal distribution of DG emissions for a particular location.

The DG scenarios developed in this effort are not based upon a detailed market penetration analysis for the various DG technologies, but rather upon studies that are currently available in the literature, APEP insights, and stakeholder feedback. The resources used include: (1) previous studies that determined a reasonable mix of technologies (e.g., Ianucci et al. 2000; Marnay et al. 2001; EPRI 2005), (2) input from the industry stakeholder workshops conducted during the phase I project, (3) input from the industry stakeholder workshop held during the phase II project, (4) current APEP understanding of technology features, (5) current penetration of certain technologies (e.g., MTGs), and (6) APEP intuition, engineering insight, and/or brainstorming.

Diesel- and petroleum distillate-fueled units are not included in the current mix of DG technologies since they are not currently permitted to run on a continual basis as distributed generators. These types of units are only permitted to run as backup generators. Although advanced diesel technologies could meet air emission standards by 2023, these technologies are not included in the technology mix considered in this report.

### *2.1.3. Emissions Specifications*

There is a wide range of emissions factors that are either available as measured data or estimated by various investigators for each of the DG technologies. Some DG technologies are environmentally friendly, with zero emissions (e.g., wind turbines, photovoltaics) or near zero emissions (e.g., fuel cell systems), while others may emit more pollutants than central power plants. There are numerous literature sources that report emission factors of different DG types. The values of emission factors vary widely amongst reports (Ianucci et al. 2000; Marnay et al.

2001; Allison and Lents 2002; Nexus 2002; NREL 2003a). In addition, some reports include projections of emissions for the future year (E2I 2004). These future estimates assume technology advances that would lead to significant emission reductions. These data sets, however, include emissions factors that are higher than the current regulated limits for DG units, some permitted by air districts (ICEs and GT) and the others certified by ARB (MG, FC, Stirling engines, and others with less than 1 MW capacity). In addition, there is a strong commitment from the regulatory agencies to apply the same emission standards to ICE and GT that are applicable to MTG and fuel cells.

Consequently, this work assumes that the emission factors for any DG type in years beyond 2020 will not exceed the 2007 ARB emission standards. Two different sources are used in this study to evaluate DG emissions. Emission factors for realistic scenarios are based on the values estimated for future years by E2I (presented in Table 4). Some of these values exceed the 2007 ARB emissions standards (shown in Table 5), and hence, these values are capped at the ARB limits shown in Table 7, which account for the CHP emission credits that depend on the total excess heat that is recovered and used by CHP. Emission factors for spanning scenarios, unless noted, were obtained from EPRI (2007) (see Table 8 through Table 11). These values assume that ICE and GT incorporate after-treatment technologies that reduce criteria pollutant emissions to within ARB limits. After-treatment technologies are specific to DG type, and are specified in Table 8 through Table 11. A new feature of the present study is the use of emission factors specific to DG unit size, as opposed to using one single factor for each DG type, as was assumed in the preceding effort.

Table 5 presents the approved California Air Resources Board emission standards (CO, VOC, $NO_X$, and PM limits) for type certification of DG. These standards apply to fuel cells and small DG units that do not fall under the jurisdiction of air districts for control of stationary point sources. The SCAQMD and SJVAPCD best available control technology (BACT) permitted levels for DG emissions are presented in Table 6.

**Table 4. Technical specifications for DG technologies estimated for the year 2030 without after-treatment**

| Type | Size, kW | Electric Efficiency[a] | CHP Heat Rate Recovery[b] | Heat Output[c] (Btu/kWh) | Emissions, lb/MWh | | | | |
|---|---|---|---|---|---|---|---|---|---|
| | | | | | $NO_X$ | CO | $SO_X$ | NMOC | $PM_{10}$ |
| *Gas Turbines* | 1000 | 0.27 | 0.17 | 2199 | 0.140 | 0.250 | 0.008 | 0.039 | 0.500 |
| | 5000 | 0.35 | 0.15 | 1462 | 0.100 | 0.210 | 0.006 | 0.032 | 0.360 |
| | 10000 | 0.37 | 0.14 | 1328 | 0.100 | 0.175 | 0.006 | 0.030 | 0.290 |
| | 25000 | 0.40 | 0.14 | 1152 | 0.090 | 0.180 | 0.005 | 0.028 | 0.300 |
| *Micro-Turbines* | 50 | 0.34 | 0.15 | 1535 | 0.100 | 0.430 | 0.006 | 0.010 | 0.230 |
| | 110 | 0.37 | 0.14 | 1328 | 0.100 | 0.180 | 0.005 | 0.010 | 0.220 |
| | 160 | 0.39 | 0.14 | 1207 | 0.090 | 0.300 | 0.005 | 0.010 | 0.190 |
| | 250 | 0.39 | 0.14 | 1207 | 0.090 | 0.380 | 0.005 | 0.010 | 0.190 |
| | 500 | 0.40 | 0.14 | 1152 | 0.090 | 0.380 | 0.005 | 0.010 | 0.150 |
| *Reciprocating Engines* | 100 | 0.34 | 0.15 | 1535 | 0.310 | 0.300 | 0.006 | 0.310 | N/A |
| | 300 | 0.35 | 0.15 | 1462 | 0.310 | 3.100 | 0.005 | 1.550 | N/A |
| | 1000 | 0.42 | 0.13 | 1048 | 0.310 | 3.100 | 0.005 | 0.310 | N/A |
| | 3000 | 0.42 | 0.13 | 1048 | 0.310 | 3.100 | 0.004 | 1.550 | N/A |
| | 5000 | 0.45 | 0.12 | 910 | 0.310 | 3.100 | 0.004 | 0.770 | N/A |
| *Fuel Cells* | 10 | 0.36 | 0.15 | 1393 | 0.050 | 0.060 | N/A | 0.010 | N/A |
| | 200 | 0.38 | 0.14 | 1266 | 0.050 | 0.040 | N/A | <0.01 | N/A |
| | 100 | 0.53 | 0.10 | 618 | 0.040 | 0.030 | N/A | <0.01 | N/A |
| | 250 | 0.49 | 0.11 | 752 | 0.040 | 0.030 | N/A | <0.01 | N/A |
| | 2000 | 0.52 | 0.10 | 650 | 0.040 | 0.030 | N/A | <0.01 | N/A |

Source: Adapted from E2I 2005

[a] Electric efficiency based on higher heating value (HHV)

[b] CHP Heat Rate Recovery calculated as $\eta_{CHP} = (\eta_{tot} - \eta_{elec}) * f_{CHP} * f_{HR}$, where $\eta_{tot}$ is DGCHP total efficiency (=0.85), $\eta_{elec}$ is the electric efficiency as reported in the table, $f_{CHP}$ is the CHP utilization factor (=0.5) and $f_{HR}$ is the heat recovery factor (=0.6). Specific values where defined based feedback from stakeholders.

[c] Heat Output calculated as 3412.14 * $\eta_{CHP}$ / $\eta_{elec}$

Note: NMOC = nonmethane organic compounds; lb/MWh = pounds per megawatt-hours; kWh = kilowatt-hour

**Table 5. Approved 2007 ARB DG emissions standards**

| Pollutant / DG type | CO lb/MWh | VOC lb/MWh | $NO_X$ lb/MWh | PM lb/MWh |
|---|---|---|---|---|
| DG Unit not integrated with Combined Heat and Power | 0.100 | 0.020 | 0.070 | An emission limit corresponding to natural gas with sulfur content of no more than 1 grain per 100 standard cubic feet (scf) |

Source: Chin et al. 2001

**Table 6. BACT guidelines for gas turbines and internal combustion engines**

| Subcategory | VOC | $NO_X$ | $SO_X$ | CO | $PM_{10}$ | Inorganic ($NH_3$) |
|---|---|---|---|---|---|---|
| NG GT < 3 MWe | | | | | | |
| ppm@15% $O_2$ | | 9 | -- | 10 | -- | 9 |
| lb/MMBtu | 0.0026 | 0.0332 | 0.0008 | 0.0224 | 0.0066 | 0.012 |
| lb/MWh | 0.0358 | 0.4638 | 0.0112 | 0.3137 | 0.0923189 | 0.170 |
| NG GT ≥ 3 MWe and < 50 MWe | | | | | | |
| ppm@15% $O_2$ | 2 | 3.6 | -- | 10 | -- | 5 |
| lb/MMBtu | 0.0026 | 0.0133 | 0.0008 | 0.0224 | 0.0066 | 0.007 |
| lb/MWh | 0.0243 | 0.1257 | 0.0076 | 0.2126 | 0.0626 | 0.064 |
| SCAQMD Non-Emergency NG ICE, <2064 bhp* | | | | | | |
| ppm@15% $O_2$ | 32.42 | 11.28 | -- | 74.18 | -- | -- |
| lb/MMBtu | 0.0415 | 0.0415 | 0.0008 | 0.1663 | 0.0066 | -- |
| grams/bhp-hr | 0.15 | 0.15 | 0.003 | 0.600 | 0.024 | -- |
| lb/MWh | 0.4431 | 0.4431 | 0.0085 | 1.7723 | 0.0704 | -- |
| SJVAPCD Non-Emergency NG ICE, >50 hp | | | | | | |
| ppm@15% $O_2$ | 25 | 9 | -- | 56 | -- | -- |
| lb/MMBtu | 0.0415 | 0.0415 | 0.0008 | 0.1663 | 0.0066 | -- |
| grams/bhp-hr | 0.15 | 0.15 | 0.003 | 0.600 | 0.020 | -- |
| lb/MWh | 0.5 | 0.5 | 0.0085 | 1.9 | 0.06 | -- |

Notes: NG GT: natural-gas gas turbine; MWe: megawatts electrical; ppm: parts per million; bhp: brake horsepower; $NH_3$ = ammonia
Sources: SCAQMD 2000, SJVAPCD 2002a
*BACT guidelines for ICE in the SoCAB do not include SCAQMD amendments to Rule 1110.2, established in 2008.

**Table 7. Emission limits for DG technologies based on the 2007 ARB standards assuming emission credits for a heat rate recovery as presented in Table 4, calculated assuming 50% of CHP utilization and 60% heat recovery**

| Type | Size[a] | Electric Efficiency | Emissions (lb/MWh) | | | | |
|---|---|---|---|---|---|---|---|
| | | | $NO_X$ | CO | $SO_X$ | VOC | $PM_{10}$ |
| Low-Temperature Fuel Cell | 1 | 0.36 | 0.099 | 0.141 | 0.011 | 0.028 | 0.088 |
| | 2 | 0.38 | 0.099 | 0.141 | 0.011 | 0.028 | 0.088 |
| | 3 | | | | | | |
| | 4 | | | | | | |
| | 5 | | | | | | |
| | 6 | | | | | | |
| High-Temperature Fuel Cell | 1 | 0.49 | 0.086 | 0.123 | 0.007 | 0.025 | 0.058 |
| | 2 | 0.49 | 0.086 | 0.123 | 0.007 | 0.025 | 0.058 |
| | 3 | 0.49 | 0.086 | 0.123 | 0.007 | 0.025 | 0.058 |
| | 4 | 0.52 | 0.086 | 0.123 | 0.007 | 0.025 | 0.058 |
| | 5 | 0.52 | 0.086 | 0.123 | 0.007 | 0.025 | 0.058 |
| | 6 | 0.52 | 0.086 | 0.123 | 0.007 | 0.025 | 0.058 |
| Micro-turbine Generators | 1 | 0.34 | 0.109 | 0.155 | 0.014 | 0.031 | 0.116 |
| | 2 | 0.39 | 0.106 | 0.151 | 0.013 | 0.030 | 0.108 |
| | 3 | 0.40 | 0.103 | 0.147 | 0.012 | 0.029 | 0.099 |
| | 4 | | | | | | |
| | 5 | | | | | | |
| | 6 | | | | | | |
| Reciprocating Engines | 1 | 0.34 | 0.104 | 0.148 | 0.012 | 0.030 | 0.103 |
| | 2 | 0.35 | 0.104 | 0.148 | 0.012 | 0.030 | 0.103 |
| | 3 | 0.42 | 0.095 | 0.136 | 0.010 | 0.027 | 0.080 |
| | 4 | 0.42 | 0.093 | 0.133 | 0.009 | 0.027 | 0.074 |
| | 5 | 0.45 | 0.091 | 0.130 | 0.008 | 0.026 | 0.069 |
| | 6 | | | | | | |
| Gas Turbines | 1 | | | | | | |
| | 2 | | | | | | |
| | 3 | 0.27 | 0.123 | 0.176 | 0.020 | 0.035 | 0.165 |
| | 4 | 0.35 | 0.113 | 0.161 | 0.016 | 0.032 | 0.130 |
| | 5 | 0.37 | 0.104 | 0.148 | 0.012 | 0.030 | 0.103 |
| | 6 | 0.40 | 0.095 | 0.135 | 0.009 | 0.027 | 0.078 |

[a] Size: (1) < 50 kW, (2) 50–250kW, (3) 250–1000 kW, (4) 1–5 MW, (5) 5–20 MW, (6) 20–50 MW

**Table 8. 2010 Accelerated Deployment Technical specifications of gas turbines considered in the scenario development (without CHP)**

| Characterization | GT | GT w/DLN | GT w/DLN | GT w/SCR | GT w/SCR |
|---|---|---|---|---|---|
| **Capacity, MW** | 1 | 3 | 10 | 25 | 40 |
| **Installed Costs, $/kW** | 1,400 | 1,100 | 900 | 725 | 675 |
| **Heat Rate, Btu/kWh** | 14,200 | 12,200 | 10,500 | 9,000 | 8,750 |
| **Electric Efficiency, %** | 24.0% | 28.0% | 32.5% | 37.9% | 39.0% |
| **O&M Costs, $/kWh** | 0.009 | 0.005 | 0.005 | 0.0045 | 0.004 |
| **$NO_X$ Emissions, lb/MWh** | 0.07 | 0.04 | 0.036 | 0.02 | 0.02 |
| **CO Emissions, lb/MWh** | 0.59 | 0.51 | 0.45 | 0.05 | 0.04 |
| **VOC Emissions, lb/MWh** | 0.023 | 0.023 | 0.02 | 0.01 | 0.01 |
| **$PM_{10}$ Emissions, lb/MWh** | 0.29 | 0.20 | 0.18 | 0.15 | 0.15 |
| **$SO_2$ Emissions, lb/MWh** | 0.0083 | 0.0069 | 0.0062 | 0.0053 | 0.0051 |
| **AT Cost, $/kW** | 200 | 150 | 110 | 75 | 70 |

Notes: DLN: Dry Low $NO_X$; SCR: Selective Catalytic Reduction; AT: After-treatment

Source: EPRI 2007

**Table 9. 2010 Accelerated Deployment Technical specifications of reciprocating engines considered in the scenario development (without CHP)**

| Characterization | RB w/TWC | EGR w/TWC | EGR w/TWC | LB w/SCR | LB w/SCR |
|---|---|---|---|---|---|
| **Capacity, kW** | 100 | 300 | 1000 | 3000 | 5000 |
| **Installed Costs, $/kW** | 1,250 | 1,200 | 980 | 900 | 875 |
| **Heat Rate, Btu/kWh** | 10,500 | 9,750 | 8,860 | 8,425 | 8,025 |
| **Electric Efficiency, %** | 32.5% | 35.0% | 38.5% | 40.5% | 42.5% |
| **O&M Costs, $/kWh** | 0.012 | 0.0125 | 0.01 | 0.008 | 0.008 |
| **$NO_X$ Emissions, lb/MWh (w/ AT)** | 0.15 | 0.04 | 0.04 | 0.124 | 0.124 |
| **CO Emissions w/AT, lb/MWh** | 0.20 | 0.17 | 0.17 | 0.31 | 0.31 |
| **VOC Emissions w/AT, lb/MWh** | 0.05 | 0.03 | 0.03 | 0.05 | 0.05 |
| **$PM_{10}$ Emissions, lb/MWh** | 0.11 | 0.01 | 0.01 | 0.01 | 0.01 |
| **$SO_2$ Emissions, lb/MWh** | 0.0062 | 0.0057 | 0.0052 | 0.0050 | 0.0047 |
| **AT Cost, $/kW** | N/A | 45 | 40 | 120 | 110 |

Notes: RB: Rich Burn; EGR: Exhaust Gas Recirculation; TWC: Three-Way Catalyst; LB: Lean Burn; SCR: Selective Catalytic Reduction; AT: After-treatment

Source: EPRI 2007

**Table 10. 2010 Accelerated Deployment Technical specifications of fuel cells considered in the scenario development (without CHP)**

| Characterization | PEMFC | SOFC | MCFC |
|---|---|---|---|
| **Capacity, kW** | 150 | 250 | 2000 |
| **Installed Costs, $/kW** | 2,700 | 2,500 | 2,200 |
| **Heat Rate, Btu/kWh** | 9,480 | 7,125 | 7,110 |
| **Electric Efficiency, %** | 36.0% | 47.9% | 48.0% |
| **O&M Costs, $/kWh** | 0.015 | 0.017 | 0.018 |
| **$NO_X$ Emissions, lb/MWh (no AT)** | 0.07 | 0.05 | 0.05 |
| **CO Emissions, lb/MWh** | 0.07 | 0.04 | 0.03 |
| **VOC Emissions, lb/MWh** | 0.01 | 0.01 | 0.01 |
| **$PM_{10}$ Emissions, lb/MWh** | 0.001 | 0.001 | 0.001 |
| **SO2 Emissions, lb/MWh** | 0.0056 | 0.0042 | 0.0042 |

Notes: PEMFC: Polymer Electrolyte Membrane Fuel Cell; SOFC: Solid Oxide Fuel Cell; MCFC: Molten Carbonate Fuel Cell
Source: EPRI 2007

**Table 11. 2010 Accelerated Deployment Technical specifications of micro-turbine generators considered in the scenario development (without CHP)**

| Characterization | Small MTG | Medium MTG | Large MTG |
|---|---|---|---|
| **Capacity, kW** | 70–100 | 250 | 500 |
| **Installed Costs, $/kW** | 1,400 | 1,300 | 1,100 |
| **Heat Rate, Btu/kWh** | 11,375 | 10,825 | 10,250 |
| **Electric Efficiency, %** | 30.0% | 31.5% | 33.3% |
| **O&M Costs, $/kWh** | 0.015 | 0.014 | 0.014 |
| **$NO_X$ Emissions, lb/MWh (no AT)** | 0.13 | 0.13 | 0.11 |
| **CO Emissions, lb/MWh** | 0.20 | 0.24 | 0.24 |
| **VOC Emissions, lb/MWh** | 0.023 | 0.023 | 0.023 |
| **$PM_{10}$ Emissions, lb/MWh** | 0.19 | 0.16 | 0.0060 |
| **$SO_2$ Emissions, lb/MWh** | 0.0067 | 0.0064 | 0.0055 |
| **AT Cost, $/kW** | N/A | 90 | 90 |

Source: EPRI 2007

The present study takes into consideration the strong commitment by SCAQMD and SJVAPCD to require all DG units to comply with 2007 ARB emissions standards. Although this requirement is not yet in place, this study assumes that by 2023 all DG units will meet the 2007 ARB emissions standards. Hence, emission factors assumed for all technologies and sizes in the realistic scenarios do not exceed the values presented in Table 5. However, some spanning scenarios consider the possibility that DG units under control of the SCAQMD and SJVAPCD could be permitted to operate under BACT standards. These scenarios help assess the sensitivity of air quality impacts of DG to changes in air emission standards.

The emissions factors presented in Table 5 indicate that the DG technologies that can be deployed in California have relatively low criteria pollutant emissions rates (i.e., they are clean DG technologies). In the preceding report (Samuelsen et al. 2005), air quality impacts of DG scenarios that considered low DG penetration by the year 2010 were typically small. Higher DG penetration in 2023 and 2030 lead to higher emissions from DG. In addition, baseline emissions in the SoCAB and the SJVAB are expected to decline in future years. As a result, the contribution of DG to the total emissions by 2023 and 2030 is more significant than the estimated for 2010.

Even though the realistic DG scenarios typically contain low DG penetration and result in small contributions to the total emissions, the air quality impacts of these DG emissions are still important. First, many locations in the SoCAB and the SJVAB are "on the edge" between compliance and non-compliance. Even a small change in ozone concentrations in those locations could keep the basin from achieving attainment. Furthermore, due to the interaction between transport and atmospheric chemistry, the relationship between emissions and air quality impacts is highly non-linear. Therefore, even small changes in emissions fields lead to measurable air quality impacts.

### 2.1.4. Spatial Distribution of DG in the SoCAB and in the SJV

It is important to capture the spatial distribution of emissions in an air basin in order to accurately determine species concentrations that contribute to air quality. The location of the emissions, together with meteorology, mass transport, photochemical reaction times, and the mixture of chemical compounds (both gases and aerosols), all contribute to the eventual air quality prediction (i.e., ozone, $NO_X$, $PM_{10}$ concentrations). In the preceding study (Samuelsen et al. 2005), reasonable estimates of DG power in 2010 were developed based strictly upon demographic and economic parameters that can be correlated to power (e.g., population data, land-use data). At the level of DG penetration assumed in the preceding study, differences in air quality impacts resulting from different spatial distribution of DG were small. In addition, land-use distribution of DG was considered as the most likely spatial distribution to occur. Furthermore, there are no demographic data available for the years of study. Therefore, the present study assumes land-use distribution as baseline for the implementation of DG. Extraction of land-use data requires the use of Geographical Information System (GIS) data. The process to obtain specific land-use data for the SoCAB and the SJV is explained in Section 2.2.

### 2.1.5. DG Duty Cycle

The DG duty cycle parameter accounts for the temporal variation of DG power production that leads to the overall capacity factor (number of hours operating/total hours) for each of the individual DG devices. The actual duty cycle for an individual DG unit depends upon maintenance schedules, economics, power demand, and many other factors. For a specific scenario some DG technologies (e.g., high-temperature fuel cells) will likely operate as baseloaded devices–that is, they will operate essentially continuously. This is due to both economic factors (high efficiency and high capital cost portend continuous operation for reasonable payback) and operational factors (high-temperature operation leads to long start-up and high thermal stresses associated with transients). On the other hand, many other DG types

are expected to operate primarily during peak hours. The combined DG duty cycle of all DG units operating in each cell results in a different set of pollutant emissions for each hour of the simulation. The air quality model can assess the air quality impacts of this duty cycle. This model is capable of accepting DG emissions profiles that vary on an hourly basis.

### 2.1.6. Emissions Displaced

Many of the DG technologies that are being and will be adopted in California will be used in combined heating cooling and power (CHP) applications because the higher overall energy efficiency of CHP improves the economics of certain DG projects. Waste heat produced during electricity generation can be captured by a heat recovery system that provides useful heat to meet facility thermal loads, which can significantly decrease operating costs. As a result, DG/CHP can replace the heat produced by burning fuel in a boiler, leading to a reduction (displacement) of boiler-associated emissions in the basin. For retrofit DG/CHP applications, old, more-polluting boilers are likely to be displaced; whereas for new applications displacement of emissions from new equipment (i.e., more efficient and lower polluting boilers) should be considered. For this study, only heat recovery for heating (no cooling) has been considered for CHP applications.

Emissions can also be displaced by application of DG to waste gases from solid landfills, oil fields, or biomass gas emissions (e.g., dairy farm gaseous emissions). In these cases the DG application displaces either direct hydrocarbon emissions or flared gas emissions, depending on the current status of the waste gas emission. According to Allison and Lents (2002), all DG units in this type of application reduce ozone-related emissions compared to a central station combined cycle power plant. However, that article assumed same emissions for natural gas-fueled DG and for biogas-fueled DG, and air quality benefits of those applications are overstated. Nevertheless, due to encouragement from the SCAQMD most landfills in the SoCAB have already implemented DG (Lenssen 2001) to substitute for flares and produce on-site power and heat. Similarly, the SJV has potential for biomass power from dairy operations. Therefore, this study includes a few scenarios for the SJV that account for emissions displacement due to power generation from this type of biomass. Other DG applications in which emissions could be displaced include the replacing of old central power plants. All of the above potential displacements of emissions are taken into account in the development of realistic DG scenarios.

#### CHP Emissions Displacement

To assess the displaced boiler emissions and net DG emissions for each of the discretized model cells in scenarios in which CHP emissions displacement is considered, the following procedure is applied:

1. Estimate a reasonable share of DG implemented in a given region that is installed with waste heat recovery equipment (e.g., $f_{CHP}$ = 60% was suggested in the stakeholder workshop).
2. Assume an average heat recovery utilization factor or heat recovery capacity factor, which includes the lost waste heat due to supply and demand mismatch (e.g., $f_{HR}$ = 50% was suggested in the stakeholder workshop).

3. Evaluate the total amount of thermal heat recovered in each hour, $Q_{HR}$, taking into account the electric energy produced by the DGs, $Q_{elec}$, the electrical and total efficiencies of each fuel-driven DG technology, $\eta_{elec,i}$ and $\eta_{total,i}$, respectively, and the particular mix of DG, $f_{DG,i}$, which can vary hour by hour due to possible differences in duty cycle for each technology.

$$Q_{HR} = Q_{elec} \sum_{i}^{n} \left( f_{DG_i} \frac{\left(\eta_{total_i} - \eta_{elec_i}\right)}{\eta_{elec_i}} \right) \cdot f_{CHP} \cdot f_{HR} \quad (1)$$

4. Evaluate the total amount of offset fuel that would otherwise be burnt in the boilers to produce the same quantity of thermal energy delivered by the DG/CHP units. Consider boilers efficiency (e.g., $ef_{boiler}$ = 0.9).

$$Q_{fuel} = \frac{Q_{HR}}{ef_{boiler}} \quad (2)$$

5. Use emissions factors for boilers ($em_{boiler}$) and calculate the avoided emissions in each cell. As an example, the expression for offset boiler CO emissions ($M_{CO,off}$) is presented below:

$$M_{CO,off} = Q_{fuel}\, em_{boiler,CO} \quad (3)$$

6. Determine the net flux of emissions for each pollutant in a cell due to DG, subtracting the displaced boiler emissions from the total DG emissions contribution. In the case of CO, the net DG emissions can be written as follows:

$$M_{CO,net} = M_{CO,DG} - M_{CO,off} \quad (4)$$

Emissions Factors for Boilers

Avoidable air emissions from old and new boilers are presented in Table 12. These values are the most up-to-date values for emission factors for boilers. The present study uses the emission factors that correspond to new boilers. However, the present study focuses in the year 2023 and beyond, a timeframe in which emissions from boilers could experience a significant decrease. Consequently, these emission factors represent an upper bound for emissions displacement due to distributed generation. In addition, SCAQMD is considering amendments to the rules 1146 and 1146.1 to reduce boiler $NO_X$ emissions from 0.036 lb/MMBtu to 0.011–0.006 lb/MMBtu, which would reduce the potential displacement of boiler emissions due to CHP by more than half. A spanning scenario is included to analyze the sensitivity of air quality impacts to changes in CHP utilization.

**Table 12. Typical boiler air emissions for new boilers and the proposed amendments to the rules 1146 and 1146.1 by the South Coast Air Quality Management District**

| | CO lb/MMBtu | VOC lb/MMBtu | $NO_X$ lb/MMBtu | $SO_X$ lb/MMBtu | $PM_{2.5}$ lb/MMBtu | $CO_2$ lb/MMBtu |
|---|---|---|---|---|---|---|
| New | $2.35 \cdot 10^{-2}$ | $5.39 \cdot 10^{-3}$ | $1.5 \cdot 10^{-2}$ | $5.90 \cdot 10^{-4}$ | $7.45 \cdot 10^{-3}$ | 118 |
| Amendment | $2.35 \cdot 10^{-2}$ | $5.39 \cdot 10^{-3}$ | $1.1\text{-}0.6 \cdot 10^{-2}$ | $5.90 \cdot 10^{-4}$ | $7.45 \cdot 10^{-3}$ | 118 |

Source: Ianucci et al. 2000; Kay 2003

Analysis of Maximum Potential Emissions Displacement for Each DG Technology

This section assesses the reduction in emissions for four representative DG technologies in the case when the heat recovery unit is running continuously, 24 hours a day and is fully utilized. This case represents the maximum theoretical emissions displacement, when both the share of CHP and the heat recovery capacity factor are equal to 100%. Therefore, this exercise gives an upper bound of emissions offsets that DG implementation scenarios would be able to provide if all DG installations included CHP. Table 13 shows CO, VOC, $NO_X$, and $CO_2$ emissions reductions when CHP is applied to four DG types (fuel cells, natural gas ICE, MTG, and gas turbine). All technologies are assumed to comply with the 2007 ARB standards, and CHP emission credits provided by the 2007 ARB standards are accounted for. However, technologies that emit below the standards without any CHP credits, such as fuel cells, will not need to receive any credits, and hence, their emissions with and without CHP are considered the same. Also, if a certain technology exceeds the standards but does not require the full emission credits, emissions for this technology will be assumed to take only partial credit. Hence, the expression to calculate DG emissions with CHP credits ($M_{X,DG}$) is as follows:

$$M_{X,DG} = \min\left\{em_{X,DG}, \left(1 + HR_{DG}\right) \cdot Std_X\right\} \quad (5)$$

where $em_{X,DG}$ is the emission factor of pollutant $X$ for a particular DG technology, $HR_{DG}$ is the excess heat recovery by that DG technology and $Std_{X,DG}$ is the emissions standard of pollutant $X$. This calculation is not applicable to $CO_2$ emissions, as efficiency of the DG unit alone is not affected by the addition of CHP capabilities.

Note that the more efficient the DG technology is, the lesser excess heat can be recuperated from it. Thus, fuel cells have the lowest potential for CHP, whereas MTG has the greatest. Emissions from boilers correspond to new boilers, as presented in Table 12. Additional calculations using the reduced $NO_X$ levels proposed in the amendments of rules 1146 and 1146.1—0.006 lb/MMBtu—are also presented in Table 13 for comparison.

**Table 13. Maximum emission displacements for four types of DG-CHP units**

| | High-Temperature Fuel Cell | Natural Gas ICE (with EGR and TWC) | Micro-turbine Generators | Gas Turbine |
|---|---|---|---|---|
| Size | 2000 | 1000 | 50 | 25000 |
| Electrical Efficiency | 0.48 | 0.41 | 0.30 | 0.39 |
| Heat recovery (kWhHR/kWhe) | 0.77 | 1.10 | 1.83 | 1.18 |
| CO | | | | |
| DG + CHP credits (lb/MWh)[a] | 0.030 | 0.210 | 0.283 | 0.180 |
| Boiler (lb/MWh) | 0.069 | 0.098 | 0.163 | 0.105 |
| Net Emissions (lb/MWh) | -0.039 | 0.112 | 0.120 | 0.075 |
| DG only (lb/MWh)[b] | 0.030 | 0.100 | 0.100 | 0.100 |
| Avoided emissions (lb/MWh) | 0.069 | -0.012 | -0.020 | 0.025 |
| Avoided emissions (%)[c] | 228.9 | -12.0 | -20.0 | 25.1 |
| VOC | | | | |
| DG + CHP credits (lb/MWh) | 0.009 | 0.042 | 0.010 | 0.028 |
| Boiler (lb/MWh) | 0.016 | 0.022 | 0.037 | 0.024 |
| Net Emissions (lb/MWh) | -0.007 | 0.020 | -0.027 | 0.004 |
| DG only (lb/MWh) | 0.009 | 0.020 | 0.010 | 0.020 |
| Avoided emissions (lb/MWh) | 0.016 | 0.000 | 0.037 | 0.016 |
| Avoided emissions (%) | 175.0 | 2.4 | 374.6 | 80.5 |
| $NO_X$ current boilers | | | | |
| DG + CHP credits (lb/MWh) | 0.040 | 0.147 | 0.100 | 0.090 |
| Boiler (lb/MWh) | 0.044 | 0.062 | 0.104 | 0.067 |
| Net Emissions (lb/MWh) | -0.004 | 0.084 | -0.004 | 0.023 |
| DG only (lb/MWh) | 0.040 | 0.070 | 0.070 | 0.070 |
| Avoided emissions (lb/MWh) | 0.044 | -0.014 | 0.074 | 0.047 |
| Avoided emissions (%) | 109.6 | -20.6 | 106.1 | 67.2 |
| $NO_X$ proposed future boilers | | | | |
| DG + CHP credits (lb/MWh) | 0.040 | 0.147 | 0.100 | 0.090 |
| Boiler (lb/MWh) | 0.016 | 0.022 | 0.038 | 0.024 |
| Net Emissions (lb/MWh) | 0.024 | 0.124 | 0.062 | 0.066 |
| DG only (lb/MWh) | 0.040 | 0.070 | 0.070 | 0.070 |
| Avoided emissions (lb/MWh) | 0.016 | -0.054 | 0.008 | 0.004 |
| Avoided emissions (%) | 39.5 | -77.7 | 10.8 | 5.9 |
| $CO_2$ | | | | |
| DG + CHP credits (lb/MWh) | 844 | 1000 | 1350 | 1038 |
| Boiler (lb/MWh) | 345 | 492 | 820 | 528 |
| Net Emissions (lb/MWh) | 499 | 508 | 530 | 511 |
| DG only (lb/MWh) | 844 | 1000 | 1350 | 1038 |
| Avoided emissions (lb/MWh) | 345 | 492 | 820 | 528 |
| Avoided emissions (%) | 40.9 | 49.2 | 60.8 | 50.8 |

[a] Calculated using Equation 5: the lowest value between the 2007 ARB limits and technology emission factors
[b] The lowest value between the 2007 ARB limits and technology emission factors, with no CHP
[c] Avoided emissions (%) are calculated as avoided emissions in % with respect to added emissions from DG only
Note: KWhHR = kilowatt-hour heat recovery; KWhe = kilowatt-hour electric

Total avoided emissions are calculated as the emissions from boilers removed minus the emission credits for a particular CHP unit. Percentagewise, avoided emissions are divided by the emissions from DG without any CHP credits. Amongst technologies, fuel cells provide the highest avoided emissions of CO and $NO_X$. Micro-turbine generators have the highest potential

to displace VOC emissions, because of their low VOC emissions and their low efficiency that provides high excess heat. Large gas turbines also achieve positive reductions in emissions due to the use of CHP. On the other end, reciprocating engines cannot meet the 2007 ARB emissions standards, and benefit in full extent to the additional emissions allowed by CHP credits.

The result is that reciprocating engines with CHP could emit 12% more CO and 20.6% more $NO_X$ than without CHP if the full emission credits are used. Combined heating and power with ICE is even more unfavorable if the newly proposed $NO_X$ emission levels for boilers are assumed, which would cause CHP to increase emissions by 77.7%. Consequently, based on criteria pollutant emissions only, although ICE is the most prevalent technology currently, it would be the least preferable technology to use in CHP applications.

Finally, all natural gas-driven CHP technologies yield to significant displacement (40.9%–60.8% reduction) of global warming $CO_2$ emissions. Even though fuel cells have the lowest potential for excess heat use, their high efficiency leads them to have the lowest $CO_2$ emissions among technologies even if CHP is used. In realistic DG scenarios, where all the above DG-CHP technologies are included in different shares and heat recovery capacity factors will be significantly less than 100%, smaller reductions in air pollutant and $CO_2$ emissions are expected.

One key component of assessing the emissions benefits of CHP is the emission levels assumed for boilers. As Table 13 shows, using the future $NO_X$ emissions proposed by SCAQMD for boilers, the potential for emission displacement by CHP diminishes substantially.

#### *Scenarios That Include Emissions Displacement From Retired In-Basin Power Plants*

If all fossil-based power plants are retired after 50 years of operation and the state's three nuclear plants (San Onofre, Diablo Canyon, and Palo Verde) are retired after first relicensing and will not be operating by 2030, then only 32.1 GW of the power plants of the total 60.6 GW in operation in 2003 will remain operational in 2030 (CERTS 2003). This implies that an additional capacity of 28.5 GW has to be installed in California besides to meet the expected growth in power demand during the period 2003–2030. This additional power could be generated in part by DG. However, substitution of conventional power plants by DG could lead to instability in the electricity system, and such a scenario is merely speculative. Consequently, this case has been included as a spanning scenario.

The approach used to develop DG emissions inventories for scenarios that include emissions displacement from in-basin power plants is as follows:

1. Locate power plants that could potentially be retired by the year of study. The database consulted is the one available in the website of the California Energy Commission for power plants in California (Energy Commission 2005b). For example, Table 14 shows the characteristics of a power plant in El Segundo, which will be older than 50 years by 2020.

**Table 14. Main characteristics of a selected power plant in the SoCAB**

| Name | Primary fuel | Technology | Online capacity (MW) | Date Online | Type |
|---|---|---|---|---|---|
| El Segundo | Natural Gas | Steam Turbine | 708 | 1964 | Baseloaded |

Source: EPRI 2007

2. Locate power plant in the emissions inventory provided by the ARB and remove emissions from inventory. Continuing with the same example, the values for criteria pollutant emissions from the power plant from El Segundo included in the inventory are shown below in Table 15.

**Table 15. Emissions from a selected power plant in the SoCAB (in tons/year)**

| Name | TOG | VOC | CO | $NO_X$ | $SO_X$ | $PM_{10}$ |
|---|---|---|---|---|---|---|
| El Segundo | 25.2 | 10.7 | 162.1 | 15.2 | 1.2 | 14.7 |

Source: ARB 2006a

3. Introduce DG emissions that correspond to total electrical power generation from DG that equals the total power removed from the central power plant. Distribution of DG follows the methodology explained in Section 2.2.3.

### *2.1.7. Other Estimates*

As some of the DG technologies are just emerging in the marketplace, certain features of these technologies, including accurate pollutant emissions rates and emissions speciation, are not readily available. In addition, understanding of features such as continuous versus peak power applicability, size of equipment, availability of fuel, and emissions stack height may need to be estimated for the current study. When data are still not available, however, reasonable estimates or assumptions are applied only as they are required for compatibility with the simulation software.

One significant factor that must be estimated for the current study is the degradation rate for technologies installed in the earlier years between now and the study year of interest. All DG technologies experience some degradation in efficiency performance and many may also degrade in the pollutant emissions performance. Scarce data is available for accurate accounting of DG vintage as it pertains to degradation in performance—so that degradation must be estimated. The adoption cumulative curve of DG power in the following year is also uncertain, and various curves (e.g., exponential, linear) are considered. Finally, some technologies are expected to substantially improve their emissions and efficiency performance over the next several years. This improvement in performance must also be estimated for accurate development of a DG scenario.

### *Speciation of Criteria Pollutants*

To make the emissions fluxes from any DG scenario compatible with the input required by the air quality model, one must provide emissions fluxes for all species that the model currently considers in its detailed chemical mechanism. As a result, the total DG emissions of some criteria pollutants ($NO_X$, $SO_X$, VOC, and PM) must be split into a representative distribution of their constituent species. Table 16 shows the speciation and weighting factors used for each of the species for which this procedure was required. The codes presented in Table 16 for the species in VOC and PM are the same as those used in the Caltech Atmospheric Chemistry Mechanism (CACM). The chemical name associated with each code is listed in Table 17.

**Table 16. Speciation used for criteria pollutants from DG scenarios**

| Criteria Pollutant | Species | | | | | | | Comments |
|---|---|---|---|---|---|---|---|---|
| **$NO_X$** | **NO** | | | **$NO_2$** | | | | APEP estimates |
| % Weight | 95 | | | 5 | | | | |
| **$SO_X$** | **$SO_2$** | | | **$SO_3$** | | | | APEP estimates |
| % Weight | 95 | | | 5 | | | | |
| **VOC** | **$CH_4$** | **HCHO** | **ALKL** | **AROH** | | **AROL** | | VOC Speciation from ARB data for gas external combustion boiler profile (www.arb.ca.gov/emisinv/speciate/speciate.htm ) |
| % Weight | 58 | 8 | 29 | 4 | | 2 | | |
| **PM** | **EC** | **OC** | **Cl**** | **Sf** | **Nt** | **K**** | **Ca**** | PM Speciation from ARB data for gas ICE profile (http://www.arb.ca.gov/emisinv/speciate/speciate.htm) |
| % Weight | 20 | 26 | 7 | 45 | 1 | 1 | 1 | |

* ALKL, AROL and AROH in the CACM mechanism are species analogous to species ALK1, ARO1 and ARO2, respectively, in the SAPRC99 mechanism.
** The Community Multi-scale Air Quality Model (CMAQ) used for the SJV simulations does not include Cl, K, and Ca.

**Table 17. Chemical names for species considered in VOC and PM CACM speciation**

| Species | Chemical Name | Criteria Pollutant |
|---|---|---|
| HCHO | Formaldehyde | VOC |
| ALKL* | C2-C6 Alkanes | VOC |
| AROL* | Low Yield Aromatics | VOC |
| AROH* | High Yield Aromatics | VOC |
| EC | Elemental Carbon | PM |
| OC | Unresolved Organic Carbon | PM |
| Cl | Chloride ion | PM |
| Sf | Sulfur (VI) | PM |
| Nt | Nitrate | PM |
| K | Potassium | PM |
| Ca | Calcium | PM |

* ALKL, AROL, and AROH in the CACM mechanism are species analogous to species. ALK1, ARO1, and ARO2, respectively, in the SAPRC99 mechanism.

#### *Performance Degradation, Operation Out of Compliance, and Geometrical Features*

The SCAQMD has detected through their inspections that a large number of permitted ICE DG units emit at emission levels out of compliance with the emission standards after some time of operation. This kind of DG performance degradation for ICE has been incorporated in two spanning scenarios for the SoCAB and the San Joaquin Valley Air Basin. These spanning scenarios include an increase in emissions to the levels reported by the SCAQMD. The remainder of the spanning scenarios assumes no degradation. Moreover, all of the scenarios included in the present study consider DG emissions to occur at ground level (i.e., no elevated emissions). A small number of DG may be installed on rooftops of tall buildings, but this factor is not included in the DG scenarios.

### *2.1.8. Approach for Estimating the Emissions Impacts of 20XX Technological Automotive Paradigm Shifts*

This section analyzes the effect that widespread use of electric vehicles could have on the electricity demand and the resulting impacts on air emissions and air quality in future years. Predicting the outcomes for such futuristic technologies is wrought with high levels of uncertainty that need to be accounted for. However, this type of scenarios sets bounds to emissions reductions from automobile sources, and is a basis for sensitivity analyses of emissions to determine air quality impacts projections in the future. The following subsections analyze a series of scenarios that consider various strategies for generating electricity in the future.

#### *Baseline Emissions From Automobiles*

Currently, there are no emission estimates available beyond 2023. Only the EMission FACtors (EMFAC) model, a model used to generate on-road mobile emissions, is capable of estimating emissions for years up to 2040. The EMFAC model is developed by the ARB, and it uses information on vehicle activity from the Department of Motor Vehicles and the California Transportation Department. The total emissions from vehicles can then be calculated using emission factors derived from vehicle testing. These emission factors depend on the number of starts, the ambient conditions, and the speed of the vehicle, among other factors. Results from the EMFAC model provide emissions from vehicle operation, as well as evaporative emissions of VOC and particle emissions from braking and tire wear (ARB 2007a).

Figure 8 shows the relative change in vehicular activity, emissions from on-road mobile sources, and fuel use for the period 2010–2040. Although the number of vehicles, trips, and vehicle miles traveled are estimated to increase, emissions of criteria pollutants are expected to decrease due to reduction of vehicle tailpipe emissions. This reduction is caused by the progressive market penetration of low-emitting vehicles and the gradual retirement of higher-emitting older models.

Table 18 presents emission source apportionment for the 2023 inventory. Emissions from on-road mobile sources account for 24%, 40%, and 36% of the total VOC, CO, and $NO_X$, respectively, in the emission inventory estimated by ARB for the year 2023. Assuming that emissions from all the sources except on-road mobile sources stay constant, emissions for up to the year 2040 may be estimated by applying the emission reductions to the mobile sources, as

shown in Figure 8. As a result, baseline emissions of VOC, $NO_x$, and CO for the year 2040 decrease to 385 tons per day (tpd), 97 tpd, and 1669 tpd, respectively; whereas $PM_{2.5}$ emissions increase to 91 tpd.

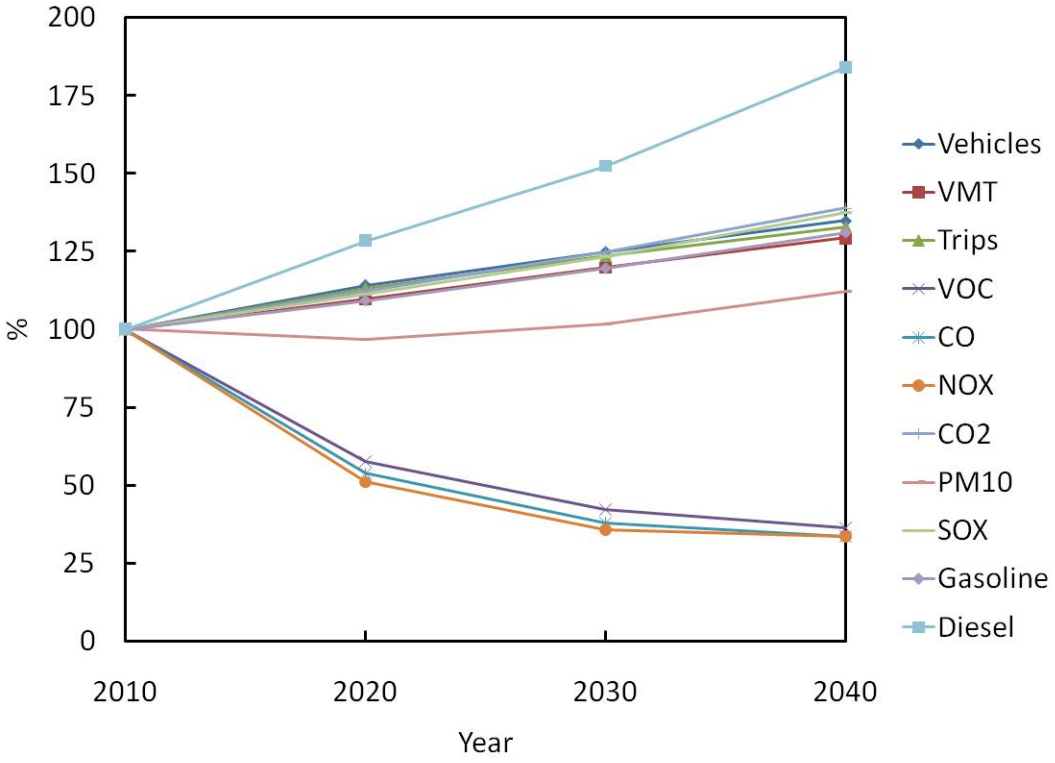


**Figure 8. Trends in on-road mobile emissions, fuel usage, and vehicular activity estimated by EMFAC Version 2.3 (November 2006) for the period 2010 to 2040 in the South Coast Air Basin of California**

**Table 18. Source apportionment of the 2023 emissions inventory and extrapolation of the total emissions for 2040 using emissions trends for on-road mobile sources projected by EMFAC for the South Coast Air Basin of California**

| | Emissions by Major Source (% with respect to total emissions in 2023) | | | | 2023 Emissions | 2040 Emissions |
|---|---|---|---|---|---|---|
| | Stationary Sources | Petroleum Production | On-Road Vehicles | Off-Road Vehicles | (tpd) | (tpd) |
| **VOC** | 44.7 | 6.5 | 23.6 | 25.2 | 420 | 385 |
| **$NO_X$** | 14.4 | 0.0 | 35.6 | 50.0 | 114 | 97 |
| **CO** | 6.1 | 0.3 | 40.4 | 53.2 | 1966 | 1669 |
| **$SO_X$** | 16.8 | 2.1 | 2.1 | 78.9 | 19 | 19 |
| **$PM_{2.5}$** | 67.6 | 1.0 | 13.7 | 17.6 | 88 | 91 |

Source: ARB 2007b (for the first four columns. Based on criteria pollutant emissions for the year 2020, www.arb.ca.gov/ei/emissiondata.htm)

### *Power Generation for Pure Electric Vehicles*

The electricity needed to power the automobile fleet is provided by DG installed in the SoCAB. Consequently, this scenario includes emissions related to production of electricity by DG inside the SoCAB, to power the electric vehicles. The amount of energy required by the fleet is calculated to be $5.37\times10^{8}$ megajoules (MJ)/day ($1.96\times10^{11}$ MJ/yr as shown in Table 19). Battery electric vehicles are three times more efficient than conventional gasoline vehicles (Idaho National Laboratory 2006), resulting in electric motor efficiency of 50%. In addition, electricity transmission losses are approximately 7% (California Energy Commission 2005a). As a result, the daily amount of electrical energy supply adds up to $1.15\times10^{9}$ MJ/day ($4.21\times10^{11}$ MJ/yr, *N* from Table 19). Electric vehicles (EV) can run up to 100 miles per full battery charge, and the average in-home recharging time is as long as 4–8 hours (www.fueleconomy.gov). High-power fast-charging stations may speed recharging times up to 2–4 hours. Although not all the vehicles will be charged at the same time, one can expect that night hours (e.g., 10 p.m.–6 a.m.) and time between morning and evening rush hours (9 a.m.–5 p.m.) would be the period of time with the highest demand for recharging power. Hence, this scenario assumes that the charging occurs evenly during eight hours at night and eight hours during the day. Based on this daily cycle, the average recharging time assumed in this scenario for the entire fleet is 16 hours/day. Considering this time span, the total capacity needed for recharge the entire fleet is 20 GW. This power is provided by a mix of DG that includes large gas turbines, fuel cells, and photovoltaic units, which are spread throughout the SoCAB following the land use distribution.

**Table 19. Estimation of the total energy required to power a vehicle fleet formed exclusively by pure electric cars**

| Equation | Parameter (Units) | 2040 |
|---|---|---|
| *A*[*] | On-road SoCAB vehicle miles traveled (mi/yr) | 1.66E+11 |
| *B*[*] | Vehicle fleet mileage (mpg) | 16.95 |
| *C=A/B* | Gallons of fuel (gas+diesel) used (gal/yr) | 9.81E+09 |
| *D*[**] | Lower heating value gasoline (MJ/kg) | 44 |
| *E*[**] | Gasoline density (kg/m$^3$) | 750 |
| *F*[**] | Gallons per cubic meter (gal/m$^3$) | 264.17 |
| *G=D*E/F* | Energy stored in gasoline (MJ/gal) | 124.92 |
| *H=C*G* | Energy to power gasoline vehicles (MJ/yr) | 1.23E+12 |
| *I*[**] | Gasoline vehicle efficiency (fraction) | 0.16 |
| *J=H*I* | Actual energy required for vehicles (MJ/yr) | 1.96E+11 |
| *K*[**] | EV efficiency (fraction) | 0.50 |
| *L=J/K* | Energy required for EV (MJ/yr) | 3.92E+11 |
| *M*[***] | Electricity transmission losses | 0.07 |
| *N=L/(1-M)* | Electricity demand for EV (MJ/yr) | 4.21E+11 |

[*] Estimates from EMFAC, Version 2.2 (2003)
[**] Values from Jacobson et al. 2005
[***] California Energy Commission 2005a

## 2.2. Extraction and Processing of GIS Land-Use Data

The use of a realistic means of defining the spatial distribution of DG is critically important to the realistic prediction of air quality impact. The sort of information required to accomplish this task is only available from special sources. These sources include the local utilities, which have spatially resolved data on electricity consumption, and local governmental agencies that have global information systems (GIS) information.

### *2.2.1. GIS Land-Use Data for the SoCAB*

Thanks to the generous donation of the organization Southern California Area Governments (SCAG), the team was provided access to GIS land-use data for the following counties: Los Angeles, Orange, San Bernardino, Riverside, Imperial, and Ventura. The latest data in this GIS data set were collected in the year 2000. Figure 9 shows how the computational domain of the air quality model for the SoCAB includes partially or wholly the counties of Orange, Los Angeles, Riverside, San Bernardino, and Ventura.

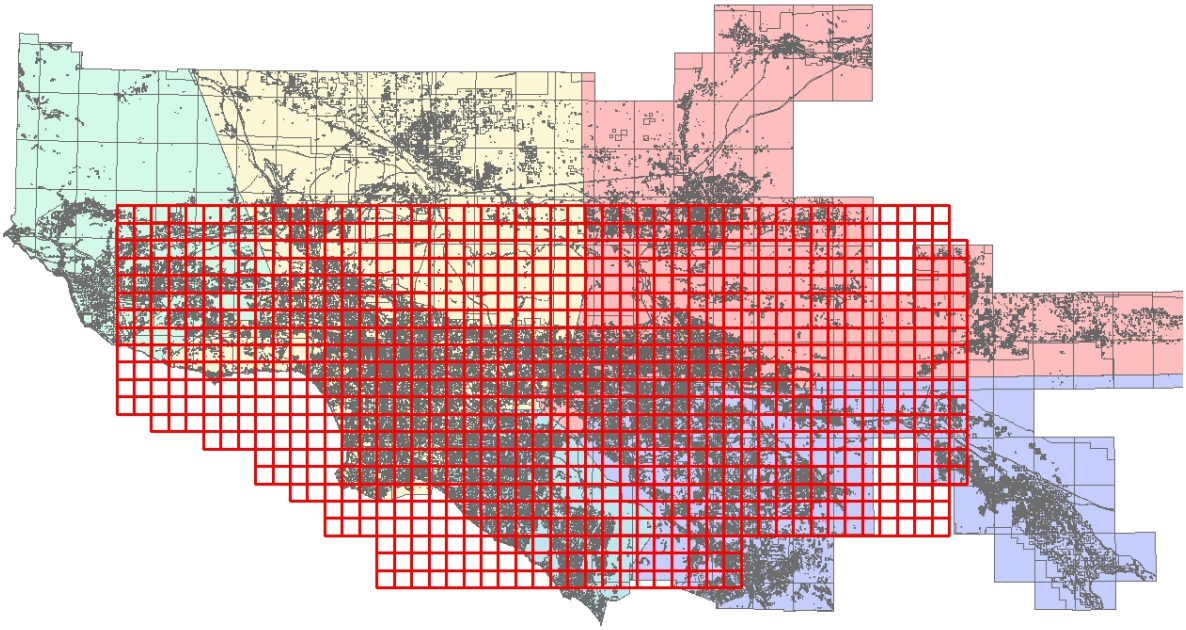

**Figure 9. Southern California Counties with land-use GIS data and the computational grid of the air quality model (in red lines)**

These data consist of each of the counties divided into land parcels (polygons) of different area and shape. The number of parcels per county is rather large. For example the total number of individual land parcels in Los Angeles County alone is more than 40,000. The land parcels have a resolution of 2 acres (0.0081 square kilometers, $km^2$). Each of the polygons has associated with it a database that contains an ID number, total area, and zone classification code. Figure 10 presents a picture of a small region near Long Beach to illustrate the typical number and resolution of the land parcel polygons. The location of the 5 km x 5 km model cells and corresponding resolution of the air quality model in this same region are represented by the red lines of Figure 10.

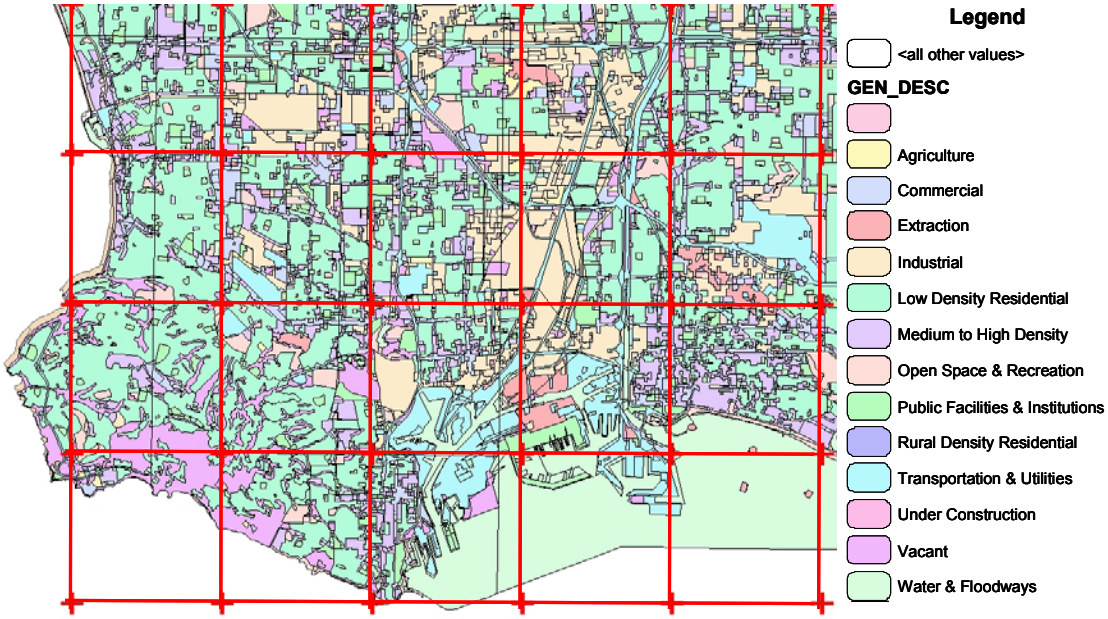


**Figure 10. Example of generic land uses in Long Beach area**

The GIS database contains 132 different specific land-use types that are aggregated into 13 generic land use types. The 13 generic land use types are the only types presented in Figure 10. Table 20, on the other hand, shows both the specific land-use types and the generic types that are contained in the GIS database.

**Table 20. Land-use codes and descriptions**

| LU CODE | LAND USE DESCRIPTION | GENERIC LAND USE TYPE |
|---|---|---|
| 1000 | Urban or Built-Up | |
| 1100 | Residential | Low Density Residential |
| 1110 | Single Family Residential | Low Density Residential |
| 1111 | High Density Single Family Residential | Low Density Residential |
| 1112 | Low Density Single Family Residential | Low Density Residential |
| 1120 | Multi-Family Residential | Medium to High Density Residential |
| 1121 | Mixed Multi-Family Residential | Medium to High Density Residential |
| 1122 | Duplexes, Triplexes & 2 or 3 Unit Condos & Townhomes | Medium to High Density Residential |
| 1123 | Low-Rise Apartments Condominiums and Townhouses | Medium to High Density Residential |
| 1124 | Medium-Rise Apartments and Condominiums | Medium to High Density Residential |
| 1125 | High-Rise Apartments and Condominiums | Medium to High Density Residential |
| 1130 | Mobile Homes and Trailer Parks | Medium to High Density Residential |
| 1131 | Trailer Parks and Mobile Home Courts High Density | Medium to High Density Residential |
| 1132 | Mobile Home Courts and Subdivisions Low Density | Medium to High Density Residential |
| 1140 | Mixed Residential | Medium to High Density Residential |
| 1150 | Rural Residential | Low Density Residential |
| 1151 | Rural Residential High Density | Low Density Residential |
| 1152 | Rural Residential Low Density | Rural Density Residential |

**Table 20. (continued)**

| | | |
|---|---|---|
| 1200 | Commercial and Services | Commercial |
| 1210 | General Office Use | Commercial |
| 1211 | Low- and Medium-Rise Major Office Use | Commercial |
| 1212 | High-Rise Major Office Use | Commercial |
| 1213 | Skyscrapers | Commercial |
| 1220 | Retail Stores and Commercial Services | Commercial |
| 1221 | Regional Shopping Mall | Commercial |
| 1222 | Retail Centers, Non-Strip Contiguous Interconnected Off-Street | Commercial |
| 1223 | Modern Strip Development | Commercial |
| 1224 | Older Strip Development | Commercial |
| 1230 | Other Commercial | Commercial |
| 1231 | Commercial Storage | Commercial |
| 1232 | Commercial Recreation | Commercial |
| 1233 | Hotels and Motels | Commercial |
| 1234 | Attended Pay Public Parking Facilities | Commercial |
| 1240 | Public Facilities | Public Facilities & Institutions |
| 1241 | Government Offices | Public Facilities & Institutions |
| 1242 | Police and Sheriff Stations | Public Facilities & Institutions |
| 1243 | Fire Stations | Public Facilities & Institutions |
| 1244 | Major Medical Health Care Facilities | Public Facilities & Institutions |
| 1245 | Religious Facilities | Public Facilities & Institutions |
| 1246 | Other Public Facilities | Public Facilities & Institutions |
| 1247 | Non-Attended Public Parking Facilities | Public Facilities & Institutions |
| 1250 | Special Use Facilities | Public Facilities & Institutions |
| 1251 | Correctional Facilities | Public Facilities & Institutions |
| 1252 | Special Care Facilities | Public Facilities & Institutions |
| 1253 | Other Special Use Facilities | Public Facilities & Institutions |
| 1260 | Educational Institutions | Public Facilities & Institutions |
| 1261 | Pre-Schools Day Care Centers | Public Facilities & Institutions |
| 1262 | Elementary Schools | Public Facilities & Institutions |
| 1263 | Junior or Intermediate High Schools | Public Facilities & Institutions |
| 1264 | Senior High Schools | Public Facilities & Institutions |
| 1265 | Colleges and Universities | Public Facilities & Institutions |
| 1266 | Trade Schools | Public Facilities & Institutions |
| 1270 | Military Installations | Public Facilities & Institutions |
| 1271 | Base Built-up Area | Public Facilities & Institutions |
| 1272 | Vacant Area | Vacant |
| 1273 | Air Field | Public Facilities & Institutions |
| 1300 | Industrial | Industrial |
| 1310 | Light Industrial | Industrial |
| 1311 | Manufacturing Assembly and Industrial Services | Industrial |
| 1312 | Motion Picture and Television Studio Lots | Industrial |
| 1313 | Packing Houses and Grain Elevators | Industrial |
| 1314 | Research and Development | Industrial |
| 1320 | Heavy Industrial | Industrial |
| 1321 | Manufacturing | Industrial |
| 1322 | Petroleum Refining and Processing | Industrial |
| 1323 | Open Storage | Industrial |
| 1324 | Major Metal Processing | Industrial |
| 1325 | Chemical Processing | Industrial |

**Table 20. (continued)**

| | | |
|---|---|---|
| 1330 | Extraction | Extraction |
| 1331 | Mineral Extraction – Other Than Oil and Gas | Extraction |
| 1332 | Mineral Extraction - Oil and Gas | Extraction |
| 1340 | Wholesaling and Warehousing | Industrial |
| 1400 | Transportation Communications and Utilities | Transportation & Utilities |
| 1410 | Transportation | Transportation & Utilities |
| 1411 | Airports | Transportation & Utilities |
| 1412 | Railroads | Transportation & Utilities |
| 1413 | Freeways and Major Roads | Transportation & Utilities |
| 1414 | Park and Ride Lots | Transportation & Utilities |
| 1415 | Bus Terminals and Yards | Transportation & Utilities |
| 1416 | Truck Terminals | Transportation & Utilities |
| 1417 | Harbor Facilities | Transportation & Utilities |
| 1418 | Navigation Aids | Transportation & Utilities |
| 1420 | Communication Facilities | Transportation & Utilities |
| 1430 | Utility Facilities | Transportation & Utilities |
| 1431 | Electrical Power Facilities | Transportation & Utilities |
| 1432 | Solid Waste Disposal Facilities | Transportation & Utilities |
| 1433 | Liquid Waste Disposal Facilities | Transportation & Utilities |
| 1434 | Water Storage Facilities | Transportation & Utilities |
| 1435 | Natural Gas and Petroleum Facilities | Transportation & Utilities |
| 1436 | Water Transfer Facilities | Transportation & Utilities |
| 1437 | Improved Flood Waterways and Structures | Transportation & Utilities |
| 1438 | Mixed Wind Energy Generation and Percolation Basin | Transportation & Utilities |
| 1440 | Maintenance Yards | Transportation & Utilities |
| 1450 | Mixed Transportation | Transportation & Utilities |
| 1460 | Mixed Transportation and Utility | Transportation & Utilities |
| 1500 | Mixed Commercial and Industrial | Industrial |
| 1600 | Mixed Urban | Industrial |
| 1700 | Under Construction | Vacant |
| 1800 | Open Space and Recreation | Open Space & Recreation |
| 1810 | Golf Courses | Open Space & Recreation |
| 1820 | Local Parks and Recreation | Open Space & Recreation |
| 1821 | Local Park Developed | Open Space & Recreation |
| 1822 | Local Park Undeveloped | Open Space & Recreation |
| 1830 | Regional Parks and Recreation | Open Space & Recreation |
| 1831 | Regional Park Developed | Open Space & Recreation |
| 1832 | Regional Park Undeveloped | Open Space & Recreation |
| 1840 | Cemeteries | Open Space & Recreation |
| 1850 | Wildlife Preserves and Sanctuaries | Open Space & Recreation |
| 1860 | Specimen Gardens and Arboreta | Open Space & Recreation |
| 1870 | Beach Parks | Open Space & Recreation |
| 1880 | Other Open Space and Recreation | Open Space & Recreation |
| 1900 | Urban Vacant | Vacant |
| 2000 | Agriculture | Agriculture |
| 2100 | Cropland and Improved Pasture Land | Agriculture |
| 2120 | Non-Irrigated Cropland and Improved Pasture Land | Agriculture |
| 2200 | Orchards and Vineyards | Agriculture |
| 2300 | Nurseries | Agriculture |
| 2400 | Dairy and Intensive Livestock | Agriculture |
| 2500 | Poultry Operations | Agriculture |
| 2600 | Other Agriculture | Agriculture |
| 2700 | Horse Ranches | Agriculture |

**Table 20. (continued)**

| | | |
|---|---|---|
| 3000 | Vacant | Vacant |
| 3100 | Vacant Undifferentiated | Vacant |
| 3200 | Abandoned Orchards and Vineyards | Vacant |
| 3300 | Vacant With Limited Improvements | Vacant |
| 3400 | Beaches (Vacant) | Open Space & Recreation |
| 4000 | Water | Water & Floodways |
| 4100 | Water | Water & Floodways |
| 4200 | Harbor Water Facilities | Water & Floodways |
| 4300 | Marina Water Facilities | Water & Floodways |
| 4400 | Water Within a Military Installation | Water & Floodways |
| 4500 | Area of Inundation (High Water) | Water & Floodways |

### *GIS Data Extraction*

The first step required to make effective use of the land-use GIS data in our DG scenarios was to correlate (i.e., scale-up) the resolution of the GIS data with the 5 km x 5 km resolution of the air quality model grid. This strategy for integrating GIS data with the AQM is described in this section of the report.

Table 21 presents a small cross-section of the model grid as a sample of the type of data that it is now available for all of the cells in the model. The *X* and *Y* coordinates of the model are presented in Table 21, followed by the square kilometers of area within each cell that correspond to Agriculture, Commercial, Extraction, Industrial, and Low Density Residential land use types.

**Table 21. Detail of some cells with GIS land-use data extracted**

| | | Agriculture | Commercial | Extraction | Industrial | Low Density Residential | ... |
|---|---|---|---|---|---|---|---|
| Ymodel | Xmodel | $A_{Agric}$ km$^2$ | $A_{Comm}$ km$^2$ | $A_{Ext}$ km$^2$ | $A_{Ind}$ km$^2$ | $A_{Lowres}$ km$^2$ | |
| 26 | 19 | 1.335 | 0.000 | 0.549 | 0.000 | 0.031 | |
| 26 | 20 | 0.012 | 0.000 | 0.503 | 0.000 | 0.000 | |
| 26 | 21 | 0.175 | 0.000 | 0.000 | 0.000 | 0.000 | |
| 26 | 22 | 5.147 | 0.000 | 0.000 | 0.000 | 0.000 | |
| 26 | 23 | 0.043 | 0.000 | 0.026 | 0.000 | 0.000 | |
| 26 | 24 | 0.040 | 0.000 | 0.137 | 0.000 | 0.000 | |
| 26 | 25 | 1.453 | 0.000 | 0.136 | 0.000 | 0.000 | |
| 26 | 26 | 0.044 | 0.000 | 1.310 | 0.000 | 0.000 | |
| 26 | 27 | 0.545 | 0.000 | 1.116 | 0.000 | 0.586 | |
| 26 | 28 | 2.896 | 0.868 | 1.498 | 1.128 | 0.685 | |
| 26 | 29 | 3.212 | 0.151 | 0.000 | 1.520 | 4.766 | |
| 26 | 30 | 0.650 | 0.125 | 0.000 | 0.120 | 5.810 | |
| 26 | 31 | 0.180 | 0.319 | 0.000 | 0.173 | 1.779 | |
| 26 | 32 | 0.123 | 0.008 | 0.932 | 0.037 | 2.120 | |
| 26 | 33 | 0.028 | 0.000 | 0.388 | 0.000 | 0.000 | |
| 26 | 34 | 0.090 | 0.000 | 0.000 | 0.018 | 0.000 | |

...

In the process of extracting the GIS data, the APEP team isolated each of the 13 generic land-use categories. These generic land use categories are listed in Table 22. Reducing the total number of land use types to the 13 generic land use types allowed reasonable identification of the spatial distribution of land use types in the SoCAB.

**Table 22. Generic land use categories**

| LAND USE CODES | GENERIC LAND USE TYPE |
|---|---|
| 1000–1112, 1150–1151 | Low Density Residential |
| 1120–1140 | Medium to High Density Residential |
| 1152 | Rural Density Residential |
| 1200–1234 | Commercial |
| 1240–1273 | Public Facilities & Institutions |
| 1300–1325, 1340, 1500, 1600 | Industrial |
| 1330–1332 | Extraction |
| 1400–1460 | Transportation & Utilities |
| 1700, 1900, 3000, 3100, 3200, 3300 | Vacant |
| 1800–1880, 3400 | Open Space & Recreation |
| 2000–2700 | Agriculture |
| 4000–4500 | Water & Floodways |

Figure 11 presents a bar chart with the total areas for the 13 generic land-use categories. Note that the "Vacant" area is by far the largest land-use category with more area (greater than 12,000 $km^2$) associated with it than any other category. The vacant area is followed by the "Low Density Residential" land use category with about 3,000 $km^2$ in the SoCAB. The third and forth land-use categories with significant area in the SoCAB are "Agriculture" and "Transportation and Utilities," respectively.

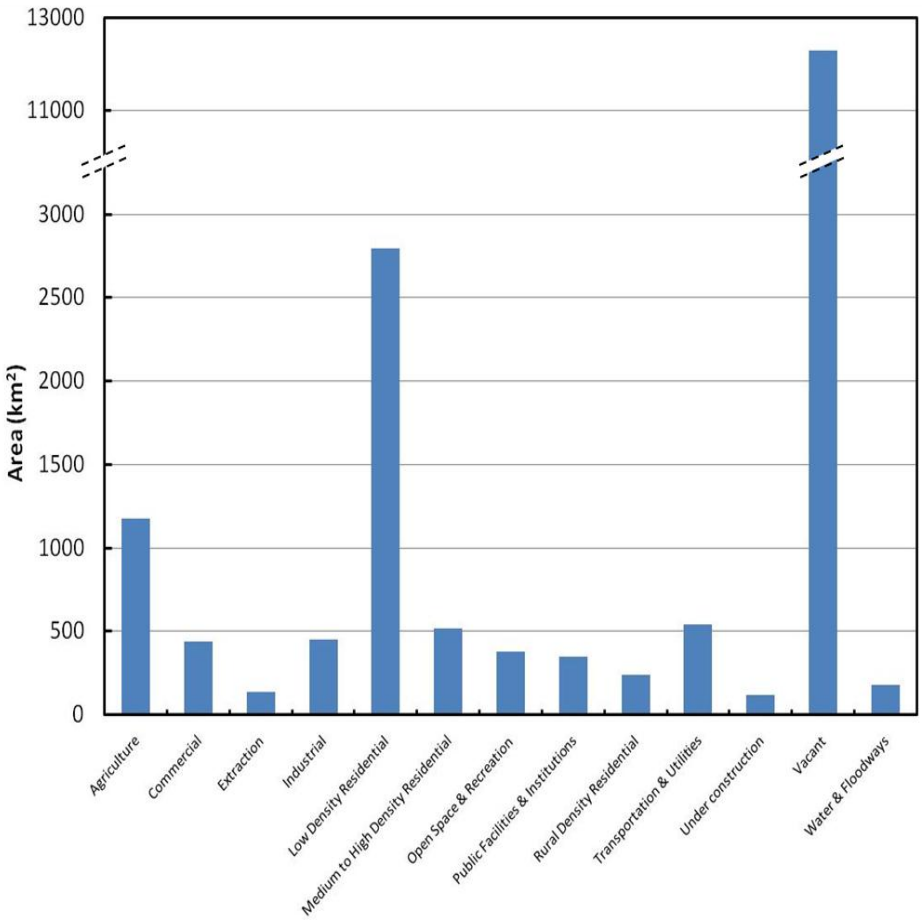


**Figure 11. Total land-use areas in the 13 generic land-use categories in the SoCAB**

### *2.2.2. GIS Land-Use Data for the SJV*

The land-use data for the SJVAB is obtained by processing GIS data acquired from the California Spatial Information Library (CaSIL). This data is available for each of the counties in California divided into land parcels (polygons) of different area and shape. Each land-parcel is associated with a particular type of land-use from 13 generic land-use categories. These data need to be processed to fit the model domain and resolution of the air quality simulation grid. This task is accomplished using advanced GIS tools and expertise available with the Network and Academic Computing Services (NACS) at the University of California, Irvine. The outcome of this task is area of each land-use type in each 4 x 4 km cell of the modeling domain. Figure 12 shows a sample of model cells near Fresno and the highest level land-use data corresponding to those cells. The overall distribution of land-use in the SJV can be placed into 13 generic categories, as shown in Figure 13. As expected, agriculture and open space dominate the land-use distribution followed by low density residential land-use.

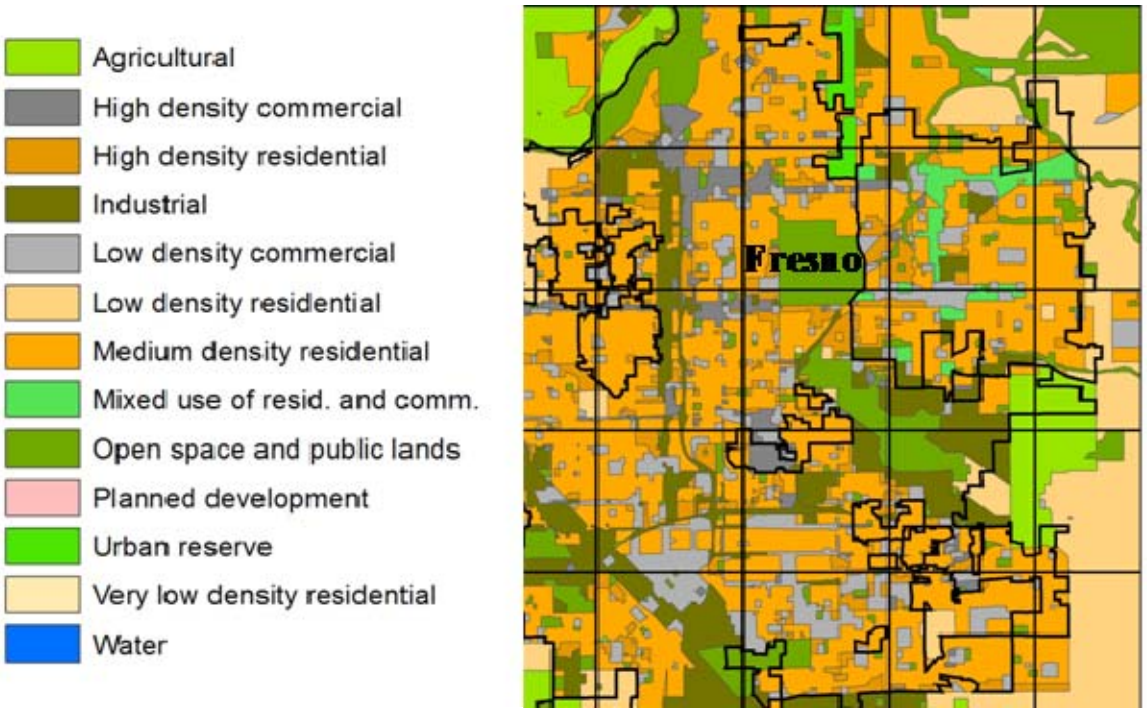


**Figure 12. Example of land-use data superimposed on model grid near Fresno**

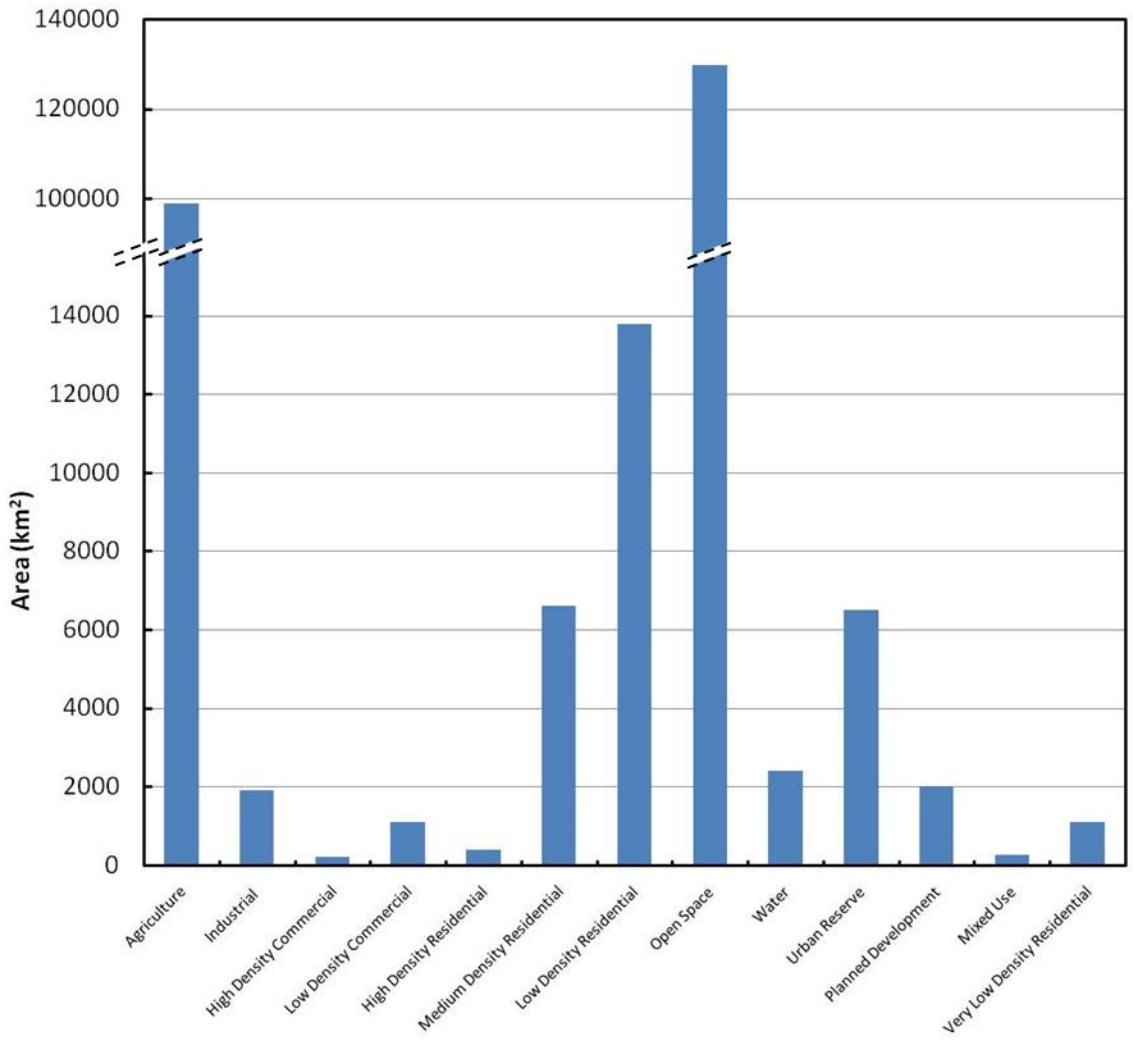


**Figure 13. Aggregate land-use distribution in the SJVAB**

### *2.2.3. Approach to Relate Land-Use Data to DG Power and DG Mix*

After extracting the areas in each cell for the 13 generic land-use categories, the next step was to design a strategy to relate land-use areas to the amount of DG power and to the mix of DG technologies assigned to each cell of the grid. Since the land-use categories generally refer to a sector of the economy that is expected to use DG (of various types and to varying degrees in various applications), the label used for groupings of land-use categories in this section is "sector."

A systematic approach to relate DG power and DG mix to land-use data was developed during the phase I project. The same systematic approach is used for the current project. However, new market studies are used to update some information on DG expected penetration in the different activity sectors. The approach presented herein was very well received by the stakeholders in the second workshop (May 21, 2003), which was organized during the phase I

project specifically to discuss the scenario development task and receive critique and feedback from DG stakeholders. Note that the approach presented herein is a comprehensive approach, but one that is amenable to modification as new market studies on future DG market estimates become available.

One limitation of this approach is the availability of GIS data for future years. The GIS information available for this study was collected in 2000. The geographical distribution and area of the different land-use sectors is continuously changing, and "vacant" areas could be occupied by other type of land-use categories within the timeframe of the current project. The current study does not analyze a change in land-use areas. However, a number of spanning scenarios are included to analyze the sensitivity of air quality impacts of DG to changes in spatial distribution of DG implementation.

The systematic approach consists of a 10-step procedure that is described in this section of the report. The nomenclature used in the equations that define the approach is presented in Table 23, together with definitions for each variable.

**Table 23. Nomenclature used in the equations that define the systematic approach for developing realistic DG scenarios**

| | |
|---|---|
| $A_{i,k}$ | Area of sector *i* in cell *k* |
| $S_{i,j}$ | Relative area of sector *i* in size category *j* |
| $A_{i,j,k}$ | Area of sector *i* in size category *j* in cell *k* |
| $A_{AB}$ | Total Area in the air basin |
| $D_{i,h}$ | Duty cycle factor in sector *i* and hour of the day *h* |
| $R_{i,j}$ | Adoption rate relative intensity (in terms of DG power/square foot) for sector *i* in size category *j* |
| $F_{power,k}$ | Factor accounting for the total DG power in each cell |
| $P_{Tot,k}$ | Total DG power (in MW) assigned to each cell |
| $P_{Tot,k,h}$ | Total DG power (in MW) assigned to each cell at hour *h* |
| $P_{Tot,AB}$ | Total DG power (in MW) estimated for the air basin in the target year |
| $P_{i,j,k}$ | DG power (in MW) of specific sector *i* in size category *j* in cell *k* |
| $P_{i,j,k,h}$ | DG power (in MW) of specific sector *i* in size category *j* in cell *k at hour h* |
| $W_{l,i,j}$ | Relative weight for DG type *l* in sector *i* and size category *j* |
| $T_{l,j,k,h}$ | Relative contribution to DG power of DG type *l* in DG size *j* in cell *k* and hour *h* |
| $P_{l,j,k,h}$ | DG power (in MW) of DG type *l*, of DG size *j*, in cell *k* at hour *h* |
| $e_{l,j,X}$ | Emission factor for species *X* of DG type *l* and DG size *j* |
| $[X]_{emiss,k}$ | Total DG emissions of species *X* in cell *k* |

In reading this section of the report one should periodically refer back to Table 23. Note that the subscript *i* refers to the sector type (i.e., groupings of land-use categories), the subscript *j* refers to the DG size class, and the subscript *k* refers to the AQM model cell. The subscript *h* refers to the hour of the day, and the subscript *l* refers to the type of DG technology. These subscripts are consistent throughout the derivation presented in this section. Note that to develop a realistic DG implementation scenario one must consider a large number of factors, as shown in Table 23.

The development of a realistic scenario based on land-use data, DG size, DG type, and other available data and insights are presented in this section as a ten (10)-step procedure. This process was vetted by the California Energy Commission, SCAQMD, SJVAPCD, and ARB staff, as well as DG stakeholders who participated in the workshops. The ten-step procedure is defined as follows.

**STEP 1.** The starting point for the DG scenario development is the extracted land-use data in 5 x 5 km resolution. These data consist of the areas (in square kilometers) of all 13 of the generic land use types for each of the computational cells of the model grid. Note that the land use categories available for the SoCAB do not correspond totally with the land use categories available for the SJV. The 13 land use area types are aggregated into 6 different sectors (i.e., low density residential, medium-to-high density residential, commercial, industrial, agriculture, and others), as shown in Table 24 and in Table 25, for the SoCAB and the SJV respectively. The amount of square kilometers of a sector type in any specific cell is represented by $A_i$.

Figure 14 presents a representative picture of the aggregated GIS land-use categories as integrated into the six (6) economic sectors for the Central Los Angeles area.

**Table 24. Integration of land-use types into energy sectors in the SoCAB**

| Sector | Land use types considered in that sector* |
|---|---|
| Low Density Residential | Low Density Residential |
| | Rural Density Residential |
| Medium to High Density Residential | Medium to High Density Residential |
| Commercial | Commercial |
| | Public Facilities & Institutions |
| Industrial | Industrial |
| Agriculture & Water Pumping | Agriculture |
| Other | Extraction |
| | Transportation & Utilities |
| | Under Construction |

* The rest of the land use categories (Vacant, Water and Flood Ways, and Open Space and Recreation) assumed to adopt zero DG power.

**Table 25. Integration of land-use types into energy sectors in the SJV**

| Sector | Land use types considered in that sector*,** |
|---|---|
| Low Density Residential | Low Density Residential |
| | Rural Density Residential |
| | Very Low Density Residential |
| Medium to High Density Residential | Medium Density Residential |
| | High Density Residential |
| Commercial | High Density Commercial |
| | Low Density Commercial |
| | Mixed Use |
| Industrial | Industrial |
| Agriculture & Water Pumping | Agriculture |

* Urban reserve is assumed to contain the same overall distribution of sectors as in the entire SJVAB.
** The rest of the land use categories (Water and Flood Ways, Open Space and Recreation, and Planned Development) assumed to adopt zero DG power

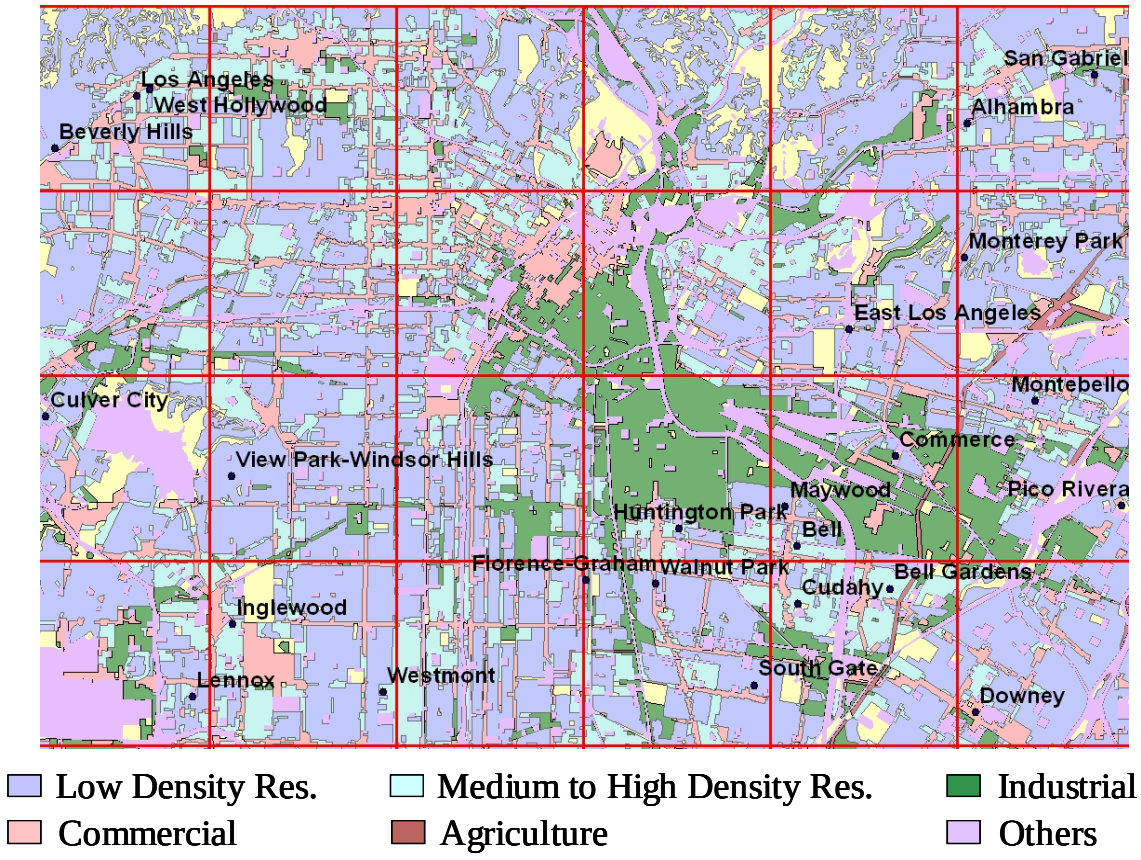


**Figure 14. Land-use parcels in central Los Angeles aggregated into six energy sector categories**

**STEP 2.** The second step is to disaggregate each of the sector areas in each cell into six (6) sub-categories according to DG size capacity. The six DG size classes that are used are:

- <50 kW,
- 50–250 kW,
- 250–1,000 kW,
- 1–5 MW,
- 5–20 MW, and
- 20–50 MW.

The bases of this disaggregating process are several reports on energy consumption surveys in the commercial, residential, and manufacturing sectors by the Energy Information Agency (EIA 2003a, 2003b, 2004). These reports are updated versions of the reports used in the phase one project. As a result, the outcome of disaggregating each activity sector in six DG size categories changes slightly from the previous study. These reports relate total floor space of various establishment types in each sector to the annual electricity consumption. From these data the average power demand for each establishment is estimated and the potential for each sector to adopt DG in each of the six size classes is determined. The results of these analyses are normalized by dividing the area of each size-category by the total area in that sector to get a relative area per sector ($i$) and per size category ($j$), which is represented by $S_{i,j}$. Two of the sectors (Agriculture and Other) required the development of estimated $S_{ij}$ since no data is currently available for these sectors. Reasonable estimates were made based on the $S_{ij}$ of the other sectors and insights of the APEP team. The equation that relates total area to area per size category for each of the sectors considered is:

$$A_{i,j,k} = S_{i,j} \cdot A_{i,k} \tag{6}$$

Table 26 shows the resulting normalized area factors that are applied to disaggregate (split) the sectors (groups of GIS land-use areas) into specific areas for each DG size category.

**Table 26. Normalized area factors ($S_{i,j}$) for each DG size category for the different sectors**

| Size Category | Low Density Residential | Medium and High Density Residential | Commercial | Industrial | Agriculture | Other |
|---|---|---|---|---|---|---|
| **< 50 kW** | 99.0 | 50.0 | 53.6 | 0.0 | 90.0 | 0.0 |
| **50–250 kW** | 1.0 | 40.0 | 24.4 | 19.3 | 10.0 | 19.3 |
| **250–1000 kW** | 0.0 | 10.0 | 11.1 | 65.5 | 0.0 | 65.5 |
| **1–5 MW** | 0.0 | 0.0 | 10.3 | 11.8 | 0.0 | 11.8 |
| **5–20 MW** | 0.0 | 0.0 | 0.6 | 3.1 | 0.0 | 3.1 |
| **20–50 MW** | 0.0 | 0.0 | 0.0 | 0.4 | 0.0 | 0.4 |

**STEP 3.** The third step is to determine DG power in each of the disaggregated (DG size class dependent) areas in each cell of the model based on a third factor included in this approach. This third factor is called the "Adoption Rate Relative Intensity" factor and has the units of DG power per square kilometer. This relative adoption rate intensity is a function of both the sector and the DG power size category, and is represented by $R_{i,j}$ in the current approach. The adoption rate relative intensity factor, $R_{i,j}$, accounts for the fact that a certain amount of land that is occupied by a certain economic sector will adopt DG technology at a rate that differs from that of other sectors.

The adoption rate relative intensity factor, $R_{i,j}$, is determined in the current approach as a function of both size category and sector based on a report that describes CHP penetration in the commercial and industrial sectors in California (EPRI 2005). Note that this report only provides combined market penetration of DG with CHP and includes both the industrial and the commercial sectors. The relative adoption rates for DG in other sectors are estimated from comparison to these data and APEP team insights. Table 27 presents the current estimates for those intensity factors. The factors should be interpreted as follows: if the DG power penetration in a square kilometer of the low density residential sector in the size category <50 kW is 1.0 MW, then the corresponding DG power penetration in the same area for the industrial sector in the range capacity 20–50 MW is 555,616 MW. The adoption rate relative intensity factors of Table 27 are well grounded in the literature and APEP insights that are currently available. However, these factors can be refined and modified at any time as additional detailed market penetration studies are completed and as information becomes available for DG market penetration in California.

**Table 27. Adoption Rate Relative Intensity per size category and per sector ($R_{i,j}$)**

| Size Category | Low Density Residential | Medium and High Density Residential | Commercial | Industrial | Agriculture | Other |
|---|---|---|---|---|---|---|
| **< 50 kW** | 1 | 5 | 86 | 0 | 7 | 0 |
| **50–250 kW** | 1 | 23 | 756 | 208 | 239 | 55 |
| **250–1000 kW** | 0 | 95 | 1758 | 98 | 0 | 26 |
| **1–5 MW** | 0 | 0 | 6377 | 6568 | 0 | 1723 |
| **5–20 MW** | 0 | 0 | 195001 | 36780 | 0 | 9647 |
| **20–50 MW** | 0 | 0 | 0 | 555616 | 0 | 145733 |

As a result of the above development of areas and factors, one can determine the total DG power in each cell as a sum of the areas per sector and per size category ($A_{i,,j,k}$) multiplied by the adoption rate relative intensity. This factor $F_{power}$ is determined for each individual cell of the air quality model as follows:

$$F_{power,k} = \sum_i \sum_j A_{i,j,k} R_{i,j} \tag{7}$$

The total DG power in real units (MW) assigned to each cell *k* of the model is then determined as a function of the assumed total implementation of DG power in the area of interest, namely the SoCAB and the SJV, (the portion of increased power demand met by DG) and the normalized power factor as follows:

$$P_{Tot,k} = \frac{F_{power,k}}{\sum_k F_{power,k}} \cdot P_{Tot,AB} \tag{8}$$

Once the total DG power in each cell is determined, DG power associated with each of the size categories in each sector can be described by the following equation:

$$P_{i,j,k} = \frac{A_{i,j,k} R_{i,j}}{F_{power}} P_{Tot,k} \tag{9}$$

Finally then, the total DG power per sector and per cell can be written as:

$$P_{i,k} = \frac{\sum_j A_{i,j} R_{i,j}}{F_{power}} P_{Tot,k} \tag{10}$$

**STEP 4.** At this point one must consider the operational duty cycle of DG units. The temporal variation of the DG power due to the variety of duty cycles of the units is introduced into this procedure as a function of the particular sector that the DG units are serving. Average load profiles are calculated for each sector based on hourly electric data obtained from the Southern California Edison web page. To apply the sector-specific duty cycle one must determine a normalized vector factor, $D_{i,h}$, which describes the hour-by-hour duty expected in each sector. The total power for a particular sector and in each size category in a cell is presented in Equation 9 as $P_{i,j,k}$. This factor is considered the peak DG power output that can occur at any one hour of the day in a particular sector. Thus, multiplying the normalized

duty cycle by the peak sector power in each cell produces the total power per sector and per cell as a function of the time of the day as:

$$P_{i,j,k,h} = P_{i,j,k} D_{i,h} \tag{11}$$

**STEP 5.** The next step consists of determining the relative contribution to total power in a cell by each of the DG types considered (namely, low-temperature (LT) fuel cells, high-temperature (HT) fuel cells, MTGs, NG ICEs, PV, gas turbine (GT), and Hybrid fuel cell systems). To accomplish this, six tables must be developed (one for each sector), in which the relative expected contribution of each DG type in each size category, $W_{i,l,j}$, is presented. Table 28 below presents the relative contributions of DG technology types ($W_{i,l,j}$) for the industrial sector as an example. The relative contribution factors all six (6) sectors are based on market penetration of DG technology types in the industrial sector, utility sector, and commercial sector (EPRI 2005) and APEP team or other expert estimates on market distribution of DG technology types in each of the size categories.

**Table 28. Estimated relative contributions of DG technology types in the Industrial sector as a function of size class**

| Size category | LT FC (%) | HT FC (%) | MTG (%) | NG ICE (%) | GT (%) | Hybrid (%) | Total (%) |
|---|---|---|---|---|---|---|---|
| **< 50 kW** | 0 | 0 | 0 | 0 | 0 | 0 | 100 |
| **50–250 kW** | 0 | 2 | 7 | 91 | 0 | 0 | 100 |
| **250–1,000 kW** | 0 | 2 | 0 | 92 | 6 | 0 | 100 |
| **1–5 MW** | 0 | 1 | 0 | 73 | 26 | 0 | 100 |
| **5–20 MW** | 0 | 0 | 0 | 16 | 83 | 0 | 100 |
| **20–50 MW** | 0 | 0 | 0 | 0 | 100 | 0 | 100 |

As a result, the equation that determines the relative contribution of each DG technology in each cell for a particular hour of the day, $T_{l,k,h}$, is given by:

$$T_{l,j,k,h} = \frac{\sum_i W_{i,l,j} \cdot P_{i,j,k,h}}{P_{Tot,k,h}} \tag{12}$$

And the total DG power in each cell supplied for each of the DG types considered is:

$$P_{l,j,k,h} = T_{l,j,k,h} \cdot P_{Tot,k,h} \tag{13}$$

**STEP 6.** At this point an estimate of the spatial distribution of DG power and the mix of DG technologies in each cell of the model and the power that each is producing at each hour of the day has been determined. The sixth step to consider is a weighting factor for relative DG adoption rates that is a function of the location within the basin that one is considering. The systematic procedure presented thus far uses average DG adoption factors for all cells throughout the basin. No local information on forecasted DG penetration in certain zones of California due to any potential driver (e.g., transmission or distribution constraints in utility grid, strong DG incentives in particular cities, anticipated larger DG installations) has been included in the approach thus far.

Since data were not available to suggest preferential DG adoption at any particular location or set of locations in the SoCAB or the SJV, only average adoption rates are used for the SoCAB and the SJV. However, if at any time preferential DG adoption rates that apply to the spatial distribution of DG in those areas become available one should apply a normalized adoption rate factor in this step. So far no local data is available and, therefore, no modification to the first five steps of this systematic approach is applied at this time in Step 6.

**STEP 7.** The seventh step is to calculate pollutant emissions in each cell and each hour of the day based on the emissions factors for each of the DG types, $e_{l,j}$. As explained in Section 2.1.3 Emissions Specifications, the emissions factors, $e_{l,j}$, for each of the DG types and sizes are determined from literature sources (E2I 2004) and APEP measurements of emissions from various DG technologies. In all realistic cases the emissions from DG within the SoCAB and the SJV are never allowed to exceed the 2007 ARB emissions standards. The emissions for all the DG pollutants considered in a given cell of the model can be determined through the following equations:

$$[CO]_{emiss,k,h} = \sum_{l}\sum_{j} P_{l,j,k,h} \cdot e_{l,j,CO} \tag{14}$$

$$[NOx]_{emiss,k,h} = \sum_{l}\sum_{j} P_{l,j,k,h} \cdot e_{l,j,NOx} \tag{15}$$

$$[VOC]_{emiss,k,h} = \sum_{l}\sum_{j} P_{l,j,k,h} \cdot e_{l,j,VOC} \quad (16)$$

$$[SOx]_{emiss,k,h} = \sum_{l}\sum_{j} P_{l,j,k,h} \cdot e_{l,j,SOx} \quad (17)$$

$$[PM]_{emiss,k,h} = \sum_{l}\sum_{j} P_{l,j,k,h} \cdot e_{l,j,PM} \quad (18)$$

$$[CO_2]_{emiss,k,h} = \sum_{l}\sum_{j} P_{l,j,k,h} \cdot e_{l,j,CO2} \quad (19)$$

Although $CO_2$ emissions do not contribute to the atmospheric chemistry, they are accounted in this step to ascertain the possible global warming impacts of DG implementation in air basins.

**STEP 8.** To fully characterize the emissions coming from potential DG operation at the level required by the air quality model, a further speciation of the above criteria pollutants, i.e., $NO_X$, CO, VOC, $SO_X$, and PM, must be applied. This step requires that one directly correlate each of the pollutant emissions calculated in the first seven steps to the pollutant flux rates that are required by the particular chemical mechanism that the AQM is using. In this particular case, the species that are considered in the AQM are those associated with the CACM and SAPRC99 chemical mechanisms. Use of the chemical mechanisms requires splitting of $NO_X$ emissions into NO and $NO_2$, $SO_X$ emissions into $SO_2$ and $SO_3$, characterization of the VOCs as five distinct hydrocarbon compounds, and supplying a distribution of particulate matter that is comprised of 19 species and eight size classes. The process of accomplishing this is presented in more detail earlier in the section on speciation of criteria pollutants.

**STEP 9.** The effects of any emissions displacement that may occur as a result of DG installations are accounted for in Step 9. Once the speciated emissions from the DG realistic scenario are known, the process described earlier to account for displaced emissions due to the operation of CHP DG units (or other emissions displacement) is applied. The resulting net emissions fluxes are calculated in this step by direct subtraction of emissions fluxes that account for displaced emissions.

**STEP 10.** The last step that is required to complete the development of a realistic scenario based upon land-use data is to take into account other realistic factors that can affect the final emissions levels for the particular date that one desires to simulate. The factors that can be included first are the date of the simulation (upon which all factors above must be scaled)

together with an adoption rate curve, or any performance degradation that one wants to include for the installed DG systems.

The performance degradation can include both an increase of criteria pollutant emissions and a decrease of electrical efficiency that will likely occur throughout the lifetime of any DG unit. As practically no public data on DG performance degradation are currently available, this study considers no performance degradation. Although this parameter may increase emissions of certain DG units, predominant technologies such as gas turbines and ICEs emit at the limits set by the 2007 ARB emission standards, and they must not exceed those limits. As a result, realistic scenarios assume no increase in emissions due to degradation.

# 3.0 DG Implementation Scenarios

Through application of the criteria presented in this report and use of all of the data and information that is currently available to the APEP team, it was determined that only a limited number of realistic scenarios can be developed and included in the current study. This is due to the fact that all available information and resources for well defining each of the parameters and factors is used to develop a "realistic" DG Scenario. The APEP team has sought and is including all possible information resources to well ground these few "realistic" DG scenarios and is then including several parametric variations (excursions) on these scenarios that either complete or complement the overall analysis of air quality impacts of DG in the SoCAB and the San Joaquin Valley Air Basin.

In addition, the APEP team is following the recommendation provided in the Industrial Stakeholder Workshops held on September 19, 2002; May 21, 2003; and April 24, 2007 to classify each of the DG scenarios in two main categories according to the "likelihood" of the scenario. Some of the scenarios that are developed in this effort are therefore classified as "realistic" implementation scenarios for distributed generation. However, for scientific completeness, for sensitivity analyses, and for determination of potential impacts for unexpected outcomes we have developed a series of scenarios that "span the spectrum." These scenarios are classified as "spanning" DG Scenarios.

These spanning scenarios should in no way be considered realistic or probable. The authors strongly caution readers to accept these spanning or "unrealistic" scenarios only in as much as they provide increased understanding or fundamental insight into DG air quality impacts. Under no circumstances do the authors suggest that the predicted impacts of a spanning scenario are realistic or expected due to the installation of DG in the SoCAB or the San Joaquin Valley Air Basin. The spanning DG scenarios are not expected and are only used for purposes of garnering insights that may be useful.

## 3.1. DG Scenarios in the SoCAB

The list of DG scenarios that is recommended includes: (1) four baseline scenarios without DG emissions, (2) ten realistic DG scenarios, (3) fifteen spanning DG scenarios for mid-term estimates, and (4) one long-term spanning scenario. These recommended DG Scenarios are presented and described below.

### *3.1.1. Baseline Scenarios (Without DG)*

#### *Scenario SoCAB-B1: 2003 AQMP Attainment for the Year 2010*

This scenario corresponds to the emissions inventory used in the 2003 AQMP developed by the SCAQMD to show attainment of the 1-hour ozone standard in the SoCAB (SCAQMD 2003a, 2003b). The base year for this emissions inventory is 1997, and then growth-and-control factors were applied to the base year emissions to achieve compliance with the 1-hour ozone standard by 2010 (Allen 2003). No DG is included in this scenario.

**Table 29. Estimated daily basinwide emissions for years 2010 (B1), 2023 (B2), and 20XX (B4) in the South Coast Air Basin of California**

| Species | 2010 Attainment (from 2003 AQMP, tons/day) | 2023 Attainment Inventory (tons/day) | 20XX Inventory (tons/day) |
|---|---|---|---|
| | Scenario SoCAB-B1 | Scenario SoCAB-B2 | Scenario Scenario-B4 |
| VOC | 453 | 420 | 385 |
| $NO_X$ | 251 | 114 | 97 |
| CO | 2064 | 1966 | 1669 |
| $SO_X$ | 33 | 19 | 19 |
| $PM_{2.5}$ | 140 | 88 | 91 |

### *Scenario SoCAB-B2: 2023 Attainment Baseline*

The ARB and South Coast AQMD developed an emissions inventory for the 2007 air quality management plan to demonstrate attainment of the 8-hour average ozone federal air quality standard by the year 2023. The final 2007 AQMP is already available (SCAQMD 2007), although the detailed gridded emissions inventory was not publicly available during the course of this project. Therefore, this report uses as an attainment scenario for the year 2023, an emissions inventory based upon scenario SoCAB-B1 and the basinwide emissions reductions described in the 2007 AQMP (see Table 29).

Emission reductions proposed by the 2007 AQMP lead to significant reductions of $NO_X$ and VOC emissions, which are the main precursors of ozone. As a result, peak ozone concentration with the emission inventory developed for this project is likely to be lower than the peak ozone concentration produced by the 2003 AQMP attainment inventory (scenario SoCAB-B1). In addition, the present project analyzes the compliance of scenario B2 with the 8-hour standard. This analysis is based on U.S. EPA's *Guidance on the Use of Models and Other Analyses in Attainment Demonstrations for the 8-hour Ozone NAAQS* (U.S. EPA 2007). This report defines the "attainment test" that allows assessing whether a reduction in emissions would lead to attainment in any monitoring station of the domain of interest. The test is based on the following equation:

$$(DVF)_I = (RRF)_I \times (DVB)_I$$

where

$(DVB)_I$ = the baseline concentration monitored at site I, units in parts per billion (ppb);

$(RRF)_I$ = the relative reduction factor, calculated near site I, unit-less. The relative reduction factor is the ratio of the future 8-hour daily maximum concentration predicted near a monitor (averaged over multiple days) to the baseline 8-hour daily maximum concentration predicted near the monitor (averaged over the same days), and

$(DVF)_I$ = the estimated future design value for the time attainment is required, ppb.

The report indicates that ozone attainment is achieved when $(DVF)_I$ is less than or equal to 84 ppb for all monitoring stations.

The most recent baseline emissions inventory for a past episode available for the SoCAB is the 1997 emissions inventory used in the 2003 Air Quality Management Plan. Hence, air quality measurements from year the 1997 can be used as $(DVB)_I$; whereas results from simulations of base year 1997 and estimated year 2023 can be used to calculate $(RRF)_I$. Finally, compliance with the 8-hour standard can be assessed by calculating $(DVF)_I$.

Scenario B2 was tested to determine whether this inventory leads to the attainment of the 8-hour standard, using the methodology described above. Based on the input data available to the APEP group, the 1997 baseline case used August 27–29 meteorology and the 1997 emissions inventory. Using the same meteorology, the "attainment" scenario was simulated using the "attainment" emissions for 2023. The peak 8-hour average concentration was calculated from the simulation results of the two cases, and the $(RRF)_I$ values were obtained for all the monitoring stations. These values are presented in Table 30.

The values of $(DVB)_I$ for all stations were obtained from ARB's database (ARB 2006b). Table 30 shows the 8-hour average ozone concentration observed in three different days in August 1997. In the modeling for August 5, ten monitoring stations measured 8-hour average ozone concentrations higher than 84 ppb. In the August 7 modeling, five monitoring stations violated the 84 ppb value; whereas on August 23, thirteen stations reported values higher than 84 ppb. The DVF values for the 8-hour average ozone concentration that was calculated using the ozone RRF and DVB values show that four and five monitoring stations exceed 84 ppb on August 5 and August 23, respectively. On August 23, only one of the (DVF) values exceeds 84 ppb. These results show that even with drastic emission reductions proposed by the AQMP, attainment of the 8-hour ozone standard might not be accomplished in some of the monitoring stations in the SoCAB. Note that some relative reduction factors, calculated as defined by U.S. EPA's guidelines, are larger than 1, which means that the emission reductions would lead to increases in ozone concentrations in some locations.

**Table 30. Ozone reduction factors $(RRF)_i$, 1997 baseline concentrations $(DVB)_i$ for selected days in August 1997, and corresponding forecasted concentrations $(DVF)_i$ for the attainment scenario at all existing monitoring stations in 1997, in the South Coast Air Basin of California**

| Code | Location | $(RRF)_i$ | $(DVB)_i$ Aug 5 | $(DVF)_i$ | $(DVB)_i$ Aug 7 | $(DVF)_i$ | $(DVB)_i$ Aug 23 | $(DVF)_i$ |
|---|---|---|---|---|---|---|---|---|
| ANAH | Anaheim-Harbor Blvd | 0.81 | 40 | 33 | 13 | 11 | 37 | 30 |
| AZUS | Azusa | 1.01 | 85 | 86 | 47 | 48 | 92 | 93 |
| BANN | Banning Airport | 0.50 | 88 | 44 | 100 | 50 | 86 | 43 |
| BURK | Burbank-W Palm Av. | 0.83 | 77 | 64 | 50 | 41 | 87 | 72 |
| CELA | Central Los Angeles | 1.11 | 56 | 62 | 30 | 33 | 65 | 72 |
| CRES | Crestline | 0.96 | 86 | 82 | 114 | 109 | 91 | 87 |
| FONT | Fontana | 0.85 | 99 | 84 | 60 | 51 | 92 | 78 |
| GLEN | Glendora-Laurel | 0.85 | 53 | 45 | 58 | 49 | 102 | 87 |
| HAWT | Hawthorne | 0.94 | 32 | 30 | 29 | 27 | 42 | 39 |
| LAHB | La Habra | 0.78 | 53 | 41 | 26 | 20 | 48 | 37 |
| LGBH | North Long Beach | 0.74 | 49 | 36 | 18 | 13 | 47 | 35 |
| LYNN | Lynwood | 0.78 | 28 | 22 | 21 | 16 | 40 | 31 |
| MTBA | Mount Baldy | 0.71 | 98 | 69 | 111 | 78 | 90 | 63 |
| NEWL | Santa Clarita | 0.64 | 64 | 41 | 83 | 53 | 101 | 65 |
| PASA | Pasadena-S Wilson Av. | 1.12 | 88 | 99 | 40 | 45 | 88 | 99 |
| PERI | Perris | 0.50 | -- | -- | 90 | 45 | 79 | 40 |
| PICO | Pico Rivera | 0.85 | 69 | 59 | 32 | 27 | 75 | 64 |
| POMA | Pomona | 0.79 | 65 | 52 | 38 | 30 | 62 | 49 |
| RDLD | Redlands-Dearborn | 0.75 | 110 | 83 | 87 | 65 | 105 | 79 |
| RESE | Reseda | 0.63 | 67 | 42 | 49 | 31 | 70 | 44 |
| RIVR | Riverside-Rubidoux | 0.82 | 118 | 97 | 81 | 67 | 99 | 81 |
| SNBO | San Bernardino-4th St. | 0.86 | 104 | 90 | 78 | 67 | 102 | 88 |
| TORO | Toro | 0.60 | 77 | 46 | 37 | 22 | 55 | 33 |
| UPLA | Upland | 0.81 | 92 | 75 | 59 | 48 | 90 | 73 |
| WSLA | West Los Angeles | 0.76 | 61 | 47 | 30 | 23 | 55 | 42 |
| Number of violations | | | 10 | 4 | 5 | 1 | 13 | 5 |

### *Scenario SoCAB-B3: 2030 Attainment Baseline*

In addition to the 2023 attainment emissions inventory, ARB and South Coast AQMD are developing an emissions inventory for year 2030 to demonstrate sustained attainment of the federal ozone air quality standard. This inventory was included in the 2007 SIP, but it was not made public during the course of this study. Therefore, preliminary estimates need to be developed by the APEP team. Estimates for the emissions inventory for 2030 will be based on the 2023 attainment emissions inventory (SoCAB-B2). The 2023 emissions are scaled up based on the increase in population from 2023 to 2030, and then controlled so that the total basinwide emission levels will be equal to the emission levels for scenario SoCAB-B2.

### *Scenario SoCAB-B4: 20XX Baseline*

Estimating emissions for a long term is difficult and implies large uncertainties. Currently, there are no emission estimates available beyond 2030. Only EMFAC, a model used to generate on-road mobile emissions, is capable of estimating emissions for years up to 2040. Therefore, estimates for the baseline long-term scenario (year 20XX) consist of estimating on-road mobile emissions estimated by EMFAC and projecting the rest of the emissions using existing trends for years up to 2030. Section 2.1.8 presents the projected vehicle emissions for this scenario.

### 3.1.2. Realistic Scenarios

As a result of applying the screening criteria described above and using all the data that are currently available, the APEP team recommends a limited number of realistic DG Scenarios (5) for years 2023 and 2030. The full characterization of these realistic scenarios uses all available reports, studies, measurements, APEP team insights, and stakeholder comments that were available on DG characteristics, performance, market penetration, and application compatibility at the time of this report writing.

Realistic scenarios are only applied to years 2023 and 2030. All the DG scenarios considered for year 20XX are assumed as spanning scenarios because of the large uncertainties associated to long-term estimates. All of the realistic scenarios are based on the 10-step methodology described in Section 2.2.3. This methodology was originally developed in a previous effort that analyzed the air quality impacts of DG in the SoCAB for the year 2010 (phase I study, Samuelsen et al. 2005). The realistic scenarios use new estimates regarding the potential application of various DG to certain applications (EPRI 2005); the degree of market penetration expected; and the size, electrical performance, efficiency, and emissions characteristics of each DG type (E2I 2004). In particular, the potential for DG market penetration per DG size category has been updated using estimates from a report to the Energy Commission by EPRI (2005). Estimates in that report differ from those used in the preceding study by Samuelsen et al 2005.

The following section presents the main changes in this report from the values used in the phase I report regarding estimates for DG penetration per activity sector, DG size category, and DG technology mix.

#### *Updated DG Technology Mix and DG Market Potential*

Updated reports are available on power size by sector (EIA 2003a; EIA 2003b; EIA 2004) and on DG market potential per DG size category and technology mix (EPRI 2005), and these reports have been used to update the results in phase II. The report by EPRI (EPRI 2005) reports estimates on traditional CHP technical market potential for existing facilities in 2004 and the fraction of these facilities that already adopted CHP by 2005. This fraction was applied to estimates on CHP technical market potential for new facilities added between 2005 and 2020. These estimates allocate total cumulative power installed from 2005 to 2020 in the different DG size categories, which differ from the estimates reported previously (ONSITE SYCOM 1999). The updated estimates on DG size distribution calculated from the estimates in EPRI 2005 and the old estimates used in the phase I project are presented in Table 31. Note that the market potential for DG in the updated report increases in the size ranges 1–5 MW and 5–20 MW with respect to the estimates in phase I project. The cumulative DG penetration in the size range 1–5 MW increases from 16% to 23%; whereas in the size range 5–20 MW increases from 27% to 40%. On the other hand, penetration in the new estimates decreases in the size range larger than 20 MW, or in the smaller than 1 MW, with respect to previous estimates used for the phase I project. This difference affects the DG size distribution in the design of realistic scenarios.

**Table 31. DG size distribution expected in California, derived from two different studies: (1) estimated DG-CHP additions in capacity from 2001 to 2017, from *Market Assessment of Combined Heat and Power in the State of California* (ONSITE SYCOM 1999); and (2) DG-CHP additions from 2005 to 2020, from *Assessment of California CHP Market and Policy Options for Increased Penetration* (EPRI 2005)**

| Size category | % Cumulative Penetration Phase I project (ONSITE SYCOM 1999) | % Cumulative Penetration Phase II project (EPRI 2005) |
|---|---|---|
| < 50 kW | 0 | 0 |
| 50–250 kW | 8 | 4 |
| 250–1,000 kW | 11 | 5 |
| 1–5 MW | 16 | 23 |
| 5–20 MW | 27 | 40 |
| 20–50 MW | 38 | 28 |
| Total | 100 | 100 |

The report by EPRI also presents a number of scenarios for the implementation of DG in combination with CHP. The report presents a base case that estimates the market penetration of DG/CHP for future years up to 2020 assuming the current incentive programs for the installation of DG/CHP units. This base case estimates that cumulative installation of DG from 2005 to 2020 will add up to 2,000 MW in California. This is approximately 15% of the increased power demand during the same period. Moreover, the base case scenario estimates that 76% of the newly installed capacity will be provided by reciprocating engines. The second largest contribution will be gas turbines, with 20% of the newly installed capacity; whereas fuel cells and MTGs will contribute only 4% (see Table 32). The high percentage of ICE estimated by EPRI is a result of computing the payback time that would be acceptable for the prospect DG users. Market studies suggest that DG users would only install DG/CHP with a payback of less than 5 years. As a result, the market favors ICE over gas turbines and novel technologies, such as fuel cells and MTG. However, the EPRI study assumes that ICE will be able to comply with the 2007 ARB 2007 emission standards by the year 2010. Currently, ICE installations have problems complying with BACT standards, as reported by the SCAQMD (SCAQMD 2008a). In addition, the SCAQMD has recently proposed a new rule for ICE that would lower the emission standards to a more stringent level than the existing BACT (SCAQMD 2008b). Consequently, penetration of ICE will be limited by their ability to comply with the emission standards. Spanning scenarios explore the sensitivity of emissions and air quality impacts to changes in the technology mix to investigate the effect of preferential adoption of specific DG technologies.

Since the EPRI report only estimates penetration of DG with CHP, no estimates on market penetration are available for PV. But regardless of the contribution of PV, the technology mix estimated for this base case is significantly different from the DG mix estimated for the phase I study, which estimated higher contribution of gas turbines and MTGs and less contribution of ICEs. The DG technology mix in the base case scenario is used as the basis for determine the technology mix for the different activity sectors needed in the 10-step methodology to develop the realistic scenarios. The resulting technology mix, presented in Table 33, is used for realistic scenarios SoCAB-R1, SoCAB-R2, and SoCAB-R3.

**Table 32. 2020 Cumulative market penetration by prime mover under different scenarios (in MW)**

| Prime Mover | Base Case | High R&D |
|---|---|---|
| Recip. Engine | 1499 | 1592 |
| Micro-turbine | 33 | 41 |
| Gas Turbine | 388 | 504 |
| Fuel Cell | 46 | 627 |
| Total | 1966 | 2764 |

Source: Appendix G, Assessment of California CHP Market and Policy Options for Increased Penetration (California Energy Commission 2005)

**Table 33. DG technology mix per activity sector for realistic scenarios SoCAB-R1, SoCAB-R2, and SoCAB-R3, based on the base case presented in the EPRI 2005 report and other APEP estimates**

| | Residential (%) | Medium and high density residential (%) | Commercial (%) | Industrial (%) | Agriculture & Water Pumping (%) | Other (%) |
|---|---|---|---|---|---|---|
| Fuel cells (LTFC) | 90 | 18 | 2 | 0 | 2 | 2 |
| Fuel cells (HTFC) | 10 | 43 | 5 | 1 | 5 | 9 |
| MTGs | 0 | 15 | 2 | 1 | 2 | 0 |
| NG ICEs | 0 | 15 | 85 | 65 | 90 | 36 |
| Gas turbines | 0 | 0 | 6 | 33 | 0 | 48 |
| Hybrid | 0 | 8 | 0 | 0 | 0 | 6 |

Among other scenarios, the EPRI report presents a case with a high level of R&D for the DG technologies. This scenario considers a rate of improvement of DG technologies accelerated by five years. As a result, this scenario includes a high penetration of Fuel Cell technology (see Table 32). This DG technology mix is the basis for the technology distribution per activity sector which is assumed in realistic scenario SoCAB-R4 (see Table 34).

**Table 34. DG technology mix per activity sector for realistic scenario SoCAB-R4, based on "the "High R&D Case" presented in the EPRI 2005 report and other APEP estimates**

| | Residential (%) | Medium and high density residential (%) | Commercial (%) | Industrial (%) | Agriculture & Water Pumping (%) | Other (%) |
|---|---|---|---|---|---|---|
| Fuel cells (LTFC) | 90 | 18 | 3 | 1 | 2 | 0 |
| Fuel cells (HTFC) | 10 | 43 | 29 | 6 | 5 | 0 |
| MTGs | 0 | 15 | 2 | 1 | 2 | 0 |
| NG ICEs | 0 | 15 | 61 | 57 | 90 | 38 |
| Gas turbines | 0 | 0 | 5 | 35 | 0 | 62 |
| Hybrid | 0 | 8 | 0 | 0 | 0 | 0 |

As a result of updating the estimates for DG market potential per DG size category and technology mix, the outcome of the 10-step methodology is different from the one presented in the phase I report. Figure 15 and Figure 17a present the resulting DG size distribution of DG among sectors and the DG mix included in the report for the phase I project. The results for the phase II project are presented in Figure 16, Figure 17b, and Figure 17c. Results presented in the phase I project were based on (1) reports from the Energy Information Agency (EIA 1999a; EIA 1999b; EIA 2000) that provide information on the power size needed by sector, and (2) various reports on DG technology mix in different sectors (Iannucci et al. 2000; Little 2000; Boedecker et al. 2000). On the other hand, results obtained for the present project are obtained from (1) newer reports by EIA (2003a, 2003b, 2004) on power size needed by sector, and (2) DG technology mix reported in the EPRI (2005) report.

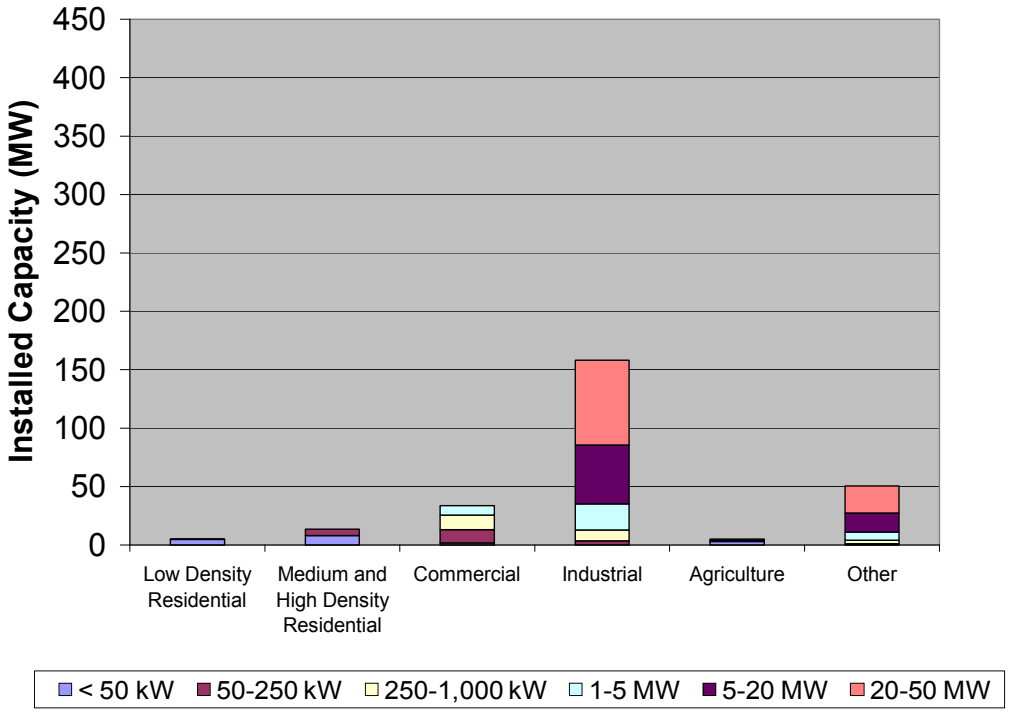


**Figure 15. Distribution of DG size per activity sector for Realistic Scenario R1 for the year 2010, as presented in Phase I Scenario Development Report**

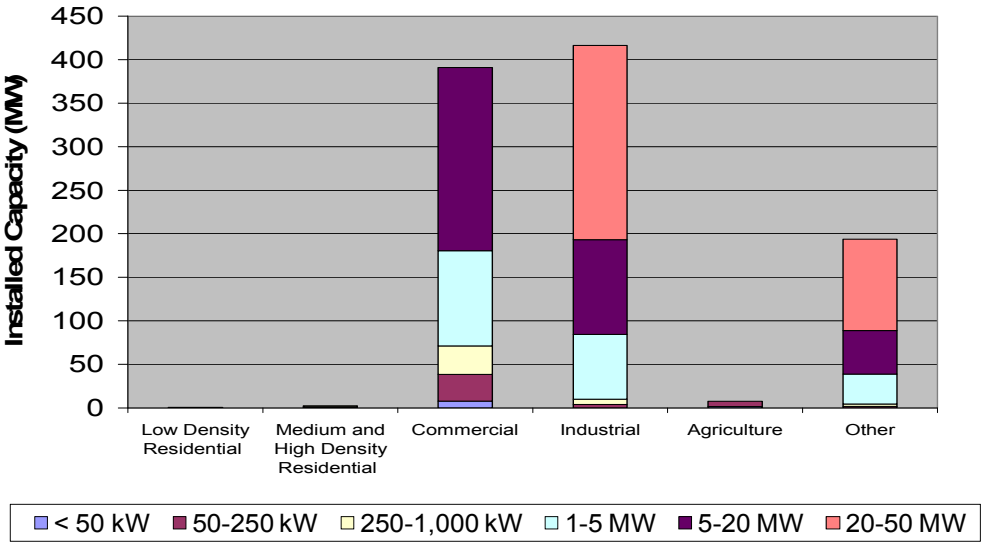


**Figure 16. Distribution of DG size per activity sector for realistic scenario SoCAB-R1 for the year 2023, using updated reports**

In phase II, the relative contribution of the DG size > 20 MW to total DG penetration is smaller than in the phase I project. In particular, the fraction of total power supplied in the range > 20 MW estimated during the phase I was near 40%; whereas in the phase II project it only accounts for 30%. On the other hand, newer estimates show that the penetration in the 1–5 MW and 5–20 MW size ranges is larger than in phase I. The relative contribution of DG in the size range of 1–5 MW increases from 13% in phase I to 21% in the present (phase II) project; whereas the relative contribution of DG in the size range of 5–20 MW increases from 27% to 35%. This is mainly due to an increase in the penetration of DG of 5–20 MW capacity in the commercial sector. As a result, the total DG capacity in the commercial sector is significantly larger than the capacity estimated during phase I, and it adds up to 39% of the total DG installations. Additionally, DG penetration in the industrial sector contributes with 41% and in the "other" sector—mining and transportation-related activities—with 19%. Finally, penetration of DG in the residential and agriculture sectors combined adds up to 1% of the total DG penetration in the SoCAB.

In brief, for the phase II project DG penetration in the commercial sector increases significantly in the range 1–20 MW in comparison with results obtained in phase I. As a result, DG penetration in the commercial sector becomes the second largest contributor to total DG penetration, slightly behind the contribution of DG in the industrial sector.

Regarding DG technology mix, new data gathered from the report by EPRI (EPRI 2005) yield to a significantly different technology distribution, with respect to the DG mix obtained during the phase I project (see Figure 17). Main differences include a dramatic decrease in the contribution of MTG to the total mix (from 16% to less than 1%), an increase in the contribution of Gas Turbines (from near 50% to 59%), and a twofold increase in the contribution of reciprocating engines to the total mix. The EPRI 2005 report projected a number of scenarios which assume different incentive programs, response from customers, and technology advancements. A case

in which there is a high level of R&D for DG technologies would lead to a larger contribution of fuel cell technologies with respect to a base case (see Figure 17b and Figure 17c), which only assumes the current incentive programs available for the implementation of DG, such as the Self-Generation Incentive Program, operative until 2014.

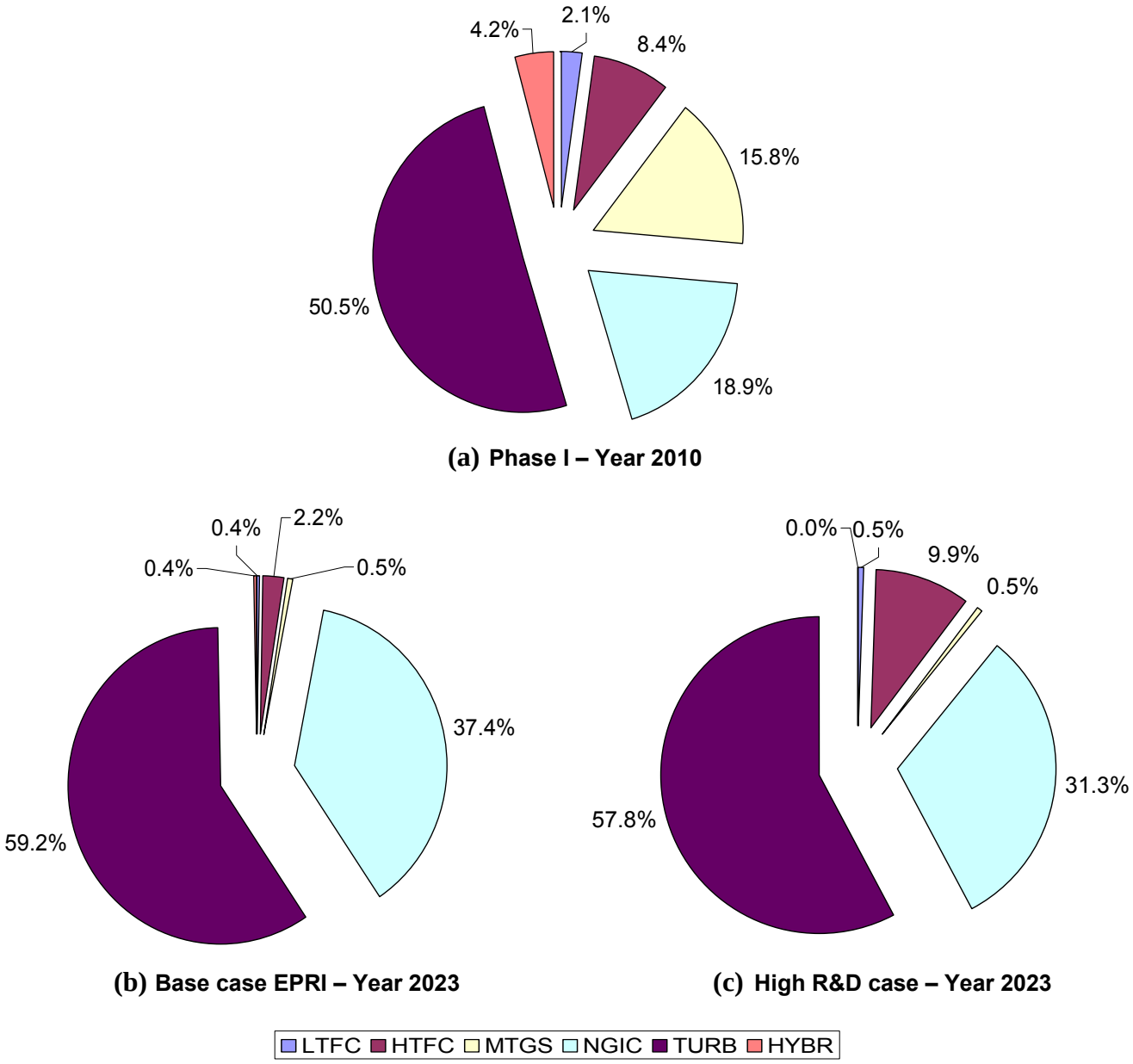


**Figure 17. DG technology mix in terms of installed capacity obtained using the 10-step methodology: (a) DG mix presented in phase I report, for realistic scenario R1 for the year 2010, (b) DG mix obtained using DG market penetration for the base case in the EPRI 2005 report for year 2023, and (c) DG mix obtained using DG market penetration for the High R&D in the EPRI/California Energy Commission 2005 report for year 2023**

### *Scenario SoCAB-R1*

This realistic scenario SoCAB-R1 (for years 2023 and 2030) is the basis for the other four realistic scenarios, which only incorporate a slight variation in one of the assumptions of the first scenario. It makes use of all the resources available to justify DG overall penetration, DG power, and DG mix in each of the discretized cells of the air quality model. This particular scenario assumes a relatively medium early adoption for DG, meaning that the cumulative DG power implemented and operating in the SoCAB is following a linear trend from 2007 to 2023 and to 2030. Also, this case assumes a DG penetration of 12% of the increased power. In addition, this scenario assumes a realistic duty cycle based on average electric hourly profiles for various energy sectors and displacement of emissions due to the heat recovery mode of most of the units installed. Table 35 presents the primary factors that contribute to the overall definition of the realistic scenario SoCAB-R1. Figure 17b presents the distribution of DG technology assumed in realistic scenarios SoCAB-R1, SoCAB-R2, and SoCAB-R3. This particular DG mix is a result of applying the 10-step methodology that uses DG market studies and land-use information to allocate DG technologies in the SoCAB.

**Table 35. Factors that contribute to the definition of realistic scenario SoCAB-R1**

| | |
|---|---|
| Factor 1.1 | Limited DG penetration, 12% of increased power |
| Factor 2.1.6 | Different mix of Certified DG in each cell based on the systematic approach to relate GIS land use data to DG mix |
| Factor 3.1.1 | Known emissions factors: literature, data, certified levels (upper bound) |
| Factor 4.4 | Different DG power in each cell based on the systematic approach to relate land use GIS data to spatial distribution of DG power |
| Factor 5.3 | Realistic duty cycle for every sector based on SCE data |
| Factor 6.3 | CHP Emissions Displaced |
| Factor 7.1.1 | PM and VOC speciation from ARB data |
| Factor 7.2 | No performance degradation |
| Factor 7.3 | No geometrical features (All DG emitting at ground level) |
| Factor 7.4.3 | Medium Early Adoption of DG Power (linear trend) |

Realistic DG Emissions Spatial Distribution

Emissions of $NO_X$ for the realistic scenario SoCAB-R1 for the year 2030 are presented in Figure 18. There are four main foci of emissions: south Los Angeles, near Long Beach, south of Anaheim, and near Riverside. This distribution is a result of applying the 10-step methodology to generate a realistic implementation of DG in the SoCAB. Consistent with results presented in Figure 16, DG is concentrated in industrial areas, such as south Los Angeles, Long Beach, and Riverside.

Scenario SoCAB-R1 assumes emissions displacement due to CHP. The values assumed for CHP utilization ($f_{CHP}$) and waste heat use ($f_{HR}$) are 60% and 50%, respectively. The resulting emissions offsets due to CHP use are higher than the emissions introduced by DG, and as a result, net emissions from DG in this scenario are negative throughout the basin.

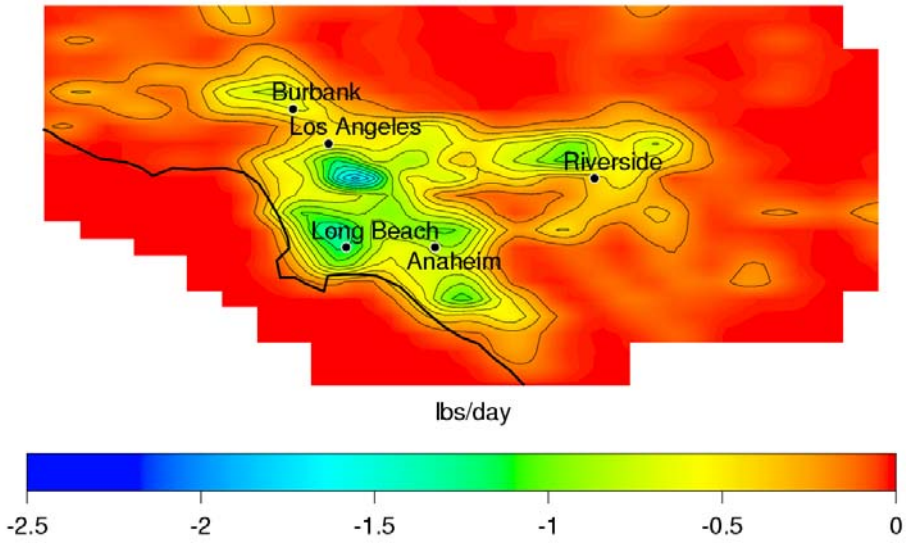


**Figure 18. DG $NO_X$ emissions for realistic scenario SoCAB-R1, for the year 2030**

### *Scenario SoCAB-R2: Low Penetration (7%) Version of SoCAB-R1*

The same assumptions in scenario SoCAB-R1 apply for SoCAB-R2. The only variation is that the parameter DG Penetration is set to a lower value (7% of the increased power demand is met by DG in 2023 or 2030).

### *Scenario SoCAB-R3: High Penetration (18%) Version of SoCAB-R1*

The same assumptions in scenario SoCAB-R1 apply for SoCAB-R3. In this case a DG Penetration parameter is set to a higher value (18% of the increased power demand is met by DG in 2023 or 2030) to account for the uncertainty associated with the future implementation of DG in the SoCAB.

### *Scenario SoCAB-R4: High Research and Development for DG Technologies*

This scenario is based on the DG technology mix and DG penetration estimated in the EPRI 2005 report for a High R&D for DG scenario. The High R&D scenario assumes an accelerated technology development that leads to a higher DG market penetration of fuel cells. The technology mix assumed for scenario SoCAB-R4 is presented in Figure 17c. The rest of the parameters are the same as the ones assumed in scenario SoCAB-R1.

### *Scenario SoCAB-R5: High Deployment of Fuel Cells Due to Environmental Forcing*

Scenario SoCAB-R5 assumes that there will be a need for further reducing greenhouse gases emissions and, consequently, penetration of high efficiency DG technologies will be favored. The incentives assumed for scenario SoCAB-R4 are prior the approval of AB 32[3] for the reduction of greenhouse gases. Scenario SoCAB-R5 assumes a penetration of fuel cells that is

[3] California Global Warming Solutions Act of 2006 [Assembly Bill 32 (Nuñez), Chapter 488, Statutes of 2006].

two times the penetration of fuel cells in scenario SoCAB-R4 to include any additional incentives created by AB32 for high efficiency electricity production like fuel cells could provide. In addition, scenario SoCAB-R5 assumes a reduced penetration of the rest of fuel-driven technologies. The total penetration in scenario SoCAB-R5 equals the total penetration in scenario SoCAB-R4.

Emissions from all realistic scenarios are summarized in Table 36 and in Figure 19. Table 36 presents the total daily emissions from DG in tons per day. Figure 19 presents the emissions in percentage of the total basinwide emissions. For realistic scenarios for the year 2023, relative emissions are calculated using baseline emissions for 2023 (SoCAB-B2). For realistic scenarios for 2030, relative emissions are calculated using 2030 baseline inventory (SoCAB-B3).

**Table 36. Daily basinwide pollutant emissions, in tons per day, from DG for all realistic scenarios in the SoCAB**

| | | Emission (ton/day) | | | | | |
|---|---|---|---|---|---|---|---|
| **Scenario** | **Electricity produced by DG (MW)** | **CO** | **$NO_X$** | **VOC** | **$SO_X$** | **$PM_{2.5}$** | **$NH_3$** |
| ***Year 2023*** | | | | | | | |
| **SoCAB-R1** | 1011.4 | 0.88 | 0.40 | 0.07 | 0.03 | 0.38 | 0.34 |
| **SoCAB-R2** | 700.2 | 0.61 | 0.27 | 0.05 | 0.02 | 0.26 | 0.23 |
| **SoCAB-R3** | 1789.4 | 1.55 | 0.70 | 0.13 | 0.06 | 0.67 | 0.60 |
| **SoCAB-R4** | 1789.4 | 1.46 | 0.67 | 0.12 | 0.06 | 0.67 | 0.60 |
| **SoCAB-R5** | 1789.4 | 1.37 | 0.64 | 0.11 | 0.05 | 0.65 | 0.58 |
| ***Year 2030*** | | | | | | | |
| **SoCAB-R1** | 1369.2 | 1.19 | 0.52 | 0.10 | 0.05 | 0.51 | 0.46 |
| **SoCAB-R2** | 798.7 | 0.69 | 0.30 | 0.06 | 0.03 | 0.30 | 0.27 |
| **SoCAB-R3** | 2053.8 | 1.78 | 0.78 | 0.15 | 0.07 | 0.77 | 0.68 |
| **SoCAB-R4** | 2053.8 | 1.67 | 0.74 | 0.14 | 0.07 | 0.77 | 0.68 |
| **SoCAB-R5** | 2053.8 | 1.57 | 0.71 | 0.13 | 0.06 | 0.74 | 0.66 |

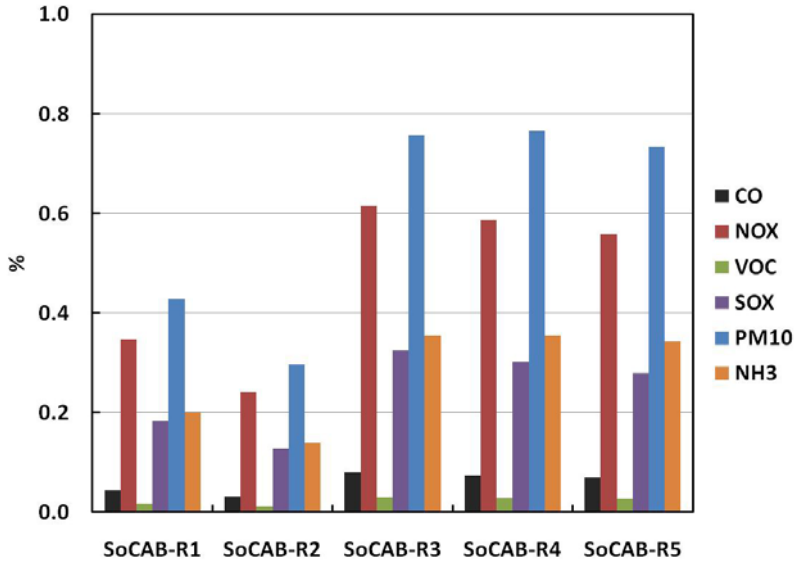


(a)

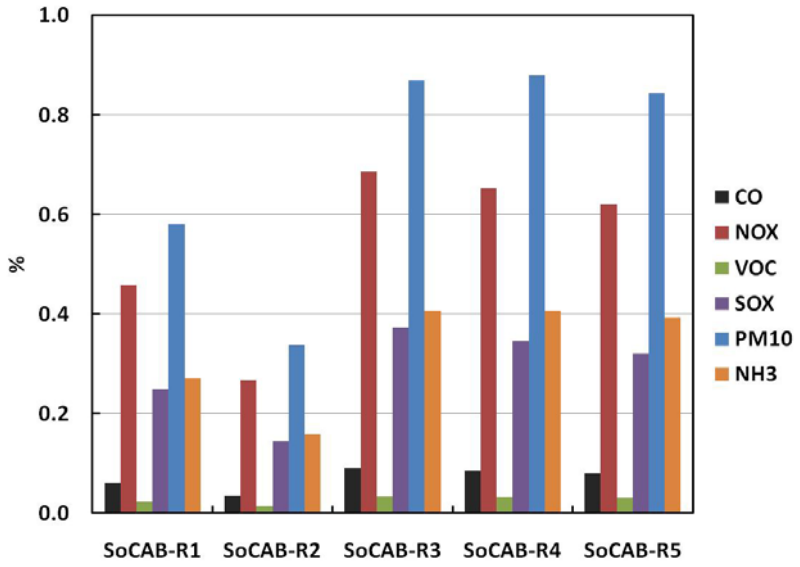


(b)

**SoCAB-R1:** Realistic DG mix and spatial distribution, Penetration: 12% increased demand
**SoCAB-R2:** Realistic DG mix and spatial distribution, Penetration: 7% increased demand
**SoCAB-R3:** Realistic DG mix and spatial distribution, Penetration: 18% increased demand
**SoCAB-R4:** Realistic spatial distribution and high R&D DG mix, Penetration: 18% increased demand
**SoCAB-R5:** Realistic spatial distribution and high deployment of fuel cells, Penetration: 18% increased demand

**Figure 19. Basinwide emissions from DG in all realistic scenarios in the SoCAB relative to total basinwide baseline emissions: (a) for the year 2023, and (b) for the year 2030 (in %)**

### 3.1.3. Spanning DG Scenarios

In the spanning DG scenarios most of the complexity of a realistic, very detailed scenario is skipped to relatively quickly develop some scenarios that can be insightful for scientific completeness, sensitivity analyses, and/or determination of potential impacts for unexpected outcomes. The 15 spanning DG scenarios are listed below and are applied to the year 2030.

#### *Scenario LU: Land-Use Weighted Scenarios*

Scenario LU contains a land-use weighted spatial distribution of emissions from an "aggregated mix" of DG technologies with an overall DG penetration of 18% of the increase in power demand between 2007 and 2030. Land use distribution is extracted from GIS data donated by the Southern California Association of Governments (SCAG). The DG mix assumed in this scenario is the same distribution used in realistic scenario SoCAB-R1 (see Figure 17b). However, this scenario assumes that all DG units operate in baseloaded mode (i.e., constantly 24 hours). In addition, no emissions displacement due to CHP is assumed here.

#### *Scenario ARB07: Certified Levels for All DG Units*

Scenario ARB07 assumes the same parameters as in scenario LU, except for the emission factors for DG technologies. In this case, all DG units emit at the 2007 ARB emissions standards, regardless of whether any technology can emit at a lower rate.

#### *Scenario BACT: All DG ICE Under BACT Levels*

Scenario BACT contains a land-use weighted spatial distribution of emissions from DG technologies that are all assumed to emit pollutants at the best available control technology (BACT) level for internal combustion engines (ICE) by the SCAQMD in the SoCAB. These BACT levels are the limits valid in 2007, and do not include the amendments to Rule 1110.2 by the SCAQMD in 2008 (SCAQMD 2008b).

#### *Scenario FC: All Fuel Cells*

Scenario FC assumes that all DG units are high-temperature fuel cells fed by natural gas. The DG size distribution in this scenario follows the same size distribution as in the realistic scenarios, but in this case, all DG sizes are covered by fuel cells. The rest of parameters are the same as in scenario LU.

#### *Scenario Peak: DG on a Peaking Duty Cycle*

Scenario Peak assumes land-use weighted spatial distribution and the same "aggregate mix" of various technologies as in scenario LU. All DG units are operating as peaking units (operating only between noon and 6 p.m.) with an installed capacity that equals 18% of the increase in power demand between 2007 and 2030. Since the DG units supply the same capacity as in LU, but only operate during six hours a day, the total emissions from DG in this scenario are one forth (1/4) of the emissions estimated for scenario LU.

#### *Scenario LDG: Large Gas Turbines Without Ammonia Slip*

Scenario LDG assumes that all DG are relatively large (50 MW) gas turbines that have emissions consistent with a SCONOX approach to emissions reduction (i.e., no ammonia emissions).

Considering the same DG penetration as in scenario S1, the number of large gas turbines required to meet the power needs is 42.

### *Scenario LDGNH3: Large Gas Turbines With Ammonia Slip*

Scenario LDGNH3 assumes that all DG are relatively large (50 MW) gas turbines that have emissions consistent with a selective catalytic reduction (SCR) approach to emissions reduction (i.e., ammonia emissions are included). This scenario considers the same specifications as in scenario S5, but it also includes ammonia emissions.

### *Scenario PGW: Population Growth Weighted*

Scenario PGW assumes that all of the DG technologies ("aggregate mix" of various technologies, same as in Scenario LU) are operating in baseload mode, and their spatial distribution follows the population growth from 2010 to 2030. Estimates of population trends during the period 2010–2030 for the SoCAB are available in the Southern California Association of Governments (SCAG) website. Total emissions considered in this scenario PGW are the same as in scenario LU. The only variation in scenario PGW with respect to scenario LU is the spatial distribution of distributed generation. Hence, comparison between S1 and S7 scenarios allows one to determine the influence of spatial distribution on the air quality impacts of distributed generation.

The 10-step methodology to generate realistic scenarios uses GIS data collected in the year 2000. There is no information available on how the land use will be distributed in the future. However, SCAG has estimated that there will be significant increases in population (and corresponding commercial and business activities) in Riverside and San Bernardino counties. The predicted increases in population could also correspond to increases in industrial activity in these counties. To study this possibility, the spanning scenario PGW uses a spatial distribution of DG that follows the growth in population between 2010 and 2030 as a basis for determining the preferential adoption of DG in these areas. Figure 20 shows the $NO_x$ emissions from DG corresponding to scenario PGW. Compared to the spatial distribution in the realistic scenarios (Figure 18), scenario S8 allocates a higher concentration of emissions at locations near Riverside, downwind from Los Angeles, and a lower concentration of emissions near Long Beach (an established industrial area that in scenario S8 is not as likely to adopt DG as new growth areas).

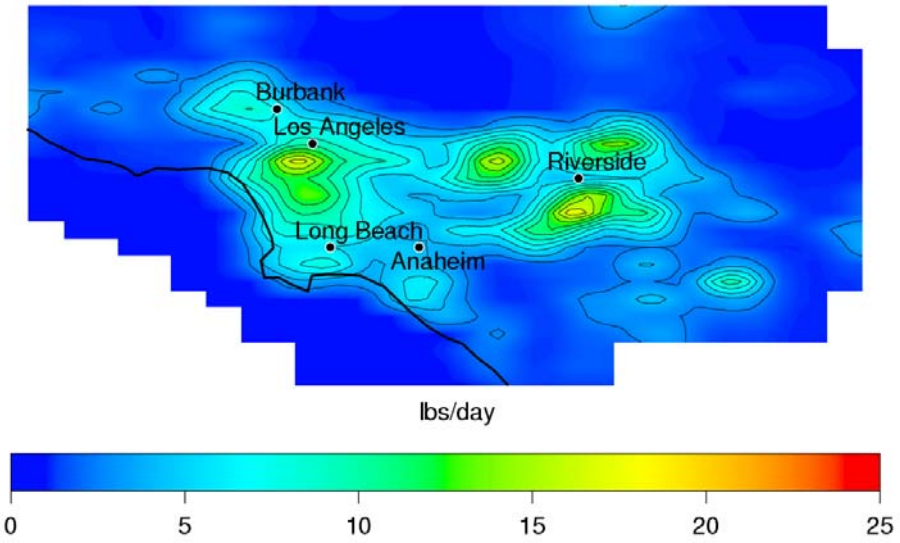


**Figure 20. DG $NO_X$ emissions for spanning scenario S7, for the year 2030. Scenario S7 corresponds to a spatial distribution of DG corresponding to the population growth between 2010 and 2030.**

### *Scenario CHP: All DG With CHP*

Scenario CHP assumes the same parameters as in scenario LU: land-use weighted spatial distribution, same DG mix, baseload operation, and DG penetration equal to 40% of the increased demand between 2007 and 2030. In addition, this scenario assumes that all DG units use CHP with appropriate emissions displacement for such technology being applied. The CHP units are assumed to recuperate 100% of the waste heat. Consequently, this scenario serves as the upper bound for emissions displacement due to CHP.

### *Scenario ARB07CHP: All 2007 ARB Certified DG With CHP Emissions Credit*

Scenario ARB07CHP assumes the same parameters as in scenario ARB07: land-use weighted spatial distribution, baseload operation, and DG penetration equal to 40% of the increased demand between 2007 and 2030. Emissions from DG units are at the 2007 ARB emission standards. In addition, DG installations include CHP, with the same levels of heat recovery as in the realistic scenarios. Namely, 60% of the available heat is recovered with a utilization factor of 50%. The 2007 ARB standards provides emission credits to DG units with CHP of 1 MWh per each 3.4 MMBtu of waste heat, allowing higher direct emissions than in scenario ARB07.

### *Scenarios EEDa and EEDb: All Electricity Emissions Displaced*

In scenarios EEDa and EEDb, a number of power plants in the SoCAB are substituted by DG units with the same total power capacity. In addition, DG units are installed to meet the 18% of the increased power demand between 2007 and 2030. This implies turning off emissions from the old existing plants and installing DG units following a land-use weighted spatial distribution. One problem that arises from these scenarios is that the emissions inventory of stationary sources is based on emission projections using 1997 emissions as a baseline. Some

power plants operating in 1997 have already been removed or repowered, as is the case of Long Beach and Huntington Beach. Hence, there is a discrepancy between the sources present in the emissions inventory and the sources that are actually operating. Two scenarios are developed to account for central generation emission displacements. The first one (EEDa) removes most large power plants present in the emissions inventory. Table 37 shows the plants removed from the inventory and Table 38 shows the total emissions from these plants included in the inventory based on 1997. Nitrogen oxide emissions reported in Table 38 are more than two times the annually averaged daily emissions reported in the U.S. EPA's Acid Rain program for 2007 (www.epa.gov/acidrain/). However, emissions from the inventory correspond to a specific day in summer, in which power plants' electricity production is expected to be higher than the annual average load. The second case (EEDb) removes power plants that will be approximately 50 years old by 2030, and emissions estimates are based on annual average emissions reported in the 2005 inventory by the ARB. As shown in Table 39, $NO_x$ emissions from power plants in this case are nearly four times lower than the emissions presented in Table 38 for scenario EEDa. The total capacity from central generation removed in these two cases is 7,980 MW and 5,543 MW. Since the emissions from power plants based on 1997 estimates are significantly higher than the emissions in the 2005 inventory, the net emissions due to the addition of DG in scenario EEDa are significantly lower. In particular, net $NO_x$ emissions in the first case are 0.83 tons/day (see Table 38); whereas net $NO_x$ emissions in scenario EEDb are 2.54 tons/day (see Table 39). Note that there is a net reduction in VOC emissions in scenario EEDa and in CO emissions in scenario EEDb due to removing existing power plants and substituting them with DG.

**Table 37. Power plants in Southern California substituted by DG. Power plants are present in the attainment inventory used in the 2003 AQMP (AQMD), which was projected using the 1997 emissions inventory as a baseline, for scenario EEDa.**

| Facility Name | Facility City | County | Year | Power (MW) |
|---|---|---|---|---|
| AES REDONDO BEACH, LLC | REDONDO BEACH | LA | 1948 | 1317 |
| EL SEGUNDO POWER, LLC | EL SEGUNDO | LA | 1964 | 708 |
| BURBANK CITY, PUB SERV DEPT | BURBANK | LA | 1943 | 82 |
| AES PLACERITA INC | NEWHALL | LA | 1988 | 150 |
| WHEELABRATOR NORWALK ENERGY CO | NORWALK | LA | 1987 | 31 |
| SUNLAW COGENERATION PARTNERS | VERNON | LA | 1984 | 112 |
| FPB COGEN PARTNERS, L.P. | LOS ANGELES | LA | 1982 | 25 |
| CARSON COGENERATION CO, CALIF | CARSON | LA | 1990 | 50 |
| LA CITY, DWP HAYNES GENERATING | LONG BEACH | LA | 1967 | 1570 |
| LA CITY, DWP SCATTERGOOD GENER | PLAYA DEL REY | LA | 1958 | 803 |
| LONG BEACH GENERATION, LLC | LONG BEACH | LA | 1976 | 577 |
| PASADENA CITY, DWP (EIS USE) | PASADENA | LA | 1965 | 162 |
| LA CITY, DWP HARBOR GENERATING | WILMINGTON | LA | 1949 | 472 |
| GLENDALE CITY, PUBLIC SERVICE | GLENDALE | LA | 1953 | 273 |
| AES HUNTINGTON BEACH, LLC | HUNTINGTON BEACH | ORA | 1958 | 880 |
| RELIANT ENERGY ETIWANDA, INC | ETIWANDA | SBD | 1963 | 770 |
| Total Power Removed | | | | 7980 |

**Source: California Energy Commission 2005b**

**Table 38. Pollutant emissions from power plants that are substituted by DG in the South Coast Air Basin of California, the emissions introduced by DG to compensate for the power capacity removed, and the increased power demand for scenario EEDa. Emissions from power plants are included in the attainment emissions inventory used in the 2003 AQMP.**

| | VOC | CO | $NO_X$ | $SO_X$ | $PM_{2.5}$ | Power (MW) |
|---|---|---|---|---|---|---|
| Plants removed from the basin | 1.67 | 4.65 | 3.87 | 0.23 | — | 7980 |
| DG that substitute central power plants | 0.62 | 6.81 | 3.74 | 0.47 | 3.77 | 7980 |
| Net change due to substituting central generation with DG | -1.05 | 2.16 | -0.13 | 0.24 | 3.77 | — |
| DG that meets the increase in power demand | 0.16 | 1.75 | 0.96 | 0.12 | 0.97 | 2054 |
| Total contribution from DG | 0.78 | 8.56 | 4.70 | 0.59 | 4.74 | 10034 |
| Net contribution (DG – Power plants) | -0.89 | 3.91 | 0.83 | 0.36 | 4.74 | 2054 |

**Table 39. Power plants in Southern California substituted by DG for scenario EEDb. The power plants that are removed are units that will be older than 50 years by 2030.**

| Facility Name | Facility City | County | Year | Power (MW) |
|---|---|---|---|---|
| AES REDONDO BEACH, LLC | REDONDO BEACH | LA | 1948 | 1317 |
| EL SEGUNDO POWER, LLC | EL SEGUNDO | LA | 1964 | 708 |
| BURBANK CITY, PUB SERV DEPT | BURBANK | LA | 1943 | 82 |
| LA CITY, DWP HAYNES GENERATING | LONG BEACH | LA | 1967 | 1144 |
| LA CITY, DWP SCATTERGOOD GENER | PLAYA DEL REY | LA | 1958 | 803 |
| LONG BEACH GENERATION, LLC | LONG BEACH | LA | 1976 | 260 |
| PASADENA CITY, DWP (EIS USE) | PASADENA | LA | 1965 | 71 |
| GLENDALE CITY, PUBLIC SERVICE | GLENDALE | LA | 1953 | 88 |
| AES HUNTINGTON BEACH, LLC | HUNTINGTON BEACH | ORA | 1958 | 430 |
| RELIANT ENERGY ETIWANDA, INC | ETIWANDA | SBD | 1963 | 640 |
| Total Power Removed | | | | 5543 |

Source: California Energy Commission 2005b

**Table 40. Pollutant emissions from power plants that are substituted by DG in the South Coast Air Basin of California, the emissions introduced by DG to compensate for the power capacity removed, and the increased power demand for scenario EEDb. Emissions from power plants are based on annually averaged daily emissions estimates by ARB for 2005.**

| | VOC | CO | $NO_X$ | $SO_X$ | $PM_{2.5}$ | Power (MW) |
|---|---|---|---|---|---|---|
| Plants removed from the basin | 0.49 | 7.38 | 1.02 | 0.20 | — | 5543 |
| DG that substitute central power plants | 0.43 | 4.73 | 2.60 | 0.33 | 2.62 | 5543 |
| Net change due to substituting central generation with DG | -0.06 | -2.66 | 1.58 | 0.13 | 2.62 | — |
| DG that meets the increase in power demand | 0.16 | 1.75 | 0.96 | 0.12 | 0.97 | 2054 |
| Total contribution from DG | 0.59 | 6.48 | 3.56 | 0.45 | 3.59 | 7597 |
| Net contribution (DG – Power plants) | 0.10 | -0.90 | 2.54 | 0.25 | 3.59 | 2054 |

### *Scenario BAU: Business as Usual With Linear Trend*

Scenario BAU assumes that the adoption rate of DG proceeds linearly throughout the SoCAB as it has been reported to occur between the years 2001 and 2004 by Southern California Edison and Los Angeles Department of Water and Power. Table 41 shows the DG installations under the Self-Generation Incentive Program in years 2001, 2002 (CPUC 2003), and 2004 (CPUC 2005). According to the California Energy Commission database of power plants, 55 MW of capacity composed of units 1 MW or more are installed annually. Linear extrapolation is used to calculate the installation of DG by 2030. Figure 21 shows the linear extrapolation of DG installations up to year 2030. The total capacity projected for 2030 using linear extrapolation is 4,190 MW. This level of DG penetration is approximately two times the adoption assumed in the realistic scenario SoCAB-R3, which assumes that 18% of the increased electricity demand from 2007 to 2030 is met by DG.

**Table 41. Active DG CPUC projects (in kW) in 2001, 2002, and 2004 (CPUC 2003; CPUC 2005)**

| Incentive Level | Total Active 2001 (kW) | Total Active 2002 (kW) | Total Active 2004 (kW) |
|---|---|---|---|
| **Level 1** | 2,291 | 26,875 | 108,800 |
| **Level 2** | 200 | 600 | 3,500 |
| **Level 3** | - | - | 49,300 |
| **Level 3N** | 15,452 | 57,625 | 107,400 |
| **Level 3R** | - | 1,585 | 7,700 |
| **Total** | 17,943 | 86,685 | 276,600 |

Source: CPUC 2005

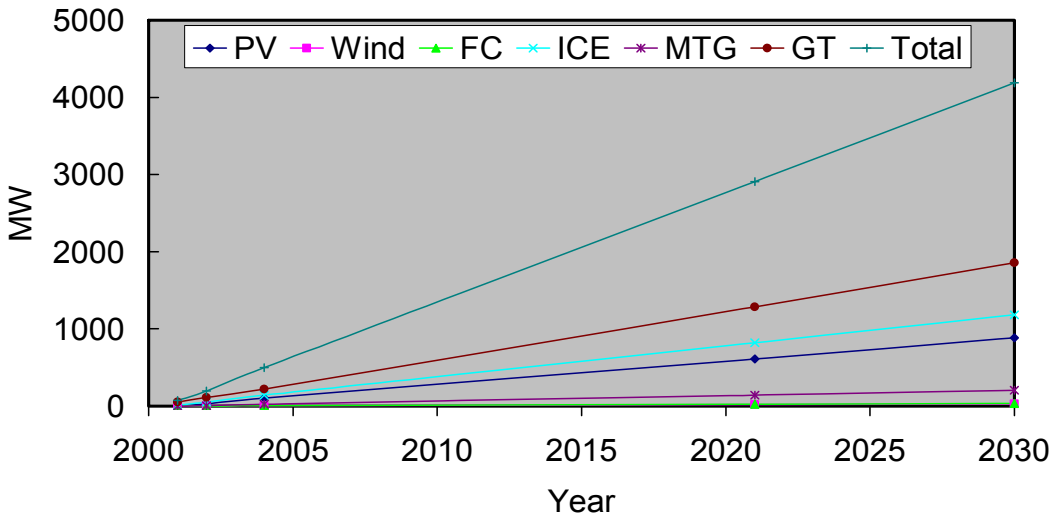


**Figure 21. Projected DG power trends in the SoCAB according to CPUC self-generation program DG data for 2001, 2002, and 2004 using a linear fit**

### *Scenario BAUP: Business as Usual With Parabolic Trend*

In the preceding study, data for years 2001 and 2002 where used to extrapolate total capacity for year 2010, following the business-as-usual trend. This linear extrapolation estimates a total capacity of 206 MW of installations active by the year 2004; whereas the CPUC's fourth-year impact assessment of the Self-Generation Incentive Program reports a total of 276.6 MW. This trend suggests that there has been acceleration in the rate of DG installation. To explore an accelerated trend, scenario BAUP assumes that the adoption rate of DG proceeds parabolically throughout the SoCAB. Figure 22 shows the parabolic extrapolation of DG installations up to year 2030. The total capacity projected for the year 2030 using parabolic extrapolation is 10,620 MW. This level of penetration represents approximately that 80% of the increase electricity demand from 2007 to 2030 will be met by distributed generation.

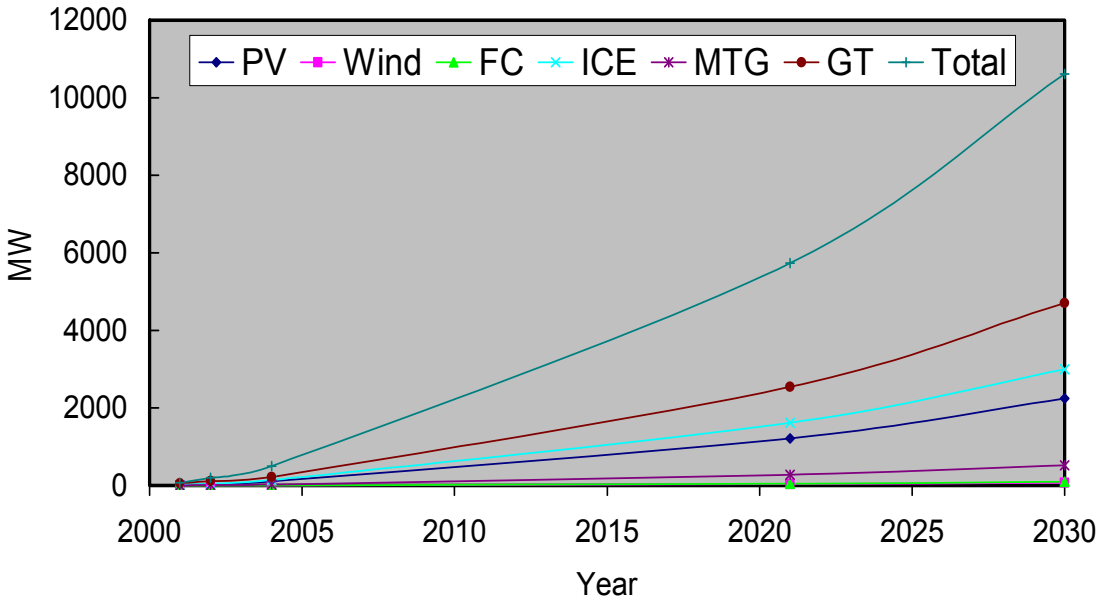


**Figure 22. Projected DG power trends in the SoCAB according to CPUC self-generation program DG data for 2001, 2002, and 2004 using a parabolic fit**

### *Scenario EHP: Extra High Penetration*

Scenario EHP assumes an extra high DG penetration that accounts for meeting 45% of the increased power demand from 2007 to 2030. According to EPRI (2005), this level of penetration, which would correspond to 5134.5 MW of total installed capacity, could be met if there were an increased level of incentives for DG installations and export of electricity were allowed. Even though this scenario is named Extra-High Penetration, the total penetration is smaller than in scenario BAUP. The DG mix and spatial distribution for this scenario are the same as in scenario LU.

### *Scenario PeakTot: Peaking Total Power*

Scenario PeakTot assumes that all of the DG technologies (same "aggregate mix" of various technologies as in LU) are operating as peaking units (operating only between noon and 6 p.m.) with a total electricity produced that equals 18% of the increase in power demand between 2007 and 2030. This implies that the total emissions in this scenario are four times the emissions in scenario Peak.

### *Scenario MSR: "Million Solar Roofs" Scenario*

The California Public Utilities Commission (CPUC) created the California Solar Initiative (CSI) in January of 2006 (CPUC 2006). The CSI consists of a $2.9 billion incentive program that will be implemented between 2007 and 2017. The main goal of this program is to install photovoltaic generation with a total capacity of 3,000 MW throughout the entire state. Considering that the SoCAB power demand is 46% of the total power demand in the state, this scenario assumes that the total capacity of PV installed in the SoCAB under the CSI incentive program will be 1,380 MW. This rate of installation is used to extrapolate the total PV capacity by 2030, which

would be 3174 MW. In California, PV systems have a typical capacity factor of 20%, and as a result, the average total power is equivalent to 635 MW of baseloaded electricity generation. The total amount of PV-generated electricity is subtracted from the total electricity generated by DG. The rest of capacity is covered by the same technology distribution assumed in the realistic scenarios. Table 42 presents the resulting DG mix for the year 2030.

**Table 42. Technology mix for the "Million Solar Roofs" scenarios for years 2023 and 2030**

| | Year 2030 | |
|---|---|---|
| | DG mix (MW) | DG mix (%) |
| GT | 840 | 40.9 |
| NGICE | 531 | 25.8 |
| MTG | 7 | 0.3 |
| HTFC | 31 | 1.5 |
| LTFC | 4 | 0.2 |
| Hybrid | 6 | 0.3 |
| PV | 635 | 30.9 |
| Total | 2054 | 100 |

HTFC=high-temperature fuel cells; LTFC = low-temperature fuel cells

### *Scenario OCLU: Out-of-Compliance Version of Spanning Scenario LU*

The SCAQMD has detected through their inspections that a large number of permitted internal combustion (ICE) DG units emit at emission levels out of compliance with the emission standards after some time of operation. Scenario OCLU assumes the same parameters as in SoCAB-R3, except for ICE emission factors. After starting a program of inspections in the year 2001, 52.4% of the inspected units were emitting at a rate higher than the standards permit. The AQMD reports a potential increase in emissions with respect to the standards of 300% if all the inspected units are taken into account. If only the non-compliant units are accounted for, the potential increase in emissions corresponds to a factor of 6.7 for $NO_X$ and 11.7 for CO. The emission factors assumed for ICE in this scenario are the emission factors of non-compliant ICE reported by the AQMD. The emission factors for the rest of technologies are the same as in the realistic scenarios. That is, all DG are emitting at regular levels, except all ICE DG units, which are emitting at three times the levels of the BACT emission standards effective in 2007.

### *Spanning Scenario Pollutant Emissions Rates and Summary*

Pollutant emissions from DG in the spanning scenarios are presented in Table 43 in tons per day and in Figure 23 as percentage of total baseline emissions. Total DG emissions in scenario PGW are equal to the emissions in scenario LU. Total emissions in scenario PeakTot are also equal to total emissions in scenario LU. However, in scenario PeakTot pollutants are emitted constantly from hour 12 to hour 18; whereas in LU pollutants are emitted constantly throughout the entire day. Emissions from scenario Peak are also released constantly from hour 12 to 18, but the total emissions are four times lower than in scenario PeakTot. Finally, emissions from scenario LDG are the same as in scenario LDG$NH_3$, except that in LDG there are no $NH_3$ emissions.

**Table 43. Daily basinwide pollutant emissions, in tons per day, from DG for selected spanning scenarios for year 2030**

| Scenario | Electricity produced by DG (MW) | Emission (ton/day) | | | | | |
|---|---|---|---|---|---|---|---|
| | | CO | $NO_X$ | VOC | $SO_X$ | $PM_{2.5}$ | $NH_3$ |
| *Spatial distribution* | | | | | | | |
| LU | 2053.8 | 1.75 | 0.96 | 0.16 | 0.12 | 0.97 | 0.83 |
| PGW | 2053.8 | 1.75 | 0.96 | 0.16 | 0.12 | 0.97 | 0.83 |
| *Duty cycle* | | | | | | | |
| Peak | 2053.8 | 0.44 | 0.24 | 0.04 | 0.03 | 0.24 | 0.21 |
| PeakTot | 2053.8 | 1.75 | 0.96 | 0.16 | 0.12 | 0.97 | 0.83 |
| *Technology Mix* | | | | | | | |
| ARB07 | 2053.8 | 2.24 | 1.56 | 0.19 | 0.16 | 1.35 | 0.83 |
| BACT | 2053.8 | 39.66 | 9.90 | 4.26 | 0.19 | 1.57 | 0.00 |
| FC | 2053.8 | 0.69 | 1.12 | 0.10 | 0.09 | 0.02 | 0.00 |
| LDG | 2053.8 | 1.79 | 0.76 | 0.16 | 0.14 | 1.57 | 0.00 |
| LDGNH3 | 2053.8 | 1.79 | 0.76 | 0.16 | 0.14 | 1.57 | 1.66 |
| MSR | 2053.8 | 1.21 | 0.66 | 0.11 | 0.08 | 0.67 | 0.58 |
| *Emissions Displacement* | | | | | | | |
| CHP | 2053.8 | 0.08 | -0.97 | 0.01 | 0.21 | 1.31 | 0.49 |
| ARB07CHP | 2053.8 | 2.27 | 1.07 | 0.19 | 0.20 | 1.62 | 0.83 |
| EEDa | 10034.0 | 3.91 | 0.83 | -0.89 | 0.36 | 4.74 | 4.07 |
| EEDb | 7597.0 | -0.90 | 2.54 | 0.10 | 0.25 | 2.97 | 3.08 |
| *DG market penetration* | | | | | | | |
| BAU | 4189.3 | 4.12 | 2.34 | 0.36 | 0.28 | 2.63 | 2.34 |
| BAUP | 10617.3 | 10.45 | 5.93 | 0.92 | 0.71 | 6.67 | 5.93 |
| EHP | 5134.5 | 4.38 | 2.40 | 0.40 | 0.30 | 2.43 | 2.08 |
| *Compliance with emission standards* | | | | | | | |
| OCLU | 2053.8 | 46.85 | 11.86 | 1.73 | 0.15 | 1.44 | 0.83 |

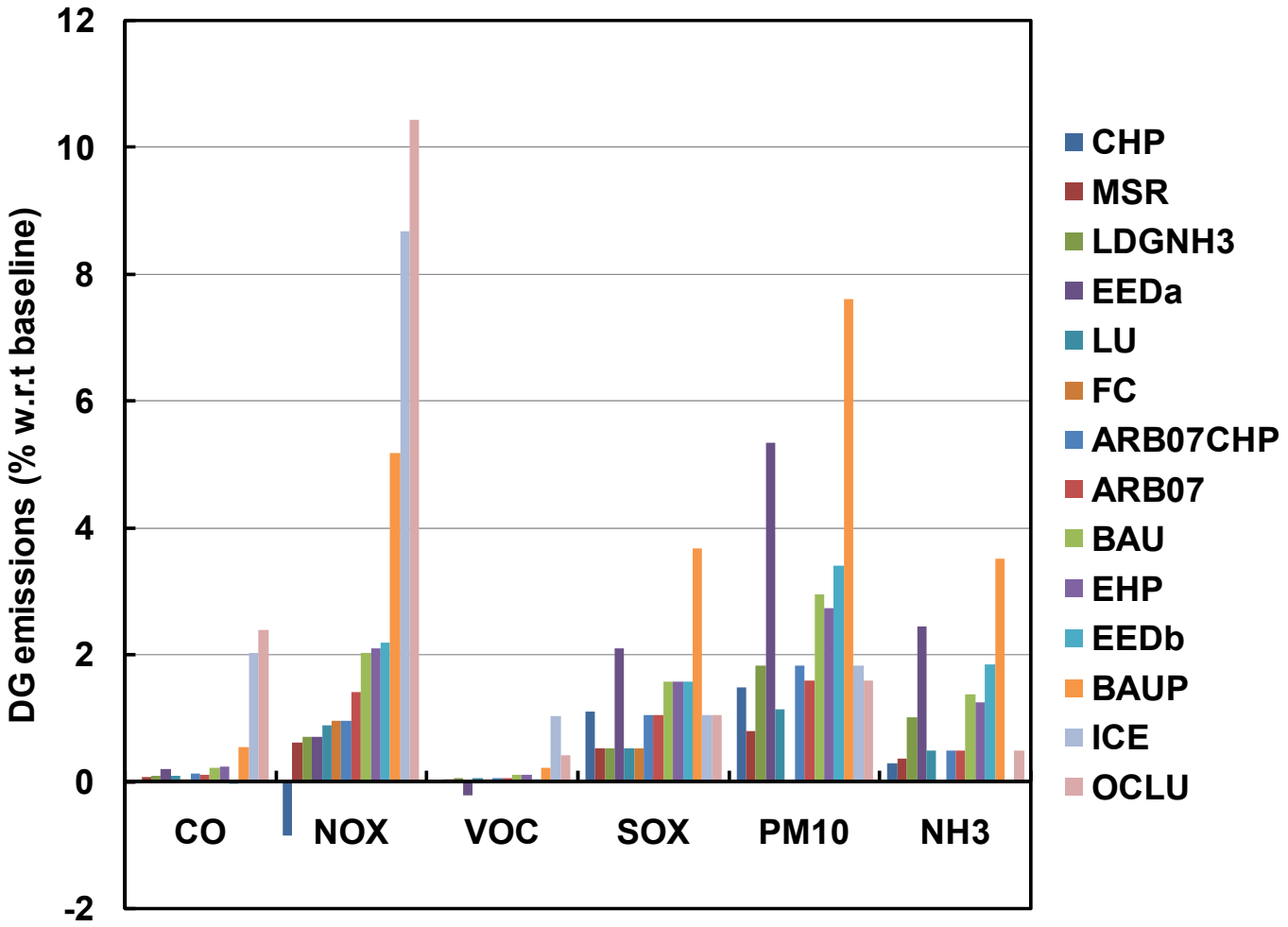


**ARB07:** Penetration: 18% of increased demand, all DG operating at ARB 2007 levels
**ARB07CHP:** Penetration: 18% of increased demand, all DG operating at ARB 2007 levels with CHP emission credits for 50% CHP utilization and 60% heat recovery (same as realistic scenarios)
**BAU:** Linear Business-as-usual projection of DG penetration and DG mix
**BAUP:** Parabolic Business-as-usual projection of DG penetration and DG mix
**CHP:** All DG with CHP, realistic DG mix, Penetration: 18% increased demand
**EEDa,b:** Existing central power plants substituted by DG, realistic DG mix
**EHP:** Penetration: 45% of increased demand, realistic DG mix
**FC:** Penetration: 18% of increased demand, all fuel cell DG
**BACT:** Penetration: 18% of increased demand, all DG are ICE operating at 2007 BACT levels
**LDGNH3:** Penetration: 18% of increased demand, all large gas turbines with $NH_3$ slip
**LU:** Penetration: 18% of increased demand, realistic DG mix, land-use spatial distribution
**MSR:** Penetration: 18% of increased demand, High penetration of PV, land-use spatial distribution
**OCLU:** Penetration: 18% of increased demand, realistic DG mix and spatial distribution, ICE emissions out of compliance

**Figure 23. Basinwide daily emissions from DG in different spanning scenarios for the year 2030, in % with respect to total baseline emissions for 2030**

### 3.1.4. Long-Term Spanning DG Scenarios: 20XX Scenarios

The scenarios that are considered in 20XX include paradigm and technology shifts that are very significant with regard to energy utilization and transmission. These technological advances imply changes in how electricity is generated and utilized. As a result, implementation of these scenarios affects significantly the amount and speciation of emissions in the SoCAB.

This section analyzes the effect that widespread use of electric vehicles could have on the electricity demand and the resulting impacts on air emissions and air quality in future years. Predicting the outcomes for such futuristic technologies is wrought with high levels of uncertainty. However, these types of scenarios sets bounds to emissions reductions from automobile sources and is a basis for sensitivity analyses of emissions to determine air quality impacts projections in the future. The following section provides a scenario for generating electricity in the future.

Even though predicting futuristic outcomes is difficult, many of the important scientific consequences of significant paradigm or technological changes must be considered before policies allow implementation of such. As a result, we propose to address the important scientific issues associated with the potential air quality impacts of quite futuristic scenarios. We will accept and address the issues of uncertainty with significant and detailed uncertainty and sensitivity analyses.

#### *Scenario 20XXEVDG: 20XX Power Generation for Pure Electric Vehicles With DG*

The electricity needed to power the automobile fleet is provided by DG installed in the SoCAB. Consequently, this scenario includes emissions related to production of electricity by DG inside the SoCAB, to power the electric vehicles. The amount of energy required by the fleet is $5.37\times10^{8}$ MJ/day ($1.96\times10^{11}$ MJ/yr as shown in Table 19). Battery electric vehicles are three times more efficient than conventional gasoline vehicles (Idaho National Laboratory 2006), resulting in electric motor efficiency of 50%. As a result, the daily amount of electrical energy supply adds up to $1.07\times10^{9}$ MJ/day ($3.91\times10^{11}$ MJ/yr). If electricity is supplied by central generation, the total electricity daily needs increase to $1.15\times10^{9}$ MJ/day ($4.21\times10^{11}$ MJ/yr) due to electricity transmission losses of approximately 7% (California Energy Commission 2005a). This scenario assumes that future electric vehicles (EV) will have a mileage range long enough to meet the average daily range, and as a result, one recharging per day per vehicle will be sufficient. As discussed in Section 2.1.8, the total capacity needed for recharge the entire fleet is 20 GW. In this scenario, this power is provided by a mix of DG that includes 50% of large gas turbines, 9% high-temperature fuel cells, 1% of low-temperature fuel cells, and 40% photovoltaic units, which are spread throughout the SoCAB following land use distribution. The photovoltaic systems include advanced storage to maintain the overall technology mix during the night charging cycle. The resulting emissions from this mix are presented in Table 44. The technology mix is only an arbitrary instance for power generation dedicated to electric automobiles. A high percentage of renewable technologies was selected because there is the synergistic opportunity to combine them with vehicle-to-grid technologies to stabilize the intermittency of renewable sources. In addition, fuel cells and gas turbines are capable to provide stable electricity

production, and in the case of gas turbines, fast response for steep increases in power demand. Internal combustion engines were excluded from this case because of their high emissions.

**Table 44. Emissions from distributed power generation to produce electricity for a pure electric vehicle fleet in the SoCAB by the year 2040 (in tons per day)**

| | $NO_X$ | VOC | CO | $SO_2$ | $PM_{2.5}$ |
|---|---|---|---|---|---|
| Distributed Generation | 6.72 | 1.84 | 9.07 | 0.77 | 7.85 |

Removing emissions from on-road mobile sources reduces the total basinwide emissions. However, new emissions from power generation are introduced in the basin, which offsets some off the emission reductions attributable to electric vehicle use. Table 45 presents the baseline emissions for 20XX and the basinwide emissions of the pure electric vehicles scenarios with distributed generation of electricity. The scenario with production of electricity with a mix of DG reduces emission of $NO_X$, VOC, CO, and $PM_{2.5}$ with respect to baseline 20XX emissions by 17%, 16%, 29% and 8%, respectively. On the other hand, $SO_X$ emissions in the case with DG increase by 2%.

**Table 45. Net basinwide emissions (tons/day) of the baseline 20XX scenario and the pure electric vehicle scenarios with electricity production via distributed generation**

| | $NO_X$ | VOC | CO | $SO_2$ | $PM_{2.5}$ |
|---|---|---|---|---|---|
| Baseline 20XX | 97.0 | 385.0 | 1669.0 | 19.0 | 91.0 |
| 20XXEVDG | 80.1 | 322.7 | 1180.8 | 19.4 | 83.8 |

## 3.2. DG Scenarios in the SJVAB

The DG scenarios that are developed for the SJVAB are classified as follows: (1) one baseline scenario without DG emissions for the target year 2023, (2) four realistic DG scenarios, (3) nine spanning DG scenarios, and (4) six DG scenarios that consider biomass technologies. These DG Scenarios are described below.

### *3.2.1. Baseline Scenario in the SJV*

#### *Scenario SJV-B1*

The ultimate objective of this study is to assess impacts of DG on regional air quality for a future year for various scenarios. Therefore, a future year base case is needed to benchmark the impacts from various DG scenarios. Spatially resolved emission inventories for future years is an important component of data that is required to predict future air quality. The year 2023 is a landmark year for SJV, because the district needs to achieve compliance with the federal 8-hour ozone standard by that year. Accordingly, the ARB and the SJVAPCD have conducted

modeling studies for the year 2023. Recently, SJVAPCD released the U.S. EPA-mandated plan that outlines the path towards the attainment of the 8-hour federal ozone standard by 2023. Therefore, the year 2023 is selected to analyze DG in the SJV.

Figure 24 shows expected $NO_X$ reductions from implementation of this plan. It is expected that total $NO_X$ emissions come down to 160 tons per day by the year 2023. Modeling studies conducted by SJVAPCD have shown that ozone concentration in the basin is more sensitive to $NO_X$ reductions than VOC reductions. Hence, the plan calls for significant reduction in $NO_X$ emissions. The VOC reductions are shown to be important in early stages of the plan. Total VOC emissions per day in the valley by 2023 are expected to be at 355 tons per day.

The future year base case for the current DG study is developed based on estimates presented in this air quality management plan (AQMP). Basinwide emissions from the 2000 inventory are scaled such that total $NO_X$ emissions are 160 tons per day and VOC emissions are 355 tons per day. This methodology was endorsed by participants from DG workshop held in Fresno on April 27, 2007.

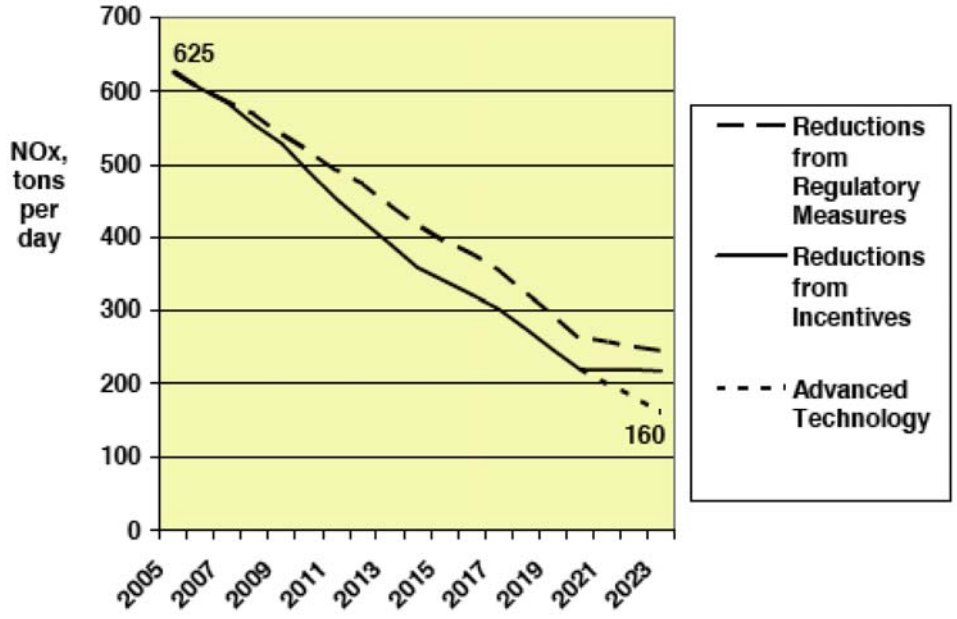


**Figure 24. Reduction in $NO_X$ emissions as proposed in the SJV ozone attainment plan**
Source: SJVAPCD

### *3.2.2. Realistic Scenarios in the SJV*

#### *Scenario SJV-R1*

This realistic scenario SJV-R1 is the basis for the other three realistic scenarios, which only incorporate variations in one of the parameters described here. This scenario makes use of all the resources available to justify DG overall penetration, DG power, and DG mix in each of the discretized cells of the air quality model. This particular scenario assumes a relatively medium early adoption for DG, meaning that the cumulative DG power implemented and operating in

the SJVAB is following a linear trend from 2007 to 2023. Accordingly, this case assumes a DG penetration of 12% of the increased power. In addition, this scenario assumes a realistic duty cycle based on average electric hourly profiles for various energy sectors and displacement of emissions due to the heat recovery mode of most of the units installed. Table 46 presents the primary factors that contribute to the overall definition of the realistic scenario SJV-R1. Figure 25a presents the distribution of DG technology assumed in realistic scenario SJV-R1. This DG technology mix is a result of applying the 10-step methodology that uses DG market studies and land-use information to allocate DG technologies in the SJVAB. Figure 26 presents the distribution of technologies by size class amongst the various land-use sectors considered in the SJVAB.

**Table 46. Factors that contribute to the definition of realistic scenario SJV-R1**

| | |
|---|---|
| Factor 1.1 | Limited DG penetration, 12% of increased power |
| Factor 2.1.6 | Different mix of Certified DG in each cell based on the systematic approach to relate GIS land use data to DG mix |
| Factor 3.1.1 | Known emissions factors: literature, data, certified levels (upper bound) |
| Factor 4.4 | Different DG power in each cell based on the systematic approach to relate land use GIS data to spatial distribution of DG power |
| Factor 5.3 | Realistic duty cycle for every sector based on PG&E and SCE data |
| Factor 6.3 | CHP Emissions Displaced |
| Factor 7.1.1 | PM and VOC speciation from ARB data |
| Factor 7.2 | No performance degradation |
| Factor 7.3 | No geometrical features (All DG emitting at ground level) |
| Factor 7.4.3 | Medium Early Adoption of DG Power (linear trend) |

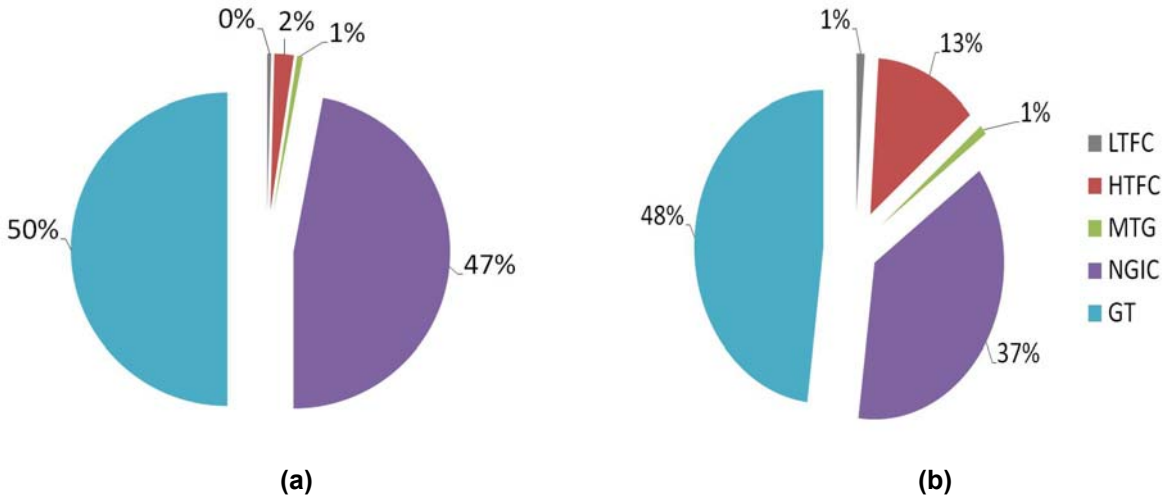


**Figure 25. DG mix obtained using the 10-step methodology: (a) DG mix in the SJV obtained using DG market penetration for the base case in the EPRI (2005) report for the year 2023, and (b) DG mix in the SJV obtained using the High R&D case in the EPRI (2005) report for the year 2023**

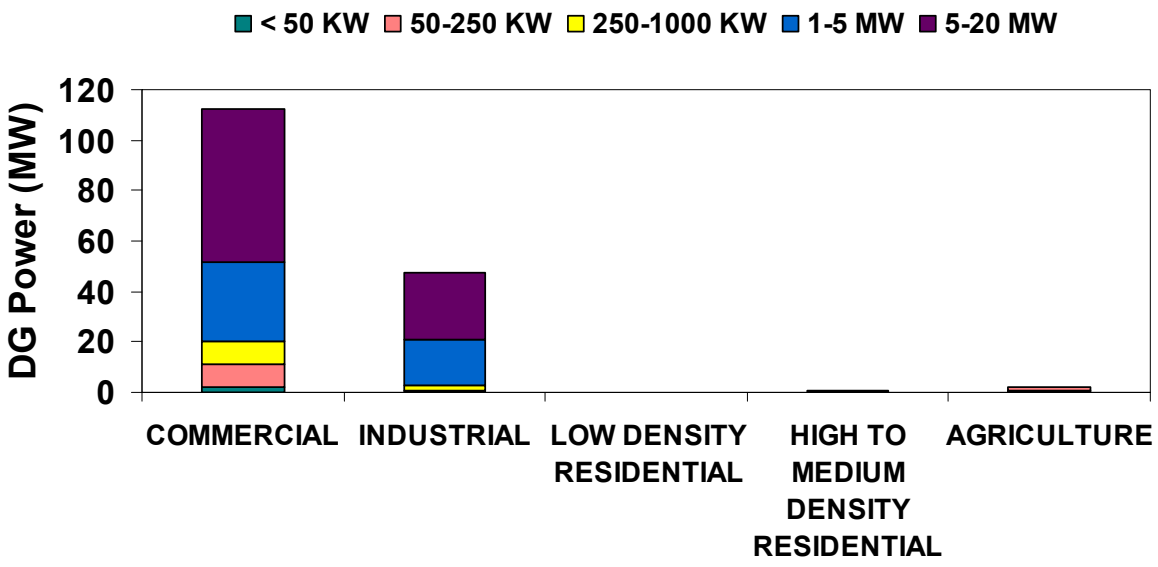


**Figure 26. Distribution of technologies by size class amongst the various land-use sectors considered in the SJVAB**

Realistic DG Emissions Spatial Distribution in the SJV

The spatial distribution of changes in ground-level $NO_X$ emissions due to DG installations for the realistic scenario SJV-R1 in the year 2023 is presented in Figure 27. Emissions are mainly concentrated in the areas around urban centers in the SJV: Bakersfield, Visalia, Fresno, and Stockton. This distribution is a result of applying the 10-step methodology to generate a realistic implementation of DG in the San Joaquin Valley Air Basin.

Scenario SJV-R1 assumes emissions displacement due to combined heating and power. The values assumed for CHP utilization ($f_{CHP}$) and waste heat use ($f_{HR}$) are 60% and 50%, respectively. The resulting emissions offsets due to CHP use are higher than the emissions introduced by DG, and as a result, net emissions from DG in this scenario are negative in many parts of the basin. The only emissions displacement considered in the realistic DG scenarios is that resulting from combined heating and power.

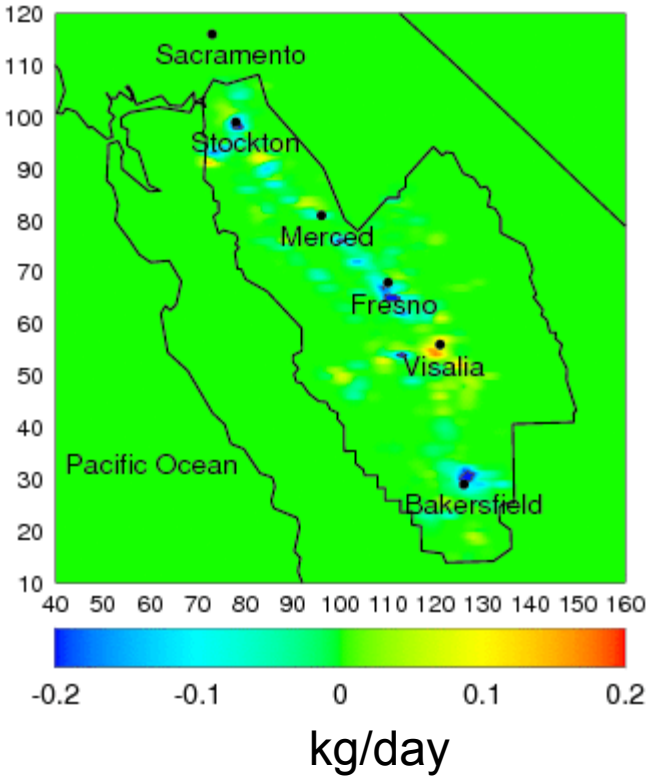


**Figure 27. DG $NO_X$ emissions for realistic scenario SJV-R1**

### *Scenario SJV-R2: High Penetration (18%) Version of SJV-R1*

All of the parameters and factors, except one, that went into developing scenario SJV-R1 were also used to develop scenario SJV-R2. The one parameter that was changed in this case is the DG penetration parameter, which is set to a higher value (18% of the increased power demand is met by DG in 2023) to account for the uncertainty associated with the future market penetration of DG in the SJVAB.

### *Scenario SJV-R3: High Research and Development for DG Technologies*

This scenario is based on the DG technology mix and DG penetration estimated in the EPRI (2005) report for a High R&D for DG scenario. The High R&D scenario assumes an accelerated technology development that leads to a higher DG market penetration of fuel cells. The total penetration assumed for this scenario is 23% of increased demand between 2007 and 2023. The technology mix assumed for scenario SJV-R3 is presented in Figure 25b. The rest of parameters are the same as the ones assumed in scenario SJV-R1.

### *Scenario SJV-R4: High Deployment of Fuel Cells Due to Environmental Forcing*

Scenario SJV-R4 assumes that there will be a need for further reducing greenhouse gas emissions and, consequently, market penetration of high efficiency DG technologies will be favored. In particular, scenario SJV-R4 assumes a penetration of fuel cells that is two times higher than the penetration in scenario SJV-R3. A corresponding reduced market penetration of the rest of fuel-driven technologies is assumed in this case. The total DG market penetration in

scenario SJV-R4 equals the total DG market penetration in scenario SJV-R3, representing 23% of the increased power demand from 2007 to 2023. Emissions in tons per day from all realistic scenarios are summarized in Table 47, and are presented graphically in Figure 28.

**Table 47. Daily basinwide pollutant emissions, in tons per day, from DG with CHP for all realistic scenarios in the San Joaquin Valley**

| Scenario | Electricity produced by DG (MW) | Emissions (ton/day) | | | | | | |
|---|---|---|---|---|---|---|---|---|
| | | CO | $NO_X$ | VOC | $SO_X$ | $PM_{2.5}$ | $NH_3$ | $CO_2$ |
| **SJV-R1** | 269 | 0.23 | 0.11 | 0.02 | 0.01 | 0.08 | 0.08 | 1854 |
| **SJV-R2** | 373 | 0.32 | 0.15 | 0.03 | 0.01 | 0.11 | 0.11 | 2571 |
| **SJV-R3** | 477 | 0.37 | 0.17 | 0.03 | 0.01 | 0.14 | 0.13 | 3261 |
| **SJV-R4** | 477 | 0.34 | 0.16 | 0.03 | 0.01 | 0.13 | 0.12 | 3216 |

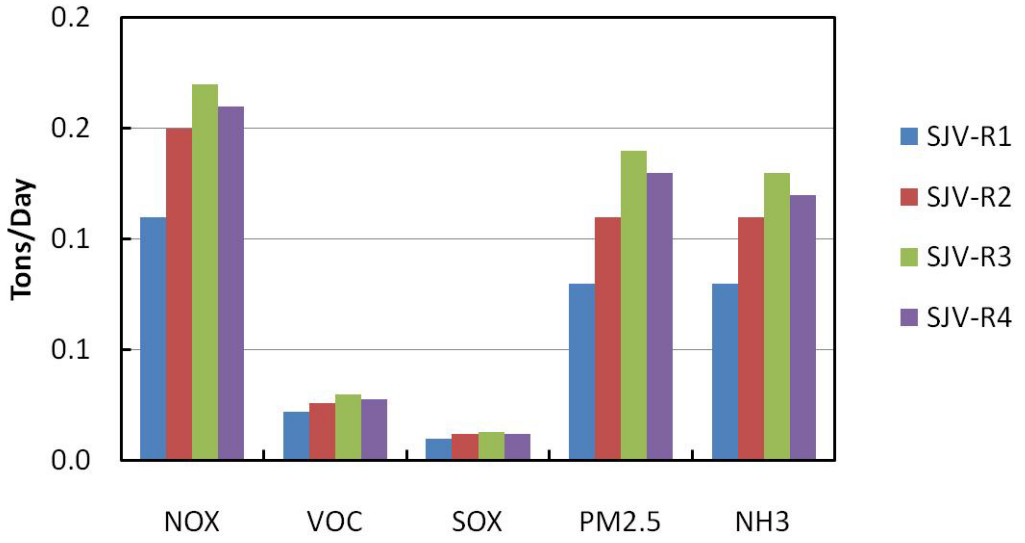


**SJV-R1:** Realistic DG mix and spatial distribution, Penetration: 12% increased demand
**SJV-R2:** Realistic DG mix and spatial distribution, Penetration: 18% increased demand
**SJV-R3:** Realistic spatial distribution and high R&D DG mix, Penetration: 23% increased demand
**SJV-R4:** Realistic spatial distribution and high deployment of fuel cells, Penetration: 23% increased demand

**Figure 28. Basinwide daily emissions from DG in all realistic scenarios for the year 2023**

### 3.2.3. Spanning DG Scenarios in the SJV

In the spanning DG scenarios, most of the complexity involved in the development of a realistic, very detailed scenario (i.e., the developed 10-step methodology described previously) is not used. As a result one can relatively quickly develop some scenarios that can be insightful for scientific completeness, sensitivity analyses, and/or determination of potential impacts for unexpected outcomes.

#### *Scenario NOCHP: Land-Use Weighted Scenario*

Scenario NOCHP contains a land-use weighted spatial distribution of emissions from an aggregated mix of DG technologies that is the same as in realistic scenario SJV-R1 (see Figure 25a) and with an overall DG penetration of 18% of the increase in power demand between 2007 and 2023. Land use distribution is obtained and processed as described in Section 2.2.3. However, this scenario assumes that all DG units operate in baseloaded mode (i.e., constantly 24 hours per day). In addition, no emissions displacement due to CHP is assumed here. Each of the remaining spanning scenarios incorporates a major variation to one of the parameters of this scenario.

#### *Scenario SJV-ARB07: Certified Levels for All DG Units*

Scenario SJV-ARB07 assumes the same parameters as in scenario NOCHP, except for the emission factors for DG technologies. In this case, all DG units emit at the 2007 ARB emissions standards, regardless of whether any technology can emit at a lower rate.

#### *Scenario ICE-BACT: Permitted Levels for ICEs*

Scenario ICE-BACT contains a land-use weighted spatial distribution of emissions from DG technologies that are all assumed to emit pollutants at the best available control technology (BACT) levels for internal combustion engines (ICE) in effect in 2007 for the SJVAPCD.

#### *Scenario ALLCHP: All DG Units With CHP*

Scenario ALLCHP assumes the same parameters as in scenario NOCHP: land-use weighted spatial distribution, same DG mix, baseload operation, and DG penetration equals to 40% (high market penetration) of the increased demand between 2007 and 2023. In addition, this scenario assumes that all DG units use CHP with appropriate emissions displacement for such technology being applied. This scenario is viewed as a significantly higher penetration of DG technologies due to higher realization of CHP benefits.

#### *Scenario SJV-EHP: Extra-High Penetration*

Scenario SJV-EHP assumes an extra-high DG penetration that accounts for meeting 45% of the increased power demand from 2007 to 2023. According to a report by EPRI (2005), this level of penetration could be met if there were an increased level of incentives for DG installations and export of electricity were allowed. The DG mix and spatial distribution for this scenario are the same as in scenario NOCHP.

#### *Scenario SJV-PeakTot: Peaking Total Power*

Scenario SJV-PeakTot assumes that all of the DG technologies (same "aggregate mix" of various technologies as in S1) are operating as peaking units (operating only between noon and 6 p.m.)

with a total electricity produced that equals 18% of the increase in power demand between 2007 and 2023.

### *Scenario OCR: Out-of-Compliance Version of Realistic Scenario SJV-R3*

The SCAQMD in the SoCAB has detected through inspections that a large number of permitted internal combustion engine DG units emit at levels that are out of compliance with the applicable BACT emission standards after some time of operation. Scenario OCR assumes the same parameters as in SJV-R3, except for the emissions factors that are applied to the ICE installations. The AQMD reports a potential increase in emissions with respect to the standards of 300% (three times) if all the inspected units are included in the average levels. If only the non-compliant units are accounted for, the potential increase in emissions corresponds to a factor of 6.7 for $NO_x$ and 11.7 for CO.

The scenario OCR takes this possibility of non-compliance into account by assuming similar conditions may apply in the SJVAB. To account for non-compliance, the emissions factors assumed for ICE in this scenario are the emission factors of non-compliant ICE reported by the AQMD. The emissions factors for the rest of the DG technologies are the same as in the realistic scenarios. That is, all DG are emitting at regular levels, except all ICE DG units, which are emitting at three times the levels of the BACT emission standards valid in the SJVAPCD in 2007.

### *Scenario LSD1: Large-Scale Deployment Scenario 1*

In scenarios LSD1, LSD2 and LSD3, DG impacts are compared with those from central generation at equivalent levels of power generation capacity. DG spatial distribution is determined based on land-use data as in realistic scenarios. In this scenario the "aggregated DG mix" is used to predict the technology distribution of DG deployment. The amount of power installed is based on recent trends of central plant power generation in the SJVAB.

In scenario LSD1 a total of 1200 MW power is assumed to be supplied by DG technologies. This capacity is equivalent to a central power plant that became operational in the SJVAB in the year 2005.

### *Scenario LSD2: Large-Scale Deployment Scenario 2*

This scenario assumes same parameters as scenario LSD1, except that emissions of ICEs are assumed to be at the existing BACT levels in 2007 in the SJV. Thus this scenario has total installed DG capacity of 1200 MW, however all DG units are operating at a maximum permissible levels of emissions.

### *Scenario LSD3: Large-Scale Deployment Scenario 3*

In this scenario, total DG power installed is 1800 MW. This is equivalent to two recent central plants that became operational in the SJVAB. This scenario assumed the "aggregate DG mix" for technology distribution.

### *Spanning Scenario Pollutant Emissions Rates and Summary*

Table 48, Figure 29, and Figure 30 show the basinwide daily emissions from DG in tons per day. As expected, emissions from scenarios that assume out-of-compliance and maximum allowed emissions (BACT) generate the highest emissions levels for moderate DG penetration. These

scenarios are followed by large-scale deployment scenarios, which use lower emitting and more realistic DG emissions rates, but that assume a much higher market penetration of DG technologies.

**Table 48. Daily basinwide pollutant emissions, in tons per day, from DG for spanning scenarios for year 2023**

| Scenario | Electricity produced by DG (MW) | Emission (ton/day) | | | | | |
|---|---|---|---|---|---|---|---|
| | | CO | $NO_X$ | VOC | $NH_3$ | $SO_X$ | $PM_{2.5}$ |
| **NOCHP** | 373.3 | 0.34 | 0.19 | 0.03 | 0.12 | 0.02 | 0.16 |
| **SJV-ARB07** | 373.3 | 0.41 | 0.28 | 0.04 | 0.12 | 0.03 | 0.24 |
| **ICE-BACT** | 373.3 | 7.21 | 1.80 | 0.77 | 0.00 | 0.04 | 0.29 |
| **ALLCHP** | 829.6 | -0.36 | -1.06 | -0.04 | 0.28 | 0.02 | 0.00 |
| **SJV-EHP** | 933.3 | 0.85 | 0.49 | 0.08 | 0.31 | 0.05 | 0.40 |
| **SJV-PeakTot** | 373.3 | 0.34 | 0.20 | 0.03 | 0.12 | 0.02 | 0.16 |
| **OCR** | 373.3 | 10.72 | 2.70 | 0.39 | 0.12 | 0.03 | 0.27 |
| **LSD1** | 1200.0 | 1.10 | 0.63 | 0.10 | 0.40 | 0.07 | 0.51 |
| **LSD2** | 1200.0 | 23.17 | 5.79 | 2.49 | 0.00 | 0.11 | 0.92 |
| **LSD3** | 1800.0 | 1.64 | 0.94 | 0.15 | 0.60 | 0.11 | 0.76 |

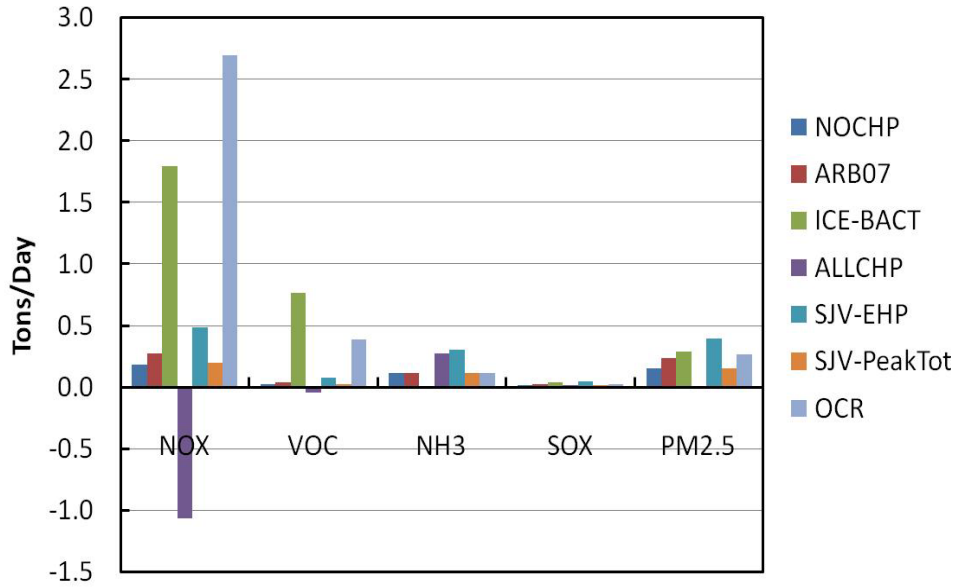


**Figure 29. Basinwide daily emissions from DG in different spanning scenarios**

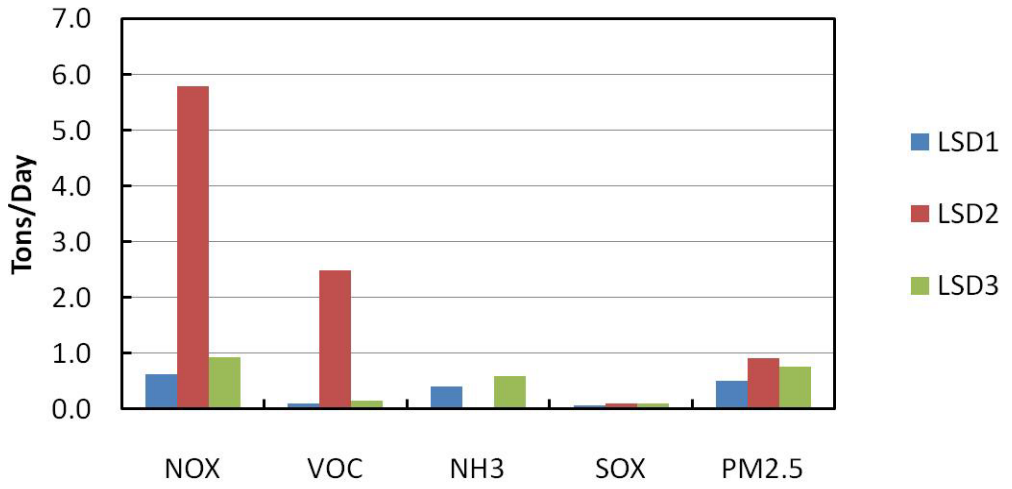


**Figure 30. Basinwide daily emissions from DG in different spanning scenarios**

### *3.2.4. Biomass DG Scenarios in the SJV*

Biomass electricity has the potential to play a major role in the future of California's power sector. Availability of diverse and large biomass resources, coupled with favorable policy outlook could lead to a significant addition of biomass generation capacity in California.

Currently, biomass power accounts for less than 3% of total in-state electricity generation. According to gross system power data reported by the California Energy Commission (2007b), 30,514 gigawatt-hours (GWh) of in-state electricity production was generated from renewables in 2006. As shown in Figure 31, this represents 13.3% of total in-state electricity production. The biomass power constitutes 18.8% of all renewable electricity that is generated in California, as shown in Figure 32.

Biomass electricity can be included as any other distributed generation technology. The size of biomass plants is typically smaller than 50 MW and these units can achieve higher overall efficiencies through the application of CHP. However, the future adoption of biomass power leads to an increase in emissions and may affect the regional air quality. In this section, future scenarios of biomass power are developed for the SJV region. These scenarios are implemented in the air quality models to study ozone and PM impacts.

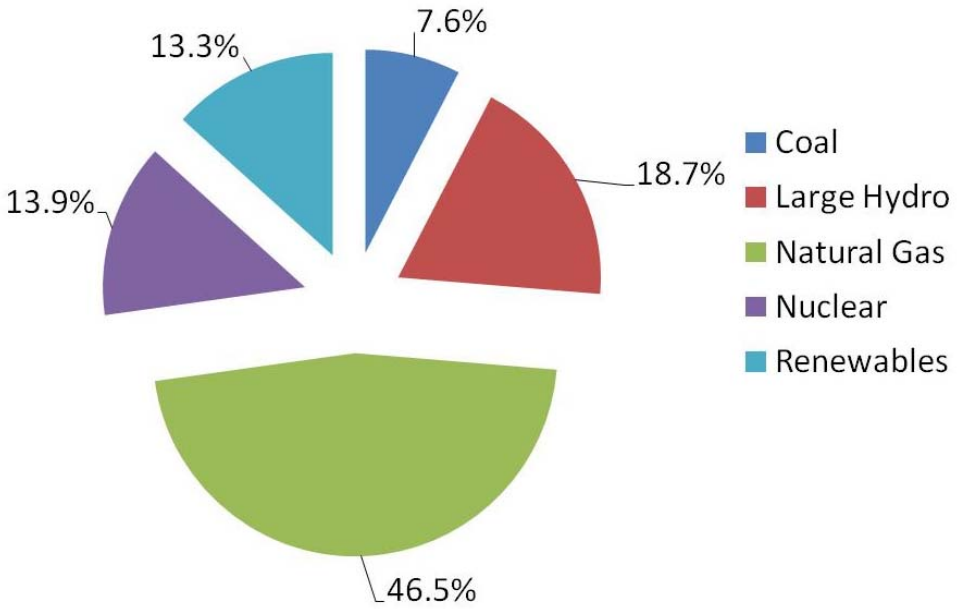


**Figure 31. Fuel mix of in-state electricity generation in California for the year 2006**
Source: California Energy Commission 2007b

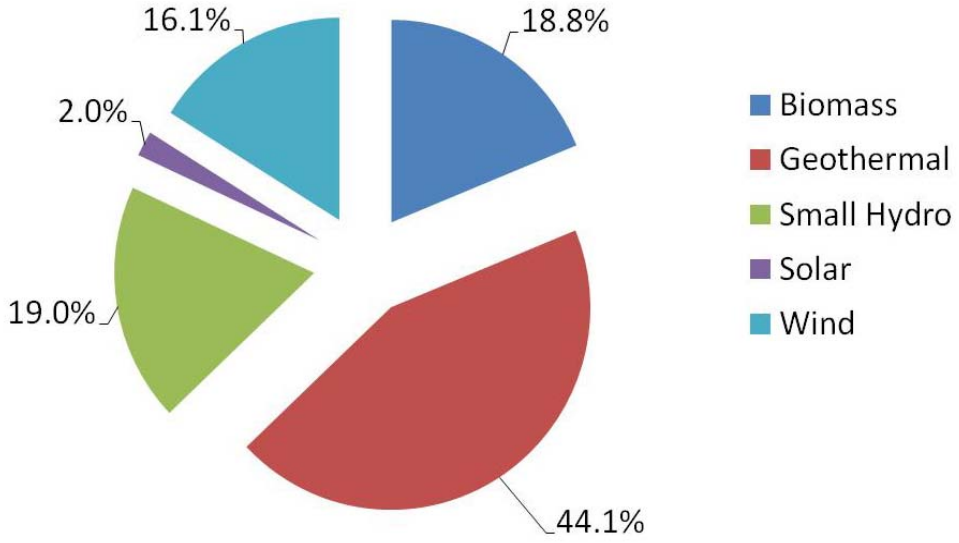


**Figure 32. Resource mix of in-state renewable electricity generation in California for the year 2006**

Source: California Energy Commission 2007b

### *Biomass Power Scenarios Development Methodology*

In order to characterize biomass scenarios and develop spatial and temporal emissions from such scenarios, a set of parameters needs to be considered that affect the extent of future biomass power in California. These parameters are: (1) aggregate power from biomass technologies, (2) spatial distribution of biomass power and location of biomass plants, (3) biomass technologies employed and emission factors for those technologies, and finally, (4) any emissions that are offset due to biomass power. Each of these parameters is described in this section.

Aggregate Power

A major driver for the development of biomass power in California is the state's renewable portfolio standard (RPS). The current RPS mandates that 20% of all retail electricity sales in California must be from renewable sources by 2010. Furthermore, the goal is to increase the share of renewables to 33% of all retail electricity sales by 2020. This will directly provide incentives to biomass power as the demand for renewable electricity from utility companies increases to comply with the RPS standard. However, biomass power has to compete with other renewables such as wind and solar power for incentives from RPS goals. Legislation to reduce GHG emissions could also lead to increased adoption of biomass power, which has significantly less net GHG emissions.

Table 49 shows an electricity demand forecast for the years 2017 and 2023 and average system power for the State of California. The demand for electricity consumption is expected to increase at an average rate of 1.29 % for years between 2008 and 2018 (California Energy Commission 2007a). This rate of increase is used to further extrapolate electricity consumption demand for the year 2023. This forecasted consumption demand translates to an average power demand of 37 GW and 44 GW in years 2017 and 2023, respectively.

Assuming that the RPS goal of 33% retail electricity demand is achieved, renewable power in California is projected to be 12.2 GW and 14.6 GW in years 2017 and 2023, respectively, as shown in Table 49. Furthermore, assuming that the biomass fraction of renewable power is maintained at 20%—near the current level—the projected biomass power in California is 2.4 GW and 2.9 GW for the years 2017 and 2023, respectively. Accounting for the currently installed biomass power capacity of 968 MW in California (California Energy Commission 2006), this would require capacity additions of 1.5 and 2.0 GW by the years 2017 and 2023. Therefore, new biomass power capacity addition is calculated based on the average power forecast, RPS goals, and the share of biomass power among all renewables.

**Table 49. Projections of statewide biomass power in California**

| Year | Electricity Demand (GWh) | Average Power (MW) | Generation from Renewables (33% RPS) (MW) | Biomass Power (MW) assuming 20% of Renewable power | Existing Biomass Capacity (MW) | Additional Biomass Capacity Addition (MW) |
|---|---|---|---|---|---|---|
| **2008** | 288976 | 32988 | | | 968 | |
| **2017** | 324310 | 37021 | 12216 | 2443 | 968 | 1475 |
| **2023** | 388055 | 44298 | 14618 | 2924 | 968 | 1956 |

*Spatial Distribution*

The spatial distribution of biomass power depends significantly on resource availability. Since the cost of transporting fuel is a major component of biomass electricity overall cost (NREL 2003b), biomass plants are usually located in the close proximity of resource base. Therefore it is expected that new biomass capacity additions will occur based on spatial distribution of future biomass resources availability.

A recent study by the California Energy Commission comprehensively evaluated total biomass resources that are available in the future and how it is distributed statewide across major categories (California Energy Commission 2006). This study estimates that generation potential from all biomass sources in California could exceed 7000 MWe by the year 2020.

Figure 33 shows distribution of this resource base among four major categories. Municipal waste includes biomass fraction of municipal solid waste (MSW), biosolids from waste water treatment operations, landfill and digester gases. Municipal waste is a major biomass resource that is available at large population centers in the state, such as Los Angeles area. Animal manure results from agricultural animal operations for diary and meat production. This is a major type of biomass resource that is available in the San Joaquin Valley. Agricultural residue biomass constitutes wood residue from crops (orchard and vineyards, field and seed, and vegetable) and food processing residues. The highest concentration of agricultural residue biomass from crops is present in the SJV due to extensive agricultural operations in the area. Forestry biomass includes mill residues, forest thinning, logging slash, and chaparral. This category of resource is mostly concentrated in the northwest region of the state.

Future biomass resource estimates for all counties are available from the Energy Commission study (California Energy Commission 2006) for the years 2017 and 2020. This data is used to predict spatial distribution of future biomass capacity addition using the expression below.

$$\mathbf{BP_{r,f} = BP_{tot} * BR_{r,f} / BR_{tot}}$$

Where $BP_{r,f}$ is projected biomass power in region r from resource type f, $BR_{r,f}$ is estimated biomass resource available in region r of type f, $BP_{tot}$ is total biomass power projected statewide, and $BR_{tot}$ is total biomass resources available in the state.

Assuming that the total statewide new biomass capacity addition is 2.0 GW and using estimated resource availability on a county-wide basis from California Energy Commission (2006), future biomass power in each of the SJV counties is estimated from major resources categories. As shown in Table 50, Fresno County is estimated to have potential for the highest biomass capacity addition at 68.8 MW, followed by Kern and Tulare counties. The future capacity addition based on RPS goals represents only a fraction of biomass resources that are estimated to be available if the share of biomass power remains as today. Assuming a 33% RPS goal, and a 20% share of biomass among all renewables, only 27% of biomass resources are used for power generation.

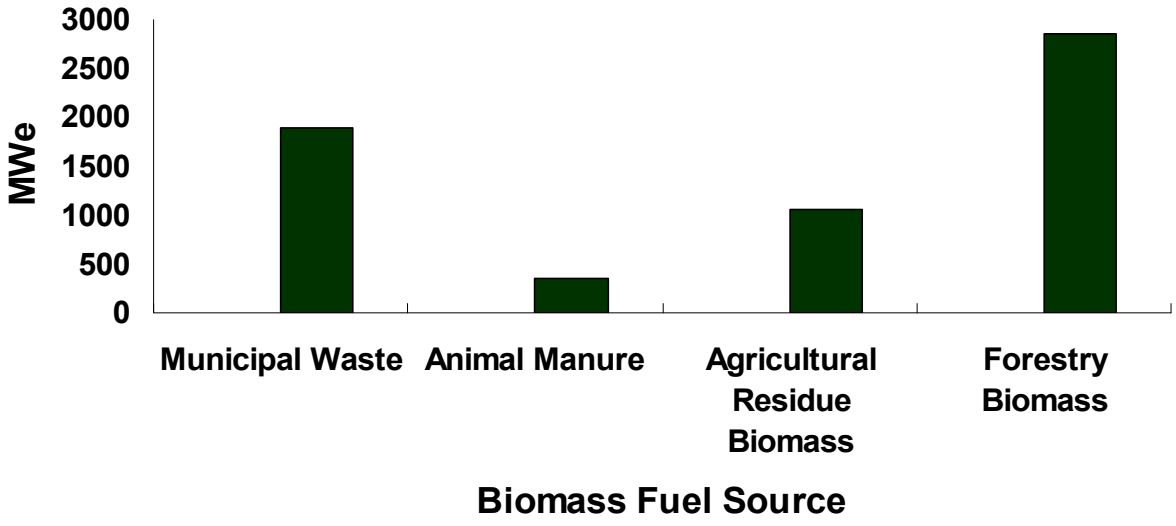


**Figure 33. Estimated biomass fuel availability in California in the year 2020**

Source: California Energy Commission 2006

**Table 50. Projected biomass power (in MW) in the SJV in 2023, assuming 33% of renewables and 20% share of biomass among renewable technologies**

| | Municipal Waste | Animal Manure | Agricultural Residue Biomass | Forestry Biomass | Total |
|---|---|---|---|---|---|
| **Fresno** | 11.2 | 8.7 | 34.7 | 14.2 | 68.8 |
| **Kern** | 10.7 | 5.2 | 25.4 | 12.3 | 53.5 |
| **Kings** | 1.6 | 6.3 | 9.8 | 0.0 | 17.8 |
| **Madera** | 1.6 | 3.3 | 13.1 | 10.7 | 28.7 |
| **Merced** | 4.1 | 12.6 | 15.8 | 0.0 | 32.5 |
| **San Joaquin** | 11.7 | 5.5 | 24.0 | 0.0 | 41.3 |
| **Stanislaus** | 7.4 | 8.5 | 14.5 | 0.5 | 30.9 |
| **Tulare** | 6.0 | 18.0 | 17.5 | 11.2 | 52.7 |
| **Total** | 54.3 | 68.1 | 154.8 | 48.9 | 326.2 |

The previous analysis provides projections of biomass capacity on a county-wide basis. However, in order to evaluate air quality impacts, the information on locations of biomass plants is also needed. The methodology to develop DG scenarios employs land-use data to predict DG emissions in the individual cells. A similar approach is adopted here. Based on the land-use, more than 40 model cells (with each cell 4 km x 4 km in resolution) are identified as potential sites that could include biomass emissions in the future. These cells are chosen so that they are in agricultural regions, yet in the proximity of industrial facilities. The potential locations of biomass plants that are selected based on land-use information are show in Figure 34.

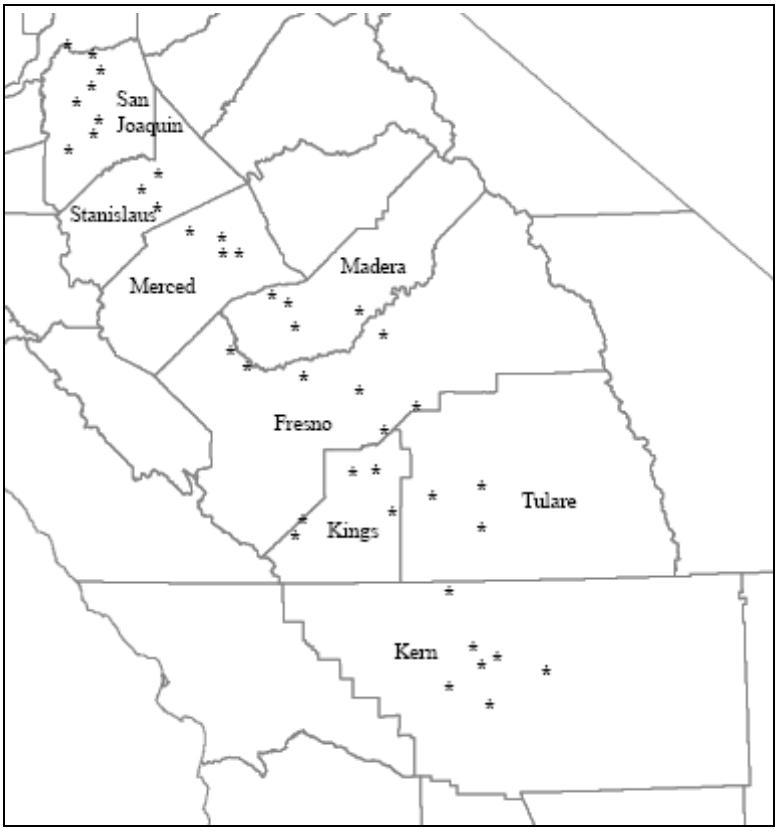


**Figure 34. Potential future biomass sites in the SJV that are selected based on land-use information**

*Biomass Power Technologies*

The major technologies that are used to produce electricity from biomass include steam and gas turbines, reciprocating engines, and fuel cells. Currently, steam turbines remain as the dominant technology for biomass electricity generation. Direct combustion of biomass is used to produce steam that drives a turbine generator. This technology offers flexibility in the choice of biomass fuel and possible co-firing using conventional fuels such as natural gas. As shown in Figure 35, direct combustion accounts for more than 72% of biomass electricity that is generated today (Biomass Collaborative 2008). Followed by direct combustion, gasification of biomass is another major route of energy conversion for biomass. Producer gas that is produced from biomass is used to drive gas turbines, reciprocating engines, and fuel cells.

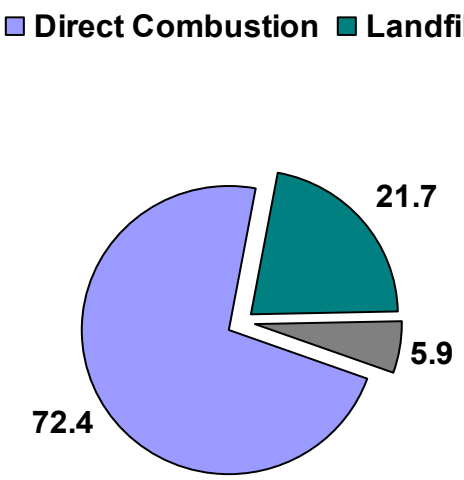


**Figure 35. Distribution of combustion technologies currently employed for generating biomass electricity (in %)**

Source: Biomass Collaborative 2008

The size of biomass plants vary widely, depending on the availability of biomass fuel and technologies employed. Direct combustion plants are usually smaller than 50 MW. The majority of plants that are currently in operation are between 5 MW and 25 MW. This study analyzes a set of scenarios that incorporate plant sizes of different ranges.

This study assumes that the direct combustion of biomass combined with steam turbines remains as the dominant technology for future biomass electricity. However, biomass presents opportunities to deploy advanced energy technologies to utilize digester gas from agricultural operations. In this study, fuel cells are considered as an option to produce electricity from animal manure. A series of scenarios is developed to analyze the effect that preferential adoption of different technologies could have on air emissions and air quality.

Emission factors for direct combustion and fuel cells are obtained from BACT guidance by the SJVAPCD (SJVAPCD 2002b), emission factors data by the U.S. EPA available in the compilation of emissions factors referred as AP-42 (U.S. EPA 2008), and ARB DG certification program. Table 51 presents these emission factors. The SJV BACT emission factors for direct combustion of biomass correspond to a biomass-fired fluidized bubbling bed combustor, which is the predominant technology in the SJV.

**Table 51. Emission factors for biomass technologies**

| | Direct Combustion | | Fuel Cells |
|---|---|---|---|
| | SJV BACT | AP-42 | ARB Certified (Fuel Cell Energy 2007) |
| **$NO_X$** | 0.100 lb/MMBtu | 0.220 lb/MMBtu | 0.017 lb/MW-hr |
| **VOC** | 0.020 lb/MMBtu | 0.017 lb/MMBtu | 0.003 lb/MW-hr |
| **$SO_X$** | 23 ppmvd | 0.025 lb/MMBtu | - |
| **PM** | 0.045 lb/MMBtu | 0.040 lb/MMBtu | - |

Sources: SJVAPCD 2002b; USEPA 2008; Fuel Cell Energy 2007

*Emissions Displacement*

Although biomass plants have stack emissions, they could lead to reduction in emissions that occur otherwise, such as those from open burning of biomass, boiler emissions, and to some extent, from dairies. Therefore such emission reductions must be estimated and offsets need to be applied to accurately quantify air quality impacts of biomass power. Similar to other DG technologies, application of combined heating and power (CHP) leads to increased overall efficiencies of biomass plants. Waste heat produced during electricity generation can be captured by a heat recovery system that provides useful heat to meet facility thermal loads, which can significantly decrease operating costs. As a result, CHP can replace the heat produced by burning fuel in a boiler leading to a reduction (displacement) of boiler-associated emissions. Emissions that are offset from boiler emissions are estimated using the same methodology discussed in the earlier section on CHP emissions displacement.

For biochemical conversion technologies, such as anaerobic digesters coupled with fuel cells, recovered waste heat is often used to maintain the temperature of the digester. Therefore, in this study, CHP emissions offset is applied only to thermo-chemical conversion technologies (i.e., direct combustion of biomass).

Emissions that are avoided when electricity is produced from agricultural residues, which are burned otherwise, represent another major source of emissions offset. However, in the SJV there are currently many restrictions on agricultural open field burning and it is expected to be completely banned in the future due to air quality concerns. Therefore, emission offsets for biomass power from agricultural waste are not considered in this study.

Dairies and animal operations constitute a major source of VOC emissions in the SJV. The use of anaerobic digesters could potentially reduce VOC emissions associated with aerobic digestion of animal manure (lagoons, storage ponds). Although animal operations are also major source of $NH_3$ emissions, a study from two diaries in the New York area showed no significant decrease in $NH_3$ emissions when anaerobic digesters are used (Martin 2004). Anaerobic digesters offer significant reductions in emissions of methane, a greenhouse gas. However, methane has a long atmospheric lifetime, is globally well-mixed, and does not significantly affect regional ozone production. Therefore, in this study only VOC emission offsets are applied when anaerobic digesters coupled with fuel cells are deployed to produce biomass electricity. These emission offsets are applied based on the emission factors reported by SJVAPCD in the air quality permitting process of dairies in the SJV (SJVAPCD 2005). The total number of dairy cows in California is approximately 2.5 million, and according to SJVAPCD emission factors, 1.0 lb/head-year[4] of VOCs are emitted from lagoons and storage ponds of diaries. Based on the total animal manure biomass fuel availability of 385 MW (see Figure 33), maximum total VOC emission reductions adds up to 0.815 lb of VOC per MWh produced by animal manure biomass. These emissions are offset when anaerobic digesters are used in the biomass scenarios of this study.

[4] lb/head-year = pounds per cow and per year

Using the parameters for biomass scenarios described in the previous section, four biomass scenarios are developed.

### *Biomass Scenario 1 (BM1)*

This scenario assumes that 33% of retail electricity consumption in 2023 is produced from renewable sources. It is assumed that biomass power contributes 20% of all renewable power, i.e., maintaining its current share among all renewable sources. These assumptions lead to total future biomass capacity addition of 326 MW in the SJV (as shown in Table 50). All plants in this scenario consist of direct combustion of biomass in a fluidized bed combined with steam turbines. The size of the plants range between 5 and 10 MW and employ combined heating and power. Furthermore, it is assumed that 60% of the waste heat is recovered, of which 50% is utilized.

### *Biomass Scenario 2 (BM2)*

This scenario assumes the same parameters as in scenario BM1. However, plant sizes are assumed to be between 10 and 15 MW. This leads to a smaller number of biomass plants in the basin, leading to more concentrated emissions as compared to scenario BM1.

### *Biomass Scenario 3 (BM3)*

This scenario assumes the same parameters as in scenario BM1. However, plant sizes are assumed to be between 15 and 25 MW. This leads to smaller number of biomass plants in the basin, leading to more concentrated sources of emissions as compared to BM1 and BM2.

### *Biomass Scenario 4 (BM4)*

This scenario assumes the same parameters as in scenario BM2. However, it assumes that all biomass from animal manure is used for power generation using anaerobic digesters coupled with fuel cells. The projected biomass power from animal manure is 68 MW from the total of 326 MW (see Table 50). Therefore, this scenario assumes that 258 MW is generated from direct combustion and 68 MW from fuel cells. Reduction of VOC emissions from diary/animal operations due to the use of anaerobic digesters is accounted for in this scenario.

### *Biomass Scenario 5 (BM5)*

This scenario assumes that policy forcing leads to increased use of biomass resource utilization through direct combustion (e.g., agricultural waste, forestry) as compared to scenario BM4. A total of 386 MW of biomass power from direct combustion, 1.5 times of that in the scenario BM4, is assumed in this scenario. As in BM4, 68 MW of power from animal manure is produced using fuel cells. Total biomass power capacity addition in this scenario is 454 MW.

### *Biomass Scenario 6 (BM6)*

This scenario assumes that policy forcing leads to increased use of biomass resource utilization from animal manure through anaerobic digesters, as compared to scenario BM4. A total of 102 MW of biomass power from anaerobic digesters coupled with fuel cells—1.5 times of that in the scenario BM4—is assumed in this scenario. As in BM4, 258 MW of power is produced from direct combustion. Total biomass power capacity addition in this scenario is 360 MW.

# 4.0 Air Quality Modeling Formulation

Tropospheric ozone is a product of photochemistry that occurs between NOx and VOCs in the ambient atmosphere in the presence of sunlight. Nitrogen oxides and VOCs, the precursors of ambient ozone, are mostly emitted from anthropogenic sources such as on-road and off-road vehicles, power plants, and industrial operations. The ambient level of ozone, on a regional scale, highly depends upon spatial and temporal profiles of precursor emissions, meteorological conditions, transport of precursors, reaction products through atmospheric transport mechanisms, and removal processes such as dry deposition and wet deposition. Therefore, comprehensive models that incorporate all these physical and chemical processes in detail, commonly known as Air Quality Models (AQMs), are widely used to understand and characterize the formation of ozone on regional scales. These AQMs numerically solve a series of atmospheric chemistry/diffusion/advection equations in order to determine ambient concentrations of pollutants over a given geographic region.

Most models employ an Eulerian representation (i.e., one that considers changes as they occur at a fixed location in the fluid, usually called a *cell* or *control volume*) of physical quantities on a three-dimensional computational grid. The atmospheric diffusion/advection equation for species *m* is given as:

$$\frac{\partial Q_m^k}{\partial t} = -\nabla \cdot \left(uQ_m^k\right) + \nabla \cdot \left(K\nabla Q_m^k\right) + \left(\frac{Q_m^k}{\partial t}\right)_{sources\,/\,sinks} + \left(\frac{Q_m^k}{\partial t}\right)_{aerosol} + \left(\frac{Q_m^k}{\partial t}\right)_{chemistry} \quad (20)$$

The above equation is numerically integrated in time for each species *m*, over a series of discrete time steps in each of the spatially distributed discrete cells of the AQM. The AQMs typically employ operator splitting, which is a numerical method that splits each term in Equation 20 so that each process is calculated separately, instead of calculating the entire differential equation at once (Yanenko 1971). Each term in the right side of Equation 20 represents a major process in the atmosphere. From left to right: (1) advective transport due to wind transport, (2) turbulent diffusion due to atmospheric stability/instability, (3) emissions (sources) and deposition (sinks) of pollutants, (4) mass transfer between gas and aerosol phases, and (5) chemical reactions. The operator-splitting method is computationally efficient and has an added advantage of providing modularity to choose between various available parameterizations of atmospheric processes and numerical algorithms.

The outputs from AQMs are spatially and temporally resolved concentration profiles of major and trace species of interest over a geographic region. In order to minimize the effects of initial conditions and conduct various analyses, air quality modeling involves simulation of episodes involving multiple days. This modeling approach greatly facilitates study of various scenarios involving changes in emissions and associated impacts on the air quality in a particular region.

However, the development and validation of an air quality model are resource-intensive tasks that require extensive software development work and experimental data from field campaigns.

In addition, the model depends upon emissions inventories and wind fields as inputs, which require many years of effort to accurately develop. Since the focus of the current project is to assess the impacts of distributed generation, the project team acquired air quality models that are well-tested and peer-reviewed extensively in the scientific literature.

## 4.1. Air Quality Modeling of the SoCAB

The gas-phase chemical mechanism used in the present simulations is the Caltech Atmospheric Chemical Mechanism (CACM, see Griffin et al. 2002a). The CACM is based on the work of Stockwell et al. 1997; Jenkin et al. 1997; and Carter 2000. It includes ozone ($O_3$) chemistry and a state-of-the-art mechanism of the gas phase precursors of secondary organic aerosol (SOA). The full mechanism consists of 361 chemical reactions and 191 gas-phase species, which describe a comprehensive treatment of VOCs oxidation.

In the current work, inorganic aerosol formation is calculated using the Simulating Composition of Atmospheric Particles at Equilibrium 2 model (SCAPE2, Meng et al. 1995); whereas organic aerosol formation is calculated using the Model to Predict the Multiphase Partitioning of Organics (MPMPO, Griffin et al. 2002b). The MPMPO allows the simultaneous formation of SOA in a hydrophobic organic phase and a hydrophilic aqueous phase. In addition, MPMPO modifies SCAPE2 to account for the interaction between organic ions present in the aqueous phase and the inorganic aerosol components. The module consists of 37 size-resolved aerosol-phase species, in 8 different size bins ranging from 0.04 to 10 microns. The integrated module allows particulate matter to undergo advection, turbulent diffusion, condensation/evaporation, nucleation, emissions, and dry deposition processes.

The California Institute of Technology (CIT) Airshed Model has been updated and modified over the course of more than a decade of work at the University of California (UC) Irvine. This model, now dubbed the UCI-CIT Airshed Model, is used as the host model for the chemical and aerosol mechanisms (Harley et al. 1993; Griffin et al. 2002b; and Meng et al. 1998). The grid used by the UCI-CIT model encompasses Orange County and part of Los Angeles, Ventura, San Bernardino, and Riverside counties (Figure 36). The grid consists of cells with an area of 25 $km^2$. Additionally the vertical resolution is described through five vertical layers with the following dimensions from ground level up: (1) 0 m–39 m, (2) 39 m–154 m, (3) 154 m–308 m, (4) 308 m–671 m, and (5) 671 m–1100 m.

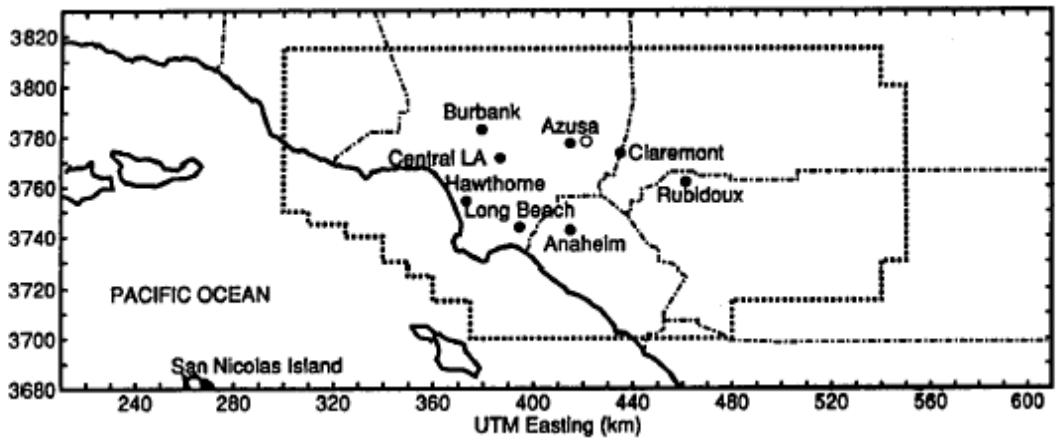


**Figure 36. UCI-CIT Airshed modeling domain of the South Coast Air Basin of California**

The Southern California Air Quality Study (SCAQS) was a comprehensive campaign of atmospheric measurements that took place in the SoCAB during August 27–29, 1987. The study collected an extensive set of meteorological and air quality data that has been used widely to validate air quality models (Meng et al. 1998; Griffin et al. 2002a; Griffin et al. 2002b; Moya et al. 2002). Zeldin et al. (1990) found that August 28, 1987, is representative of the meteorological conditions in the SoCAB, which makes it suitable for modeling. In addition, the August 27–28, 1987, episode is statistically within the top 10% of severe ozone-forming meteorological conditions. Hence, meteorological conditions for August 28 are used here as the basis to evaluate air quality impacts of DG.

The SCAQS episode in August 27–29, 1987 was characterized by a weak onshore pressure gradient and warming temperatures aloft. The wind flow was characterized by a sea breeze during the day and a weak land-mountain breeze at night. The presence of a well-defined diurnal inversion layer at the top of neutral and unstable layers near the surface, along with a slightly stable nocturnal boundary layer, facilitated the accumulation of pollutants over the SoCAB, which lead to a high ozone concentration occurrence.

Model performance needs to be analyzed and compared with available observations, since simulation of an air quality episode requires various input parameters, each subject to some level of uncertainty. Griffin et al. (2002a) validated results obtained with the UCI-CIT model and the CACM chemical mechanism using the August 27–29, 1987, meteorology and emissions inventory. They also reported comparisons between observed and simulated data at Pasadena and Riverside. In general, ozone concentrations in Pasadena are under-predicted each day; whereas NO concentrations at this location compare reasonably well with observation, except for the third day. In Riverside, ozone concentrations agree with observed data for the second and third day. However, NO concentrations are under-predicted during the daylight hours and over-predicted at nighttime. A statistical analysis was conducted to determine the overall performance of the model versus observed data (see Table 52). Results show a typical level of agreement for current three-dimensional air quality models.

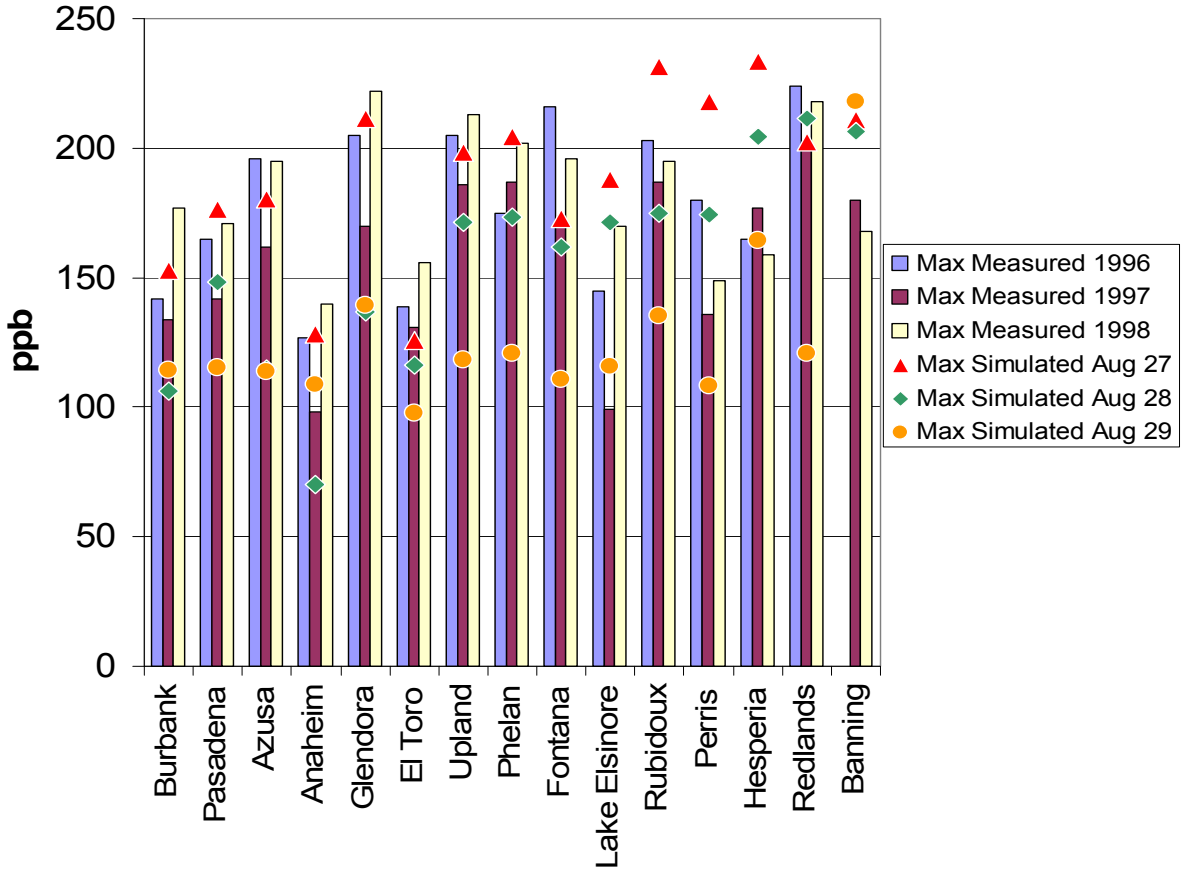


**Figure 37. Comparison between measured maximum concentration of ozone in years 1996–1998, and concentration of ozone simulated using 1997 emission inventory and a high ozone-forming potential episode (SCAQS August 27–29, 1987, meteorology)**

Figure 37 shows a comparison between model predictions and observations of maximum ozone concentrations at different monitoring stations using August 27–29 meteorology and the emission inventory for year 1997. Measured maximum ozone concentrations reported in Figure 37 correspond to observations in the period from 1996 to1998 at the selected stations. Note that simulated data refers to a specific episode; whereas measured data refers to maximum concentrations during the entire year. This comparison shows that simulation results fall within the range of measured ozone values at each station. Although not a strict validation, these results provide additional understanding on the validity of the simulation results.

**Table 52. Statistical analysis of model performance versus observed data on August 28, 1987, for $O_3$ and $NO_2$**

| Statistical Measure | $O_3$ | $NO_2$ |
|---|---|---|
| Bias, ppb | 15.9 | -0.4 |
| Normalized bias, % | 21.7 | 12.6 |
| $\sigma$ of residuals, ppb | 55.3 | 28.1 |
| Gross error, ppb | 39.5 | 21.4 |
| Normalized gross error, % | 41.1 | 51.6 |

Source: Griffin et al. 2002a

## 4.2. Air Quality Modeling of the SJV

### *4.2.1. Ozone Modeling for the SJVAB*

Two candidate models for ozone simulation that were acquired and tested for applicability to the current effort were the Community Multi-scale Air Quality Model (CMAQ) and Comprehensive Air Quality Model with Extensions (CAMx). The CMAQ code was selected for simulation of particulate matter in SJV since it has been the most widely used model for simulating particulate matter (PM) in this region. The CAMx model is selected for the ozone analysis component of this study, as this model is currently being used for regulatory applications for the Central California region, including the San Joaquin Valley. This choice of model greatly facilitates the coordination of this work across various collaborative groups and regulatory agencies, including SJVAPCD and ARB.

#### *CAMx: Comprehensive Air Quality Model With Extensions*

The CAMx model is under continuous development by the ENVIRON Corporation and is approved by the U.S. EPA for regulatory applications. Currently, CAMx is being used for several State Implementation Plans (SIPs) and many other regulatory studies. The model source code and detailed documentation is available from the model website: www.camx.com. Table 53 presents a brief description of each of describes the modules of the CAMx model. These modules are those that are required to simulate the major physical processes identified in Equation 20.

The choice of mechanism that simulates atmospheric chemistry is important, because the prediction of ozone concentrations throughout the basin greatly depends upon the representation of chemical reactions that occur in the atmosphere, as well as the particular chemical species that are considered to participate in these reactions. The SAPRC99 chemical mechanism is chosen for this study for several reasons. First, the mechanism is well documented and validated in the scientific literature. Secondly, the CACM chemical mechanism that is being used for the SoCAB study is similar to the SAPRC99 mechanism (Carter 2000) in the representation of species and reactions that contribute to the formation of ozone. Therefore, this choice enables the team to maintain consistency with modeling approaches being used for DG impact studies to the extent possible. Finally, the SAPRC99 mechanism is being used for SIP studies as well, and hence the emissions inventory data sets that have been developed by ARB

for this process can be used for the current study without major adaptations that will be required for alternate mechanisms.

**Table 53. Overview of modules in CAMx for key atmospheric processes**

| Atmospheric Process | Module Description | Numerical Algorithm |
|---|---|---|
| Horizontal atmospheric transport through advection/diffusion | Eulerian continuity equation closed by K-theory | Bott or PPM solver for advection, explicit diffusion |
| Vertical transport | Eulerian continuity equation closed by K-theory | Implicit advection and diffusion |
| Atmospheric Chemistry | Carbon Bond IV or SAPRC99 mechanism | ENVIRON CMC solver or IEH solver |
| Dry deposition | Resistance models for gases and aerosols | Deposition velocity as surface boundary condition for vertical diffusion |

### *SAPRC99 Chemical Mechanism*

The SAPRC99 chemical mechanism is the latest version of the Statewide Air Pollution Research Center (SAPRC) chemical mechanism (Carter 2000). This mechanism has been extensively validated against environmental and environmental chamber data. The mechanism has assignments for over 400 types of VOCs and can be used to estimate reactivities for 550 VOC categories. Common reactive organic products are represented by a total of 24 model species, of which 11 are used for organic compounds that are represented explicitly and 13 are lumped species. The SAPRC99 mechanism used in this study consists of 56 gas phase species and 211 reactions.

### *Model Inputs From the Central California Ozone Study (CCOS)*

CAMx requires input data that describes atmospheric conditions (e.g., wind, temperature, and relative humidity), a spatially, chemically and temporally resolved emission inventory for the region, and physical data such as rate constants for chemical reactions. Such input datasets are typically developed using predictions from prognostic models (such as the Pennsylvania State University / National Center for Atmospheric Research mesoscale model, MM5) in combination with observational data from extensive field campaigns. This development of input data for air quality modeling purposes is often an iterative process, which involves statistical analysis of model performance, refinement of estimates used to develop emission inventories, and improved representation of physical processes in AQMs. Figure 38 presents the modeling domain being considered in the CAMx model, which is consistent with the input data sets and modeling domain used in the Central California Ozone Study (CCOS).

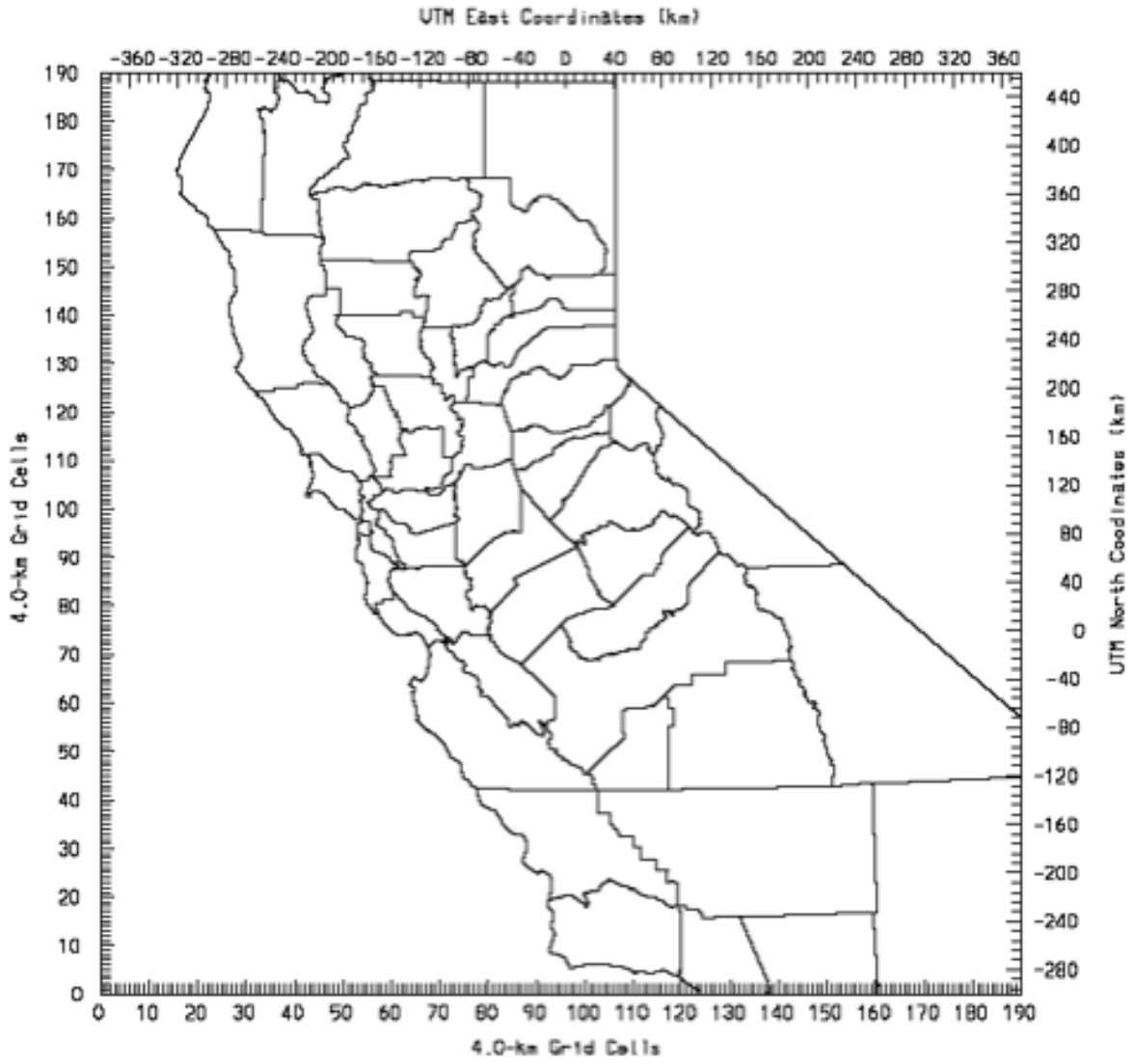


**Figure 38. The modeling domain using CCOS input dataset**

For this study, the model input data for an air quality episode was acquired from ARB. These data were developed as a part of the CCOS project, which was a multi-agency campaign conducted in the summer of 2000 with the aim of acquiring extensive ambient data and developing a better modeling apparatus that enables the study of ozone formation in air basins of the Central California region. Currently, the dataset developed during this campaign is being used in regulatory applications for the region.

The acquired input data simulates an air quality episode that occurred from July 29, 2000, through August 2, 2000. Two sets of meteorological data were acquired from ARB for the purpose of this study. The first set was developed from model predictions of the prognostic MM5 model. The second set, called a hybrid data set, was developed using the California Meteorological (CALMET) model from both observational data and the MM5 model-predicted

data of air temperatures and wind speed components. As per the analysis of Jackson et al. (2006), the model performance is improved by the use of this hybrid data set compared to pure MM5 model predictions. Hence for this study, a hybrid data set is used to conduct air quality simulations.

In the current effort, the team made no attempt to validate or update the hybrid wind fields, the temperature or the humidity fields that were provided to us by the CCOS group. Rather, the team trusted the findings of the CCOS group for the generation of good meteorological data sets for use in the AQM.

### *Modeling Domain*

Figure 38 shows the modeling domain for this study. The domain extends from Los Angeles County in the south to the California/Oregon border in the north, and from the Pacific Ocean on the west to Nevada in the east. As seen in Figure 38, the San Joaquin Valley region is in the middle of the current modeling domain and hence suffers minimally from boundary effects on the predicted species profiles.

For computational purposes, the modeling domain is discretized into 189 by 189 horizontal cells of 4 km by 4 km horizontal resolution. The domain extends up to 5000 meters in the vertical direction, which is resolved into 16 discrete layers using a terrain-following coordinate system. The height of individual layers, presented as meters above ground level (AGL), is shown in Table 54.

**Table 54. Vertical structure of modeling domain**

| Layer | Height (m AGL) |
|---|---|
| 1 | 20 |
| 2 | 60 |
| 3 | 100 |
| 4 | 200 |
| 5 | 300 |
| 6 | 400 |
| 7 | 600 |
| 8 | 800 |
| 9 | 1000 |
| 10 | 1500 |
| 11 | 2000 |
| 12 | 2500 |
| 13 | 3000 |
| 14 | 3500 |
| 15 | 4000 |
| 16 | 5000 |

### *CCOS Base Case Results*

The CAMx model was successfully acquired, compiled, and run using the input data set. The main outputs of the model are spatially and temporally resolved profiles of ambient concentration of selected species over the computational grid, as described in the previous section. Figure 39 shows the spatial distribution of maximum 1-hour average ozone concentration for each day of the simulation. For each of the days simulated, urban areas in the SJV, especially Fresno and Bakersfield, experience high ozone concentrations. Forest fires that occurred during this episode cause high ozone in the southeastern part of the domain for the first three days of the simulation.

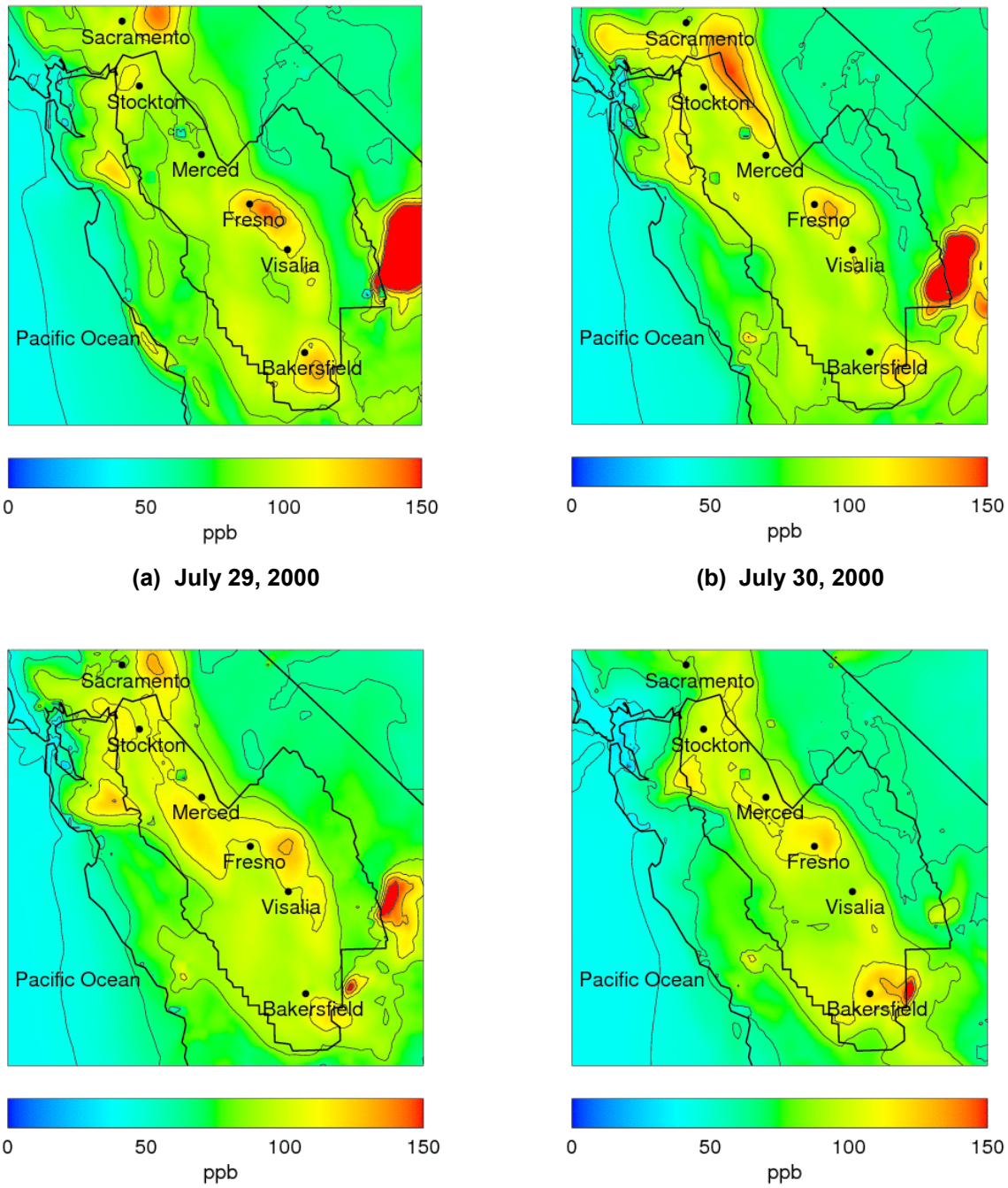


**Figure 39. Simulated distribution of maximum local ground-level ozone concentrations in the San Joaquin Valley for the four-day episode using meteorological conditions from the CCOS study of July 29–August 1, 2000**

### *Comparison With Observations*

It is important to compare observations with model predictions to gain confidence in the model performance. The comparative analysis is typically done using statistical methods, which calculate Unpaired Peak Ratio (UPR), Normalized Bias, and Gross Error (GE). These types of analyses for this dataset have already been extensively conducted by ARB in support of SIP plans for air basins in the central California region. The model domain is divided into nine zones, and statistical performance parameters are calculated for each of these zones. The SJV region falls in to zones 6, 7, and 8 of the CCOS domain. The statistical measures of predictive accuracy obtained for the zones comprising the SJV region are presented in Table 55.

Further, the current analyses included comparing model predictions with the observations for three urban locations, as shown in Figure 40, Figure 41, and Figure 42. The model under-predicts ozone concentrations near Fresno, Bakersfield, and Sacramento for the first day of the simulation. However, the performance is satisfactory throughout the basin for the later days in the simulation.

**Table 55. Statistical measures of model predictive performance**

| Sub-region | Obs. Peak | Sim. Peak | UPR | NB (%) | GE (%) |
|---|---|---|---|---|---|
| | | **July 29, 2000** | | | |
| Zone 6 | 121 | 147 | 1.21 | +13 | 22 |
| Zone 7 | 129 | 144 | 1.12 | -03 | 17 |
| Zone 8 | 128 | 149 | 1.16 | -02 | 25 |
| | | **July 30, 2000** | | | |
| Zone 6 | 110 | 149 | 1.35 | +04 | 17 |
| Zone 7 | 118 | 138 | 1.17 | +06 | 18 |
| Zone 8 | 115 | 132 | 1.15 | -07 | 20 |
| | | **August 1, 2000** | | | |
| Zone 6 | 110 | 145 | 1.08 | -02 | 19 |
| Zone 7 | 118 | 132 | 1.12 | -05 | 21 |
| Zone 8 | 115 | 120 | 1.04 | -10 | 19 |
| | | **August 2, 2000** | | | |
| Zone 6 | 110 | 137 | 1.05 | -09 | 20 |
| Zone 7 | 118 | 137 | 1.04 | -02 | 22 |
| Zone 8 | 115 | 140 | 0.92 | -07 | 20 |

Source: SJVAPCD 1-hour ozone attainment plan

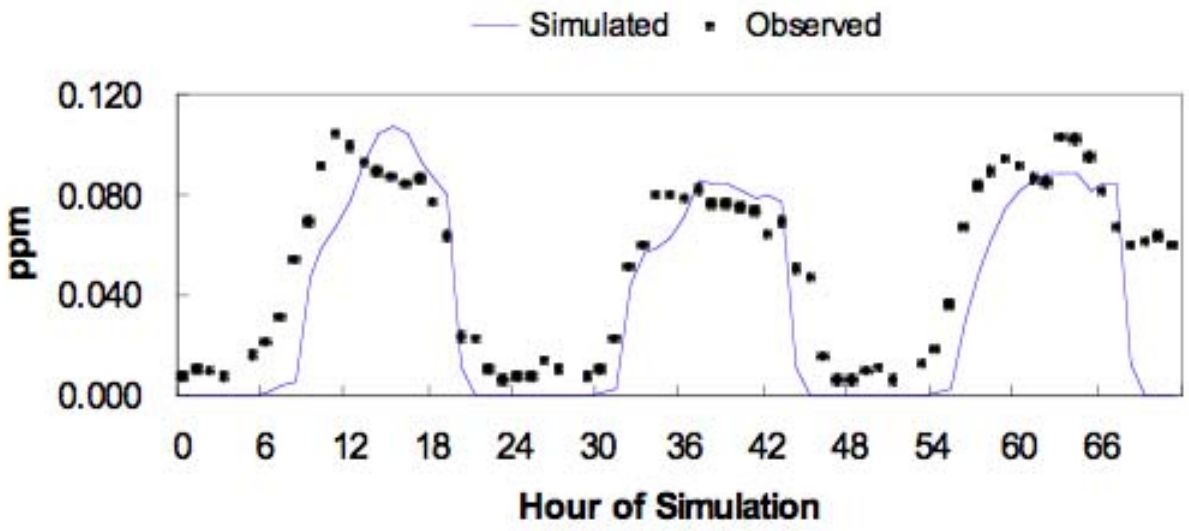


**Figure 40. Comparison of observed ozone concentrations with model predictions at a Bakersfield site**

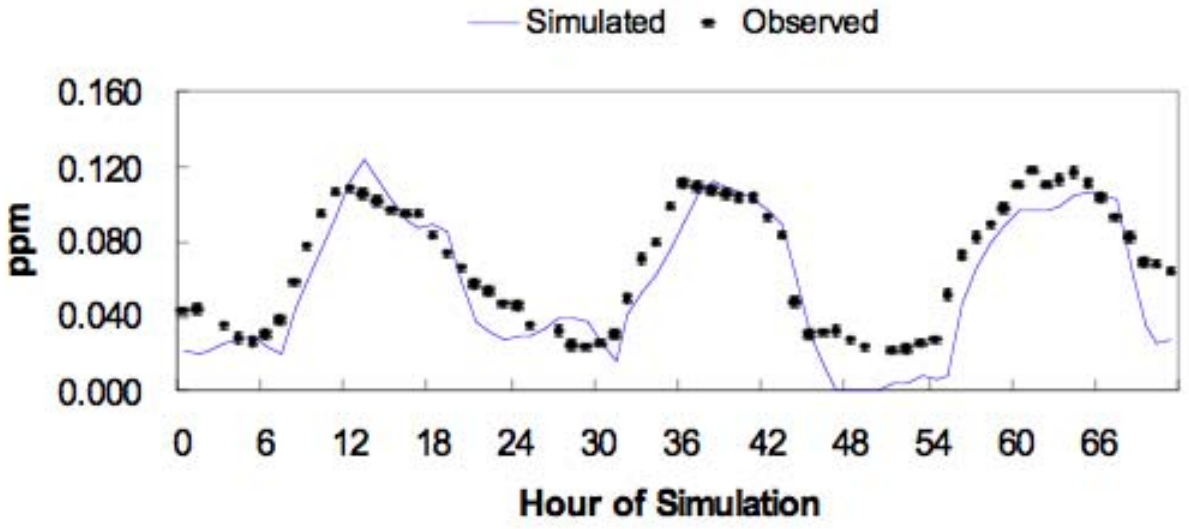


**Figure 41. Comparison of observed ozone concentrations with those of model predictions at a Fresno site**

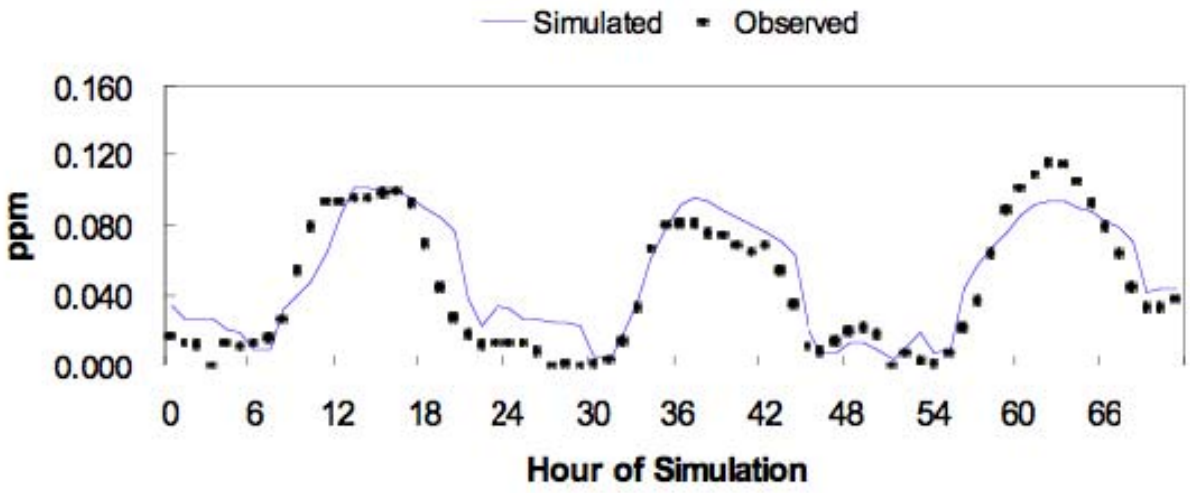


**Figure 42. Comparison of observed ozone concentrations with those of model predictions at a Sacramento site**

### *4.2.2. Particulate Matter Modeling for the SJVAB*

Particulate matter is another major criteria pollutant that is linked to adverse health effects and climate impacts. Particulate matter is a complex mixture of airborne solid particles and aerosols that are either directly emitted into the atmosphere or formed in the atmosphere from secondary processes. The direct or primary sources of PM include automobiles, power plants, and diesel-powered vehicles. Secondary PM is formed from atmospheric transformation of nitrogen oxides, sulfur dioxide and volatile organic compounds that are present in gas-phase emissions. The size distribution is an important characteristic of ambient PM, as health effects and atmospheric lifetime of particles are determined by particle size. Fine and ultrafine particles, such as diesel PM, reach alveolar regions of the lung and are shown to be carcinogenic. Consequently, federal and state air quality standards are defined based on size of particles. Federal $PM_{2.5}$ and $PM_{10}$ standards regulate mass concentrations of ambient particles with aerodynamic diameter smaller than 2.5 and 10 microns, respectively. The San Joaquin Valley region is designated as a nonattainment region for $PM_{10}$ and $PM_{2.5}$ standards.

As shown in the Figure 43, PM concentrations peak during winter months. Hence, the majority of PM studies in the SJV are conducted during wintertime, and modeling episodes are developed for winter days with high PM concentrations. The Integrated Monitoring Study (IMS95) conducted in the fall and winter of 1995 is a planning study for more intensive California Regional Particulate Air Quality Study (CRPAQS). During the IMS95 field study, wintertime $PM_{10}$ is dominated by ammonium nitrate (50%), mobile sources (20%), and vegetative burning (15%), with approximately 70%–80% of the $PM_{10}$ present as $PM_{2.5}$ (Magliano et al. 1999). A large fraction of observed ammonium nitrate ($NH_4NO_3$) is formed when the air masses from urban areas with high $NO_X$ mixes with downwind ammonia emissions from agricultural activities.

Modeling studies were conducted using the data obtained from IMS95 in order to better understand the dynamics of ammonium nitrate formation and PM in general. Kleeman et al. (2005) has shown that the ammonium nitrate formation is limited by nitric acid ($HNO_3$). Furthermore, the study also concluded that the formation of nitric acid is limited by $NO_X$ rather than VOC emissions. The data from the most recent field campaign, the California Regional Particulate Air Quality Study (CRPAQS), is currently undergoing extensive analysis. The CRPAQS study also led to the development and validation of a modeling episode that will be used in this study.

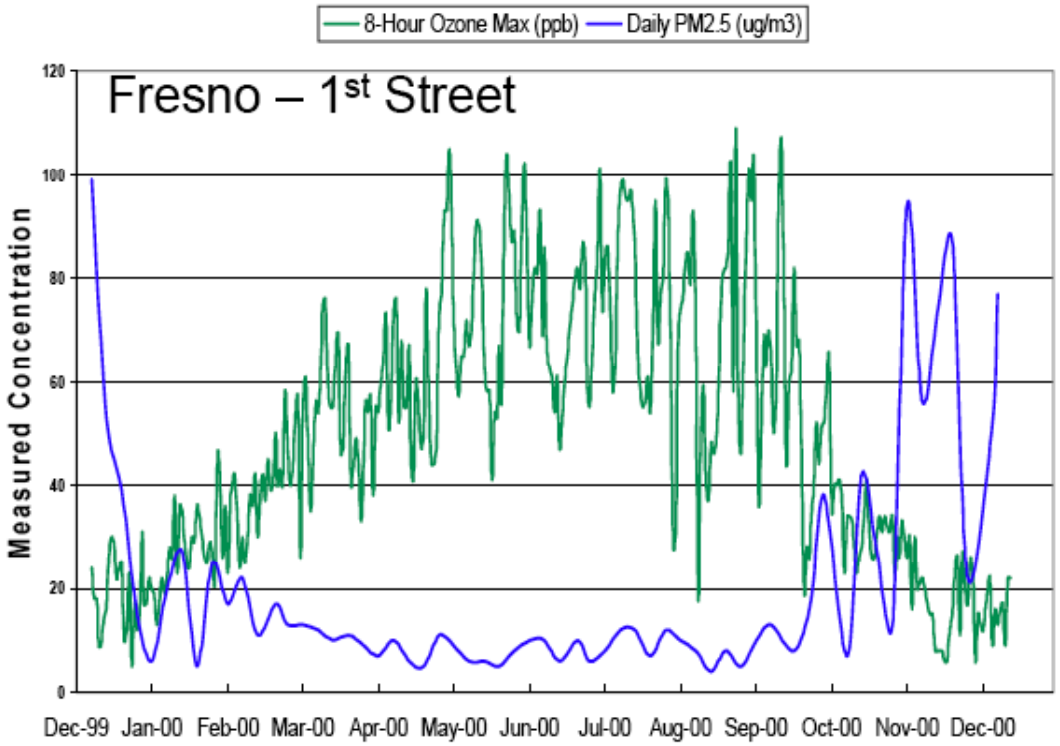


**Figure 43. Observed concentrations of PM2.5 and 8-hour ozone maximum for the year 2000 at a Fresno Site in the SJV**

Source: Kaduwela 2005

### *Community Multi-Scale Air Quality (CMAQ) Model*

Modeling of PM is more challenging than ozone modeling due to the nature of ambient aerosol formation. Particulate matter characterization includes number, mass, and size distributions as well as the chemical composition of the particles. Therefore PM modeling is more complex, computationally expensive and data intensive. The current team chose to use the CMAQ model to evaluate impacts of DG on PM in the central valley. The CMAQ model is a comprehensive air quality modeling system developed by the U.S. EPA, and it is widely used for many regulatory air quality simulation applications. The source code and technical formulation of the model are

available from the CMAQ website (www.cmaq-model.org). The CMAQ model is designed from the "one atmosphere" perspective and is used for studies on tropospheric ozone, particulate matter, acid deposition, and visibility. The CMAQ system includes a meteorological modeling system (MM5), emissions modeling system (EMS), and chemical transport modeling system (CTMS).

Although U.S. EPA develops and maintains a standard version of the CMAQ model, several groups have modified and advanced the CMAQ modeling framework. Such modifications are mainly to include certain modules or to suit characteristics of a particular region. Of particular interest to the current effort are modifications that ARB has made to the CMAQ model for the simulations they have conducted in the SJV. The ARB has modified the standard version of the CMAQ model to obtain better model performance when applied to the central California region. The APEP team has acquired the source code of the ARB-modified model and compiled the code successfully. This version of the CMAQ model is the one used throughout the current study, to allow ease of comparison with other SJV studies.

### *Aerosol Model*

The aerosol component of the CMAQ model predicts the formation of sulfates, nitrates, ammonium, and organic compounds, and it is derived from the Regional Particulate Model (RPM) (Binkowski and Shankar 1995). The CMAQ model represents particle size distribution as a superimposition of three log-normal modes. Fine particulate ($PM_{2.5}$) is represented by two interacting fine modes. The smaller mode within these fine particles, the Aitken mode, represents fresh particles. The second, larger fine mode represents aged particles, which is typically called the accumulation mode. The coarse mode represents particles between $PM_{2.5}$ and $PM_{10}$. Modeling of aerosol dynamics in CMAQ is based on Whitby et al. (1991) and Whitby and McMurry (1997). The aerosol component also includes mechanisms for dry deposition and cloud processing of aerosols.

### *Model Inputs From California Regional Particulate Air Quality Study (CRPAQS)*

The CRPAQS study also led to development of a modeling episode using the CMAQ modeling system. The episode is a 22-day episode that occurred from December 15, 2000, to January 7, 2001. The modeling domain for this study (presented in Figure 38) is identical to that of the ozone component of this study. The APEP team acquired all model inputs that are required to simulate the 22-day winter CRPAQS episode. The current DG study uses the same meteorological input dataset to simulate all DG scenarios and the base case. Figure 44 and Figure 45 show sample input data (ground level temperature and pressure distributions, respectively, for the second day of the simulation at hour 15:00).

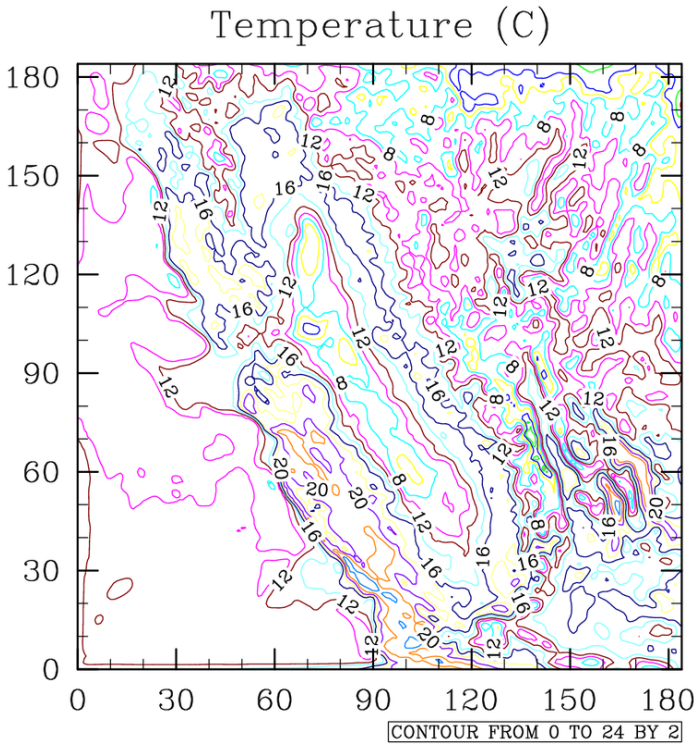


**Figure 44. Input temperature field for the second day of simulation at the hour 15:00**

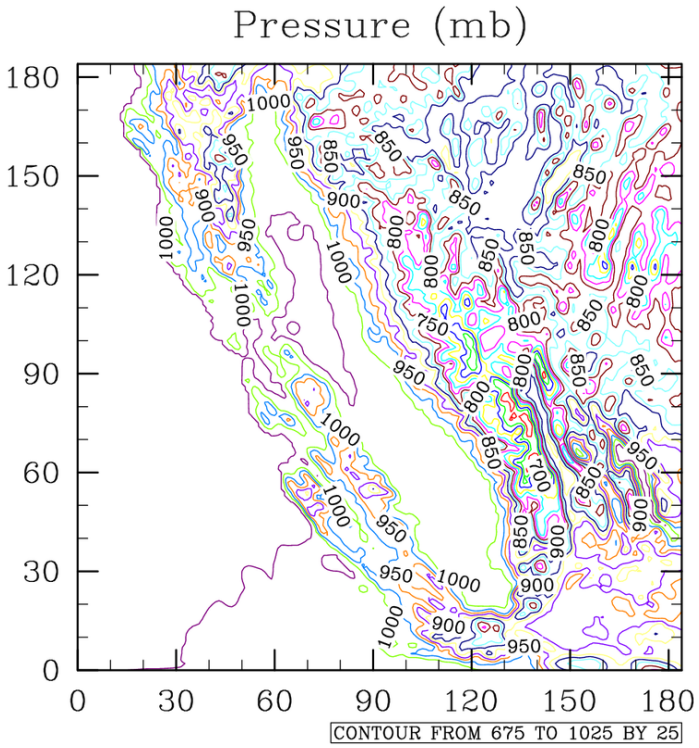


**Figure 45. Input pressure field for the second day of simulation at the hour 15:00**

### *Model Results*

Figure 46 and Figure 47 show 24-hour average concentrations of $PM_{2.5}$ and $PM_{10}$, respectively, on the final day of the simulation. Although most of the basin shows high levels of PM, downwind areas of Stockton, Fresno, and Bakersfield exhibit the highest 24-hour average PM concentrations. These observations are consistent with other modeling and field studies (Kleeman et al. 2005). In the SJV region, particulate ammonium nitrate is a major component of $PM_{2.5}$.

A future year base case is constructed in order to assess the impacts of DG on $PM_{2.5}$ and $PM_{10}$ in future years. This is accomplished by taking the emissions inventory produced by ARB for the year 2000 and scaling the emissions to account for future growth in population, industrial activity, and transportation in each of the counties throughout the SJV (at a county-by-county level). Then the total basinwide emissions are scaled back to the expected levels that are in the SIP for future year compliance (2023). Emissions of $NO_X$ and VOC are scaled using the same ratios that are used to construct future year emissions for the ozone simulations. There is a considerable decrease in PM concentrations with the decreased emissions that are expected in future years.

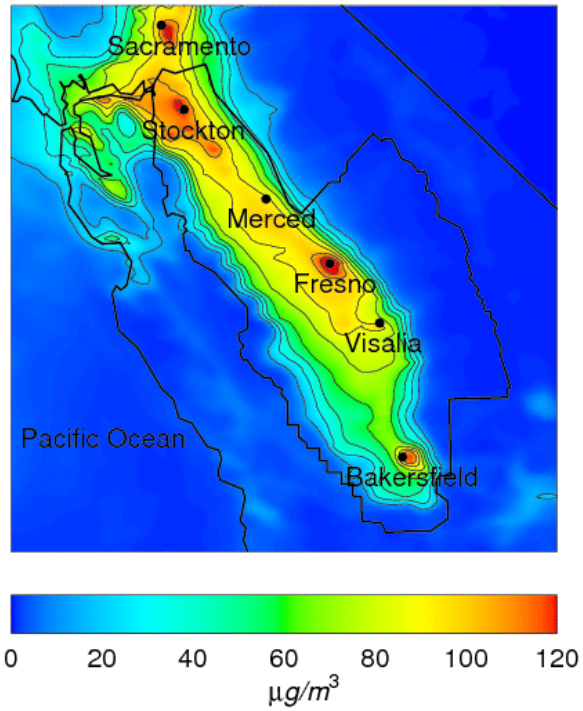


**Figure 46. 24-hour average concentration of $PM_{2.5}$ on the final day of the simulation for the baseline case**

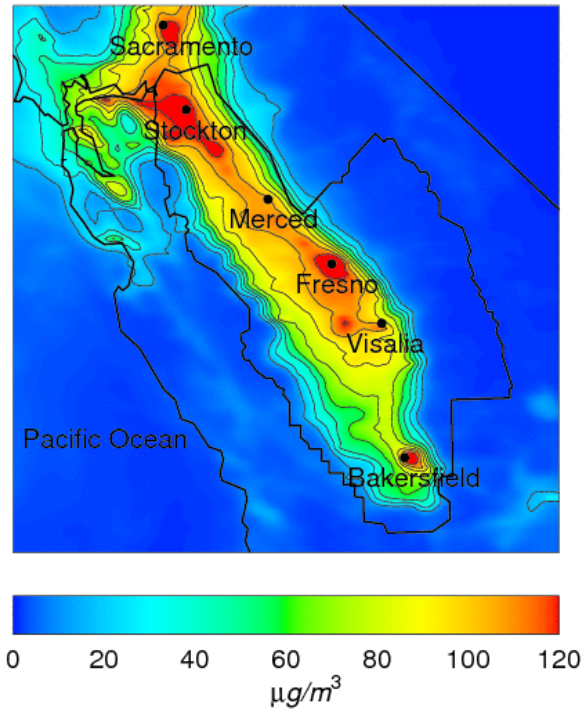


**Figure 47. 24-hour average concentration of $PM_{10}$ on the final day of the simulation for the baseline case**

# 5.0 Air Quality Impacts of DG

## 5.1. Air Quality Impacts of DG Scenarios in the SoCAB

This study presents an assessment of air quality impacts caused by the deployment of DG systems throughout the SoCAB. Installation of such technologies by the year 2030 will depend upon market penetration for each DG type. Factors that will influence the degree of market penetration include the application for which DG is required, the cost of installation, and the ability of each technology to comply with pollutant emission standards. A set of 26 DG scenarios has been developed and divided into two categories: (1) realistic, and (2) spanning scenarios. Realistic DG scenarios are developed to reflect an expected level of DG deployment by the years 2023 and 2030. Spanning DG scenarios are developed for scientific completeness, for sensitivity analyses, and for determination of potential impacts due to unexpected outcomes. Additionally, spanning scenarios help to set upper bounds for air quality impacts due to DG installation. Moreover, long-term spanning scenarios are developed to project power needs in the future, that may be the result of a widespread implementation of novel technologies such as electric vehicles. A brief description of the parameters that define each scenario is summarized in Table 58 and Table 66. Air quality impacts are assessed through comparison of pollutant concentrations in each DG scenario and a base case that does not include DG penetration. The base cases for the SoCAB are described below.

### *5.1.1. Baseline Air Quality in Target Years*

This section presents simulation results using the emission inventory for the years 2010, 2023, and 2030, and the meteorological conditions of the August 27–29, 1987 episode. Emissions for 2010 correspond to the emissions inventory used in the 2003 AQMP developed by the SCAQMD to show attainment of the 1-hour ozone standard in the SoCAB. The base year for this emissions inventory is 1997, and then growth-and-control factors were applied to the base year emissions to achieve compliance with the 1-hour ozone standard by 2010. South Coast AQMD and ARB developed an emissions inventory for the 2007 air quality management plan to demonstrate attainment of the 8-hour average ozone federal air quality standard by the year 2023. A draft of the 2007 AQMP that contains basinwide emissions for 2023 is already available, although the gridded emissions inventory has not been made public yet. The gridded emissions for 2023 are obtained using the 2010 emissions and applying basinwide emissions reductions from 2003 AQMP to 2007 AQMP emissions, as described in Table 56. Therefore, the emissions inventory for 2023 used herein represents an estimate of the attainment scenario for the year 2023. Finally, estimates for the emissions inventory for 2030 are based on the 2023 attainment emissions inventory. The 2023 emissions are scaled up based on the population increase from 2023 to 2030, and then controlled so that the total basinwide emission levels will be equal to the emission levels for the year 2023.

**Table 56. Estimated daily basinwide emissions for years 2010 and 2023 in the South Coast Air Basin of California as estimated in the 2003 AQMP and 2007 AQMP by the South Coast Air Quality Management District**

| Species | 2003 AQMP Attainment (tons/day) Year 2010 | 2007 Attainment Inventory (tons/day) Year 2023 | Reductions from 2003 to 2007 Attainment Inventories (%) |
|---|---|---|---|
| VOC | 453 | 420 | 7 |
| $NO_X$ | 251 | 114 | 55 |
| CO | 2064 | 1966 | 5 |
| $SO_X$ | 33 | 19 | 42 |
| $PM_{2.5}$ | 140 | 88 | 37 |

Sources: SCAQMD 2003b; SCAQMD 2007

Emission reductions proposed by the 2007 AQMP lead to significant reductions of $NO_X$ and VOC emissions, which are the main precursors of ozone. As a result, peak ozone concentration in scenario B2, baseline for the year 2023 (based on 2007 AQMP) is lower than the peak ozone concentration simulated for scenario SoCAB-B1, baseline for the year 2010 (based on 2003 AQMP attainment inventory). As shown in Figure 48, peak ozone concentrations in scenario SoCAB-B1 are considerably higher than in scenarios SoCAB-B2 and SoCAB-B3, throughout the basin. Table 57 reports the maximum measured concentrations of some criteria pollutants. Results in Figure 48 show that ozone and $PM_{2.5}$ concentrations peak at locations downwind from Los Angeles, where the largest focus of emissions is located. On the other hand, CO concentrations peak in Central Los Angeles (not shown). Ozone, $NO_2$, and $PM_{2.5}$ peaks occur downwind from the main emissions because they are secondary pollutants; whereas CO is a primary pollutant, and its concentrations depend mainly on direct emissions.

Baseline simulations for the years 2023 and 2030 are based upon emission inventories that have been developed for the 2007 AQMP. Although air quality simulations performed by the SCAQMD show attainment of ozone and $PM_{2.5}$ air quality standards using those emissions, the model used in this project predicts that ozone and $PM_{2.5}$ concentrations exceed the established air quality standards in some locations. This is because the CACM chemical mechanism used for in the UCI-CIT model predicts higher oxidative capacity that leads to higher concentrations of $O_3$ than those predicted by some other chemical mechanisms, such as SAPRC-99, which has been used in the AQMP (Jimenez et al. 2003). Basinwide peak ozone concentration in scenario B3 is slightly higher than in scenario B2 because emissions for 2030 are redistributed toward inland locations, leading to lower peak ozone concentrations near the coast. On the other hand, peak ozone concentrations increase in inland locations, in particular in the northeastern corner, where the basinwide maximum occurs. The $PM_{2.5}$ concentrations are less sensitive to the different spatial distribution of pollutants between 2023 and 2030, and no major changes in $PM_{2.5}$ occur in the basin, as shown in Table 57 and in Figure 48.

**Table 57. Maximum concentration of pollutants on August 29 in baseline cases for the years 2010, 2023, and 2030, along with the applicable ambient air quality standards**

| Pollutant | USEPA[(1)]/CAAQS[(2)] Standard | Year 2010 | Year 2023 | Year 2030 |
|---|---|---|---|---|
| 1-hour $O_3$ | 120 ppb [(1)] | 235 ppb | 150 ppb | 152 ppb |
| 8-hour $O_3$ | 84 ppb [(1)] | 222 ppb | 128 ppb | 129 ppb |
| 1-hour CO | 20 ppm [(2)] | 3.0 ppm | 1.6 ppm | 1.7 ppm |
| 1-hour $NO_2$ | 180 ppb [(2)] | 121 ppb | 78 ppb | 77 ppb |
| 24-hour $PM_{2.5}$ | 35 $\mu g/m^3$ [(1)] | 123 $\mu g/m^3$ | 60 $\mu g/m^3$ | 60 $\mu g/m^3$ |

[1] National Ambient Air Quality Standard is applied
[2] California Ambient Air Quality Standard is applied
$\mu g/m^3$ = microgram per cubic meter

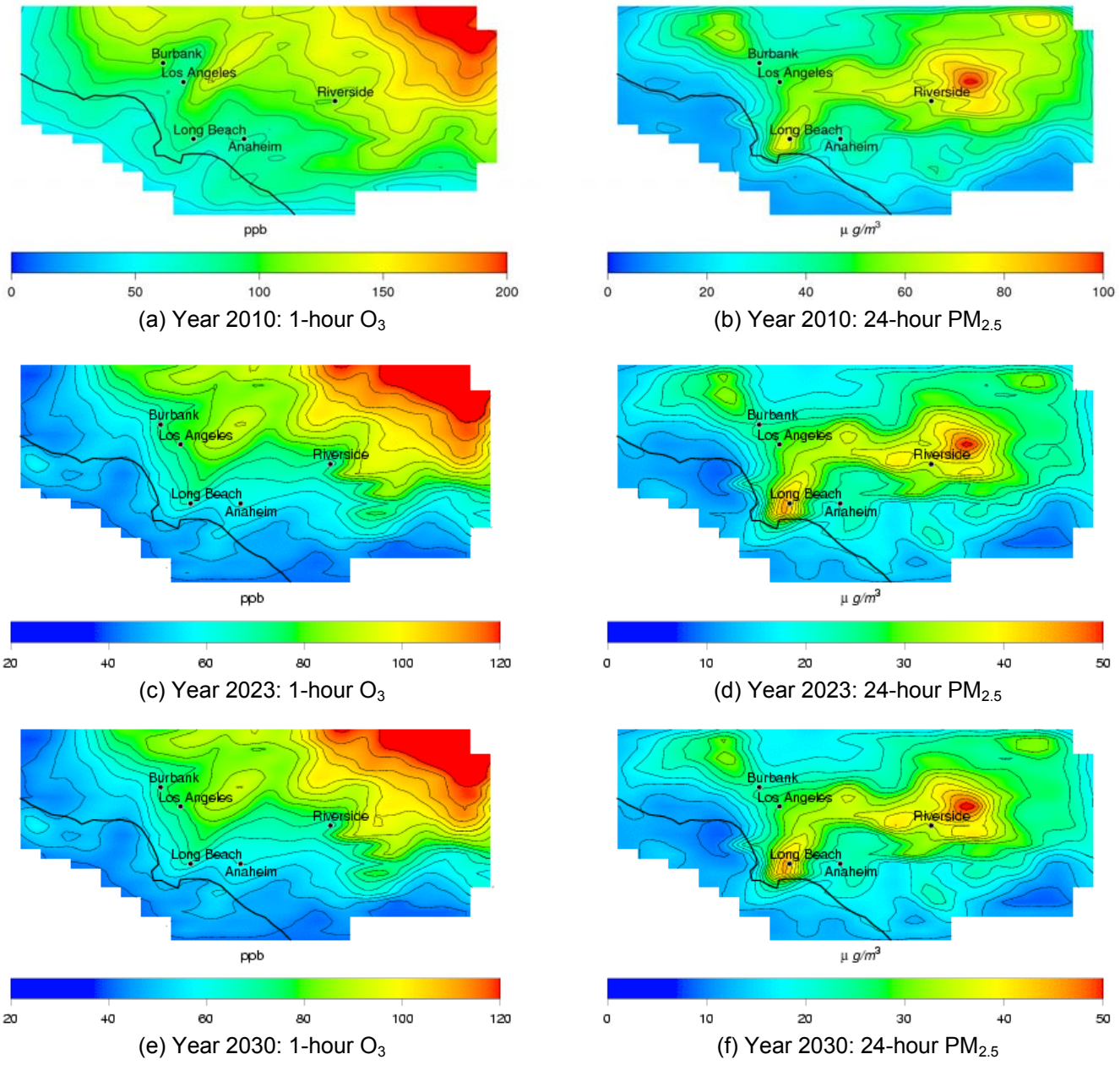


**Figure 48. Peak 1-hour ozone concentration and 24-hour average $PM_{2.5}$ concentrations in the South Coast Air Basin of California, for the baseline years 2010, 2023, and 2030**

The synoptic conditions in the SoCAB create a regime of circulation that favors transport of pollutants, emitted mainly in Los Angeles and Long Beach, toward the northeast. In the northeastern part of the domain there are mountain ranges that trap the pollution arriving from upwind, leading to accumulation of ozone concentration. Near Riverside, a high density of dairy farms releases significant amounts of ammonia. This ammonia reacts with nitric acid formed via oxidation of nitrogen oxides emitted upwind to form secondary particulate matter, leading to the high $PM_{2.5}$ near Riverside. Two other foci of $PM_{2.5}$ concentration develop near Central Los Angeles and the Port of Long Beach. The former originates from direct emissions from vehicles; whereas the latter originates from direct emissions due to the activity at the port, where there are high emissions from trucks, trains, and ships.

Although the increase of basinwide emissions in all cases is relatively small compared to total emissions, each scenario considers the implementation of a different DG technology mix and the DG systems themselves are installed to operate according to different duty cycles. In addition, each DG technology has different emission factors and is implemented differently according to its use by activity sector. As a result, chemically resolved emissions vary widely in space and time. Furthermore, the effects of emissions fluxes on ambient concentrations depend upon a host of coupled processes including bulk transport, diffusion, and chemical and photochemical reactions. Hence, localized air quality impacts can be determined only through use of the three-dimensional air quality models.

### *5.1.2. Air Quality Impacts of Realistic DG Scenarios*

The analysis of air quality impacts of DG was conducted with the overall assumption that DG emissions are always added to the baseline emissions inventory. This was done to clearly identify and investigate the potential air quality impacts of DG in future years. Note that it is likely that DG will be employed to displace current basin emissions from older electricity generation, in which case the implementation of DG would be more favorable with respect to air quality than what is presented in the current analyses. The only significant accounting of emissions displaced by DG in the analyses for realistic scenarios is for combined heating and power. A few cases that explore additional impacts of emissions that may be displaced by implementation of DG (for example by substituting for older power plants) are considered in the analysis for spanning scenarios.

Table 58 shows a brief description of the parameters considered in each realistic scenario. Realistic scenarios assume sector-specific duty cycles for DG technologies, shown in Figure 49. Table 59 shows the overall DG technology mix obtained through the methodology described in Section 2.0.

**Table 58. Brief description of DG realistic scenario parameters**

| DG Scenario | Parameters that describe each scenario |
|---|---|
| **SoCAB-R1** | • 12% of increased power demand from 2007 to 2023/2030 met by DG<br>• Technology mix according to activity sector distribution (see Table 59 and Figure 17b)<br>• Spatial distribution according to GIS land use distribution<br>• Realistic duty cycle per each sector (see Figure 49)<br>• CHP emission displaced<br>• Linear trend for DG power adoption |
| **SoCAB-R2** | • 7% of increased power demand from 2007 to 2023/2030 met by DG<br>• Same assumptions as in SoCAB-R1 for the rest of parameters |
| **SoCAB-R3** | • 18% of increased power demand from 2007 to 2023/2030 met by DG<br>• Same assumptions as in SoCAB-R1 for the rest of parameters |
| **SoCAB-R4** | • High R&D scenario with high penetration of fuel cells (technology mix shown in Figure 17c)<br>• Same assumptions as in SoCAB-R3 for the rest of parameters |
| **SoCAB-R5** | • High penetration of fuel cells due to environmental forcing<br>• Fuel cell penetration 4 times the penetration in SoCAB-R3<br>• Same assumptions as in SoCAB-R3 for the rest of parameters |

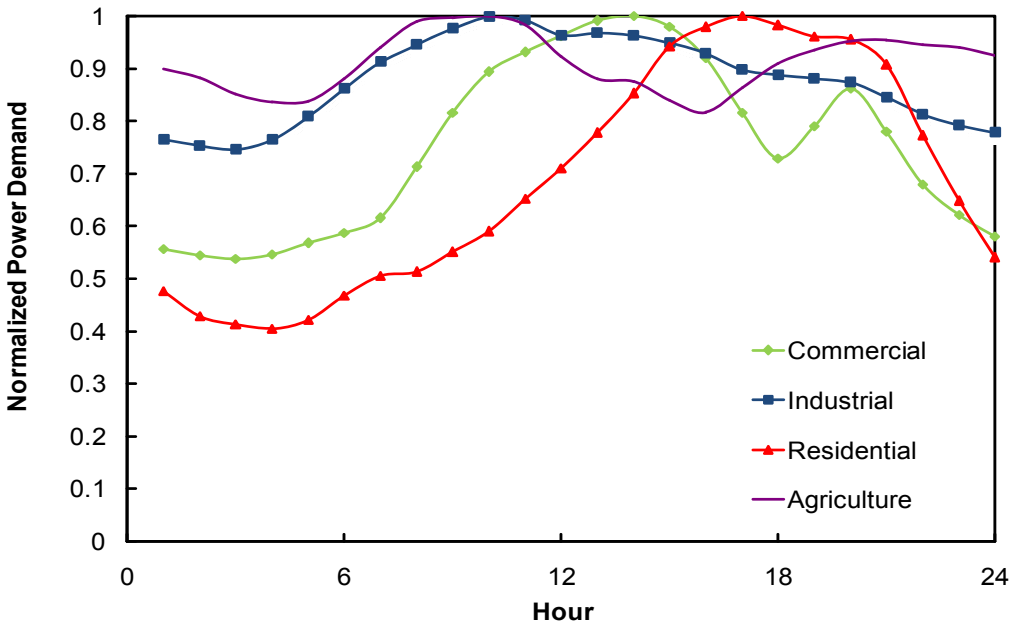


**Figure 49. Duty cycle for different activity sectors. Each duty cycle is normalized with respect to the maximum demand of that particular sector.**

Source: Southern California Edison Load Profiles (www.sce.com/AboutSCE/Regulatory/loadprofiles/, last accessed 2005)

**Table 59. Power distribution by activity sector, DG power size, and DG technology, in percentage (%) with respect to total power provided by DG in realistic scenario SoCAB-R1**

| Sector | DG Size | DG Technologies | | | | | |
|---|---|---|---|---|---|---|---|
| **Commercial** | | | | | | | |
| | | **LTFC** | **HTFC** | **MTGS** | **NGIC** | **TURB** | **HYBR** |
| | <50 kW | 0.21 | 0.03 | 0.03 | 0.49 | | |
| | 50–250 kW | 0.04 | 0.18 | 0.32 | 2.52 | | |
| | 250 kW–1 MW | | 0.22 | 0.01 | 2.97 | 0.03 | |
| | 1–5 MW | | 0.34 | | 10.00 | 0.50 | |
| | 5–20 MW | | 0.70 | | 11.87 | 8.38 | |
| | 20–50 MW | | | | | | |
| **Industrial** | | | | | | | |
| | | **LTFC** | **HTFC** | **MTGS** | **NGIC** | **TURB** | **HYBR** |
| | <50 kW | | | | | | |
| | 50–250 kW | | 0.01 | 0.03 | 0.35 | | |
| | 250 kW–1 MW | | 0.01 | 0.00 | 0.56 | 0.04 | |
| | 1–5 MW | | 0.05 | | 5.35 | 1.94 | |
| | 5–20 MW | | 0.03 | | 1.77 | 8.97 | |
| | 20–50 MW | | 0.07 | | | 22.10 | |
| **Low Density Residential** | | | | | | | |
| | | **LTFC** | **HTFC** | **MTGS** | **NGIC** | **TURB** | **HYBR** |
| | <50 kW | 0.06 | 0.00 | | | | |
| | 50–250 kW | 0.00 | 0.00 | | | | |
| | 250 kW–1 MW | | | | | | |
| | 1–5 MW | | | | | | |
| | 5–20 MW | | | | | | |
| | 20–50 MW | | | | | | |
| **High and Medium Density Residential** | | | | | | | |
| | | **LTFC** | **HTFC** | **MTGS** | **NGIC** | **TURB** | **HYBR** |
| | <50 kW | 0.02 | 0.00 | 0.00 | 0.00 | | 0.00 |
| | 50–250 kW | 0.01 | 0.03 | 0.05 | 0.01 | | 0.01 |
| | 250 kW–1 MW | | 0.07 | 0.00 | 0.02 | | 0.01 |
| | 1–5 MW | | | | | | |
| | 5–20 MW | | | | | | |
| | 20–50 MW | | | | | | |
| **Agriculture** | | | | | | | |
| | | **LTFC** | **HTFC** | **MTGS** | **NGIC** | **TURB** | **HYBR** |
| | <50 kW | 0.04 | 0.01 | 0.01 | 0.09 | | |
| | 50–250 kW | 0.01 | 0.03 | 0.06 | 0.48 | | |
| | 250 kW–1 MW | | | | | | |
| | 1–5 MW | | | | | | |
| | 5–20 MW | | | | | | |
| | 20–50 MW | | | | | | |
| **Others** | | | | | | | |
| | | **LTFC** | **HTFC** | **MTGS** | **NGIC** | **TURB** | **HYBR** |
| | <50 kW | | | | | | |
| | 50–250 kW | 0.00 | 0.03 | | 0.11 | | 0.02 |
| | 250 kW–1 MW | | 0.05 | | 0.17 | 0.03 | 0.03 |
| | 1–5 MW | | 0.22 | | 1.53 | 1.47 | 0.14 |
| | 5–20 MW | | 0.08 | | 0.33 | 4.46 | 0.05 |
| | 20–50 MW | | 0.18 | | | 9.85 | 0.11 |

Deployment of DG in most cases implies an increase of in-basin emissions of primary pollutants using the current approach, although the use of CHP reduces some of these emissions. However, the use of CHP in the realistic scenarios does not offset totally the emissions from DG, resulting in a net increase in emissions due to DG implementation. Table 60 shows the increase in criteria pollutant emissions for each realistic DG scenario. Table 61 presents the increase in percentage of pollutant emissions relative to the total in-basin emissions.

In general, emissions of CO and VOC from DG units contribute to less than 0.1% to total basinwide emissions. Even though CHP is used in all realistic scenarios, emissions displaced from boilers do not offset $NO_X$ emissions from DG. However, the resulting net emissions from DG with CHP correspond to less than 1% of the total emissions. The DG emissions of $SO_X$ and $NH_3$, which are precursors for particulate matter, contribute less than 1% to total emissions; whereas direct emissions of $PM_{2.5}$ from DG contribute to up to 0.37%. Consequently, air quality impacts of DG are expected to be small, although the temporal and spatial distribution of emissions may lead to significant effects at some locations. Model results from spanning scenarios show trends in air quality impacts of DG similar to the ones observed through analysis of realistic scenarios. However, impacts from spanning scenarios are more noticeable because the range of emissions is significantly larger than in the realistic scenarios. Hence, despite the small changes in emissions, the air quality model is sensitive and shows small yet meaningful changes in pollutant concentrations. That is, air quality impacts of realistic DG scenarios are small, because the impacts of DG on total basinwide emissions are small. A more detailed discussion of air quality impacts is presented in the following subsections.

**Table 60. Daily basinwide pollutant emissions, in tons per day, from DG for all realistic scenarios**

| Scenario | Electricity produced by DG (MW) | Emission (ton/day) | | | | | |
|---|---|---|---|---|---|---|---|
| | | CO | $NO_X$ | VOC | $SO_X$ | $PM_{2.5}$ | $NH_3$ |
| ***Year 2023*** | | | | | | | |
| **SoCAB-R1** | 1011.4 | 0.88 | 0.40 | 0.07 | 0.03 | 0.38 | 0.34 |
| **SoCAB-R2** | 700.2 | 0.61 | 0.27 | 0.05 | 0.02 | 0.26 | 0.23 |
| **SoCAB-R3** | 1789.4 | 1.55 | 0.70 | 0.13 | 0.06 | 0.67 | 0.60 |
| **SoCAB-R4** | 1789.4 | 1.46 | 0.67 | 0.12 | 0.06 | 0.67 | 0.60 |
| **SoCAB-R5** | 1789.4 | 1.37 | 0.64 | 0.11 | 0.05 | 0.65 | 0.58 |
| ***Year 2030*** | | | | | | | |
| **SoCAB-R1** | 1369.2 | 1.19 | 0.52 | 0.10 | 0.05 | 0.51 | 0.46 |
| **SoCAB-R2** | 798.7 | 0.69 | 0.30 | 0.06 | 0.03 | 0.30 | 0.27 |
| **SoCAB-R3** | 2053.8 | 1.78 | 0.78 | 0.15 | 0.07 | 0.77 | 0.68 |
| **SoCAB-R4** | 2053.8 | 1.67 | 0.74 | 0.14 | 0.07 | 0.77 | 0.68 |
| **SoCAB-R5** | 2053.8 | 1.57 | 0.71 | 0.13 | 0.06 | 0.74 | 0.66 |

**Table 61. Daily basinwide pollutant emissions, in % with respect to baseline emissions, from DG for all realistic scenarios**

| Scenario | Electricity produced by DG (MW) | Emission (%) | | | | | |
|---|---|---|---|---|---|---|---|
| | | CO | $NO_X$ | VOC | $SO_X$ | $PM_{2.5}$ | $NH_3$ |
| ***Year 2023*** | | | | | | | |
| **SoCAB-R1** | 1011.4 | 0.04 | 0.35 | 0.02 | 0.20 | 0.18 | 0.43 |
| **SoCAB-R2** | 700.2 | 0.03 | 0.24 | 0.01 | 0.14 | 0.13 | 0.30 |
| **SoCAB-R3** | 1789.4 | 0.08 | 0.62 | 0.03 | 0.35 | 0.33 | 0.76 |
| **SoCAB-R4** | 1789.4 | 0.07 | 0.59 | 0.03 | 0.35 | 0.30 | 0.77 |
| **SoCAB-R5** | 1789.4 | 0.07 | 0.56 | 0.03 | 0.34 | 0.28 | 0.74 |
| ***Year 2030*** | | | | | | | |
| **SoCAB-R1** | 1369.2 | 0.06 | 0.46 | 0.02 | 0.27 | 0.25 | 0.58 |
| **SoCAB-R2** | 798.7 | 0.04 | 0.27 | 0.01 | 0.16 | 0.15 | 0.34 |
| **SoCAB-R3** | 2053.8 | 0.09 | 0.69 | 0.03 | 0.41 | 0.37 | 0.87 |
| **SoCAB-R4** | 2053.8 | 0.09 | 0.65 | 0.03 | 0.41 | 0.35 | 0.88 |
| **SoCAB-R5** | 2053.8 | 0.08 | 0.62 | 0.03 | 0.39 | 0.32 | 0.84 |

Figure 50 presents air quality impacts of realistic scenario R1 for 2010 (from the phase I project—see Samuelsen et al. 2005) and SoCAB-R1 for the years 2023 and 2030. The point of presenting a single DG implementation scenario for three separate future years is to show the impacts of future baseline emissions assumptions (i.e., those used for 2010, 2023, and 2030) on the effects of DG on air quality. Emissions of ozone precursors—CO, VOC, and $NO_X$—from DG are less than 1% of the total emissions. As a result, the difference in peak ozone concentration between the R1 DG scenarios and their respective baseline case—with no DG—is less than 1 ppb. In addition, increases of $SO_X$ and PM due to DG implementation are less than 1% in all cases. As a result, differences in simulated 24-hour average $PM_{2.5}$ concentrations between these realistic DG cases and their respective baseline cases throughout the basin end up being smaller than 1 $\mu g/m^3$.

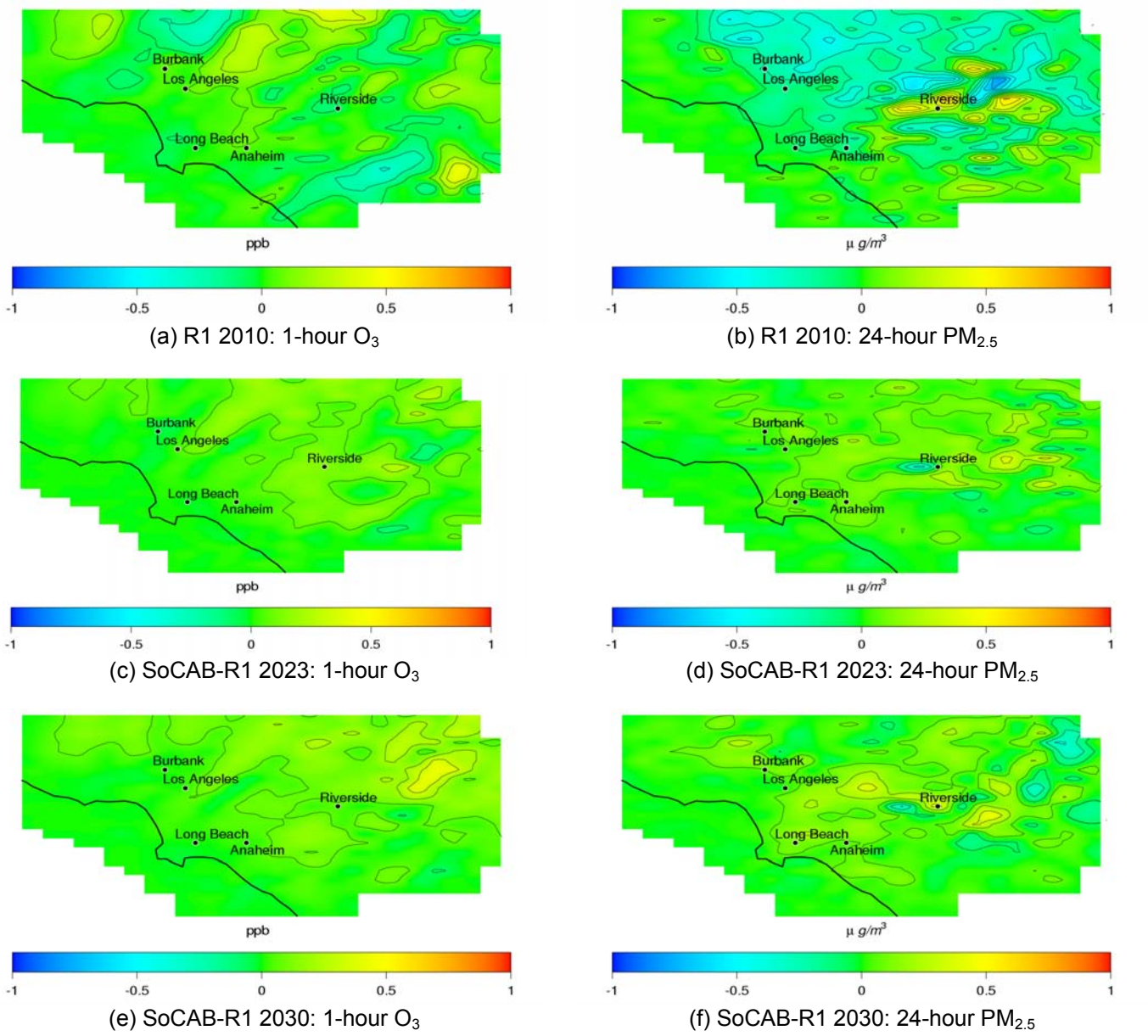


(a) R1 2010: 1-hour $O_3$

(b) R1 2010: 24-hour $PM_{2.5}$

(c) SoCAB-R1 2023: 1-hour $O_3$

(d) SoCAB-R1 2023: 24-hour $PM_{2.5}$

(e) SoCAB-R1 2030: 1-hour $O_3$

(f) SoCAB-R1 2030: 24-hour $PM_{2.5}$

**Figure 50. Difference in peak 1-hour average ozone concentrations and in 24-hour average $PM_{2.5}$ concentrations between the realistic DG scenario R1 and the baseline air quality (no DG case) for the target years 2010, 2023, and 2030 (the 1-hour $O_3$ California Ambient Air Quality Standards (CAAQS) = 90 ppb, and the 24-hour $PM_{2.5}$ CAAQS = 35 μg/m$^3$)**

Emissions from DG in scenario R1 for 2010 assumes DG penetration from 2003 to 2010. The DG installations implemented before 2007 are regulated by the ARB 2003 standards, which are less restrictive than the 2007 ARB standards. As a result, emissions from DG in the 2010 case are approximately twice the emissions released by DG in the 2023 and 2030 scenarios, in which all DG emit below the 2007 emission standards. Although total emissions of ozone precursors from DG in scenario R1 2010 are more than twice the emissions in scenarios SoCAB-R1 in 2023 and

2030, the magnitude of air quality impacts attributable to DG are comparable. In addition, in scenario R1 2010, the use of CHP that offsets old boiler emissions lead to a net decrease in $NO_X$ emissions; whereas in scenarios SoCAB-R1 for 2023 and 2030, CHP does not completely offset DG emissions, leading to net increase in emissions. Implementation of DG in the three cases leads to slight increases in ozone concentration, despite that in 2010 DG slightly reduces $NO_X$ emissions. This is due to the difference in baseline $NO_X$ emissions levels between the year 2010 and later years. The total basinwide $NO_X$ emissions in the year 2010 are projected to be three times the $NO_X$ emissions in 2023 and 2030. High levels of $NO_X$ present in 2010 provide VOC-limited conditions under which small decreases in $NO_X$ emissions lead to increases in ozone concentration. On the other hand, low levels of baseline $NO_X$ estimated for 2023 provide $NO_X$-limited conditions, in which increases of $NO_X$ emissions due to DG lead to increases in ozone concentrations.

Implementation of DG increases direct emissions of particles that may contribute to increasing concentrations of $PM_{2.5}$. In addition, increases in emissions of $NO_X$ and $SO_X$ in scenarios for 2023 and 2030 also contribute to the secondary formation of particles. As a result, DG implementation in scenarios SoCAB-R1-2023 and SoCAB-R1-2030 leads to increases in $PM_{2.5}$ concentrations. On the other hand, DG implementation in 2010 leads to decreases in $NO_X$ emissions, reducing the formation of nitric acid. Reduction of nitric acid concentration offsets the increase in particle formation from $SO_X$ emissions, and as a result, DG in 2010 produces mixed impacts; namely, it reduces $PM_{2.5}$ by less than 1 $\mu g/m^3$ in some areas and increases $PM_{2.5}$ by less than 1 $\mu g/m^3$ in some other areas.

Table 62 through Table 64 present the maximum air quality impacts of all realistic DG scenarios for 2023 and 2030. Impacts on peak and hourly ozone concentration are smaller than 1.0 ppb. Impacts on 8-hour average concentrations are smaller than 0.5 ppb. Finally, impacts of DG on 24-hour average $PM_{2.5}$ concentration are smaller than 1.2 $\mu g/m^3$.

In conclusion, realistic DG implementation leads to small perturbations in pollutant emissions that result in small differences in ozone and $PM_{2.5}$ concentrations with respect to baseline air quality. Distributed generation emissions are directly related to the level of DG market penetration. In addition, the resulting emissions from DG depend on the technology mix estimated for the SoCAB and the emissions associated with each technology. For realistic scenarios in 2023 and 2030, ICE and gas turbines are assumed to meet the 2007 ARB emissions standards, which are more restrictive than the current BACT emissions limits. These factors directly affect emissions from DG, and consequently, may affect the air quality impacts resulting from DG implementation. The following subsections analyze the effects of market penetration and technology mix on the potential air quality impacts of DG in the SoCAB. Other factors considered include emission factors used for DG technologies and the level of CHP implementation that determines the extent of emissions displacement that DG implementation could achieve. These factors are extensively analyzed using the spanning scenarios. Results of these analyses are presented in Section 5.1.3.

**Table 62. Impacts of DG realistic scenarios on peak and 1-hour average ozone concentrations with respect to the baseline cases for 2023 and 2030**

| | | Δ peak $O_3$ | | Δ 1-hour $O_3$ | |
|---|---|---|---|---|---|
| | Peak $O_3$ | Maximum increase | Maximum decrease | Maximum increase | Maximum decrease |
| Scenario | (ppb) | (ppb) | (ppb) | (ppb) | (ppb) |
| 2023 | | | | | |
| Baseline | 150.0 | | | | |
| SoCAB-R1 | 150.1 | 0.5 | -0.5 | 0.5 | -0.3 |
| SoCAB-R2 | 149.9 | 0.5 | -0.4 | 0.5 | -0.2 |
| SoCAB-R3 | 150.1 | 0.6 | -0.8 | 0.4 | -0.3 |
| SoCAB-R4 | 150.2 | 0.6 | -0.8 | 0.4 | -0.2 |
| SoCAB-R5 | 150.1 | 0.5 | -0.8 | 0.4 | -0.2 |
| 2030 | | | | | |
| Baseline | 152.0 | | | | |
| SoCAB-R1 | 152.2 | 0.8 | -1.2 | 0.7 | -0.2 |
| SoCAB-R2 | 152.2 | 0.6 | -0.8 | 0.6 | -0.3 |
| SoCAB-R3 | 152.2 | 0.7 | -0.9 | 0.7 | -0.3 |
| SoCAB-R4 | 152.3 | 0.9 | -0.9 | 0.6 | -0.3 |
| SoCAB-R5 | 152.2 | 0.6 | -0.9 | 0.6 | -0.3 |

**Table 63. Impacts of DG realistic scenarios on 8-hour average ozone concentrations with respect to the baseline cases for 2023 and 2030**

| | | Δ max 8-hour average $O_3$ | |
|---|---|---|---|
| | 8-hour $O_3$ | Maximum increase | Maximum decrease |
| Scenario | (ppb) | (ppb) | (ppb) |
| 2023 | | | |
| Baseline | 127.8 | | |
| SoCAB-R1 | 127.8 | 0.2 | -0.1 |
| SoCAB-R2 | 127.8 | 0.2 | -0.1 |
| SoCAB-R3 | 127.9 | 0.3 | -0.1 |
| SoCAB-R4 | 127.8 | 0.2 | -0.1 |
| SoCAB-R5 | 127.8 | 0.3 | -0.1 |
| 2030 | | | |
| Baseline | 128.8 | | |
| SoCAB-R1 | 128.9 | 0.3 | -0.1 |
| SoCAB-R2 | 128.8 | 0.3 | -0.1 |
| SoCAB-R3 | 129.1 | 0.3 | -0.1 |
| SoCAB-R4 | 128.9 | 0.4 | -0.1 |
| SoCAB-R5 | 129.0 | 0.3 | -0.1 |

**Table 64. Impacts of DG realistic scenarios on 24-hour average $PM_{2.5}$ concentrations with respect to the baseline cases for 2023 and 2030**

| | | Δ 24-hour $PM_{2.5}$ | |
|---|---|---|---|
| | 24-hour $PM_{2.5}$ | Maximum increase | Maximum decrease |
| Scenario | ($\mu g/m^3$) | ($\mu g/m^3$) | ($\mu g/m^3$) |
| 2023 | | | |
| Baseline | 60.0 | | |
| SoCAB-R1 | 60.1 | 0.7 | -0.7 |
| SoCAB-R2 | 60.0 | 0.7 | -0.6 |
| SoCAB-R3 | 60.1 | 1.1 | -0.5 |
| SoCAB-R4 | 60.0 | 1.0 | -0.4 |
| SoCAB-R5 | 60.0 | 0.7 | -0.5 |
| 2030 | | | |
| Baseline | 59.7 | | |
| SoCAB-R1 | 59.8 | 0.9 | -0.8 |
| SoCAB-R2 | 59.7 | 0.8 | -1.0 |
| SoCAB-R3 | 59.8 | 0.9 | -0.6 |
| SoCAB-R4 | 59.9 | 0.9 | -0.7 |
| SoCAB-R5 | 59.8 | 1.1 | -0.8 |

### *Effects of DG Market Penetration*

Distributed generation market penetration for scenario SoCAB-R1 corresponds to 12% of the increased power demand from 2007 to 2030. This level of penetration is based on market studies by EPRI (2005) that assumed a scenario that maintained the current incentives for DG installations. Thus, this level of DG penetration is sensitive to the incentives available for DG installation. The EPRI report suggests that in a scenario without incentives, market penetration of DG could be as low as 7% of the increased power demand; whereas in a scenario with increased incentives it could rise to 18% of the increased demand from 2005 to 2020. These two extremes are examined in this section.

Scenario SoCAB-R2 assumes the lowest DG penetration, which corresponds to 7% of the increased demand from 2007 to 2030, and as a result introduces the lowest emissions from distributed generation. Consequently, the air quality impacts of DG in scenario SoCAB-R2 are very small. Peak ozone concentration in scenario SoCAB-R2 is not affected by DG in most of the central part of the domain. Only in the northeastern portion of the domain the peak ozone is affected. The peak in this area is less than 0.5 ppb higher than in the base case, due to the slight increase of $NO_X$ (see Figure 51a and c, for years 2023 and 2030, respectively). Increases of $NO_X$ and $SO_X$ emissions due to DG increase the formation of nitrate and sulfate aerosols. In addition, DG also increases the emissions of PM, leading to an overall increase in the $PM_{2.5}$ concentration. As a result, DG produces maximum increases in $PM_{2.5}$ of 0.8 $\mu g/m^3$, due to the small perturbation in emissions (see Figure 52a and c for years 2023 and 2030, respectively).

On the other end of the market penetration spectrum, scenario SoCAB-R3 presents the highest DG penetration amongst realistic scenarios. Nevertheless, the perturbations in emissions of scenario SoCAB-R3 are smaller than 0.9%, which results in increases of less than 0.7 ppb in peak

ozone concentration (see Figure 51b and d), and changes in $PM_{2.5}$ smaller than 1.1 $\mu g/m^3$ (see Figure 52b and d). However, the area in which peak ozone is affected by DG in scenario SoCAB-R3 is larger than in scenario SoCAB-R1 and SoCAB-R2, covering most of the basin.

In conclusion, even though the total DG penetration in 2030 is expected to be larger than in 2010, results suggest that air quality impacts will be small. In particular, none of the DG realistic scenarios increase the overall maximum 8-hour average ozone concentration. Consequently, DG implementation as proposed in the realistic scenarios would not affect compliance with ozone standards. Emissions from DG estimated for 2010 included units that could emit at the less restrictive 2003 ARB standards. On the other hand, emissions estimates for 2023 and 2030 assume that all DG will emit at the most restrictive 2007 ARB standards, which leads to smaller impacts than the ones estimated for 2010. A series of spanning scenarios are analyzed to quantify the effect of increasing the values of emission factors for DG on air quality.

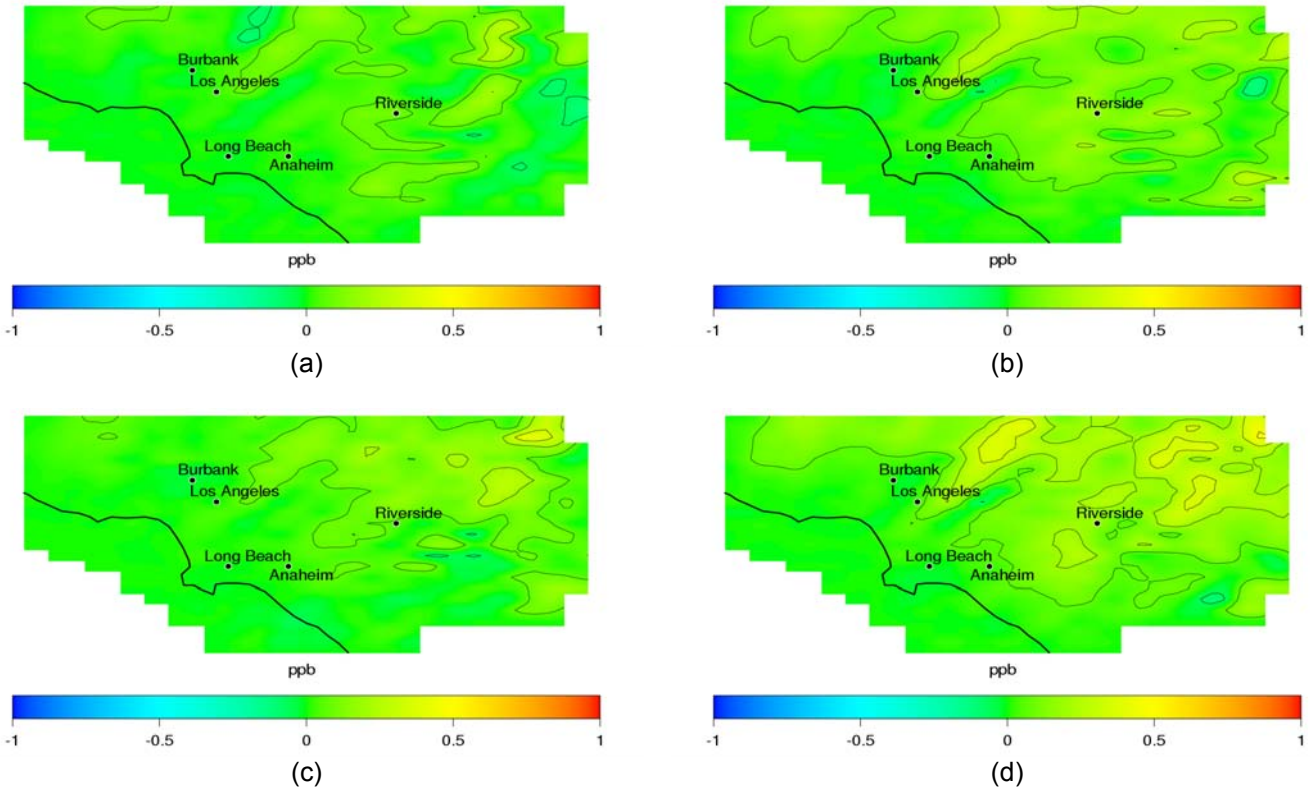


**Figure 51. Impacts of realistic scenarios on peak $O_3$ as a function of DG market penetration: (a) Scenario SoCAB-R2, year 2023, (b) Scenario SoCAB-R3, year 2023, (c) Scenario SoCAB-R2, year 2030, (d) Scenario SoCAB-R3, year 2030**

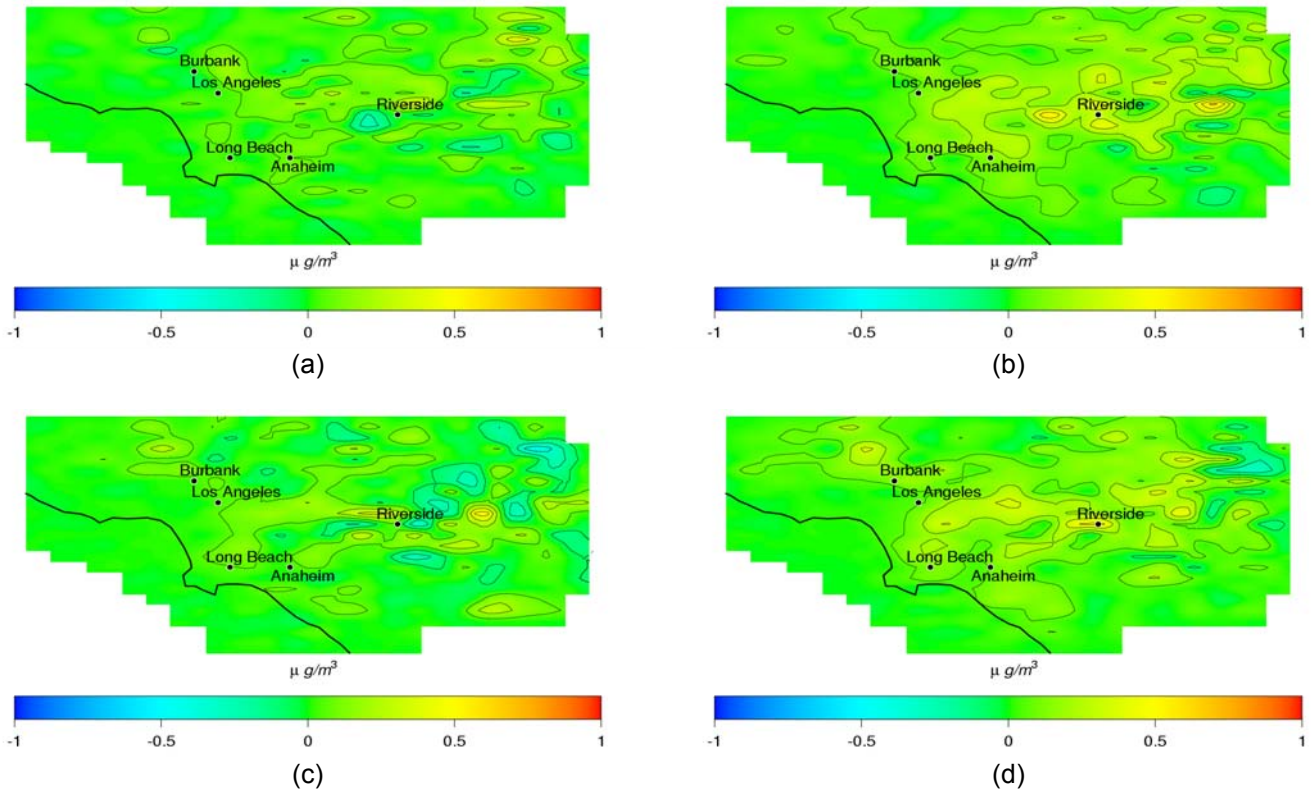


**Figure 52. Impacts of realistic scenarios on 24-hour average $PM_{2.5}$ as a function of DG market penetration: (a) Scenario SoCAB-R2, year 2023, (b) Scenario SoCAB-R3, year 2023, (c) Scenario SoCAB-R2, year 2030, (d) Scenario SoCAB-R3, year 2030**

### *Effects of DG Technology Mix*

Technology mix in scenario SoCAB-R1 through SoCAB-R3 are based on estimates by EPRI (2005), which considered not only customer power needs, but also customer response as a function of economical parameters and emission regulations. As a result, most DG installations for these three realistic scenarios consist of gas turbines and internal combustion engines; whereas penetration of fuel cells only adds up to 3% of the total installed capacity. However, the EPRI report suggested that with increased incentives and higher investment in R&D, penetration of FC could increase up to 10%, by the year 2020.

Scenario SoCAB-R4 evaluates the air quality impacts of such scenarios. In particular, scenario SoCAB-R4 considers the same parameters as in scenario SoCAB-R3 but increases penetration of fuel cells up to 10% of the total DG capacity, in detriment of ICE, mostly. Since fuel cells are more efficient than ICE, the excess heat available for CHP in scenario SoCAB-R4 is lower than in scenario SoCAB-R3. Thus, the reduction in $NO_x$ emissions due to the use of fuel cells, which emit at a lower rate than ICE, is not offset by the reduction in emission displacements due to combined heating and power. However, the result is a small decrease in emissions of some pollutants from DG in scenario SoCAB-R4, with respect to scenario SoCAB-R3. The incentives assumed for scenario SoCAB-R4 are prior the approval of AB32 for the reduction of greenhouse gases.

Scenario SoCAB-R5 assumes a penetration of fuel cells that is two times the penetration of fuel cells in scenario SoCAB-R4 to include any additional incentives created by AB32 for high-efficiency electricity production. As a result, emissions from DG in scenario SoCAB-R5 are lower than in scenario SoCAB-R4.

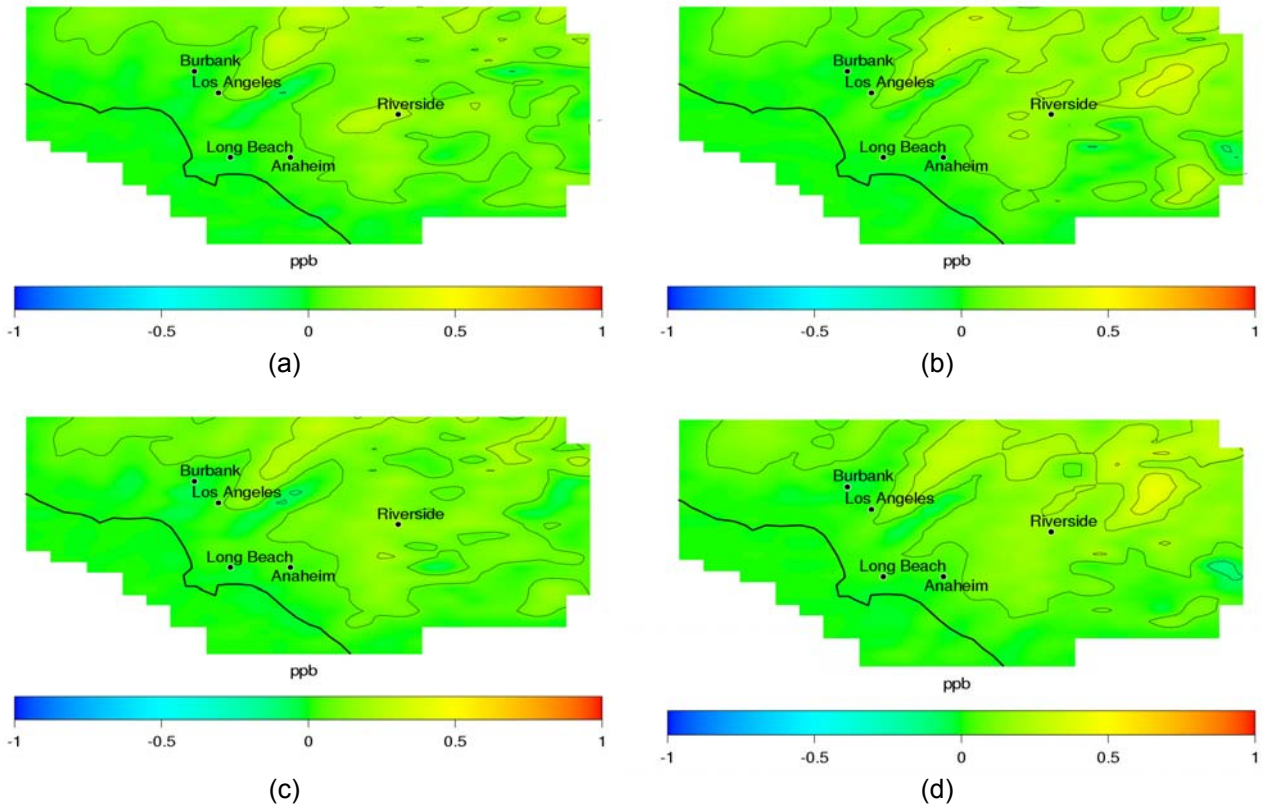


**Figure 53. Impacts on peak $O_3$ for realistic scenarios with high penetration of fuel cells: (a) Scenario SoCAB-R4, year 2023, (b) Scenario SoCAB-R4, year 2030, (c) Scenario SoCAB-R5, year 2023, (d) Scenario SoCAB-R5, year 2030**

As $NO_X$ emissions in scenarios SoCAB-R4 and SoCAB-R5 are slightly lower than in scenario SoCAB-R3, reductions in peak ozone concentration in scenarios SoCAB-R4 and SoCAB-R5 are slightly smaller than those of scenario SoCAB-R3 (see Figure 53). Also, emissions of $SO_X$ and PM from DG in scenarios SoCAB-R4 and SoCAB-R5 are slightly lower than in scenario SoCAB-R3, which leads to impacts on 24-hour average $PM_{2.5}$ of up to 1.1 $\mu g/m^3$, which are comparable to scenario SoCAB-R3 (see Figure 54 and Table 64).

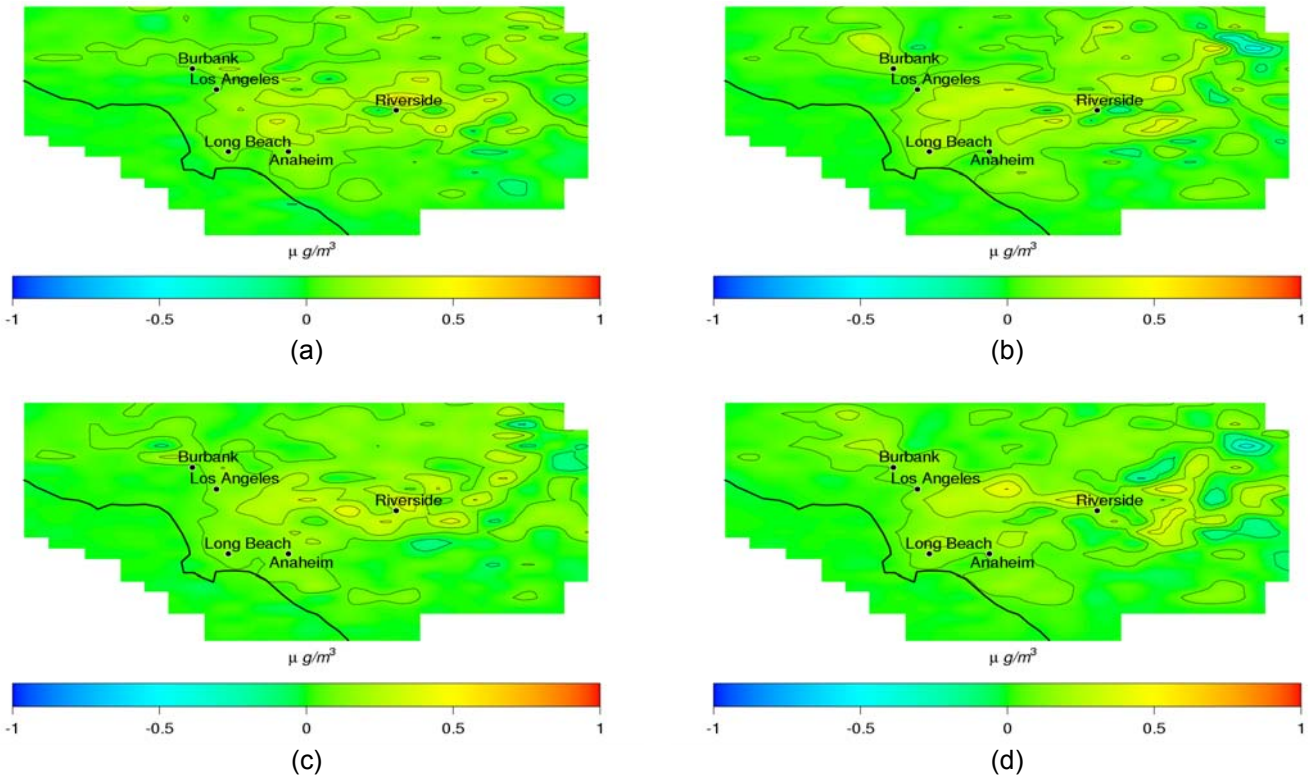


**Figure 54. Impacts on 24-hour average $PM_{2.5}$ for realistic scenarios with high penetration of fuel cells: (a) Scenario SoCAB-R4, year 2023, (b) Scenario SoCAB-R4, year 2030, (c) Scenario SoCAB-R5, year 2023, (d) Scenario SoCAB-R5, year 2030**

In summary, emissions from DG in realistic DG scenarios lead to impacts on peak ozone concentration and 24-hour average $PM_{2.5}$ concentrations that are smaller than 1.0 ppb and 1.1 μg/m$^3$, respectively. Although DG penetration in the year 2030 could supply more than 2 GW of power capacity, emissions from DG correspond to less than 1.0% of the total baseline emissions, and their associated air quality impacts are very small. Note that ICE and gas turbines are assumed to meet the 2007 ARB emissions standards for all realistic scenarios. A series of spanning scenarios has been developed to analyze the impact of less restrictive emissions standards, namely the BACT emissions standards. The use of CHP in conjunction with the implementation of DG reduces DG emissions but does not completely offset them, resulting in a net increase in $NO_X$ emissions, which leads to slight increases in peak ozone concentrations. In addition, implementation of DG could slightly increase $PM_{2.5}$ concentrations due to direct emissions of particles and the formation of particles from $SO_X$ and $NO_X$.

### *5.1.3. Air Quality Impacts of Spanning DG Scenarios*

Spanning scenarios are developed to assess the effects that some parameters of DG scenarios have on air quality. Because the air quality impacts presented for the realistic DG scenarios are small due to the level of DG penetration, the analysis in this section is based on the year 2030. This year assumes the highest DG penetration amongst the target years and shows more noticeable air quality impacts, and hence, the year 2030 is more illustrative than 2023 for showing the effects of DG parameters on air quality.Table 65 presents the list of spanning

scenarios with a short descriptive name that identifies the most characteristic features of each scenario and Table 66 presents a brief description of the main parameters assumed in each DG spanning scenario. These two tables are for quick reference of the spanning scenarios. For complete description of the spanning scenarios, see Section 3.1.3.

**Table 65. List of acronyms for spanning scenarios and their respective description**

| Acronym | Descriptive name |
|---|---|
| LU | Land-Use weighted |
| BACT | All internal combustion engines emitting at BACT levels of 2007 |
| ARB07 | All DG units emit at the 2007 ARB standards |
| FC | All fuel cell |
| Peak | Peak duty cycle |
| LDG | All large gas turbines (49 MW) |
| LDGNH3 | All large gas turbines (49 MW) with ammonia slip |
| PGW | Population growth weighted |
| CHP | All units with combined heating and power and 100% heat use |
| ARB07CHP | All DG units emit at 2007 ARB limits, and using emission credits for CHP with 60% heat recovery and 50% utilization factor |
| EEDa,b | Electricity emissions displaced from existing central power plants |
| BAU | Business-as-usual linear projections |
| BAUP | Business-as-usual parabolic projections |
| EHP | Extra-high DG market penetration |
| PeakTot | Peak duty cycle with total electricity equal to LU case |
| MSR | Million solar roofs |
| OCLU | Version of LU scenario with out-of-compliance emissions for ICE |

**Table 66. Brief description of DG spanning scenario parameters**

| DG Scenario | Parameters that describe each scenario |
|---|---|
| **LU** | • 18% of increased power demand from 2007 to 2030 met by DG<br>• Spatial distribution following GIS land use distribution<br>• Technology mix same as in realistic scenario SoCAB-R1<br>• Baseloaded duty cycle<br>• No emission displacement<br>• No performance degradation |
| **BACT** | • Technology Mix – all DG are ICE operating under BACT criteria (see Table 67 for BACT emission guidelines)<br>• Same assumptions as in LU for the rest of parameters |
| **ARB07** | • All DG units emit at 2007 ARB emission standards<br>• Same assumptions as in LU for the rest of parameters |
| **FC** | • Technology Mix – All DG are Fuel Cells<br>• Same assumptions as in LU for the rest of parameters |
| **Peak** | • Peaking duty cycle (6 hours a day)<br>• Peak power demand is equal to baseload demand in LU (18% of increased power demand from 2007 to 2030)<br>• Total power delivered by DG during duty cycle<br>• Same assumptions as in LU for the rest of parameters |
| **LDG** | • Technology Mix – all DG are 49 MW GT<br>• No ammonia emissions from DG considered<br>• GT distributed in populated areas with high industrial activity<br>• Same assumptions as in LU for the rest of parameters |
| **LDGNH3** | • Ammonia emissions from GT considered<br>• Same assumptions as in LDG for the rest of parameters |
| **PGW** | • Spatial distribution of DG following population growth spatial distribution from 2010 to 2030<br>• Same assumptions as in LU for the rest of parameters |
| **CHP** | • CHP emissions displaced with 100% heat recovery and 100% utilization factor<br>• Same assumptions as in LU for the rest of parameters |
| **ARB07CHP** | • CHP emissions displaced with 60% heat recovery and 50% utilization factor (same as realistic scenarios)<br>• Same assumptions as in LU for the rest of parameters |
| **EED** | • All Electricity Emissions Displaced from in-basin Electricity Generators<br>• Same assumptions as in LU for the rest of parameters |
| **BAU** | • Linear extrapolation from current data on 2001 through 2004 DG installations in the SoCAB to determine total DG power installed in 2030, which corresponds to 37% of the increased power demand from 2007 to 2030<br>• Technology Mix – Mix of permitted and Certified DG from current DG mix data<br>• Same assumptions as in LU for the rest of parameters |
| **BAUP** | • Parabolic extrapolation from current data to determine total DG power installed in 2030, which corresponds to 93% of the increased power demand from 2007 to 2030<br>• Same assumptions as in BAU for the rest of parameters |
| **EHP** | • Extra high DG penetration: 50% of the increased power demand from 2007 to 2030<br>• Same assumptions as in LU for the rest of parameters |
| **PeakTot** | • Peaking duty cycle (6 hours a day)<br>• Peak power demand is 4 times the baseload demand in PW2010 so that Total cumulative electricity delivered by DG during duty cycle equals the DG electricity in LU<br>• Same assumptions as in LU for the rest of parameters |
| **MSR** | • Penetration of PV according to the California Solar Initiative in substitution of other DG units: 31% of DG capacity is PV, rest follows same DG technology mix as in LU<br>• Technology mix of the rest of DG is as in LU<br>• Same assumptions as in LU for the rest of parameters |
| **OCLU** | • Emission factors of ICE for $NO_X$ and CO are 3 times the values of BACT standards.<br>• Same assumptions as in LU for the rest of parameters |

**Table 67. SCAQMD BACT guidelines for non-emergency natural gas internal combustion engines with power rating smaller than 2064 horsepower. Guidelines do not include amendments to Rule 1110.2 by the SCAQMD in 2008.**

| Emission factors | VOC | $NO_X$ | $SO_X$ | CO | $PM_{10}$ | Inorganic ($NH_3$) |
|---|---|---|---|---|---|---|
| ppm@15% $O_2$ | 32 | 11 | -- | 74 | -- | -- |
| grams/bhp-hr | 0.150 | 0.150 | 0.003 | 0.600 | 0.024 | -- |
| lb/MWh | 0.443 | 0.443 | 0.009 | 1.772 | 0.070 | -- |

Source: SCAQMD 2000

Total emissions from DG in all spanning scenarios are presented in Table 68, in tons per day, and in Table 69, in % with respect to 2030 baseline emissions. Scenario LU assumes the same parameters as realistic scenario SoCAB-R3, except that LU considers no CHP emissions displacement, and a constant baseload operation during 24 hours. As a result, pollutant emissions from DG in scenario LU are up to 1.75 times higher than in SoCAB-R3. In addition, since emissions displacement due to CHP is not accounted for in scenario LU, net $NO_X$ emissions are positive.

The rest of spanning scenarios consider variations of one or two parameters that determine scenario LU. To evaluate the effect of spatial distribution of DG, scenario PGW introduces the same emissions levels as in LU, with a different spatial distribution that follows population growth from 2010 to 2030.

To evaluate the effect of an operational duty cycle, Peak and PeakTot scenarios assume that DG units operate during six hours a day. Scenario Peak assumes that during those six hours of operation DG emit at the same level as in scenario LU during the same period of time; whereas PeakTot assumes that emissions in six hours of operation are equal to total daily emissions in scenario LU. As a result, PeakTot and LU assume the same total emissions, although they are released following different temporal cycles; whereas scenario Peak introduces emissions that are one forth (1/4) of the emissions in scenario LU.

To evaluate the effect of technology mix, six scenarios were developed. The scenario ARB07 assumes that all units emit at the 2007 ARB standards regardless of the DG technology. This sets the upper bound for DG emissions regulated by the 2007 ARB emissions standards. Emissions in this scenario are up to 60% higher than in scenario LU, because some technologies are expected to emit below the 2007 ARB standards by 2030. The scenario BACT assumes that all units are ICE operating at BACT levels valid in 2007 (see Table 6), which are significantly less restrictive than the 2007 ARB emissions standards, assumed for ICE in scenario LU and in the realistic scenarios. As a result, emissions of CO, $NO_X$, and VOC from DG in scenario BACT are 10–25 times the emissions in LU. Scenario FC assumes that all units are high-temperature fuel cells with on-site natural gas reformers. Overall, FC emit at a lower rate than the technology mix in LU, except for $NO_X$ emissions. Large gas turbines, which contribute to a large percentage of DG in scenario LU, emit $NO_X$ at a lower level than FC, and as a result $NO_X$ emissions in scenario LU are slightly lower than in scenario FC. Scenarios LDG and LDG$NH_3$ assume that all DG units are 49-MW gas turbines. Because gas turbines are the dominant DG technology in

scenario LU, emissions in LDG, LDGNH3, and LU are similar. To evaluate the sensitivity PM formation to ammonia emissions, scenario LDG does not include ammonia emissions. For the rest of the pollutants, LDG and LDGNH3 present the same emissions. Finally, scenario MSR evaluates the effect of introducing PV in the DG mix in substitution of a fraction of all other emitting technologies. The result is a decrease in emissions from DG of 31%, with respect to DG emissions in scenario LU.

**Table 68. Daily basinwide pollutant emissions, in tons per day, from DG for selected spanning scenarios for year 2030**

| Spanning Scenario | Electricity produced by DG (MW) | Emission (ton/day) | | | | | |
|---|---|---|---|---|---|---|---|
| | | CO | $NO_X$ | VOC | $SO_X$ | $PM_{2.5}$ | $NH_3$ |
| *Spatial distribution* | | | | | | | |
| LU | 2053.8 | 1.75 | 0.96 | 0.16 | 0.12 | 0.97 | 0.83 |
| PGW | 2053.8 | 1.75 | 0.96 | 0.16 | 0.12 | 0.97 | 0.83 |
| *Duty cycle* | | | | | | | |
| Peak | 2053.8 | 0.44 | 0.24 | 0.04 | 0.03 | 0.24 | 0.21 |
| PeakTot | 2053.8 | 1.75 | 0.96 | 0.16 | 0.12 | 0.97 | 0.83 |
| *Technology Mix* | | | | | | | |
| ARB07 | 2053.8 | 2.24 | 1.56 | 0.19 | 0.16 | 1.35 | 0.83 |
| BACT | 2053.8 | 39.66 | 9.90 | 4.26 | 0.19 | 1.57 | 0.00 |
| FC | 2053.8 | 0.69 | 1.12 | 0.10 | 0.09 | 0.02 | 0.00 |
| LDG | 2053.8 | 1.79 | 0.76 | 0.16 | 0.14 | 1.57 | 0.00 |
| LDGNH3 | 2053.8 | 1.79 | 0.76 | 0.16 | 0.14 | 1.57 | 1.66 |
| MSR | 2053.8 | 1.21 | 0.66 | 0.11 | 0.08 | 0.67 | 0.58 |
| *Emissions Displacement* | | | | | | | |
| CHP | 2053.8 | 0.08 | -0.97 | 0.01 | 0.21 | 1.31 | 0.49 |
| ARB07CHP | 2053.8 | 2.27 | 1.07 | 0.19 | 0.20 | 1.62 | 0.83 |
| EEDa | 10034.0 | 3.91 | 0.83 | -0.89 | 0.36 | 4.74 | 4.07 |
| EEDb | 7597.0 | -0.90 | 2.54 | 0.10 | 0.25 | 2.97 | 3.08 |
| *DG market penetration* | | | | | | | |
| BAU | 4189.3 | 4.12 | 2.34 | 0.36 | 0.28 | 2.63 | 2.34 |
| BAUP | 10617.3 | 10.45 | 5.93 | 0.92 | 0.71 | 6.67 | 5.93 |
| EHP | 5134.5 | 4.38 | 2.40 | 0.40 | 0.30 | 2.43 | 2.08 |
| *Compliance with emission standards* | | | | | | | |
| OCLU | 2053.8 | 46.85 | 11.86 | 1.73 | 0.15 | 1.44 | 0.83 |

**Table 69. Daily basinwide pollutant emissions, in % with respect to baseline emissions, from DG for selected spanning scenarios for year 2030**

| Spanning Scenario | Electricity produced by DG (MW) | Emissions (%) | | | | | |
|---|---|---|---|---|---|---|---|
| | | CO | $NO_X$ | VOC | $SO_X$ | $PM_{2.5}$ | $NH_3$ |
| *Spatial distribution* | | | | | | | |
| LU | 2053.8 | 0.09 | 0.84 | 0.04 | 0.63 | 1.10 | 0.50 |
| PGW | 2053.8 | 0.09 | 0.84 | 0.04 | 0.63 | 1.10 | 0.50 |
| *Duty cycle* | | | | | | | |
| Peak | 2053.8 | 0.02 | 0.21 | 0.01 | 0.16 | 0.28 | 0.12 |
| PeakTot | 2053.8 | 0.09 | 0.84 | 0.04 | 0.63 | 1.10 | 0.50 |
| *Technology Mix* | | | | | | | |
| ARB07 | 2053.8 | 0.11 | 1.37 | 0.05 | 0.85 | 1.53 | 0.49 |
| BACT | 2053.8 | 2.02 | 8.69 | 1.01 | 1.00 | 1.78 | 0.00 |
| FC | 2053.8 | 0.04 | 0.98 | 0.02 | 0.49 | 0.03 | 0.00 |
| LDG | 2053.8 | 0.09 | 0.67 | 0.04 | 0.73 | 1.78 | 0.00 |
| LDGNH3 | 2053.8 | 0.09 | 0.67 | 0.04 | 0.73 | 1.78 | 0.99 |
| MSR | 2053.8 | 0.06 | 0.58 | 0.03 | 0.44 | 0.76 | 0.34 |
| *Emissions Displacement* | | | | | | | |
| CHP | 2053.8 | 0.00 | -0.85 | 0.00 | 1.49 | 0.29 | 1.10 |
| ARB07CHP | 2053.8 | 0.12 | 0.94 | 0.04 | 1.06 | 1.84 | 0.49 |
| EEDa | 10034.0 | 0.20 | 0.73 | -0.21 | 1.89 | 5.39 | 2.42 |
| EEDb | 7597.0 | -0.05 | 2.23 | 0.02 | 1.32 | 3.38 | 1.83 |
| *DG market penetration* | | | | | | | |
| BAU | 4189.3 | 0.21 | 2.05 | 0.09 | 1.48 | 2.99 | 1.39 |
| BAUP | 10617.3 | 0.53 | 5.20 | 0.22 | 3.74 | 7.58 | 3.53 |
| EHP | 5134.5 | 0.22 | 2.11 | 0.09 | 1.58 | 2.76 | 1.24 |
| *Compliance with emission standards* | | | | | | | |
| OCLU | 2053.8 | 2.38 | 10.40 | 0.41 | 0.79 | 1.63 | 0.50 |

Scenarios CHP, ARB07CHP, and EED are three examples of the potential air quality impacts of substituting existing boilers and central power plants with distributed generation. Scenario CHP assumes that 100% of the DG units use CHP and that these units use 100% of excess heat that is thermodynamically reusable. As a result, DG implementation in scenario CHP leads to net reductions in $NO_X$. Because recuperating 100% of the heat is practically impossible for all applications due to mismatch between electricity and heat loads, this scenario sets the upper bound for emissions displacements due to combined heating and power. Scenario ARB07CHP represents a case in which CHP utilization and heat recovery factors are the same as in the realistic scenarios. However, this case assumes that all technologies use the totality of the CHP emission credits. This implies that some technologies will emit at a higher rate than what are expected to emit by 2030.

Finally, scenarios EEDa and EEDb introduce the same DG penetration as in scenario LU, in addition to 8 and 5.5 GW, respectively, of DG power in substitution of all the power plants

included in the 2010 attainment inventory that were installed before 1980. Substituting existing power plants leads to a net decrease in VOC emissions and lower $NO_X$ emissions compared to scenario LU, but it also leads to increases in CO, $SO_X$, and $NH_3$ with respect to scenario LU. In addition, particle emissions from power plants were not available, and as a result, the EED scenario leads to a net increase in $PM_{2.5}$ emissions.

Market penetration, one of the key parameters that determine the resulting emissions from DG and air quality impacts of a range of market penetration, is presented in the realistic scenarios section. Market penetration for realistic scenarios is based on market studies reported by EPRI (2005) and represents the most plausible range based on current understanding of the DG market. Nevertheless, three additional scenarios—BAU, BAUP, and EHP—are presented here to analyze unexpected outcomes that would lead to extra high penetration. Linear extrapolation of the DG penetration during 2001 through 2004 leads to a total penetration of 4.2 GW, which is approximately two times the penetration in scenario LU. As extrapolation is obtained individually for each DG technology type, the technology mix in BAU is different than in LU. In particular, business-as-usual projections suggest a larger penetration of MTG, up to 5%, in detriment of fuel cells and gas turbines. The resulting emissions are approximately 2.5 times the emissions in scenario LU. Although future projections by EPRI (2005) estimate a DG market penetration that is lower than the linear business-as-usual projections, the trends from year 2001 to 2004 show an acceleration of the rate of installations that are being placed in California. Scenario BAUP uses a parabolic extrapolation to represent the effect that this acceleration in market penetration would have on air quality if the acceleration were sustained until 2030. The result is a total DG penetration of 10.6 GW, which is 5.2 times the penetration in scenario LU, and total pollutant emissions that are approximately six times the emissions in LU. The third scenario with extra high penetration, scenario EHP, assumes a total DG penetration of 5.1 GW, which corresponds to EPRI estimates for a scenario with increased incentives and electricity exports enabled. Scenario EHP assumes the same technology mix as in LU, and the resulting emissions are 2.5 times higher.

Finally, scenario OCLU assumes the same DG penetration and technology mix as in scenario LU. However, in scenario OCLU, $NO_X$, and CO emission factors for ICE are three times the BACT levels in 2007, which reflect the findings from inspections of ICE installations by SCAQMD. The emissions factors for ICE for the rest of pollutants correspond to the BACT levels. The resulting DG emissions for the OCLU scenario are significantly higher than the DG emissions in scenario LU. In particular, CO and $NO_X$ emissions in scenario OCLU are approximately 27 and 12 times the emissions in scenario LU, respectively, leading to the scenario with the highest $NO_X$ and CO emissions.

In summary, emissions from DG in scenarios with market penetration of 2 GW and emission factors that comply with 2007 ARB standards correspond to 1.1%, or less, of total basinwide emissions. Scenarios that assume extra-high penetration introduce emissions that add up to a 5.2% increase in emissions of $NO_X$ and to a 7.6% increase in emissions of $PM_{2.5}$, respectively. Moreover, scenarios that assume the BACT standards for ICE, which are less restrictive than the 2007 ARB emissions standards limits, or that the BACT standards are exceeded introduce emissions that add up to 8.7% of the total $NO_X$ in the basin.

**Table 70. Impacts of DG spanning scenarios on peak and 1-hour average ozone concentrations with respect to the baseline case for 2030**

| | | Δ peak $O_3$ | | Δ 1-hour $O_3$ | |
|---|---|---|---|---|---|
| | Peak $O_3$ | Maximum increase | Maximum decrease | Maximum increase | Maximum decrease |
| | (ppb) | (ppb) | (ppb) | (ppb) | (ppb) |
| Baseline | 152.0 | | | | |
| *Spatial distribution* | | | | | |
| LU | 152.2 | 0.8 | -0.3 | 0.8 | -0.9 |
| PGW | 152.4 | 1.1 | -0.2 | 1.1 | -1.1 |
| *Duty cycle* | | | | | |
| Peak | 152.0 | 0.5 | -0.2 | 0.6 | -0.3 |
| PeakTot | 152.3 | 0.7 | -0.1 | 0.7 | -0.6 |
| *Technology Mix* | | | | | |
| ARB07 | 152.5 | 0.9 | -0.5 | 0.9 | -1.8 |
| BACT | 154.5 | 4.6 | -3.6 | 5.4 | -9.3 |
| HTFC | 152.4 | 0.7 | -0.4 | 0.8 | -1.3 |
| LDG | 152.4 | 0.5 | -0.2 | 0.6 | -0.8 |
| LDGNH3 | 152.4 | 0.7 | -0.2 | 0.7 | -0.8 |
| MSR | 152.1 | 0.9 | -0.2 | 0.9 | -0.8 |
| *Emissions Displacement* | | | | | |
| CHP | 151.6 | 0.5 | -0.6 | 1.5 | -0.7 |
| ARB07CHP | 152.2 | 0.8 | -0.3 | 0.8 | -1.3 |
| EEDa | 152.4 | 2.5 | -4.0 | 5.3 | -4.6 |
| EEDb | 153.4 | 2.8 | -2.0 | 3.1 | -6.2 |
| *DG market penetration* | | | | | |
| BAU | 152.6 | 1.2 | -0.8 | 1.3 | -2.6 |
| BAUP | 153.2 | 2.6 | -2.3 | 3.1 | -6.3 |
| EHP | 152.6 | 1.2 | -0.7 | 1.4 | -2.3 |
| *Compliance with emission standards* | | | | | |
| OCLU | 155.1 | 6.2 | -3.9 | 6.7 | -12.1 |

**Table 71. Impacts of DG spanning scenarios on 8-hour average ozone concentrations with respect to the baseline case for 2030**

| | | Δ 8-hour $O_3$ | |
|---|---|---|---|
| | Maximum 8-hour $O_3$ | Maximum increase | Maximum decrease |
| | (ppb) | (ppb) | (ppb) |
| Baseline | 128.8 | | |
| *Spatial distribution* | | | |
| LU | 129.0 | 0.4 | -0.1 |
| PGW | 129.0 | 0.5 | -0.1 |
| *Duty cycle* | | | |
| Peak | 128.9 | 0.2 | -0.1 |
| PeakTot | 129.0 | 0.4 | -0.1 |
| *Technology Mix* | | | |
| ARB07 | 129.3 | 0.6 | -0.2 |
| BACT | 131.6 | 3.0 | -1.3 |
| HTFC | 129.1 | 0.5 | -0.2 |
| LDG | 128.9 | 0.4 | -0.1 |
| LDGNH3 | 129.0 | 0.4 | -0.1 |
| MSR | 129.0 | 0.4 | -0.1 |
| *Emissions Displacement* | | | |
| CHP | 128.4 | 0.2 | -0.5 |
| ARB07CHP | 129.0 | 0.4 | -0.1 |
| EEDa | 129.5 | 1.3 | -1.7 |
| EEDb | 130.1 | 1.5 | -0.8 |
| *DG market penetration* | | | |
| BAU | 129.4 | 0.7 | -0.3 |
| BAUP | 130.1 | 1.6 | -0.8 |
| EHP | 129.4 | 0.7 | -0.3 |
| *Compliance with emission standards* | | | |
| OCLU | 132.3 | 3.7 | -1.3 |

**Table 72. Impacts of DG spanning scenarios on 24-hour average $PM_{2.5}$ concentrations with respect to the baseline case for 2030**

| | | Δ 24-hour $PM_{2.5}$ | |
|---|---|---|---|
| | Maximum 24-hour $PM_{2.5}$ | Maximum increase | Maximum decrease |
| | ($\mu g/m^3$) | ($\mu g/m^3$) | ($\mu g/m^3$) |
| Baseline | 59.7 | | |
| *Spatial distribution* | | | |
| LU | 59.8 | 1.1 | -0.6 |
| PGW | 59.9 | 0.9 | -0.7 |
| *Duty cycle* | | | |
| Peak | 59.7 | 1.0 | -1.0 |
| PeakTot | 59.8 | 0.9 | -0.9 |
| *Technology Mix* | | | |
| ARB07 | 59.9 | 1.0 | -0.8 |
| BACT | 59.9 | 2.6 | -1.0 |
| HTFC | 59.7 | 0.9 | -0.7 |
| LDG | 59.9 | 1.1 | -0.6 |
| LDGNH3 | 59.9 | 1.0 | -0.7 |
| MSR | 59.8 | 0.8 | -0.8 |
| *Emissions Displacement* | | | |
| CHP | 59.8 | 0.8 | -1.0 |
| ARB07CHP | 59.9 | 1.0 | -0.8 |
| EEDa | 60.2 | 2.0 | -0.8 |
| EEDb | 60.0 | 2.0 | -0.6 |
| *DG market penetration* | | | |
| BAU | 60.0 | 1.6 | -0.7 |
| BAUP | 60.3 | 3.4 | -0.2 |
| EHP | 59.9 | 1.4 | -0.6 |
| *Compliance with emission standards* | | | |
| OCLU | 59.8 | 3.1 | -0.8 |

### *Effects of Spatial Distribution of DG*

This section explores the sensitivity of air quality impacts of DG to changes in the spatial distribution of DG units. Figure 55 and Figure 56 present the impact on maximum 1-hour average ozone concentration and 24-hour average $PM_{2.5}$ concentration in scenarios LU and PGW, with respect to baseline peak ozone concentrations. The two scenarios introduce an increase of 0.84% in $NO_X$ emissions and 1.1% in $PM_{2.5}$ emissions with respect to the base case, which results in an increase in maximum 1-hour average ozone concentration and 24-hour average $PM_{2.5}$ concentration of approximately 1 ppb and 1 $\mu g/m^3$, respectively. Because PGW introduces a higher penetration of DG in San Bernardino and Riverside counties, compared to scenario LU, the increase in peak ozone and 24-hour average $PM_{2.5}$ concentration in PGW occurs farther downwind. In addition, peak ozone in scenario PGW is slightly higher than in the LU scenario.

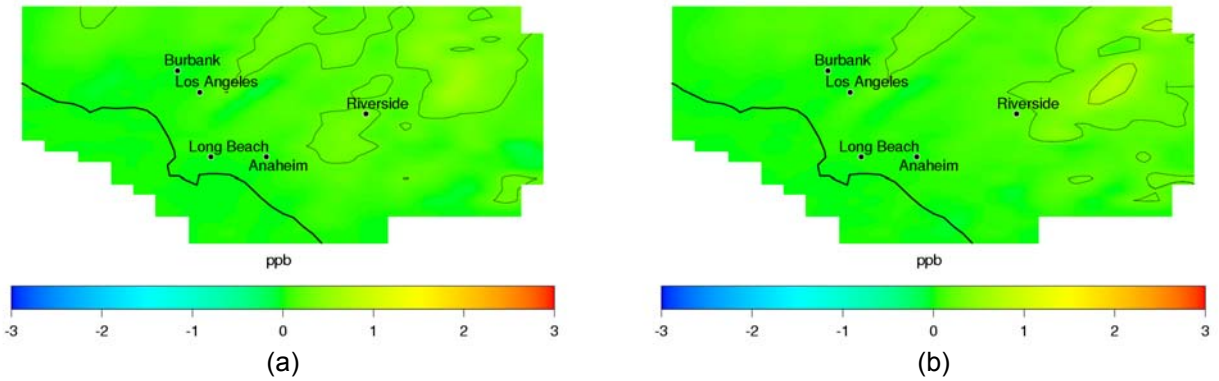


**Figure 55. Impacts of spanning scenarios on maximum 1-hour average $O_3$ as a function of DG spatial distribution: (a) Land use-weighted scenario (LU), and (b) population-weighted scenario (PGW)**

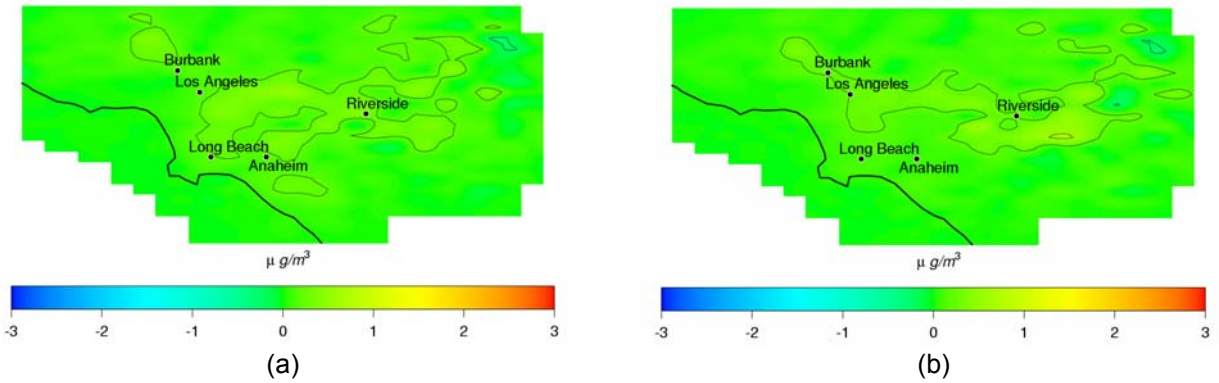


**Figure 56. Impacts of spanning scenarios on 24-hour average $PM_{2.5}$ as a function of DG spatial distribution: (a) Land use-weighted scenario (LU), (b) population-weighted scenario (PGW)**

### *Effects of the DG Technology Mix*

This section evaluates the sensitivity of air quality impacts of DG to changes in the technology mix distribution. Scenario ARB07 assumes that all DG units emit at the 2007 ARB standards. Hence, considering that some technologies are currently able to emit below the ARB standards (e.g., fuel cells), this scenario represents the upper bound for DG emissions and air quality impacts if all the DG units have to comply eventually with those standards. In particular, emissions of $NO_X$ from DG in scenario ARB07 are nearly 60% higher than in scenario LU. However, overall DG emissions in scenario ARB07 correspond to approximately 1.5% of the baseline emissions or less. As a result, peak ozone in scenario ARB07 is slightly higher than in scenario LU. Similarly, the magnitude of the impacts of DG on $PM_{2.5}$ in scenario ARB07 are comparable to the impacts in scenario LU and the area of $PM_{2.5}$ concentrations affected by DG in scenario ARB07 is slightly larger than in scenario LU.

Scenario BACT assumes that all DG units are ICE emitting at BACT levels present in 2007. As those BACT standards are far less restrictive than ARB 2007 emissions standards, the impact on ozone and $PM_{2.5}$ concentrations is more intense than in scenario ARB07. In particular, peak ozone concentration in scenario BACT is up to about 5 ppb higher than in the base case, and these increases occur in the northeastern region of the domain, which typically experiences the highest ozone concentrations in the basin (see Figure 57b). Note that the scale is truncated at 3 ppb so that the air quality impacts depicted by the contour plot are comparable to the rest of the panels in Figure 57. Also, 24-hour average $PM_{2.5}$ concentrations are up to 2.6 $\mu g/m^3$ higher than in the base case, and the maximum increases appear downwind from Riverside, where the basinwide $PM_{2.5}$ peak generally occurs (Figure 58b).

Scenario FC assumes that all DG units are high-temperature fuel cells with on-site reformers, which emit below the 2007 ARB standards. Resulting $NO_X$ emissions in scenario FC are approximately 10% higher than in scenario LU. The increase in $NO_X$ emissions with respect to scenario LU leads to an enlargement of the area in which peak ozone concentration increases, although maximum increases in peak ozone are 1 ppb, which are of the same order as in scenario LU (Figure 57c). On the other hand, emissions of $PM_{2.5}$ from DG in scenario FC are 50 times lower than in scenario LU, and as a result, the impact of DG on $PM_{2.5}$ concentration is negligible (Figure 58c).

Scenarios LDG and LDGNH3 assume that all DG units are 49-MW gas turbines operating with selective catalytic reduction (SCR) as after-treatment technology. As a result, $NO_X$ emissions from these two scenarios are 20% lower than in scenario LU, and lead to increases in peak $O_3$ concentration of 0.5 and 0.7 ppb, respectively (Figure 57d and e). Due to lower $NO_X$ emissions, the area in which peak ozone is affected is smaller than in scenario LU. On the other hand, PM emissions in scenario LDG are approximately 60% higher than in scenario LU, which results in a more widespread increase in $PM_{2.5}$ concentrations (Figure 58d). However, maximum increases in 24-hour average $PM_{2.5}$ add up to 1.1 $\mu g/m^3$, which are of the same order as in scenario LU. Emissions of ammonia from DG in scenario LDGNH3 increases the formation of particles with respect to scenario LDG, enlarging the area in which $PM_{2.5}$ concentrations are affected (Figure 58e). However, maximum increases in 24-hour average $PM_{2.5}$ concentration with respect to the

base case is the same (1 μg/m$^3$) in the two DG scenarios because DG ammonia emissions in LDGNH3 correspond only to 1.66% of the total basinwide emissions. In other words, at the level of DG penetration considered in this study, ammonia emissions from DG show a limited impact on particulate matter concentrations.

Finally, scenario MSR assumes that 31% of the power is supplied by PV, reducing the installed capacity of the rest of fuel-driven DG technologies, and hence, reducing emissions by the same percentage with respect to scenario LU. The result is a less widespread increase in peak ozone and in 24-hour average $PM_{2.5}$ concentration. The maximum increase in peak ozone concentration and 24-hour average concentration with respect to the base case are less than 1 ppb and 1 μg/m$^3$ (Figure 57f and Figure 58f, respectively).

In summary, DG implementation at the level of penetration expected for 2030 would have a marginal impact on air quality if DG units emit at the ARB 2007 standards levels, regardless of the DG technology. Fuel cells have low PM emissions associated that could reduce the impact of DG on $PM_{2.5}$ concentrations. Zero-emission technologies, such as photovoltaics, could contribute to reducing emissions from DG installations, and hence, they could reduce the impact on ozone and $PM_{2.5}$. On the other hand, if DG emits at the BACT emissions levels in place in 2007—as in the ICE BACT scenario—DG implementation could lead to increases in ozone and $PM_{2.5}$ concentrations that could compromise compliance with air quality standards.

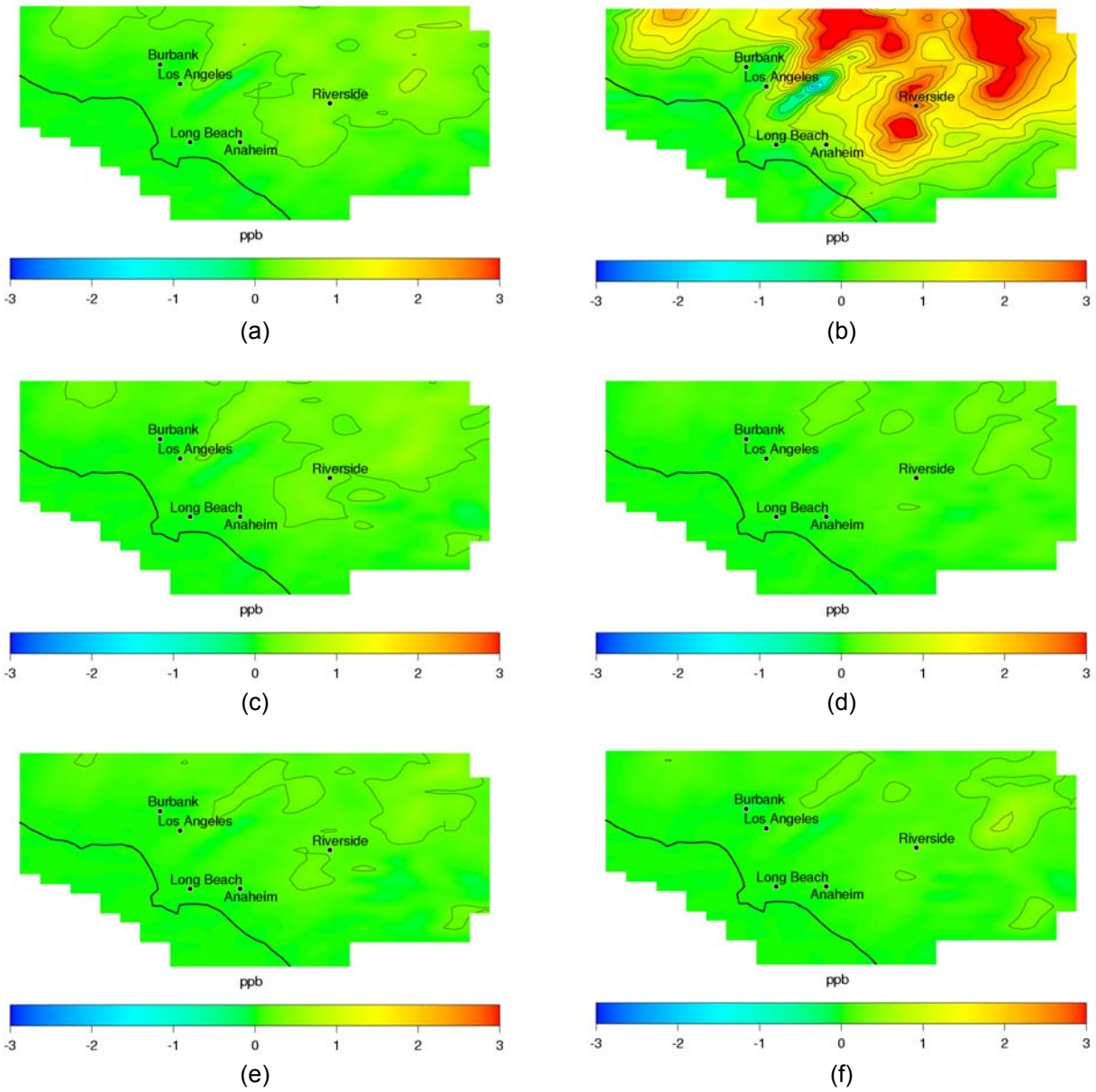


**Figure 57. Impacts of spanning scenarios on peak $O_3$ as a function of DG technology mix: (a) All DG emit at ARB 2007 standards, (b) All DG are ICE emitting at BACT standards in 2007 (BACT), (c) all DG are high-temperature fuel cells (HTFC), (d) all DG are large gas turbines (LDG), (e) all DG are large gas turbines with ammonia slip (LDGNH3), (f) high penetration of photovoltaic units— "Million Solar Roofs" scenario (MSR)**

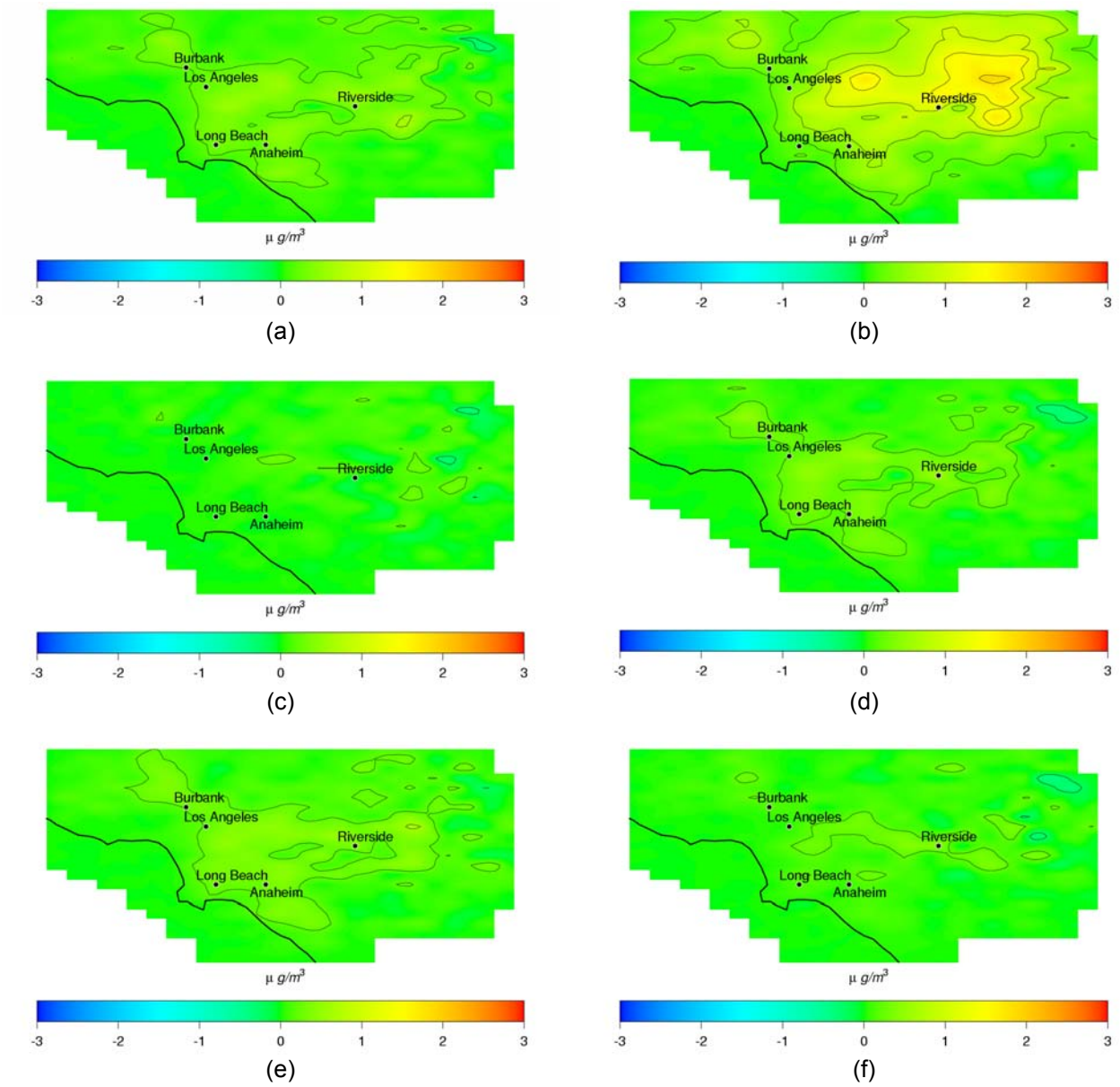


**Figure 58. Impacts of spanning scenarios on 24-hour average $PM_{2.5}$ as a function of DG technology mix: (a) All DG emit at ARB 2007 standards (ARB07), (b) All DG are ICE emitting at BACT standards in 2007 (BACT), (c) all DG are high-temperature fuel cells (HTFC), (d) all DG are large gas turbines (LDG), (e) all DG are large gas turbines with ammonia slip (LDGNH3), (f) high penetration of photovoltaic units—"Million Solar Roofs" scenario (MSR)**

### *Effects of DG Duty Cycle*

This section evaluates the effect of changing the timing of DG emissions on pollutant concentrations. Two different scenarios are considered: scenario Peak and scenario PeakTot. Scenario Peak assumes that all DG units operate during six hours supplying the same power capacity as in scenario LU for the same period of time. The emissions from DG during hour 11 through hour 17 are exactly the same as in scenario LU, and the rest of the time DG units do not operate, and hence, do not emit. As a result, emissions from DG in scenario Peak are four times

lower than in scenario LU, and hence, DG implementation in this scenario does not produce any significant effect on peak ozone and 24-hour average $PM_{2.5}$ concentration (Figure 59a and Figure 60a, respectively). Scenario PeakTot assumes that all units operate during the same period of time as in scenario Peak, but the power supplied by DG is four times the capacity installed in scenario Peak. As a result, the daily electrical energy produced in scenario PeakTot equals the daily production of electricity in scenario LU. Consequently, DG emissions in scenario PeakTot from hour 11 to hour 17 are four times the emissions in scenario LU, but the total daily emissions are the same in both cases. Thus, scenario PeakTot serves as reference to evaluate the effect of the timing of emissions, with respect to scenario LU.

The maximum increase in peak ozone concentration in scenario PeakTot (Figure 59b) is less than 1 ppb, similarly as in scenario LU (Figure 55a). However, the area in which peak ozone is increased in scenario PeakTot is larger than in scenario LU. This occurs because ozone concentration generally peaks in the afternoon hours, and adding emissions from DG during the afternoon increases peak ozone concentrations more intensively than if the emissions are added during all day. On the other hand, scenario PeakTot (Figure 60b) produces smaller impacts on $PM_{2.5}$ concentrations than in scenario LU, and the area in which $PM_{2.5}$ concentrations are affected by DG in PeakTot is smaller than in LU (Figure 56a). This smaller impact from DG occurs because $PM_{2.5}$ concentrations generally peak in the morning rush hour, due to direct emissions, and at night, due to the formation of secondary particles. The morning $PM_{2.5}$ peak occurs near Los Angeles and Long Beach; whereas the night $PM_{2.5}$ peak occurs around Riverside. As emissions from DG are released in the afternoon, they do not contribute to the morning peak near Los Angeles, but they contribute to the peak at night that develops near Riverside. As a result, DG implementation in scenario PeakTot does not produce a significant effect on 24-hour average $PM_{2.5}$ concentration near Los Angeles and Long Beach, and produces small impacts on 24-hour average $PM_{2.5}$ concentration near Riverside.

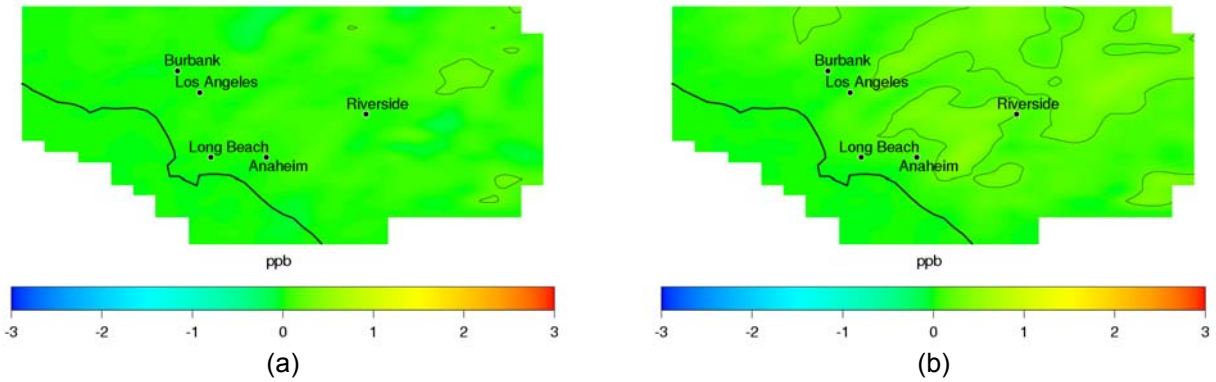


**Figure 59. Impacts of spanning scenarios on peak $O_3$ as a function of DG duty cycle: (a) Peak scenario (Peak), with all units operating from hour 11 to hour 17 meeting the same power as in LU, (b) Peak scenario (PeakTot), with all units operating from hour 11 to hour 17 meeting the same total daily electrical energy as in LU, which represents a power capacity four times higher than scenario Peak**

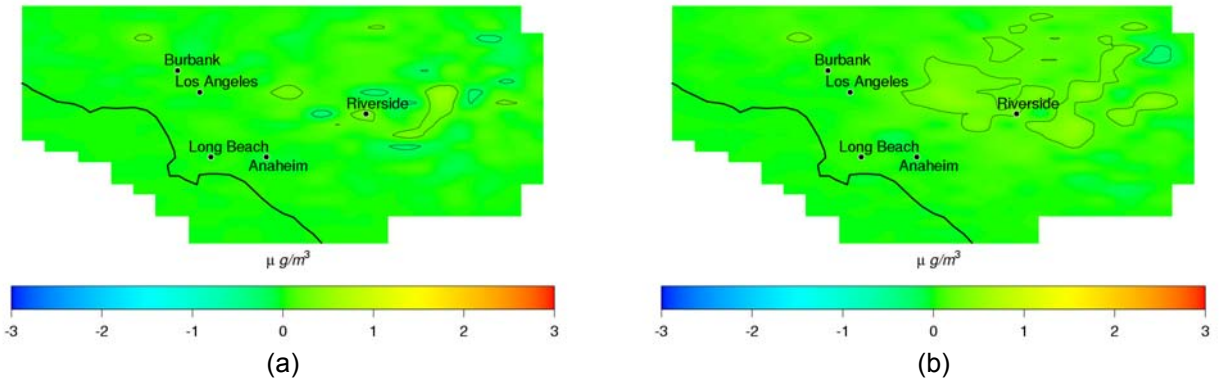


**Figure 60. Impacts of spanning scenarios on 24-hour average $PM_{2.5}$ as a function of DG duty cycle: (a) Peak scenario (Peak), with all units operating from hour 11 to hour 17 meeting the same power as in LU, (b) Peak scenario (PeakTot), with all units operating from hour 11 to hour 17 meeting the same total daily electrical energy as in LU, which represents a power capacity four times higher than scenario Peak**

### *Effects of Emissions Displacement*

This section considers the potential of DG to substitute existing facilities, such as boilers or power plants. Scenario CHP considers that all DG units include CHP capabilities and that there is a total match between the electric load and the heating load—that is, that all excess heat from DG can be utilized for heating and air conditioning. This extreme is unlikely, but this scenario sets the upper bound for the air quality benefits from utilizing CHP. However, the use of CHP provides emission credits for DG installations, allowing them to emit at a higher rate than units without combined heating and power. As a result, this scenario leads to a net decrease in $NO_X$ emissions of less than 1%, with respect to baseline emissions. As a result, peak 1-hour ozone concentration decreases by up to 0.6 ppb in the northeastern part of the domain where the basinwide peak ozone typically occurs (Figure 61a and Table 70). Moreover, net reductions in $NO_X$ emissions reduce secondary formation of particles. However, these reductions are compensated by the increase in direct PM emissions due to the higher emissions that CHP units are allowed to release. As a result, impacts of scenario CHP on 24-hour average $PM_{2.5}$ concentrations are very small (Figure 62a).

Scenario ARB07CHP assumes that all the DG units incorporate CHP capabilities with 50% CHP utilization and 60% heat recovery, and that all DG units emit at the 2007 ARB standards. Hence, direct emissions from DG in scenario ARB07CHP are higher than in scenario ARB07, because the 2007 ARB standards allow additional emissions equivalent to 1 MWh per each 3.4 MMBtu of heat recuperated (Table 68). However, the increase in emissions due to CHP credits is offset in part by the removal of existing boilers that are substituted by the CHP installations. The result is a net decrease in $NO_X$ and VOC emissions with respect to scenario ARB07. On the other hand, increases in emissions of PM and $SO_X$ due to CHP emissions credits are larger than the emissions from boilers. As a result, emissions of PM and $SO_X$ in scenario ARB07CHP are higher than in scenario ARB07 (Table 68). Because of lower $NO_X$ and VOC emissions, the impact on ozone 1-hour average concentration in scenario ARB07CHP (Figure 61b) is slightly smaller than in scenario ARB07 (Figure 57a). In addition, lower $NO_X$ emissions lead to less secondary

formation of nitrate particles. However, lower $NO_x$ emissions are compensated by the fact that direct PM emissions in scenario ARB07CHP are higher than in scenario ARB07. For this reason, the resulting air quality impacts on $PM_{2.5}$ in scenarios ARB07 and ARB07CHP are very similar (Figure 58a and Figure 62b, respectively).

Scenarios EEDa and EEDb (electricity emissions displaced) consider the effect of removing existing power plants and installing DG systems as a replacement technology. The emissions associated with the existing power plants are thus removed in these scenarios. As a result, localized foci of emissions are removed (central power plants) and new sources of emissions are introduced (DG units), which are more widely spread throughout the basin than the existing power plants. Table 73 and Table 74 show the net direct emissions from the removal of central power plants and the addition of DG to meet the removed central power capacity, and from the addition of DG to meet 18% of the increased power demand from 2007 to 2030.

In scenario EEDa, the net change due to substituting existing central generation with DG produces a net decrease in VOC and $NO_x$ emissions (Table 73, third row). This means that VOC and $NO_x$ emissions from DG are lower than the emissions from the power plants removed from the system. On the other hand, $SO_x$, PM, and CO emissions from central power plants are lower than the emissions introduced due to DG. In scenario EEDb (Table 74), substituting existing power plants with DG leads to a net decrease in VOC and CO emissions and to an increase in $SO_x$, PM, and $NO_x$ emissions (Table 74, third row). The additional installation of DG to meet 18% of the increased power demand from 2007 to 2030 leads to a basinwide net increase in $NO_x$ emissions in scenario EEDa (Table 73, sixth row) and a basinwide net increase in VOC emissions in scenario EEDb (Table 74, sixth row). Removing power plants decreases peak ozone concentration by up to 4 ppb in areas near Long Beach, Los Angeles, and Huntington Beach, where large power plants are removed. On the other hand, peak ozone concentration increases by up to 2.8 ppb in downwind locations, due to the addition of DG emissions (Figure 61c and d). Although there are some local decreases in ozone concentration due to the removal of power plants, these decreases occur near the coast, where ozone concentrations are typically in compliance with the air quality standards. In contrast, peak ozone concentrations increase at downwind locations in the northeastern part of the domain, where the basinwide peak ozone generally occurs and exceeds the air quality standards. In conclusion, scenarios EEDa and EEDb cause a reduction in ozone concentration where ozone peak is already low, but increases ozone concentrations in areas where peak ozone needs to be reduced.

The impacts on ozone concentration of scenarios EEDa and EEDb should be compared to the impacts of scenario LU. Emissions of $NO_x$ and VOC from scenario EEDa are lower than in scenario LU. However, peak ozone concentration in EEDa is higher than in scenario LU, because some $NO_x$ and VOC emissions from the central power plants, from which the highest emissions are mostly concentrated near Long Beach, are redistributed to inland areas following the land-use distribution. As a result, $NO_x$ and VOC emissions are pushed inland, producing lower ozone peaks around Long Beach and higher ozone peaks farther downwind. Emissions of $NO_x$ in scenario EEDb are higher than in scenario LU (Table 70), and in turn, higher than scenario EEDa. As a result, increases in peak ozone concentration in scenario EEDb are more pronounced than in scenario EEDa.

The effect of scenarios EEDa and EEDb on $PM_{2.5}$ cannot be fully assessed, because direct PM emissions from central power plants were not included in the emissions inventory. However, secondary formation of PM from $NO_X$, $SO_X$, and ammonia plays a key role in the total concentration of $PM_{2.5}$. For instance, the removal of $NO_X$ and $SO_X$ emissions from the power plants located near the port of Long Beach leads to local reductions in $PM_{2.5}$ of up to 1 $\mu g/m^3$ (Figure 62c and d). On the other hand, emissions from DG contribute to the increase in $PM_{2.5}$ in most of the domain, and in particular, in Los Angeles and Riverside, where 24-hour average $PM_{2.5}$ generally peaks. In conclusion, reduction of emissions due to the removal of existing power plants is offset by the introduction of DG emissions, which leads to increases in the basinwide peak ozone and $PM_{2.5}$ concentrations.

**Table 73. Pollutant emissions from power plants that are substituted by DG in the South Coast Air Basin of California, and the emissions introduced by DG to compensate for the power capacity removed (in tons/day) and the increased power demand for scenario EEDa**

| | VOC | CO | $NO_X$ | $SO_X$ | $PM_{2.5}$ | Power (MW) |
|---|---|---|---|---|---|---|
| Central power plants removed from the basin | 1.67 | 4.65 | 3.87 | 0.23 | -- | 7980 |
| DG that substitute central power plants | 0.62 | 6.81 | 3.74 | 0.47 | 3.77 | 7980 |
| Net change due to substituting central generation with DG | -1.05 | 2.16 | -0.13 | 0.24 | 3.77 | -- |
| DG that meets the increase in power demand | 0.16 | 1.75 | 0.96 | 0.12 | 0.97 | 2054 |
| Total contribution from DG | 0.78 | 8.56 | 4.70 | 0.59 | 4.74 | 10034 |
| Net contribution (DG – Power plants) | -0.89 | 3.91 | 0.83 | 0.36 | 4.74 | 2054 |

**Table 74. Pollutant emissions from power plants that are substituted by DG in the South Coast Air Basin of California, and the emissions introduced by DG to compensate for the power capacity removed (in tons/day) and the increased power demand for scenario EEDb**

| | VOC | CO | $NO_X$ | $SO_X$ | $PM_{2.5}$ | Power (MW) |
|---|---|---|---|---|---|---|
| Central power plants removed from the basin | 0.49 | 7.38 | 1.02 | 0.20 | -- | 5543 |
| DG that substitute central power plants | 0.43 | 4.73 | 2.60 | 0.33 | 2.62 | 5543 |
| Net change due to substituting central generation with DG | -0.06 | -2.66 | 1.58 | 0.13 | 2.62 | |
| DG that meets the increase in power demand | 0.16 | 1.75 | 0.96 | 0.12 | 0.97 | 2054 |
| Total contribution from DG | 0.59 | 6.48 | 3.56 | 0.45 | 3.59 | 7597 |
| Net contribution (DG – Power plants) | 0.10 | -0.90 | 2.54 | 0.25 | 3.59 | 2054 |

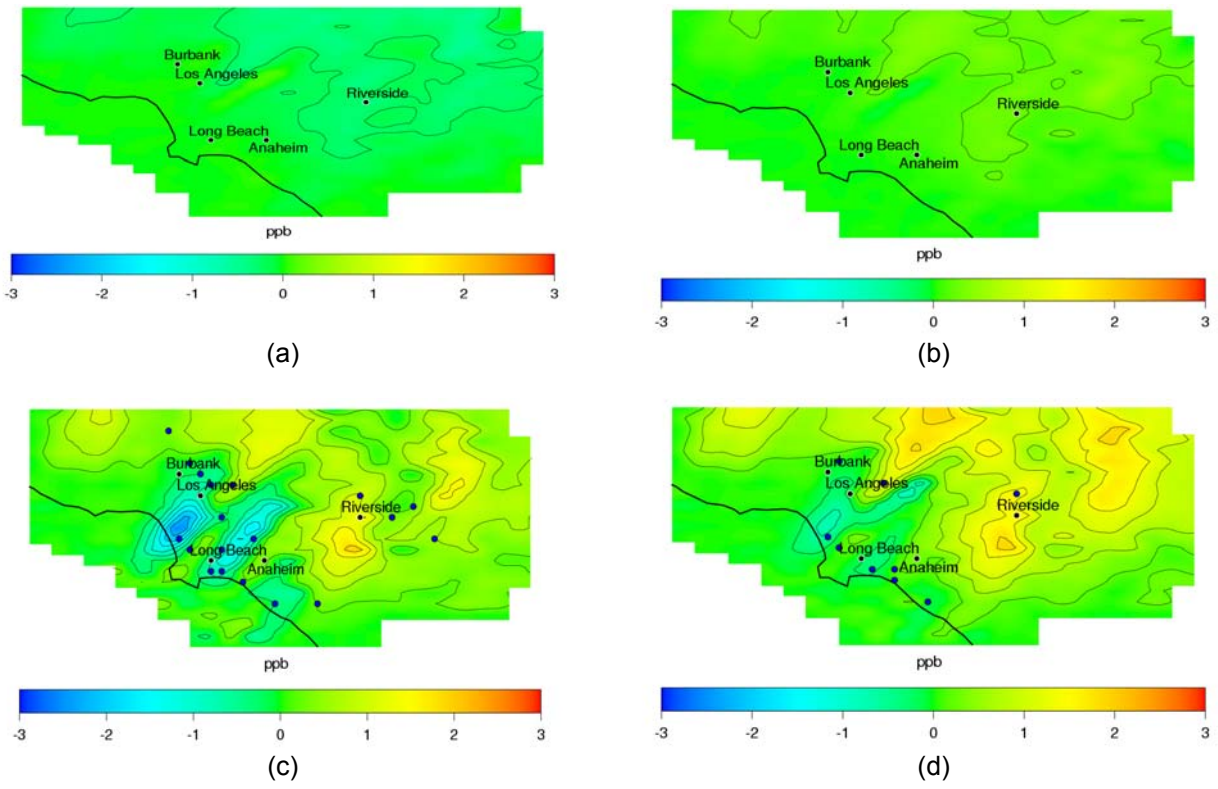


**Figure 61. Impacts of spanning scenarios on peak 1-hour $O_3$ as a function of the amount of emissions displaced by DG: (a) scenario with all units operating with combined heating and power (CHP) assuming 100% of heat recovery and 100% CHP utilization (CHP), (b) scenario with all units operating with combined heating and power assuming 60% recovery and 50% CHP utilization, same as in realistic scenarios (ARB07CHP), (c) emissions displaced from existing power plants by new DG installations (EEDa), (d) emissions displaced from existing power plants by new DG installations (EEDb). Blue dots correspond to the power plants removed from the basin.**

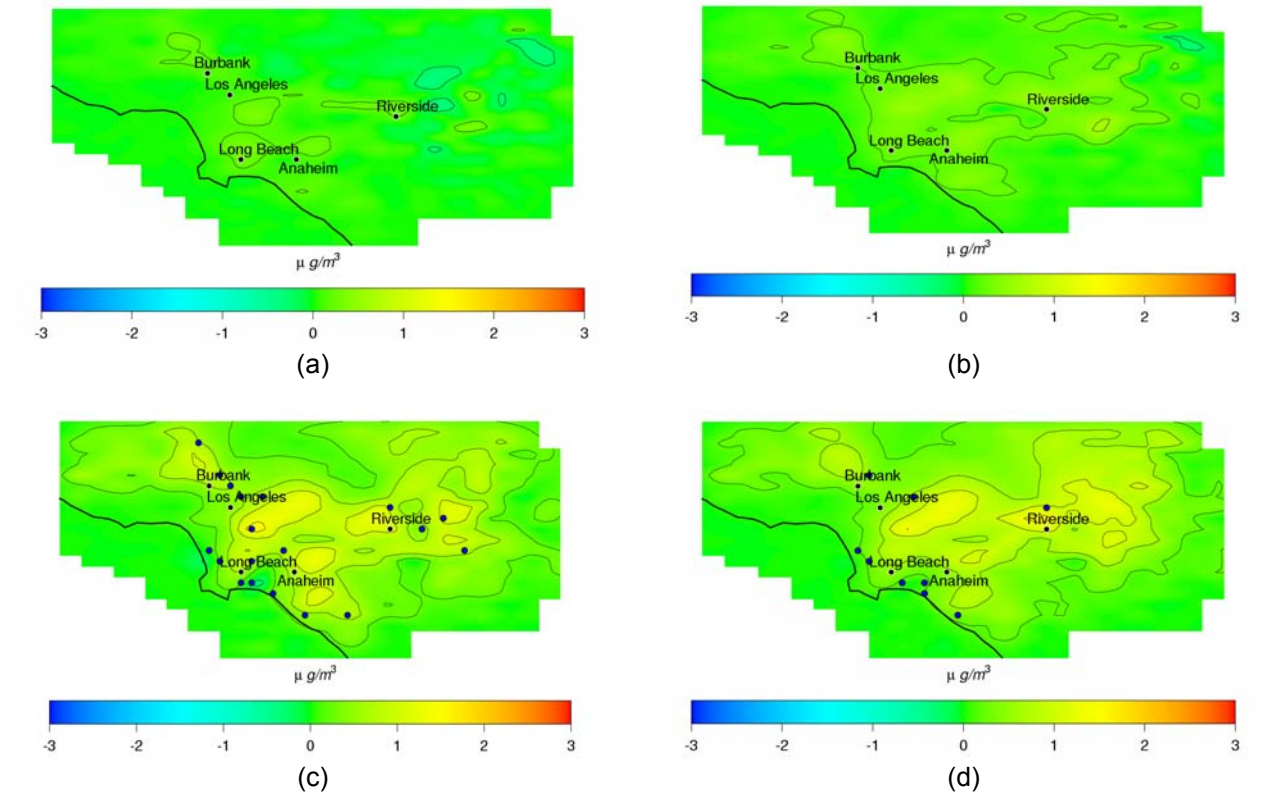


**Figure 62. Impacts of spanning scenarios on 24-hour average $PM_{2.5}$ as a function of the amount of emissions displaced by DG: (a) scenario with all units operating with combined heating and power (CHP) assuming 100% of heat recovery and 100% CHP utilization (CHP), (b) scenario with all units operating with combined heating and power assuming 60% recovery and 50% CHP utilization, same as in realistic scenarios (ARB07CHP), (c) emissions displaced from existing power plants by new DG installations (EEDa), (d) emissions displaced from existing power plants by new DG installations (EEDb). Blue dots correspond to the power plants removed from the basin.**

### *Effects of DG Market Penetration*

Distributed generation market penetration affects directly the total emissions of DG, and hence, air quality impacts of DG depend strongly on this value. Sensitivity of air quality impacts of DG with respect to DG market penetration was investigated for realistic scenarios, using a plausible penetration range according to market studies. This section expands the range of market penetration to investigate unexpected outcomes and to determine the model sensitivity with respect to market penetration.

Two scenarios were developed using business-as-usual trends: BAU, which extrapolates linearly the current trends of DG deployment, and BAUP, which extrapolates parabolically current trends. A third scenario, scenario EHP, was developed based on estimates by EPRI (EPRI 2005) of a scenario that assumes optimistic DG market penetration because electricity exports from DG to the grid are allowed. As a result, DG penetration in scenario EHP is 2.5 times the market penetration in scenario LU, i.e., 45% of the increased power demand from

2007 to 2030. Results show that linear extrapolation of business-as-usual projects a market penetration that is 20% lower than the penetration in EHP. On the other hand, parabolic projection of business-as-usual trends projects a penetration that is twice the penetration in scenario EHP, which is already considered as optimistic. Consequently, scenario BAUP is unrealistic, and it is only used to illustrate model sensitivity to DG market penetration.

Although scenario EHP introduces 20% more DG capacity than in scenario BAU, the technology mix in scenario BAU assumes a higher penetration of MTG and a lower penetration of fuel cells and gas turbines. The resulting $NO_X$ emissions from DG in scenario EHP are only 3% higher than in scenario BAU, and $PM_{2.5}$ emissions in scenario EHP are 8% lower than in scenario BAU. As a result, DG implementation in scenarios BAU and EHP lead to similar impacts on peak ozone concentration and on 24-hour average $PM_{2.5}$ concentration. Maximum increases in peak ozone concentration with respect to the base case are of the order of 1 ppb in both scenarios (Figure 63a and c, and Table 70); whereas maximum increases in $PM_{2.5}$ are 1.6 $\mu g/m^3$ (Figure 64a and c, and Table 72). Moreover, the area in which ozone concentrations and $PM_{2.5}$ concentrations are affected is similar. In scenario BAUP, emissions from DG are 2.5 times the emissions in scenario BAU, and the contribution of $NO_X$ and $PM_{2.5}$ emissions from DG to the total basinwide emissions adds up to 5.2% and 7.6%, respectively. As a result, impacts of DG on ozone and $PM_{2.5}$ are more intense than in the other two scenarios. In particular, peak ozone concentration increases by up to 3 ppb and 24-hour average $PM_{2.5}$ increases by 3 $\mu g/m^3$, with respect to the base case (Figure 63b and Figure 64b).

In summary, air quality impacts of DG in scenario with high DG penetration present small increases in ozone and $PM_{2.5}$ concentrations. Only if the market penetration increases substantially, following a parabolic extrapolation of the current trends in DG installed capacity, the air quality impacts exceed increases in pollutant concentrations by more than 1 ppb (ozone) and 1 $\mu g/m^3$ ($PM_{2.5}$). However, such high penetration is unrealistic. Low air quality impacts are generally caused by the low emissions associated with all DG units, which are assumed to meet the ARB 2007 standards. High penetration of technologies that emit at a higher rate could lead to more significant air quality impacts, as suggested by scenario BACT.

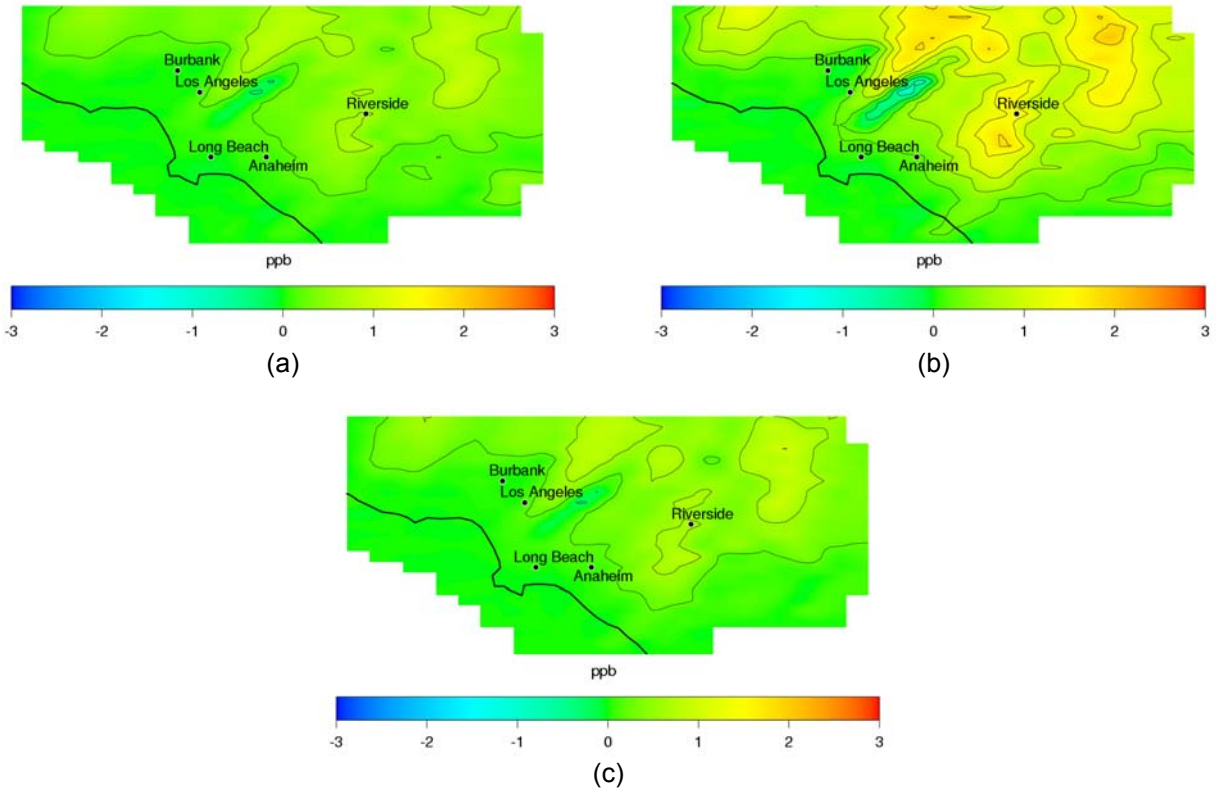


**Figure 63. Impacts of high penetration spanning scenarios on peak $O_3$: (a) scenario with linear extrapolation of business-as-usual trends in DG market penetration (BAU), (b) scenario with parabolic extrapolation of business-as-usual trends in DG market penetration (BAUP), (c) extra-high penetration scenario due to electricity export (EHP)**

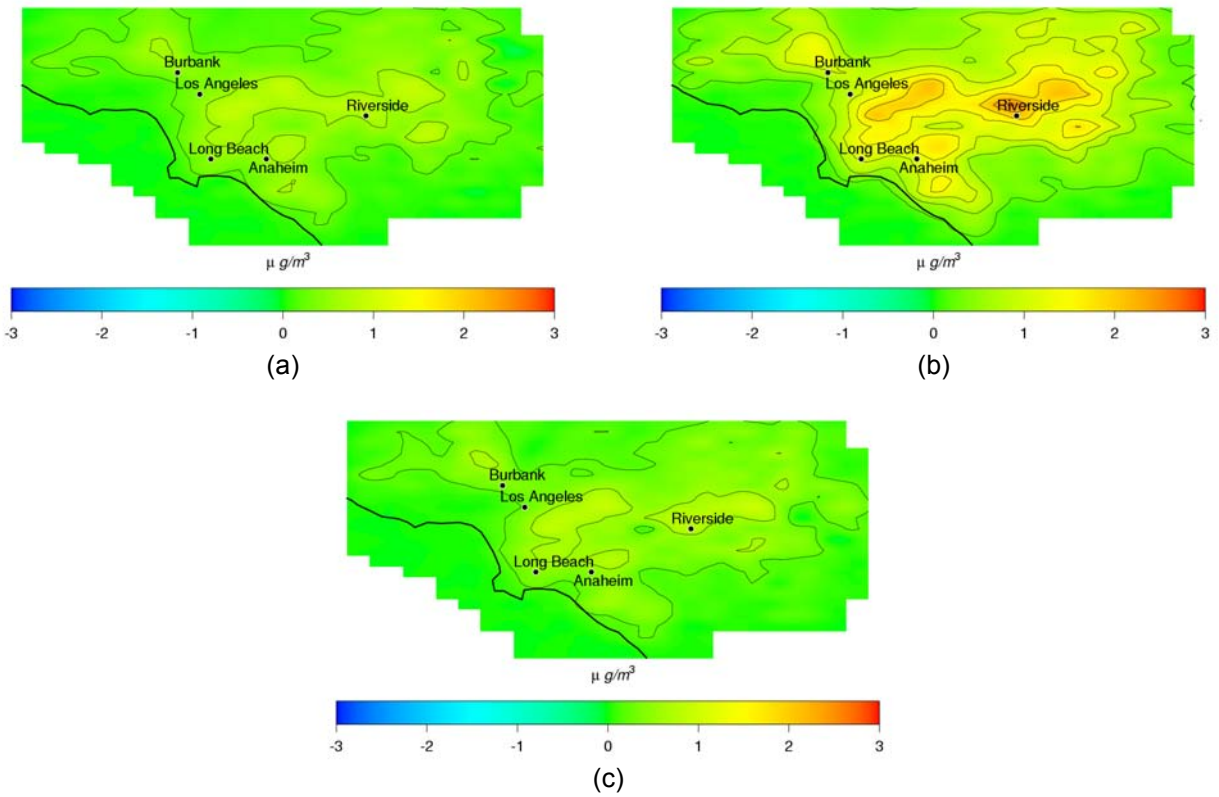


**Figure 64. Impacts of high-penetration spanning scenarios on 24-hour average $PM_{2.5}$: (a) scenario with linear extrapolation of business-as-usual trends in DG market penetration (BAU), (b) scenario with parabolic extrapolation of business-as-usual trends in DG market penetration (BAUP), (c) extra-high penetration scenario due to electricity export (EHP)**

### *Effect of Out-of-Compliance Emission Factors*

As shown in previous sections, emissions from DG lead to small air quality impacts if DG units are emitting at the ARB 2007 emission limits. Scenario BACT, which assumes that all the units are ICE emitting at BACT levels of 2007, suggests that DG implementation could lead to increases in ozone concentration of approximately 5 ppb, which would challenge attainment of the ozone air quality standards. In addition, such emissions levels could increase $PM_{2.5}$ concentrations by approximately 3 μg/m$^3$, making things difficult for the attainment of the $PM_{2.5}$ air quality standards. Consequently, results suggest that application of ARB 2007 limits for all DG units would limit air quality impacts of DG.

Through inspections of ICE installations from 2001 through 2005, SCAQMD found that some units were emitting at rates over six times higher than the permitted levels under BACT standards (Kay 2006). Over 50% of all units were operating exceeding the emissions levels, and the overall emissions of all the units inspected exceeded by 300% the 2007 BACT limits. Scenario OCLU assumes the same parameters as in scenario LU, except for the emission factors for ICE. The emission factors for $NO_X$ and CO are three times the 2007 BACT emission levels for ICE. Since only $NO_X$ and CO emissions were report by AQMD, the emission factors assumed for the rest of pollutants correspond to those for the BACT standards. As a result, scenario OCLU

presents the highest emissions of $NO_X$ and CO amongst all DG scenarios, which add up to 2.4% and 10.4% of the total basinwide emissions, respectively.

Consequently, peak ozone concentrations in scenario OCLU are the highest amongst DG scenarios, and in some areas peak ozone concentration increases by 6 ppb with respect to the base case (see Figure 65a. Note that the scale in the figure is capped at 3 ppb for the sake of comparison with air quality impacts presented in scenario LU shown in Figure 55a). Moreover, increases in ozone concentrations occur at downwind locations in the northeastern part of the domain, where the highest ozone concentrations typically occur. On the other hand, direct emissions of $PM_{2.5}$ add up to 1.6%, which is slightly lower than in scenario BACT. Despite not assuming the highest direct emissions of $PM_{2.5}$, scenario OCLU presents the second highest increases in $PM_{2.5}$, after scenario BAUP, mainly due to the increase in secondary formation of particle through oxidation of $NO_X$. In particular, increases in 24-hour average $PM_{2.5}$ concentration with respect to the base case exceed 3 $\mu g/m^3$ in areas downwind from Riverside (Figure 65b). In conclusion, these results suggest that violations of emissions standards, such as reported by the AQMD, which could be an outcome of poor maintenance and/or defective operating conditions of DG installations, could lead to significant increases in ozone and $PM_{2.5}$ concentrations.

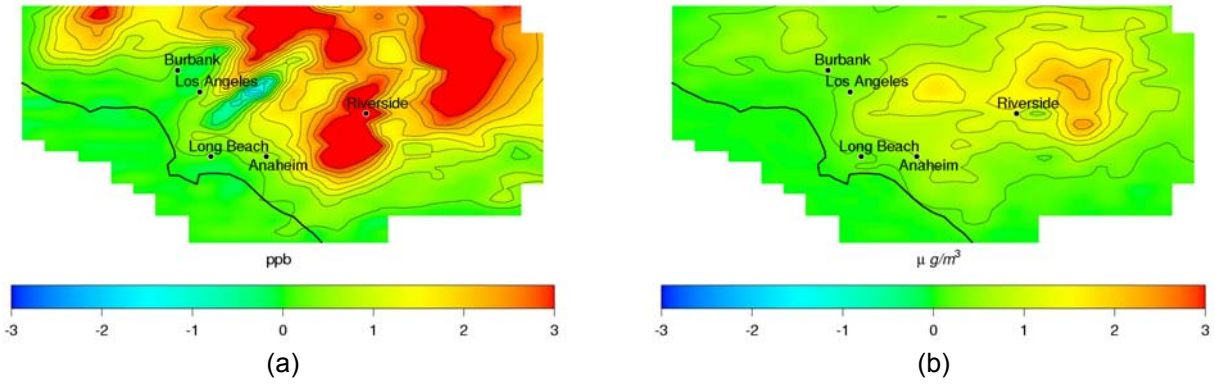


**Figure 65. Air quality impacts of land-use scenario with ICE emitting at three times the BACT standards of 2007 (OCLU): (a) impact on peak $O_3$, and (b) impact on 24-hour average $PM_{2.5}$**

### *5.1.4. Air Quality Impacts of Long-Term DG Implementation*

This section analyzes the effect that widespread use of electric vehicles could have on the electricity demand, and the resulting impacts on air emissions and air quality in future years. Predicting the outcomes for such futuristic technologies is wrought with high levels of uncertainty that need to be considered. However, this type of scenario sets bounds to emissions reductions from automobile sources and is a basis for sensitivity analyses of emissions to determine air quality impacts projections in the future. The following section provides a scenario for generating electricity in the future.

As estimated in the earlier discussion of Scenario S16, the total capacity needed for recharge the entire fleet of electric vehicles that would replace the existing mix of vehicles in the year 2040 is 20 GW. This power is provided by a mix of DG that includes 50% large gas turbines, 9% high-

temperature fuel cells, 1% low-temperature fuel cells—all of which spread throughout the SoCAB following land use distribution—and 40% photovoltaic units. The resulting emissions from this mix are presented in Table 75. In addition, Table 75 presents the total emissions in the baseline inventory for the year 20XX, total emissions resulting from removing existing vehicles in 20XX and adding the EVs, and the DG infrastructure to power the fleet. Scenario 20XX EV reduces emissions of $NO_X$, VOC, CO, and $PM_{2.5}$ with respect to baseline 20XX emissions by 17%, 16%, 29%, and 8%, respectively. On the other hand, $SO_X$ emissions increase by 2%.

**Table 75. Basinwide emissions (tons/day) from the DG used to power the entire fleet of electric vehicles, the total basinwide emissions (tons/day) in the baseline 20XX scenario, and the pure electric vehicle scenario with electricity production via distributed generation**

| | $NO_X$ | VOC | CO | $SO_2$ | $PM_{2.5}$ |
|---|---|---|---|---|---|
| DG for EV | 6.72 | 1.84 | 9.07 | 0.77 | 7.85 |
| Baseline 20XX | 97.0 | 385.0 | 1669.0 | 19.0 | 91.0 |
| Scenario 20XXEVDG | 80.1 | 322.7 | 1180.8 | 19.4 | 83.8 |

The decrease in $NO_X$ and VOC emissions due to implementation of a widespread EV infrastructure leads to a decrease in the peak ozone concentrations throughout the entire basin. In particular, maximum reductions in peak ozone concentrations are nearly 6 ppb (Figure 66a), and they occur in the northeastern part of the domain, where ozone concentrations are typically the highest. In addition, reductions of direct emissions of particles in conjunction with $NO_X$ reductions contribute to the reduction in 24-hour average $PM_{2.5}$ concentration. Particularly, $PM_{2.5}$ concentrations decrease by 4 $\mu g/m^3$ in the vicinity of Riverside, where the peak in $PM_{2.5}$ develops generally (Figure 66b).

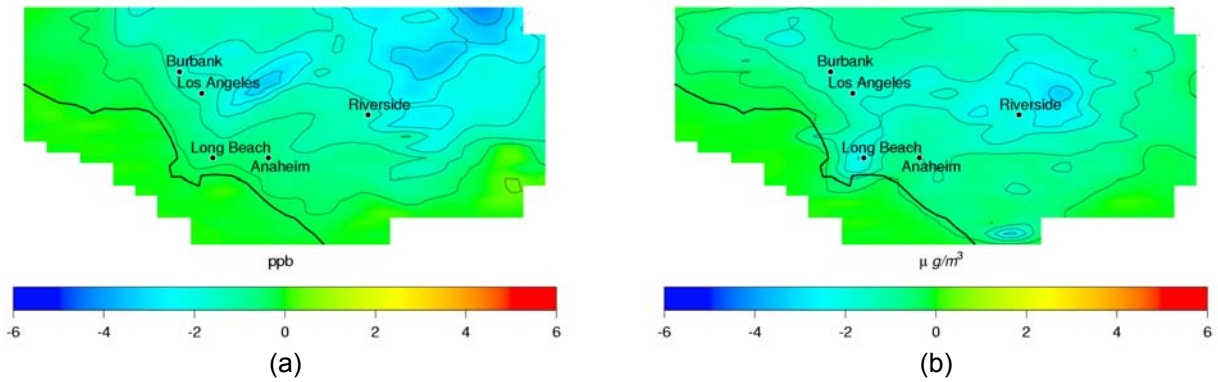


**Figure 66. Air quality impacts of scenario 20XXEVDG with respect to baseline 20XX: (a) impacts on peak ozone concentration, and (b) impacts on 24-hour average $PM_{2.5}$ concentration**

In conclusion, the widespread use of EV coupled with DG to produce the required electricity could significantly reduce emissions. Despite the introduction of additional in-basin emissions from power generation needed to supply electricity for the EV fleet, emissions from power generation are significantly lower than the vehicle emissions that were reduced by EV use. As a result of these emissions reductions, implementation of a DG-EV infrastructure would lead to large reductions in ozone and $PM_{2.5}$ that could help maintain the compliance with air quality standards. Note that these benefits to air quality from the DG-EV case depend upon a high percentage of renewable power—40% renewable—in the DG mix, as well as the ARB 2007 emission limits to for all NG-fueled units. Lower penetration of renewable power and/or more permissive emission standards for DG could increase the emissions from electricity generation for EV and even offset the benefits of using electric vehicles with DG, leading to increases in air pollutant concentrations.

## 5.2. Air Quality Impacts of DG Scenarios in the SJV

### *5.2.1. Baseline Air Quality in Target Year*

The baseline emissions for the target year 2023 are developed using the methodology described in the earlier discussion on Scenario B1. Figure 67 shows 1-hour ozone maximum ground level concentrations that are predicted after these reductions in emissions are accounted for in the four days of simulation. As compared to results from the 2000 base case shown in Figure 39, major reductions are seen in maximum 1-hour ozone concentrations. Similarly, maximum 8-hour ozone concentrations decrease considerably (not shown). Note that for the purposes of developing 2023 emission estimates, the 2000 emission inventory version without the emissions from forest fires that occurred during the 2000 episode is used. Therefore, the effect of forest fires seen in 2000 base case results in the eastern portion of the domain is not seen for the future year simulation. Figure 69 shows 24-hour average $PM_{2.5}$ concentrations for the target year. Similar to ozone concentrations, significant decrease in 24-hour average $PM_{2.5}$ concentrations are predicted using the baseline emissions for the target year 2023 in comparison with year 2000 emissions.

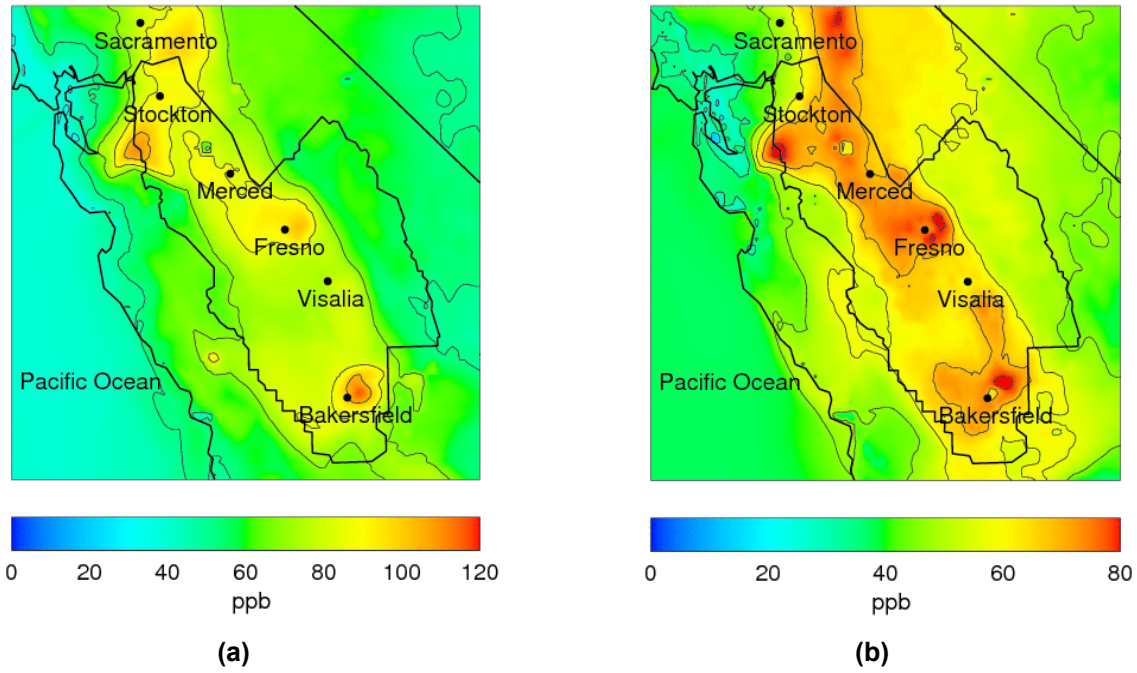


**Figure 67. Base case ground-level ozone concentrations for the year 2023. (a) Peak 1-hour ozone concentrations, and (b) Peak 8-hour ozone concentration.**

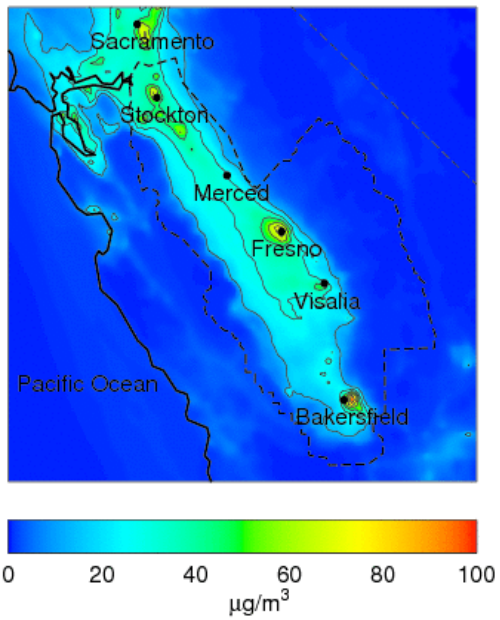


**Figure 68. Base case ground-level 24-hour average $PM_{2.5}$ concentrations for the year 2023**

### 5.2.2. Air Quality Impacts of Realistic DG Scenarios

The parameters that describe realistic scenarios are presented in Section 3.2.2. As shown in Table 47, emissions resulting from all realistic scenarios are quite small in comparison with basinwide emissions. All the realistic scenarios include emission credit for combined heating and power. However, as in the case of the SoCAB, CHP emissions displacement does not offset completely the emissions from DG, resulting in net positive $NO_X$ emissions. Figure 69 shows the peak ground-level 1-hour averaged ozone concentration impacts of DG emissions from realistic scenarios (SJV-R1, SJV-R2, SJV-R3, and SJV-R4). As expected, the impacts are very low with the highest impact being less than 0.1 ppb for all realistic scenarios. Table 76 and Table 77 present domain-wide maximum increase and decrease in peak 1-hour and 8-hour ozone concentrations for all scenarios. Although there are some localized decreases in ozone concentration due to ozone titration by additional $NO_X$ from DG, in general the addition of $NO_X$ leads to increases in ozone concentrations in all four realistic scenarios, as shown in Figure 69. Even though consistent spatial trends are observed in ozone impacts from the realistic implementation of DG, overall impacts are negligible.

Figure 70 shows the impacts of the realistic DG implementation scenarios on 24-hour average ground-level particulate matter concentrations throughout the SJVAB during the winter episode described in Section 4.2.2. Impacts on $PM_{2.5}$ are smaller than 0.5 $\mu g/m^3$ for all realistic DG scenarios. The maximum increase in $PM_{2.5}$ is 0.43 $\mu g/m^3$, and it occurs in scenario SJV-R3. The impacts occur primarily near the urban centers of Stockton, Fresno, Visalia, and Bakersfield, and along parts of State Route 99. The winter meteorology in SJV is characterized by very low wind speeds and stagnant conditions. Therefore, impacts appear to be localized in urban areas where DG emissions are predicted to occur. Table 78 presents domain-wide maximum increase and decrease of 24-hour $PM_{2.5}$ for all realistic scenarios. Although there are some localized decreases in $PM_{2.5}$, Figure 70 shows that most of the SJV experiences an increase in $PM_{2.5}$ concentration due to DG emissions. Decreases in 24-hour average $PM_{2.5}$ emissions are attributed to the nighttime chemistry of nitrogen oxides. Addition of $NO_X$ from DG at nighttime titrates ozone and decreases oxidation capacity of the atmosphere, reducing secondary formation of PM in some locations.

**Table 76. Peak 1-hour ozone impacts in the SJVAB from all spanning scenarios**

| | | Δ 1-hour $O_3$ | |
|---|---|---|---|
| | Maximum 1-hour $O_3$ | Maximum increase | Maximum decrease |
| | (ppb) | (ppb) | (ppb) |
| Baseline | 116.83 | | |
| *Realistic Scenarios* | | | |
| SJV-R1 | 116.84 | 0.02 | 0.01 |
| SJV-R2 | 116.84 | 0.03 | 0.02 |
| SJV-R3 | 116.84 | 0.03 | 0.02 |
| SJV-R4 | 116.84 | 0.03 | 0.02 |

**Table 77. Peak 8-hour ozone impacts in the SJVAB from all spanning scenarios**

| | | Δ 8-hour $O_3$ | |
|---|---|---|---|
| | Maximum 8-hour $O_3$ | Maximum increase | Maximum decrease |
| | (ppb) | (ppb) | (ppb) |
| Baseline | 84.56 | | |
| *Realistic Scenarios* | | | |
| SJV-R1 | 84.58 | 0.02 | 0.01 |
| SJV-R2 | 84.58 | 0.03 | 0.02 |
| SJV-R3 | 84.58 | 0.03 | 0.02 |
| SJV-R4 | 84.58 | 0.03 | 0.02 |

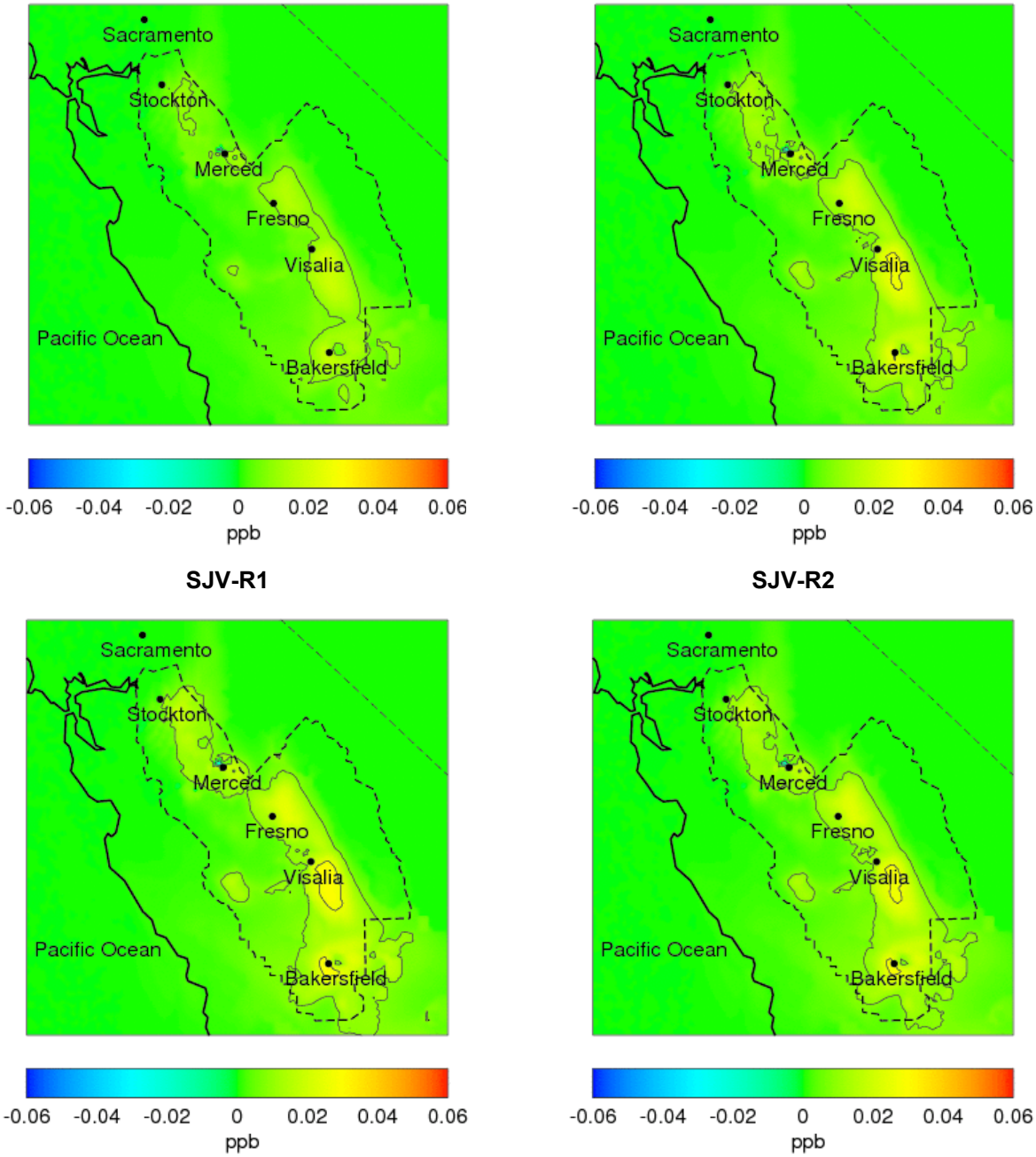


**Figure 69. Impact of emissions from realistic DG scenarios on peak 1-hour average ground-level ozone concentrations in the SJV: (SJV-R1) Medium market penetration of DG technologies, (SJV-R2) High market penetration of DG technologies, (SJV-R3) High research and development of DG technologies, (SJV-R4) High deployment of fuel cells due to environmental forcing**

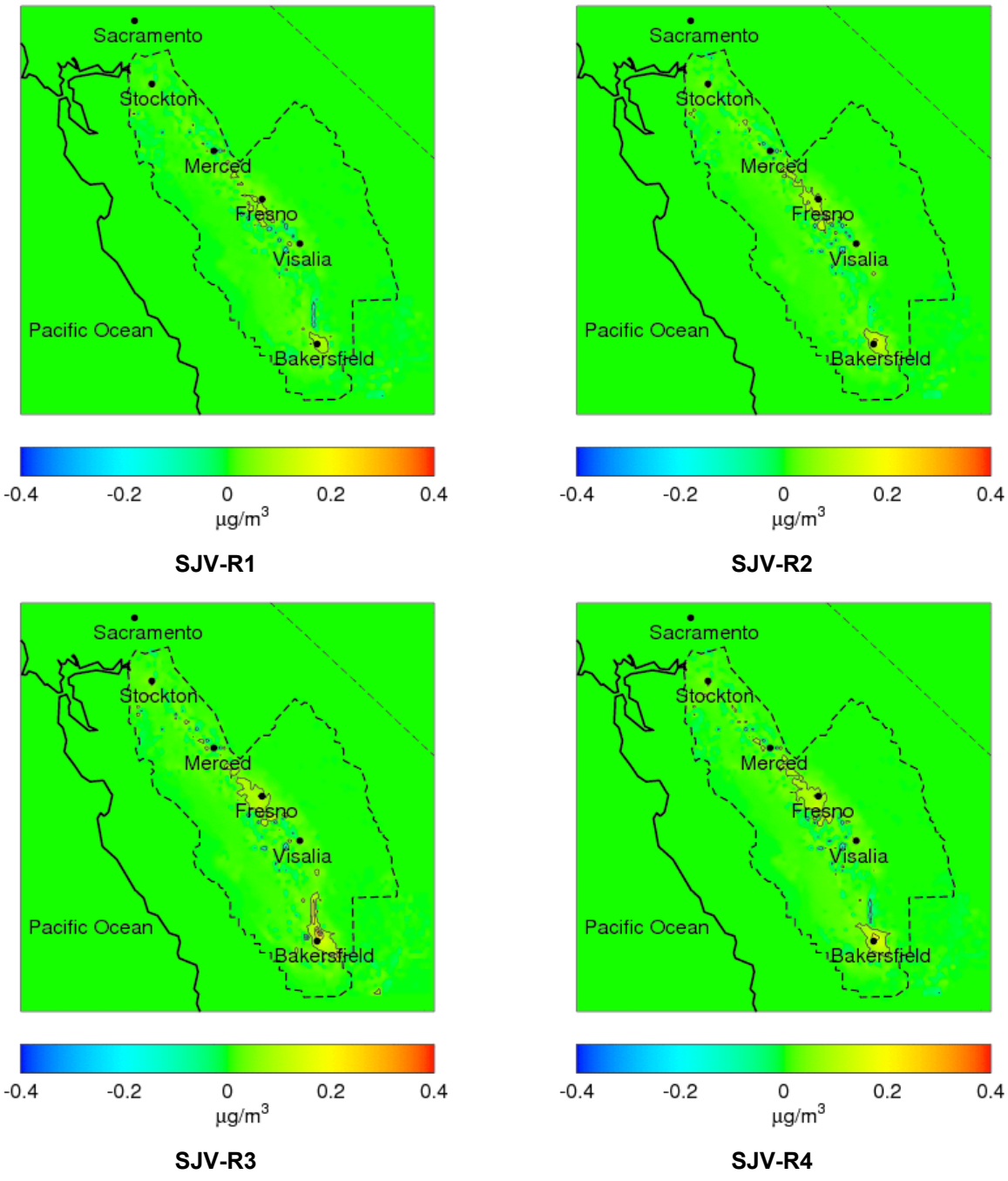


**Figure 70. Impacts of emissions from realistic DG scenarios on 24-hour average ground-level $PM_{2.5}$ concentrations in the SJV: (SJV-R1) Medium market penetration of DG technologies, (SJV-R2) High market penetration of DG technologies, (SJV-R3) High research and development of DG technologies, (SJV-R4) High deployment of fuel cells due to environmental forcing**

**Table 78. Peak 24-hour PM impacts in the SJVAB from all spanning scenarios**

| | | Δ 24-hour $PM_{2.5}$ | |
|---|---|---|---|
| | Maximum 24-hour $PM_{2.5}$ | Maximum increase | Maximum decrease |
| | $\mu g/m^3$ | $\mu g/m^3$ | $\mu g/m^3$ |
| Baseline | 98.50 | | |
| *Realistic Scenarios* | | | |
| SJV-R1 | 98.59 | 0.14 | 0.17 |
| SJV-R2 | 98.62 | 0.17 | 0.20 |
| SJV-R3 | 98.65 | 0.43 | 0.29 |
| SJV-R4 | 98.65 | 0.24 | 0.21 |

### *5.2.3. Air Quality Impacts of Spanning DG Scenarios*

Realistic scenarios were constructed based on consensus projections of DG deployment in the future. However, in order to obtain a broader view of the potential air quality impacts of DG in SJV, many additional scenarios were created that explore a particular aspect of DG implementation. These scenarios are described in Section 3.2.3.

Scenario NOCHP does not apply emissions credits towards CHP benefits from DG power. Consequently, net emissions from DG are higher than in scenario SJV-R2, which assumes the same level of DG market penetration. Total DG power installed under this scenario is 334 MW, which is under baseload operation. All other parameters (e.g., emissions factors, technology mix, relative penetration) are the same as SJV-R2 scenario. Figure 71a shows increases in peak ozone concentration from this scenario. The predicted impact is small; however it is greater than those observed in realistic scenarios. Highest impact of 0.05 ppb increase due to DG emissions is observed in the downwind area of Visalia (Table 79). The Fresno and Bakersfield areas experience impacts of nearly 0.05 ppb. It is important to note that no decreases of ozone are observed except in a few model cells near Merced area. This could be because $NO_X$ emissions in the basin are at a level where ozone production is not VOC limited. Therefore, an increase in $NO_X$ emissions in the SJVAB leads to increases in ground-level ozone concentrations. This observation is in contrast to the DG impacts that are predicted for the SoCAB region for the year 2010. Predicted ozone for the SoCAB in 2010 is VOC limited and hence, addition of $NO_X$ from DG leads to a decrease in ozone concentrations in urban areas of the basin.

Figure 72a shows the impacts of emissions from the spanning scenario NOCHP on $PM_{2.5}$ during the winter. A maximum impact of 0.2 $\mu g/m^3$ is predicted to occur in the Bakersfield area. In comparison with ozone impacts, $PM_{2.5}$ impacts appear to be more localized, closer to the source of DG emissions. As noted previously, PM in the SJV region has a significant fraction that originates from secondary processes where gas-phase $NH_3$ emissions play a major role. As shown in Table 48, DG deployment introduces additional $NH_3$ emissions and thereby enhancing the formation of ammonium nitrate, which contributes to secondary particulate matter.

Scenario SJV-ARB07 assumes that all DG emit at the 2007 ARB emission standards levels. The rest of DG parameters are the same as in scenario NOCHP. Since in scenario NOCHP some DG technologies emit below the 2007 ARB standards, emissions in scenario SJV-ARB07 are higher than in scenario NOCHP. Scenario SJV-ARB07 can be seen as an upper bound for DG emissions if all DG technologies must comply with 2007 ARB standards. As a result, air quality impacts in scenario SJV-ARB07 are more intense than in scenario NOCHP. Impacts of scenario SJV-ARB07 on peak ozone concentration is shown in Figure 71b. Highest increases of 0.05 ppb occur downwind from Visalia. Also, the Fresno and Bakersfield areas experience increases of nearly 0.05 ppb. Although the highest increases in peak ozone in scenarios NOCHP and SJV-ARB07 are the same, increases in scenario S2 spread throughout a larger area than in scenario SJV-ARB07. Impacts on $PM_{2.5}$ concentration in scenario SJV-ARB07 are slightly larger than in scenario NOCHP (as shown in Figure 72b). In particular, $PM_{2.5}$ concentrations increase by up to 0.29 $\mu g/m^3$ in Bakersfield, and Visalia and Fresno experience increases of up to 0.2 $\mu g/m^3$.

Scenario ICE-BACT considers DG implementation with emissions from ICEs operating at the level of BACT guidelines valid in 2007 in the SJV. Total installed DG power in this scenario is 334 MW. The BACT standards are significantly less restrictive than the 2007 ARB standards. Hence, as shown in Table 48, emissions from this scenario are significantly higher compared to scenario NOCHP, although the level of DG market penetration and other parameters are the same in both cases. For this spanning scenario ICE-BACT, $NO_X$ emissions are about 10 times higher and VOC emissions are about 25 times higher than the NOCHP scenario. It is interesting to note that small decreases in peak 1-hour ozone concentrations are observed for the spanning scenario ICE-BACT just northwest of Merced. This result is similar to that observed for the spanning scenario NOCHP, even though spanning scenario ICE-BACT comprises the addition of comparatively high amounts of $NO_X$. This is attributed to the local ozone chemistry in that area being VOC limited.

Figure 71c shows increases in peak ground-level ozone concentrations throughout the basin that result from the DG installation associated with this scenario ICE-BACT. The largest impacts are observed near Visalia, which experiences an increase of 0.4 ppb. This is followed by two other major urban areas in the SJV, Bakersfield, and Fresno, which experience an impact on the order of 0.3 ppb. Figure 72c shows the impacts of the DG emissions of spanning scenario ICE-BACT on the 24-hour average ground-level $PM_{2.5}$ concentrations throughout the San Joaquin Valley Air Basin. Peak impacts, up to 0.4 $\mu g/m^3$, are observed near the Bakersfield and Fresno areas. Note that $PM_{2.5}$ is predicted to decrease at some locations in this scenario. The observed decreases in 24-hour average $PM_{2.5}$ in these locations is attributed to the nighttime chemistry of nitrogen oxides. Addition of $NO_X$ from DG at nighttime titrates ozone and decreases oxidation capacity of the atmosphere. Consequently, secondary PM formation decreases and leads to the overall reduction in 24-hour average $PM_{2.5}$.

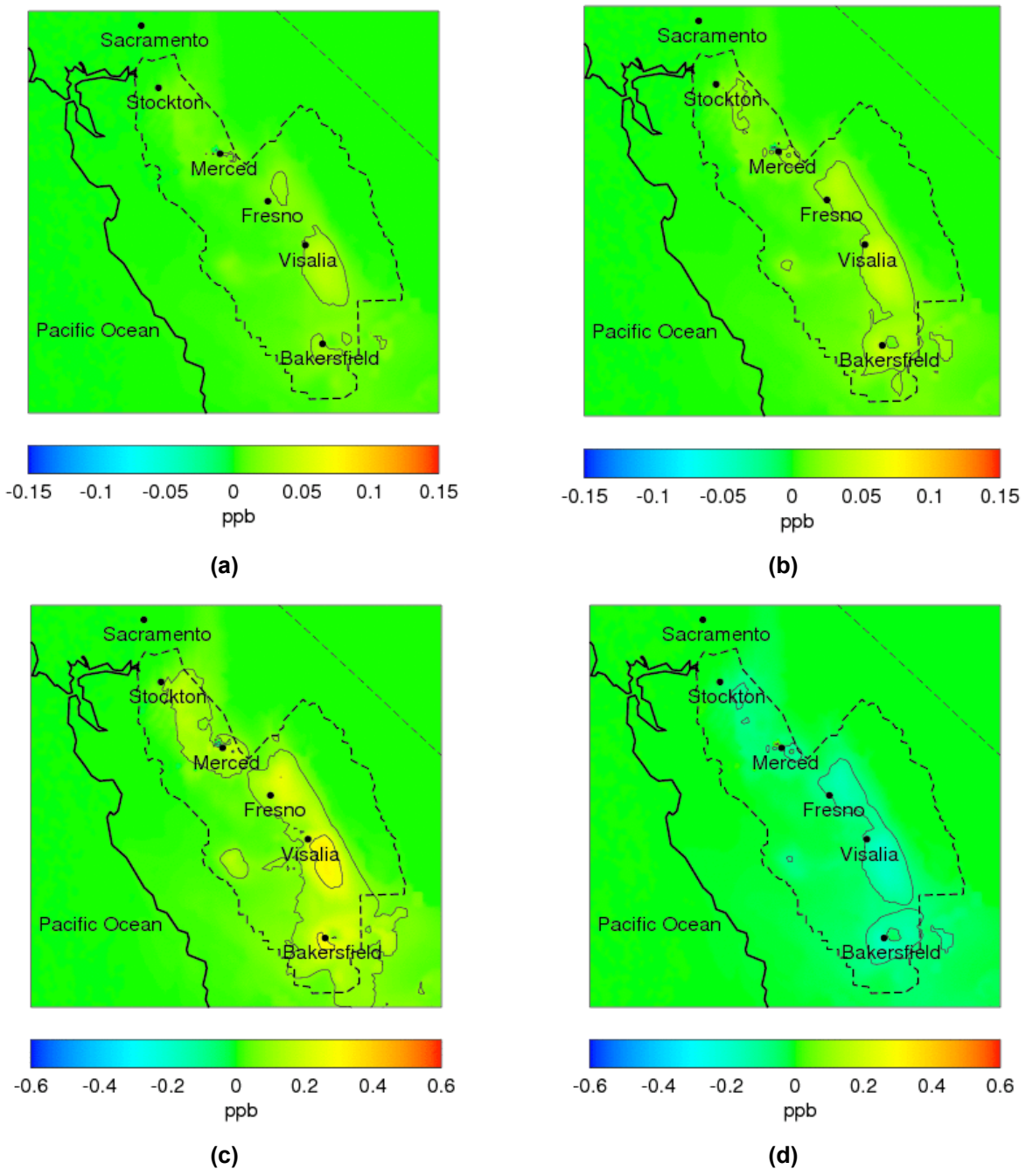


**Figure 71. Impact of emissions from DG spanning scenarios on peak ground-level ozone concentration in the SJV: (a) SJV-R1 scenario without CHP emission credits (NOCHP), (b) All DG emitting at certified levels (SJV-ARB07), (c) All ICE emitting at BACT emission standards of 2007 (ICE-BACT), (d) High penetration of DG technologies with 100% CHP emission credits (ALLCHP)**

A major incentive for deployment of DG is the benefit from CHP application of technologies. The scenario ALLCHP explores the possibility of aggressive DG deployment and utilization of full CHP potential from DG installations. In this scenario, total installed power of DG is assumed to be 830 MW. In this scenario emission credit is applied assuming 100% of DG units use CHP, and 100% heat is thermodynamically extractable. Since 100% utilization of CHP potential is impossible due to mismatch between electricity and heat loads, this scenario sets the upper bound for emission displacements due to combined heating and power. Consequently, this scenario leads to net reduction in CO, $NO_X$, and VOC emissions. As shown in Table 48, $NO_X$ emissions decrease by about 1 ton per day.

Figure 71d shows the impacts of spanning scenario ALLCHP DG emissions on ozone peak concentrations throughout the San Joaquin Valley Air Basin. Spanning scenario ALLCHP was particularly designed to assess the effects of emissions reductions associated with combined heating and power. One can deduce from the ozone decreases throughout the basin, and especially in comparison to the ozone increases observed for scenarios NOCHP, SJV-ARB07, and ICE-BACT, that CHP has a significant effect on the potential air quality impacts of DG in the San Joaquin Valley Air Basin. Note that the spatial distribution of impacts is similar to those of NOCHP, SJV-ARB07, and ICE-BACT. The highest reductions of 0.1 ppb are observed near Visalia area, followed by Fresno and Bakersfield areas.

Figure 72d shows impacts of $PM_{2.5}$ from scenario ALLCHP. An increase in $PM_{2.5}$, up to 0.4 $\mu g/m^3$, is predicted for this scenario. The increase is attributed to nighttime chemistry of nitrogen oxides. Since $NO_X$ emissions are reduced in the S4 scenario, a higher ozone concentration is present in the night. This concentration would lead to higher secondary PM formation when compared with the base case. However, note that impacts are highly localized and occur in relatively small number of model cells. Furthermore, this scenario assumes higher levels of $NH_3$ and direct PM emissions compared to NOCHP, SJV-ARB07, and ICE-BACT scenarios due to higher level of DG penetration. Direct PM and $NH_3$ also lead to an increase in overall 24-hour $PM_{2.5}$.

There are some inherent uncertainties in estimating future adoption of DG power. Adoption of DG power is influenced by regulatory, economic, and other factors. In spanning scenario SJV-EHP5 we assume an extra-high penetration of DG technologies. In this scenario, 45% of increased demand is assumed to be supplied by DG units. As shown in Figure 73a, peak 1-hour ground-level ozone increases up to 0.10 ppb. The $PM_{2.5}$ impacts (see Figure 74a) are predicted to be as high as 0.74 $\mu g/m^3$ for this scenario. Scenario SJV-EHP illustrates that DG impacts are sensitive to amount of power supplied by DG units, keeping all other parameters the same as in scenario S1, although the impacts are in the same order of magnitude for the extent of DG penetration that is studied here.

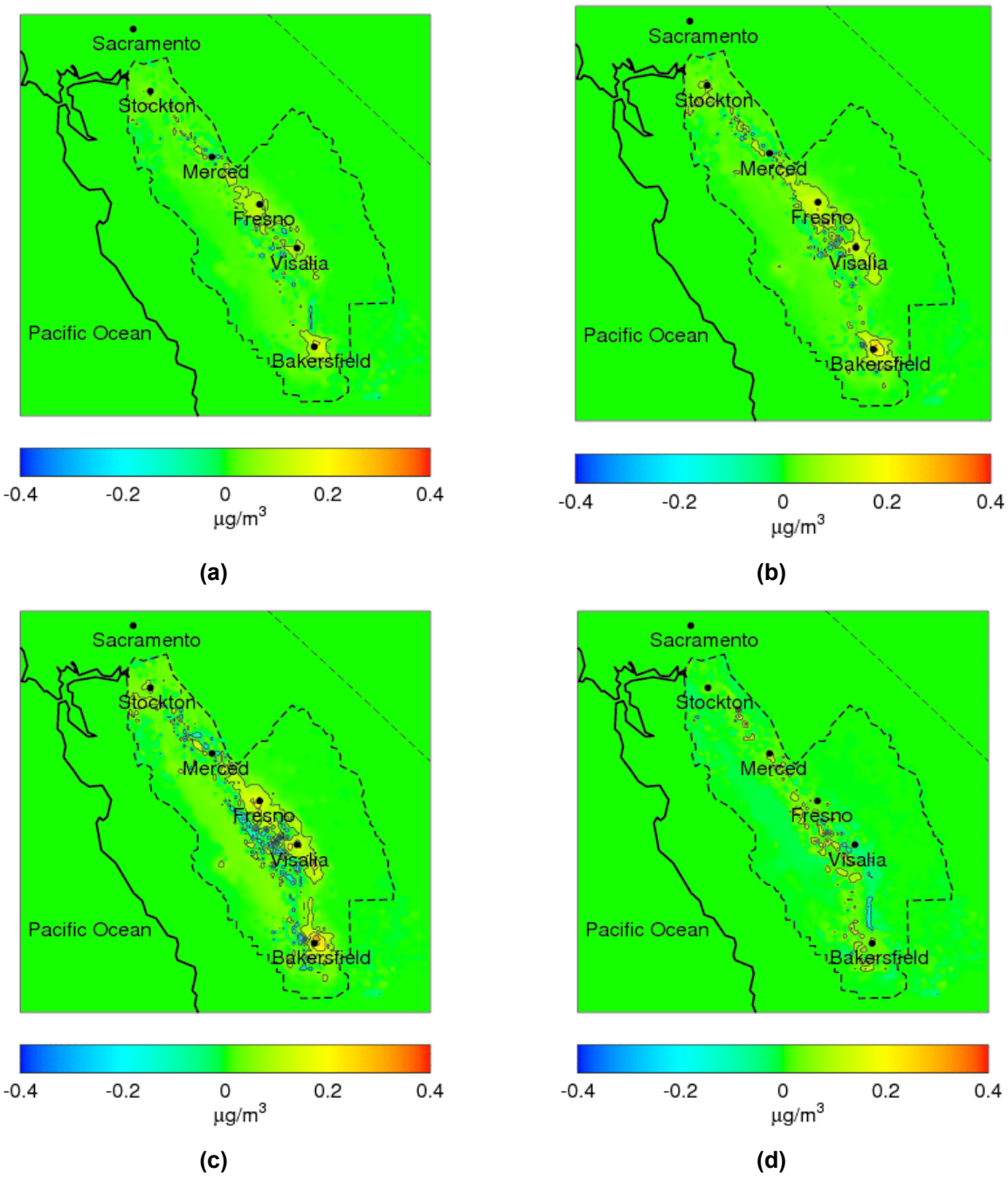


**Figure 72. Impact of emissions from DG spanning scenarios on 24-hour average PM concentration in the SJV: (a) SJV-R1 scenario without CHP emission credits (NOCHP), (b) All DG emitting at certified levels (SJV-ARB07), (c) All ICE emitting at BACT emission standards of 2007 (ICE-BACT), (d) High penetration of DG technologies with 100% CHP emission credits (ALLCHP)**

To investigate the effects of duty cycle on air quality impacts, the spanning scenario SJV-PeakTot installs DG sufficient to meet 18% of the increased power demands in the SJV between 2007 and 2023. These DG, however, are only operated during the peak power demand time period (between 12 noon and 6 p.m.), producing just as much total daily electricity and emissions as spanning scenario NOCHP, but only during a much briefer six-hour peak period. As a result, spanning scenario SJV-PeakTot leads to higher peak 1-hour average ground-level ozone concentration impacts compared to spanning scenario NOCHP, as shown in Table 79b. However, the differences are very small, suggesting that operating DG in peaking modes in the SJV may not have severe adverse effects on ozone concentrations, compared to baseload operation. The impacts of peaking operation for scenario SJV-PeakTot on 24-hour average $PM_{2.5}$ concentrations in the SJV basin are presented in Figure 74b and in Table 81. Note that $PM_{2.5}$ impacts for spanning scenario SJV-PeakTot are almost same as scenario NOCHP, again indicating a relative insensitivity of PM concentrations to DG operation in a peaking mode.

As shown for previous scenarios, especially with realistic projections of DG penetration, air quality impacts are relatively small when ARB 2007 emissions limits are used. Scenario ICE BACT demonstrates that DG impacts on ground level 1-hour ozone concentrations in SJV could increase up to 0.35 ppb if more-polluting DG units are deployed. In the South Coast, the SCAQMD found out through inspections that some units were emitting at rates over six times higher than the permitted levels under BACT standards (Kay 2006). Over 50% of the units were operating with emissions exceeding the permitted levels, and the overall average emissions of all the units inspected exceeded the BACT limits by 300%. The scenario OCR, shown in Figure 74c), explores impacts from such a possibility. In this scenario, the emissions factors for $NO_X$ and CO are assumed to be at three times the BACT emissions levels for ICE. Figure 73c shows the impacts of spanning scenario S7 on peak ozone concentrations in San Joaquin Valley Air Basin. Peak ozone increases by 0.7 ppb in the areas downwind of Visalia and by 0.5 ppb near Fresno and Bakersfield area. The $PM_{2.5}$ increases by 0.32 $\mu g/m^3$ near Visalia and Bakersfield. As in previous scenarios, some model cells experience a decrease in $PM_{2.5}$ concentration. This is attributed to nighttime $NO_X$ chemistry. Since $NO_X$ emissions are particularly high in this scenario as compared to previous spanning scenarios, decrease in PM concentrations are more prominent.

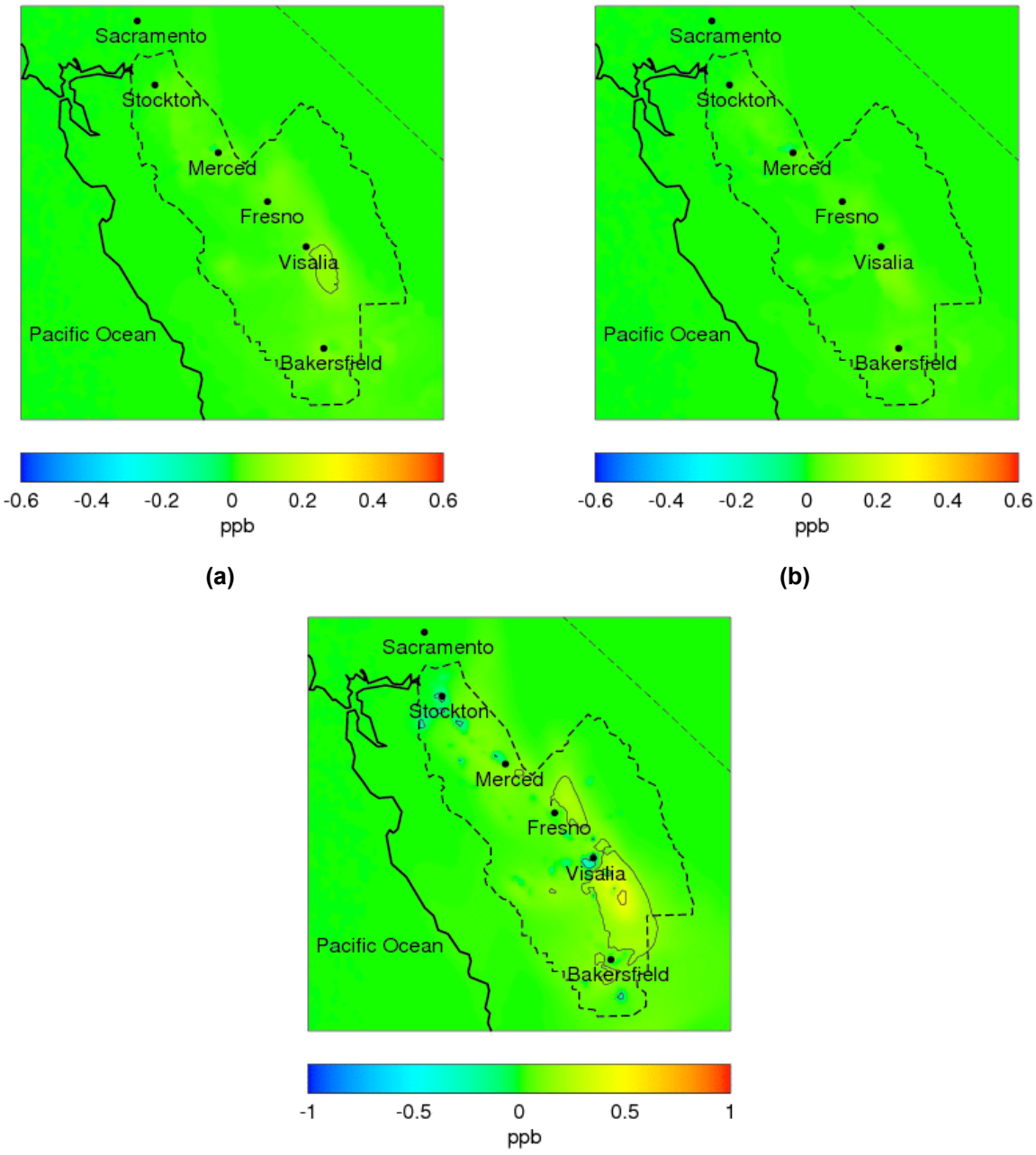


**Figure 73. Impact of emissions from DG spanning scenarios on peak ozone concentration in the SJV: (a) Extra high penetration of DG technologies without CHP emission credits (SJV-EHP), (b) All DG is operated as peaking units (SJV-PeakTot), (c) ICEs are assumed to be out-of-compliance and emitting at much higher level than permitted levels of emissions (OCR)**

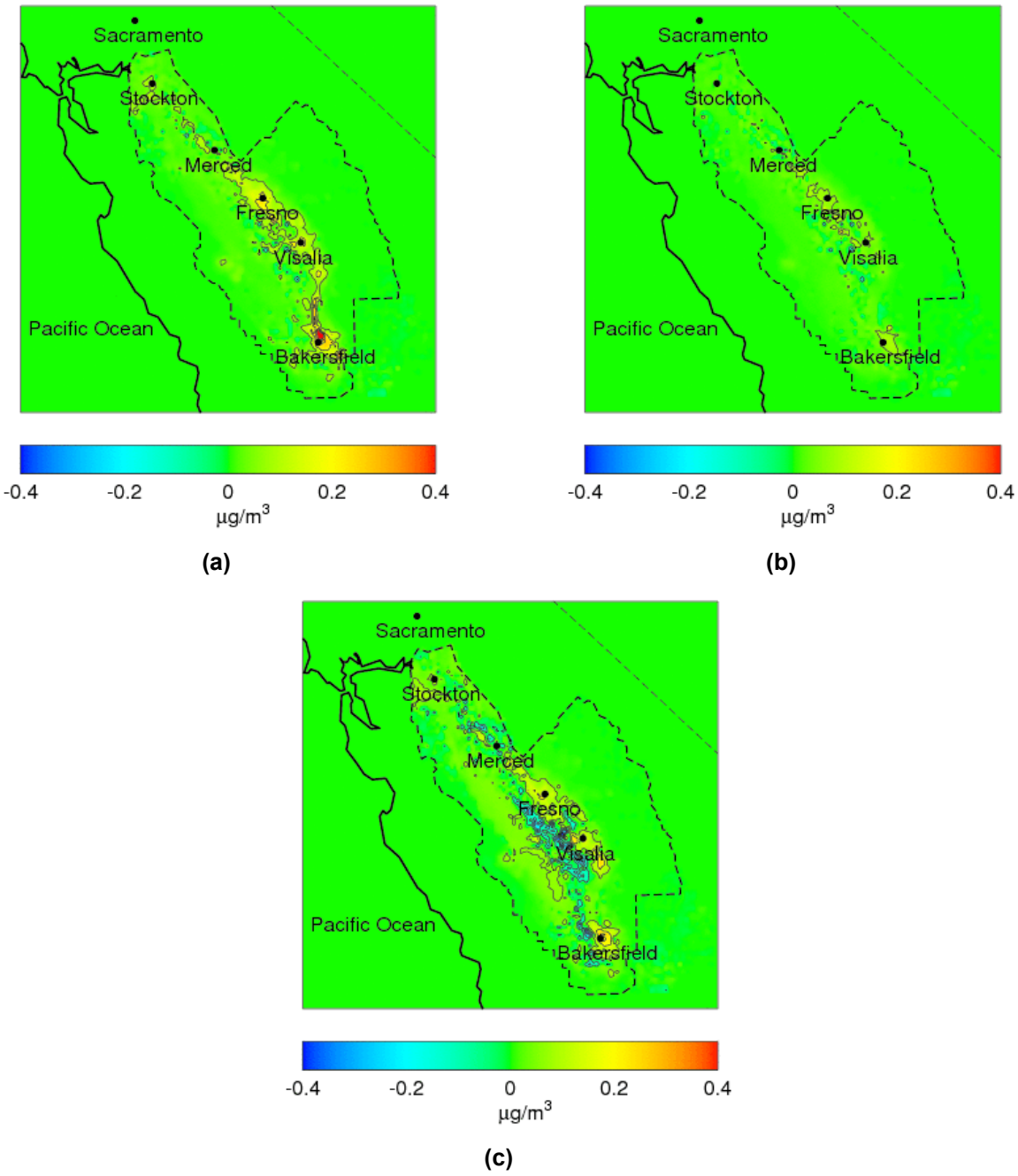


**Figure 74. Impact of emissions from DG spanning scenarios 24-hour average PM concentration in the SJV: (a) Extra high penetration of DG technologies without CHP emission credits (SJV-EHP), (b) All DG is operated as peaking units (SJV-PeakTot), (c) ICEs are assumed to be out-of-compliance and emitting at much higher level than permitted levels of emissions (OCR)**

### *Large-Scale Deployment Scenarios*

In this section the authors consider large-scale deployment of DG power. Total power from DG technologies in these scenarios is equivalent to some central generation plants in the SJV basin. In scenarios LSD1 and LSD2, total power generated by DG is assumed to be 1200 MW. This is equivalent to the power generated by a central power plant that recently became operational in the San Joaquin Valley. In scenario LSD3, DG power is equivalent to a central power plant of 1800 MW capacity. Scenarios LSD1 and LSD3 assume an aggregated technology mix; whereas LSD2 assumes that DG emissions are at the BACT levels in place in 2007. Note that the LSD3 scenario assumes the highest installed capacity amongst all scenarios. However, it assumes an aggregate mix of DG technologies, as opposed to scenario LSD2, which assumes emissions at BACT levels for all distributed generation. As a result, scenario LSD2 introduces the highest emissions amongst all scenarios. As shown in Figure 30, each of these scenarios contributes significantly to total emissions in the basin. Figure 75 and Figure 76 show the impacts of spanning scenarios LSD1, LSD2 and LSD3 on ground-level 1-hour average ozone and 24-hour average $PM_{2.5}$ concentrations in the SJV basin. Maximum 1-hour average ozone concentrations increase up to 0.1 ppb, 1 ppb, and 0.2 ppb, respectively, for S8, S9, and S10 scenarios respectively. The 24-hour average $PM_{2.5}$ increases up to 0.7 $\mu g/m^3$, 1.1 $\mu g/m^3$, and 1.0 $\mu g/m^3$, respectively, for the LSD1, LSD2 and LSD3 scenarios. The spatial distribution of impacts from these scenarios is similar to those observed in other spanning and realistic scenarios, even though the total DG emissions introduced are much higher. Table 79 and Table 80 summarize results from all spanning scenarios for peak 1-hour and 8-hour ozone concentrations respectively. Peak 8-hour ozone impacts show the same spatial trends as 1-hour ozone impacts. Table 81 summarizes 24-hour $PM_{2.5}$ impacts for all spanning scenarios.

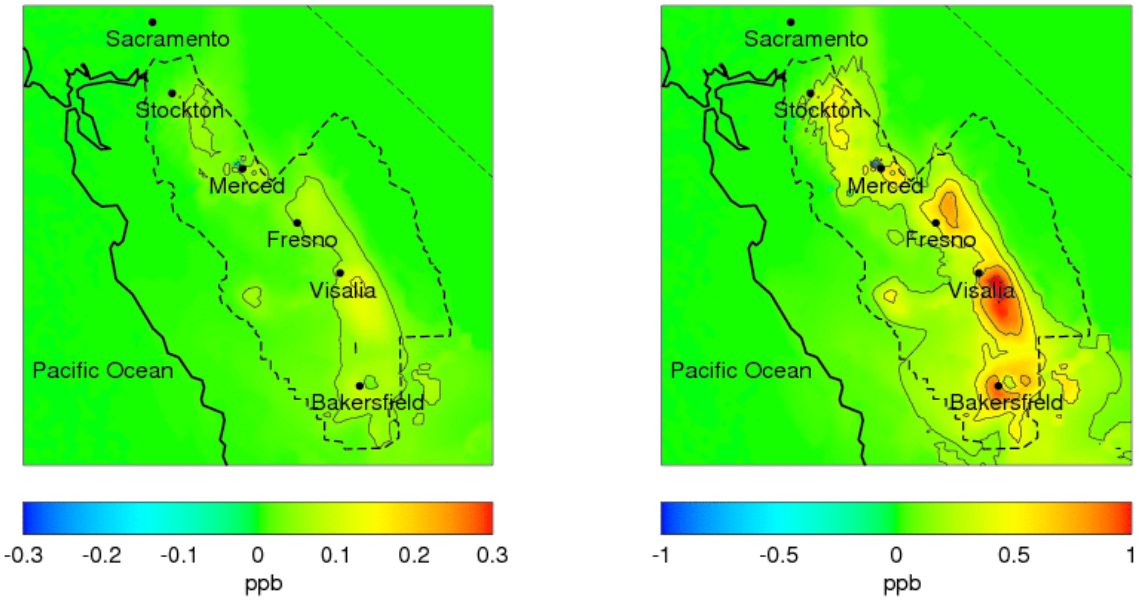


**Figure 75. Impact of emissions from large-scale deployment (LSD) scenarios on peak ozone concentration in the SJV: (a) 1200 MW of DG with an "aggregated" technology mix (LSD1), (b) 1200 MW of DG units emitting at 2007 BACT levels (LSD2), (c) 1800 MW of DG with an "aggregated" technology mix (LSD3)**

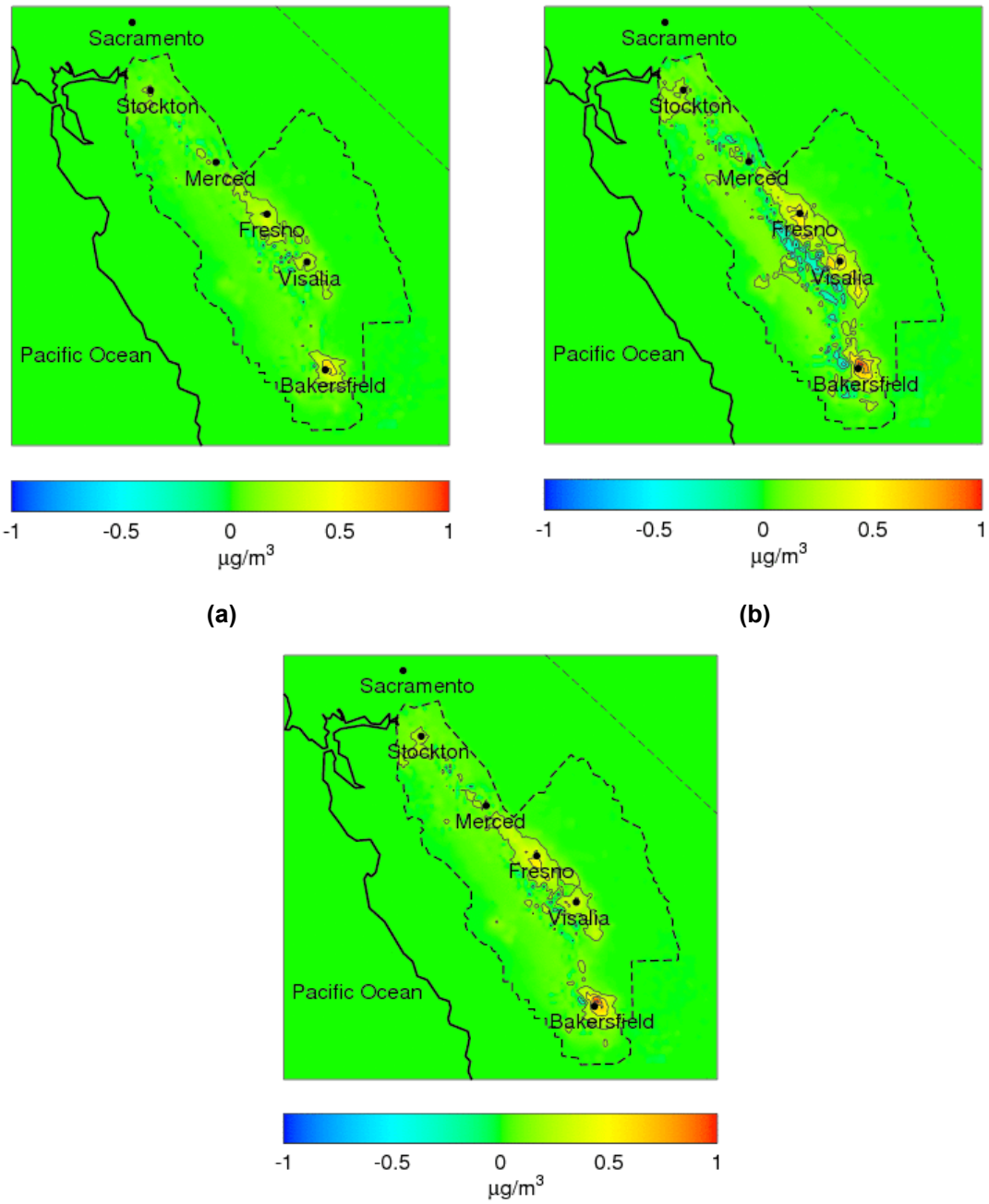


**Figure 76. Impact of emissions from large-scale deployment (LSD) scenarios on 24-hour average PM concentration in the SJV: (S8) 1200 MW of DG with an "aggregated" technology mix (LSD1), (S9) 1200 MW of DG units emitting at 2007 BACT levels (LSD2), (S10) 1800 MW of DG with an "aggregated" technology mix (LSD3)**

**Table 79. Peak 1-hour ozone impacts in the SJVAB from all spanning scenarios**

| | | Δ Peak 1-hour $O_3$ | |
|---|---|---|---|
| | Peak 1-hour $O_3$ | Maximum increase | Maximum decrease |
| | (ppb) | (ppb) | (ppb) |
| Baseline | 116.83 | | |
| *Technology mix* | | | |
| SJV-ARB07 | 116.84 | 0.05 | 0.03 |
| ICE BACT | 116.94 | 0.35 | 0.18 |
| *Emissions displacement* | | | |
| NOCHP | 116.84 | 0.05 | 0.005 |
| ALLCHP | 116.78 | 0.10 | 0.10 |
| *DG market penetration* | | | |
| SJV-EHP | 116.85 | 0.10 | 0.006 |
| *Duty cycle* | | | |
| SJV-PeakTot | 116.84 | 0.11 | 0.007 |
| *Compliance with emissions standards* | | | |
| OCR | 116.95 | 0.66 | 0.40 |
| *Large-scale deployment* | | | |
| LSD1 | 116.86 | 0.13 | 0.008 |
| LSD2 | 117.17 | 1.08 | 0.64 |
| LSD3 | 116.87 | 0.20 | 0.12 |

**Table 80. Peak 8-hour ozone impacts in the SJVAB from all spanning scenarios**

| | Peak 8-hour $O_3$ | Δ Peak 8-hour $O_3$ | |
|---|---|---|---|
| | | Maximum increase | Maximum decrease |
| | (ppb) | (ppb) | (ppb) |
| Baseline | 84.56 | | |
| *Technology mix* | | | |
| SJV-ARB07 | 84.58 | 0.03 | 0.03 |
| ICE-BACT | 84.70 | 0.24 | 0.21 |
| *Emissions displacement* | | | |
| NOCHP | 84.57 | 0.03 | 0.02 |
| ALLCHP | 84.48 | 0.13 | 0.13 |
| *DG market penetration* | | | |
| SJV-EHP | 84.59 | 0.07 | 0.05 |
| *Duty cycle* | | | |
| SJV-PeakTot | 84.59 | 0.06 | 0.02 |
| *Compliance with emissions standards* | | | |
| OCR | 84.74 | 0.45 | 0.36 |
| *Large-scale deployment* | | | |
| LSD1 | 84.77 | 0.10 | 0.06 |
| LSD2 | 86.47 | 0.76 | 0.60 |
| LSD3 | 84.87 | 0.14 | 0.10 |

**Table 81. 24-hour average $PM_{2.5}$ impacts in the SJVAB from all spanning scenarios**

| | | Δ 24-hour $PM_{2.5}$ | |
|---|---|---|---|
| | Maximum 24-hour $PM_{2.5}$ | Maximum increase | Maximum decrease |
| | μg/m³ | μg/m³ | μg/m³ |
| Baseline | 98.50 | | |
| *Technology mix* | | | |
| SJV-ARB07 | 98.72 | 0.29 | 0.29 |
| ICE-BACT | 98.75 | 0.35 | 0.35 |
| *Emissions displacement* | | | |
| NOCHP | 98.66 | 0.22 | 0.23 |
| ALLCHP | 98.54 | 0.38 | 0.18 |
| *DG market penetration* | | | |
| SJV-EHP | 98.79 | 0.74 | 0.22 |
| *Duty cycle* | | | |
| SJV-PeakTot | 98.59 | 0.26 | 0.25 |
| *Compliance with emissions standards* | | | |
| OCR | 98.73 | 0.32 | 0.26 |
| *Large-scale deployment* | | | |
| LSD1 | 99.00 | 0.70 | 0.33 |
| LSD2 | 99.32 | 1.11 | 0.69 |
| LSD3 | 99.25 | 1.04 | 0.35 |

### *5.2.4. Air Quality Impacts of Future Biomass Power in SJV*

Emission profiles from each of the biomass scenarios are developed using the methodology described in the earlier section on the biomass power scenarios development methodology. Table 82 presents aggregate emissions from all these scenarios. Scenario BM5, which assumes the highest amount of biomass power from direct combustion, introduces the highest emissions among all scenarios considered here. When fuel cells are employed to produce power from animal manure, biomass scenarios lead to a net reduction in VOC emissions. The reduction in VOC emissions is from offsets due to lower emissions from storage ponds and lagoons that potentially occur when anaerobic digesters are used to treat animal manure.

**Table 82. Total emissions from biomass scenarios**

| Biomass Scenario | Biomass Power (MW) | $NO_X$ (tons/day) | VOC (tons/day) | $SO_X$ (tons/day) | PM (tons/day) |
|---|---|---|---|---|---|
| BM1 | 326 | 0.35 | 0.03 | 0.07 | 0.17 |
| BM2 | 326 | 0.35 | 0.03 | 0.07 | 0.17 |
| BM3 | 326 | 0.35 | 0.03 | 0.07 | 0.17 |
| BM4 | 326 | 0.31 | -0.37 | 0.06 | 0.14 |
| BM5 | 454 | 0.46 | -0.35 | 0.09 | 0.21 |
| BM6 | 360 | 0.33 | -0.74 | 0.06 | 0.14 |

Emissions from the biomass scenarios are added to the baseline emissions and introduced as inputs for the air quality models used to assess ozone and PM air quality impacts. Sections 3.2.4 and 4.2 present details of the air quality modeling tools and meteorological and basinwide emissions data. Air quality impacts from biomass scenarios are quantified by analyzing the changes in maximum 1-hour ozone and 24-hour average PM concentrations attributable to biomass electricity generation with respect to the baseline case.

Figure 77, Figure 79, and Table 83 show an increase in the maximum 1-hour ozone concentrations for all biomass scenarios. Table 84 shows the impact of biomass scenarios on the maximum ozone 8-hour average. Peak ozone concentration is predicted to increase by about 0.1 ppb in all biomass scenarios. Scenarios BM1, BM2, and BM3 add the same amount of total emissions to the basin. However, the spatial distribution is different among these three scenarios. Scenario BM3, which assumes biomass plants with higher capacity, has more concentrated emissions than scenarios BM2 and BM1, which assume smaller plant sizes. Consequently, impacts in scenario BM3 are more concentrated than in scenarios BM2 and BM1. Similarly, scenario BM2, which assumes larger plant sizes than BM1, has more concentrated impacts than BM1. Scenario BM4, which assumes deployment of fuel cells for animal manure, has similar impacts as scenarios that assume all direct combustion (BM1, BM2, and BM3). Although fuel cells have far lower emissions than direct combustion plants, only a small fraction of total biomass can be utilized through fuel cells. As noted before, utilization of anaerobic digesters and fuel cells leads to a net reduction of VOCs in the basin. However, the impact of this reduction in VOCs is only minimal because ozone formation in the SJVAB is $NO_X$ limited.

In comparison with impacts from distributed generation using advanced technologies, biomass scenarios show higher impacts for comparable amount of additional total power in the basin. Ozone impacts of DG from realistic scenarios are negligible as presented in Section 5.2.2. However, biomass scenarios show a small but non-negligible level of impacts.

Figure 78, Figure 80, and Table 85 show an increase in 24-hour average $PM_{2.5}$ concentrations for all biomass scenarios. Results show maximum increases in 24-hour $PM_{2.5}$ of up to 0.63 $\mu g/m^3$. Note that the scale in Figure 78 and Figure 80 has been truncated to show better resolution. The $PM_{2.5}$ impacts are more localized than ozone impacts and are predicted to occur around the location of the biomass plants. As discussed in previous sections, emissions and pollutants are

transported northward during wintertime in the SJV region. A similar phenomena, although at a smaller scale, is also observed for biomass scenarios. Model cells that are north of cells with biomass plants experience increases in 24-hour average $PM_{2.5}$ for all scenarios.

**Table 83. Peak 1-hour ozone impacts in the SJVAB from all biomass scenarios**

| | Peak 1-hour $O_3$ | Maximum increase | Maximum decrease |
|---|---|---|---|
| | (ppb) | (ppb) | (ppb) |
| Baseline | 116.83 | | |
| *Biomass Scenarios* | | | |
| BM1 | 116.84 | 0.11 | 0.01 |
| BM2 | 116.84 | 0.12 | 0.01 |
| BM3 | 116.84 | 0.12 | 0.02 |
| BM4 | 116.80 | 0.09 | 0.03 |
| BM5 | 116.80 | 0.10 | 0.04 |
| BM6 | 116.80 | 0.09 | 0.03 |

**Table 84. Peak 8-hour ozone impacts in the SJVAB from all biomass scenarios**

| | Peak 8-hour $O_3$ | Maximum increase | Maximum decrease |
|---|---|---|---|
| | (ppb) | (ppb) | (ppb) |
| Baseline | 84.56 | | |
| *Biomass Scenarios* | | | |
| BM1 | 84.58 | 0.05 | 0.1 |
| BM2 | 84.58 | 0.06 | 0.2 |
| BM3 | 84.58 | 0.06 | 0.2 |
| BM4 | 84.56 | 0.04 | 0.2 |
| BM5 | 84.57 | 0.05 | 0.1 |
| BM6 | 84.56 | 0.04 | 0.2 |

**Table 85. 24-hour $PM_{2.5}$ impacts in the SJVAB from all biomass scenarios**

| | Maximum 24-hour PM | Maximum increase | Maximum decrease |
|---|---|---|---|
| | $\mu g/m^3$ | $\mu$ g/m$^3$ | $\mu$ g/m$^3$ |
| Baseline | 98.50 | | |
| *Biomass Scenarios* | | | |
| BM1 | 98.58 | 0.33 | 0.32 |
| BM2 | 98.57 | 0.44 | 0.19 |
| BM3 | 98.56 | 0.63 | 0.20 |
| BM4 | 98.57 | 0.44 | 0.20 |
| BM5 | 98.61 | 0.45 | 0.21 |
| BM6 | 98.57 | 0.44 | 0.20 |

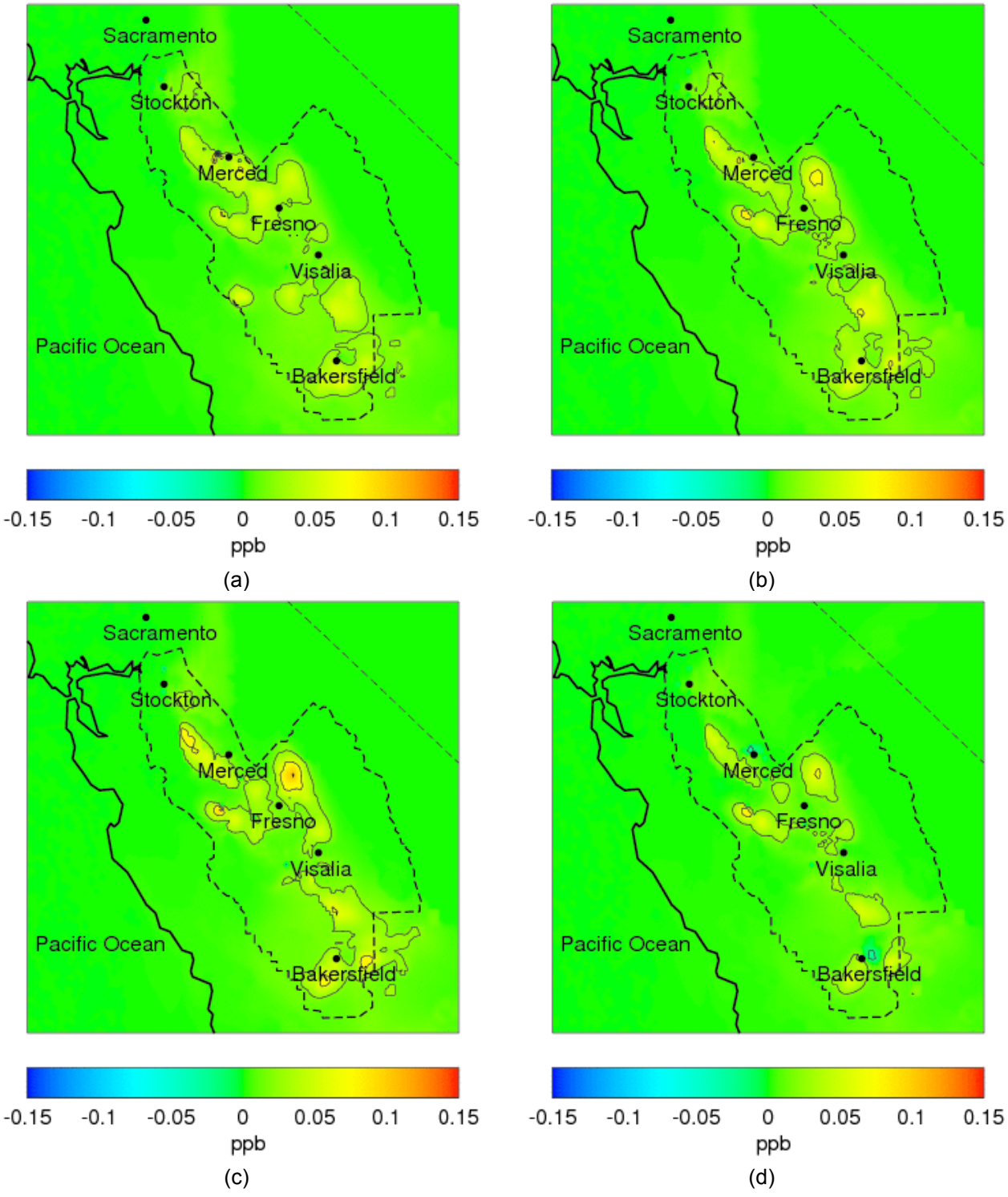


**Figure 77. Increase in maximum 1-hour ozone concentrations from biomass power in 2023 from scenarios (a) BM1, (b) BM2, (c) BM3, and (d) BM4**

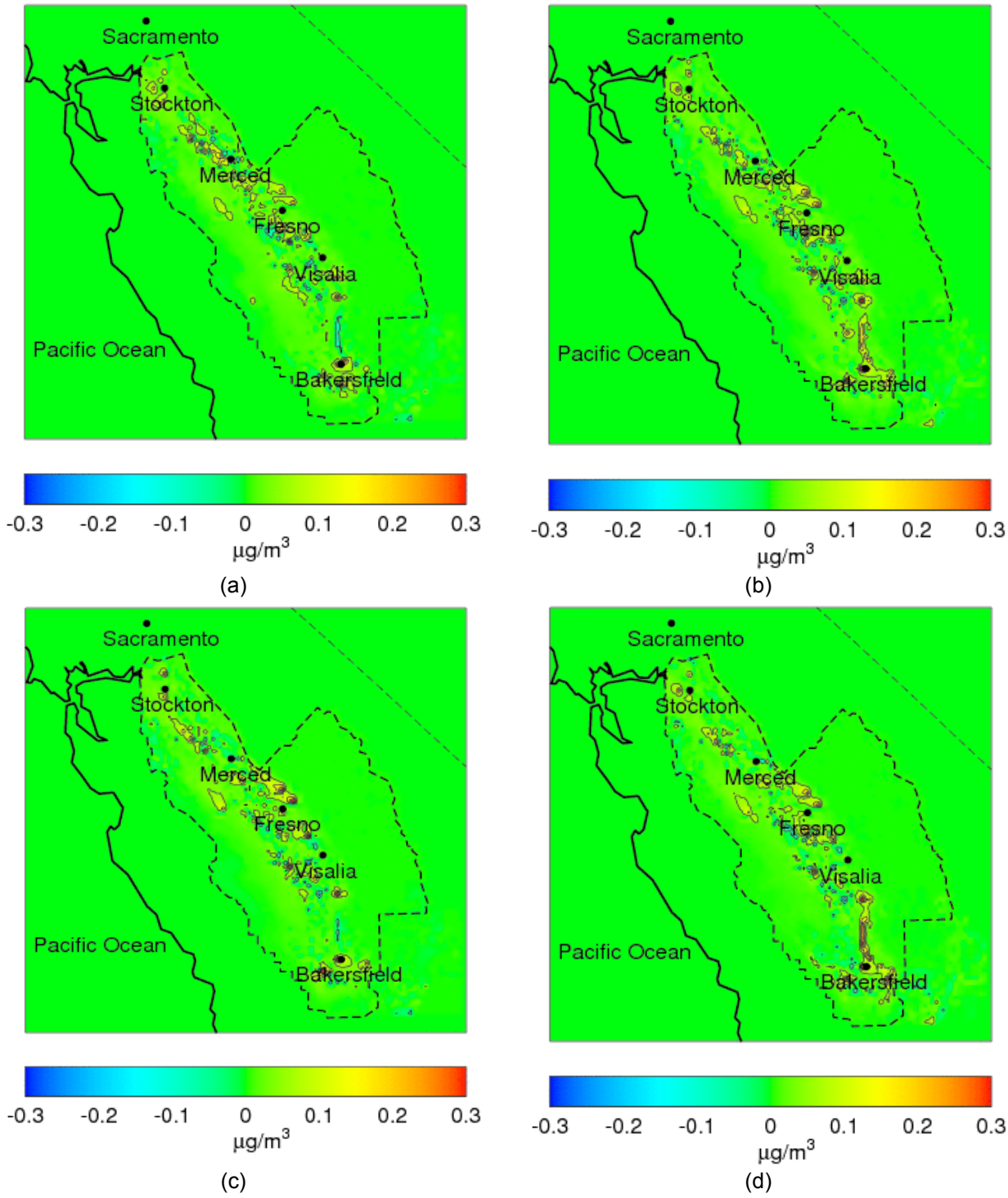


**Figure 78. Increase in 24-hour average concentration of PM from biomass power in 2023 from scenarios (a) BM1, (b) BM2, (c) BM3, and (d) BM4. Note that scale is truncated to 0.3 µg/m$^3$ to show better contrast. For absolute maximum values, see Table 85.**

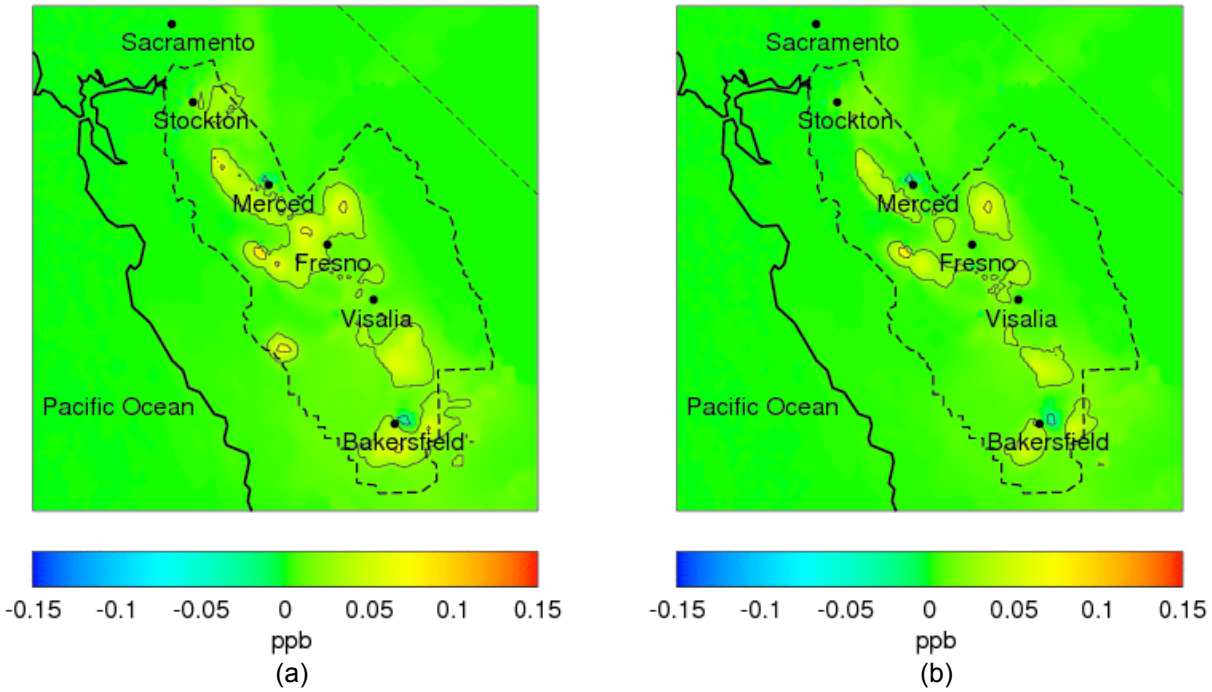


**Figure 79. Increase in maximum 1-hour ozone concentrations from biomass power in 2023 from scenarios (a) BM5 and (d) BM6**

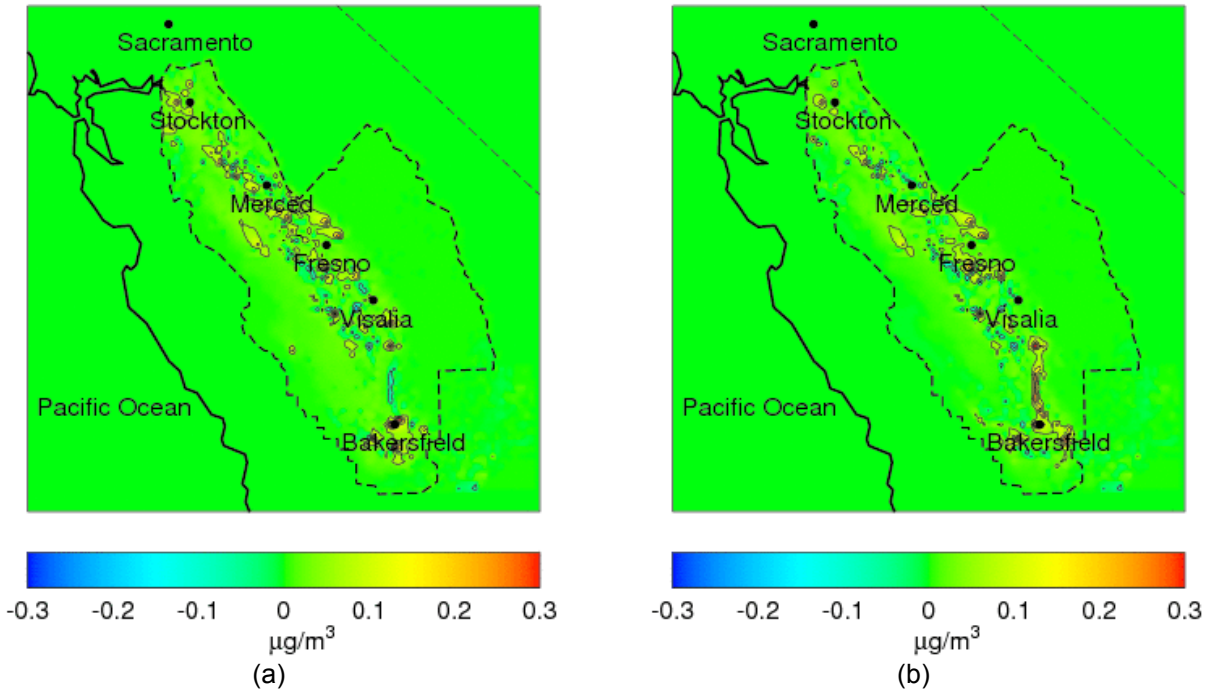


**Figure 80. Increase in 24-hour average PM concentrations from biomass power in 2023 from scenarios (a) BM5 and (d) BM6. Note that scale is truncated to 0.3 µg/m$^3$ to show better contrast. For absolute maximum values, see Table 85.**

# 6.0 Impacts on Greenhouse Gases From DG Implementation

## 6.1. Greenhouse Gas (Primarily $CO_2$) Emissions in the Electricity Sector

The emission of $CO_2$ (and other greenhouse gases) in the electricity sector depends upon the mix of power generation technologies used to meet the electrical demand. According the report *Carbon Dioxide Emissions for the Generation of Electric Power in the United States,* (U.S. DOE/U.S. EPA 2000), the 1999 national average output rate was 1.341 pounds of $CO_2$/kilowatt-hour (kWh) generated.

However, this value differs significantly for the State of California due to less use of coal, more use of natural gas and large hydropower, and more use of renewable sources in the California electrical supply. In the report *Inventory of California Greenhouse Gas Emissions and Sinks: 1990 to 2002 Update* (California Energy Commission 2005c), it is mentioned that since 1990, in-state electricity produced 185 to 280 metric tons of $CO_2$ per gigawatt-hour, while imported electricity from fossil-fuel and renewable electric generators out-of-state produced 660–1350 metric tons of $CO_2$ per gigawatt-hour. Such wide variations in carbon intensity are due to year-to-year availability of hydropower and wind power, fossil-fueled generator types that dominate portions of peak and baseload power, and other factors. The same report also states that out-of-state electricity generation comprises 22% to 32% of California's total electrical energy consumption. Nonetheless, out-of-state electricity production comprises approximately 50% of the total GHG emissions associated with serving California's electricity demand. So, an average value for in-state $CO_2$ emissions is 232 metric tons of $CO_2$ per gigawatt-hour while that for out-of-state electricity generation is 1005 metric tons of $CO_2$ per gigawatt-hour. Taking into account the percentage in the electrical demand for each case, 1.023 pounds of $CO_2$/kWh is a rough estimate for the composite $CO_2$ emissions in California for the electricity generation sector.

From the same report (California Energy Commission 2005c) and for the specific year of 2002, one can produce another estimate for the $CO_2$ emissions in California in the electricity generation sector. It has been estimated that in 2002, a total of 493 million metric tons of $CO_2$ was emitted from generators meeting California's energy demands. The trend of the $CO_2$ emissions equivalent in California is presented in Figure 81. The $CO_2$ equivalent emissions include all GHG emissions, each weighted by their respective radiant cross-section to produce a similar greenhouse effect. The primary contribution to $CO_2$ equivalent emissions remains $CO_2$ in most cases. Note that roughly 35% of the $CO_2$ equivalent emissions are produced in the transportation sector and that roughly 20% of the $CO_2$ equivalent emissions are produced in the electricity sector.

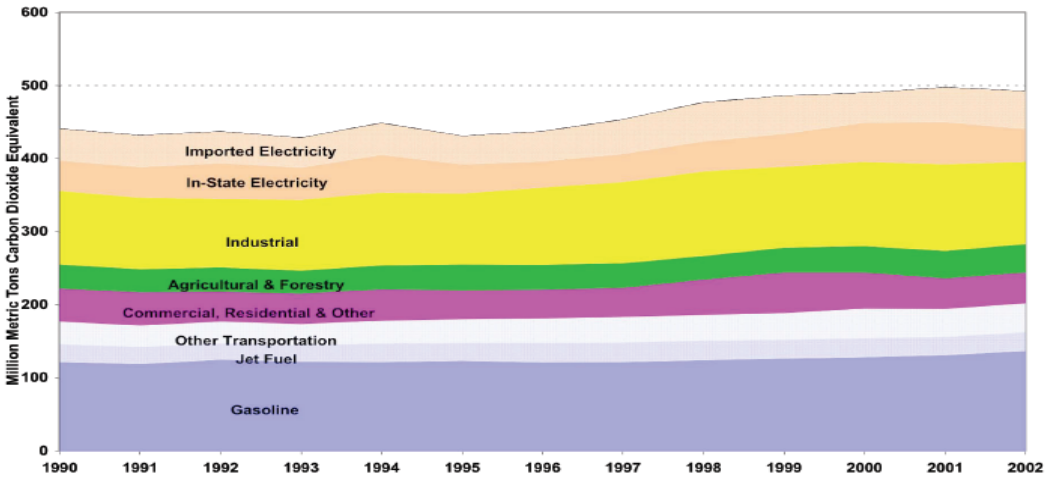


**Figure 81. Carbon dioxide emissions equivalent in the State of California**

Source: California Energy Commission 2005c

In 2002, the total electrical energy demand in California was 209,600 GWh, and it represents 19.6% of the total $CO_2$ emitted in California. From these figures, the $CO_2$ emissions per unit of electrical energy in California can be estimated by:

$$\frac{0.196 * 493 * 10^6}{209{,}600} = 461\, tons\ of\ CO_2 / GWh = 1014\, lb\ of\ CO_2 / MWh \qquad (22)$$

This value is consistent with the previous estimate of $CO_2$ emissions in California attributed to the electricity generation sector. The total GHG emissions for the years 1990 and 2002 are reported in Table 86.

**Table 86. California greenhouse gas (GHG) emissions**

| Year | GHG *(millions of metric tons of $CO_2$ equivalent)* |
|---|---|
| 1990 | 442 |
| 2002 | 493 |

Source: California Energy Commission 2005c

It is apparent from the 1990 to 2002 total GHG emissions data of Table 86 that California GHG emissions rose nearly 12% over this 12-year period. However, the same report (California Energy Commission 2005c) indicates that a 24% increase in GHG emissions is expected from 1990 to 2020 (30 years), if current trends continue. Taking this into account, the forecast emissions growth for the year 2050 is 48% greater than 1990 emissions. The GHG emissions estimates on this basis are presented in Table 87.

**Table 87. California GHG emissions forecast**

| Year | GHG *(millions of metric tons of $CO_2$ equivalent)* |
|---|---|
| 2020 | 548 |
| 2050 | 654 |

## 6.2. Potential Impacts of DG in the California Electricity Generation Sector

One of the most interesting characteristics of DG deployment is the capacity to recover part of the waste heat for useful applications. In the analyses presented in this section, 60% of the DG units are assumed to have CHP applications, and 50% of the heat available from the CHP units will be used—the same assumption that was used in the realistic scenarios for the SoCAB and the San Joaquin Valley. The emissions displaced by the waste heat recovery have been evaluated as those that would otherwise have been emitted by a boiler with an efficiency of 90% (direct $CO_2$ emissions in this case are 118 lb/MMBtu).

This study has considered six different DG technologies that can be implemented in six different size configurations. The electrical efficiency and the $CO_2$ emissions per electrical energy output for each technology using NG as fuel are presented in Table 88. Only high-temperature fuel cells (HTFC), internal combustion engines (NGIC) larger than 1 MW, and gas turbine-fuel cell hybrid systems emit at a lower rate than 1014 lb/MWh, the average California grid $CO_2$ emissions. However, if emissions displacements due to CHP are included, other technologies could become competitive with central generation $CO_2$ emissions.

The total amount of thermal heat recovered by DG technology *i* is determined by the relative heat rate $\left(\frac{Q_{HR}}{Q_{elec}}\right)_i$, which represents the heat rate $Q_{HR}$ used by the CHP application per total electricity production by the DG unit. The relative heat rate takes into account the electrical and total efficiencies of each fuel-driven DG technology, $\eta_{elec,i}$ and $\eta_{total,i,}$, respectively. In addition, it accounts for the CHP and heat utilization factors, $f_{CHP}$ and $f_{HR}$, respectively. The expression is as follows:

$$\left(\frac{Q_{HR}}{Q_{elec}}\right)_i = f_{CHP} \cdot f_{HR} \cdot \frac{\left(\eta_{total\,i} - \eta_{elec\,i}\right)}{\eta_{elec_i}} \quad \left[\frac{\mathrm{MWh_{HR}}}{\mathrm{MWh_e}}\right] \tag{23}$$

**Table 88. Electrical efficiency and $CO_2$ emissions from the DG units considered**

| | Electrical Efficiency (%) | | | | | |
|---|---|---|---|---|---|---|
| **Size** | **LTFC** | **HTFC** | **MTG** | **NGIC** | **TURB** | **HYBR** |
| <50 kW | 36.0 | 47.9 | 30.0 | 32.5 | | 70.0 |
| 50–250 kW | 36.0 | 47.9 | 31.5 | 32.5 | | 70.0 |
| 250 kW–1 MW | | 47.9 | 33.0 | 38.5 | 24.0 | 70.0 |
| 1–5 MW | | 48.0 | | 40.5 | 28.0 | 70.0 |
| 5–20 MW | | 48.0 | | 42.5 | 32.5 | 70.0 |
| 20–50 MW | | 48.0 | | | 39.0 | 70.0 |
| | **Emission Factor (lb/MWh)** | | | | | |
| **Size** | **LTFC** | **HTFC** | **MTG** | **NGIC** | **TURB** | **HYBR** |
| <50 kW | 1128 | 848 | 1353 | 1249 | | 580 |
| 50–250 kW | 1128 | 848 | 1289 | 1249 | | 580 |
| 250 kW–1 MW | | 848 | 1230 | 1055 | 1692 | 580 |
| 1–5 MW | | 846 | | 1002 | 1450 | 580 |
| 5–20 MW | | 846 | | 955 | 1249 | 580 |
| 20–50 MW | | 846 | | | 1041 | 580 |

The calculated values for relative heat rate for each of the DG technologies are presented in Table 89. Once the recovered heat from each technology is obtained, avoided boiler emissions per unit electricity produced can be estimated with the following expression:

$$M_{CO_2,boiler} = \left(\frac{Q_{HR}}{Q_{elec}}\right)_i \frac{em_{boiler,CO_2}}{ef_{boiler}} \quad \left[\frac{\text{lbs CO}_2}{\text{MWh}_e}\right] \tag{24}$$

where $ef_{boiler}$ is the boiler efficiency and $em_{boiler}$ is the boiler emission factor. The net emissions from DG with CHP, presented in Table 89, are obtained by subtracting the avoided boiler emissions from the emission factors from DG presented in Table 88. The resulting net emission factors suggest that low-temperature fuel cells, ICE of size range 250 kW–1 MW, and gas turbines larger than 20 MW can emit at a lower rate than the California grid if these technologies use CHP, in addition to the technologies that can emit less than the California mix without CHP. Furthermore, net emissions from 250 kW micro-turbines are close to the average California grid mix, and small improvements in efficiency could make these technologies competitive with central generation, in terms of $CO_2$ emissions. On the other hand, emissions from small micro-turbines, small ICE, and small gas turbines are still higher than from the average California grid, even with the use of combined heating and power. In general, high-temperature fuel cells and hybrid gas turbine/fuel cell systems are the technologies that minimize the most $CO_2$ emissions.

It is interesting to note that preferred DG technologies based upon criteria pollutant emissions differ in some cases from preferred technologies based upon $CO_2$ emissions. On the one hand, high-temperature fuel cells and GT-FC hybrid systems have both low criteria pollutant emissions and $CO_2$ emissions, and hence, are good candidates to reduce greenhouse gases and pollutant emissions from electricity generation. On the other hand, there are technologies, such as natural gas ICE, that have $CO_2$ emissions that are competitive with California grid emissions, but they have high criteria pollutant emissions. Another example is the case of gas turbines, which typically have lower pollutant emissions than ICE, but emit $CO_2$ at a higher rate than the average California grid emissions levels unless CHP is used to recover the waste heat.

**Table 89. Potential relative heat rate of DG technologies assuming CHP utilization $f_{CHP}$ = 60% and a heat rate utilization $f_{HR}$ = 50%, and net $CO_2$ emissions from DG technologies after subtracting avoided boiler $CO_2$ emissions**

| | Relative Heat Rate ($kWh_{HR}/kWh_e$) | | | | | |
|---|---|---|---|---|---|---|
| **Size** | **LTFC** | **HTFC** | **MTG** | **NGIC** | **TURB** | **HYBR** |
| <50 kW | 0.41 | 0.23 | 0.55 | 0.48 | | 0.06 |
| 50–250 kW | 0.41 | 0.23 | 0.51 | 0.48 | | 0.06 |
| 250 kW–1 MW | | 0.23 | 0.47 | 0.36 | 0.76 | 0.06 |
| 1–5 MW | | 0.23 | | 0.33 | 0.61 | 0.06 |
| 5–20 MW | | 0.23 | | 0.30 | 0.48 | 0.06 |
| 20–50 MW | | 0.23 | | | 0.35 | 0.06 |
| | **Net Emission Factor (lb/MWh)** | | | | | |
| **Size** | **LTFC** | **HTFC** | **MTG** | **NGIC** | **TURB** | **HYBR** |
| <50 kW | 945 | 744 | 1107 | 1032 | | 551 |
| 50–250 kW | 945 | 744 | 1061 | 1032 | | 551 |
| 250 kW–1 MW | | 744 | 1019 | 892 | 1351 | 551 |
| 1–5 MW | | 742 | | 855 | 1177 | 551 |
| 5–20 MW | | 742 | | 821 | 1032 | 551 |
| 20–50 MW | | 742 | | | 883 | 551 |

New information on DG performance and $CO_2$ emissions benefits is available from the California Public Utilities Commission (CPUC) *Self-Generation Incentive Program Sixth Year Impact Evaluation Report* (CPUC, 2007). This report presents metered data and estimates of heat recovery for some DG systems, including fuel cells, internal combustion engines, and micro-turbine generators. Efficiencies are evaluated under two regulatory frameworks: (1) PUC 216.6b, which requires that that the sum of the electric generation and half of the heat recovery of the system exceeds 42.5% of the energy entering the system as fuel, and (2) AB 1685, which requires that the total efficiency exceeds 60%. Data reported in the sixth year impact report of the Self-Generation Incentive Program (SGIP) suggest that only fuel cells installations can meet the two requirements, operating at 55% and 70% efficiencies, as calculated under PUC 216.6b and AB 1685 criteria, respectively. Data on internal combustion engines show that the majority

of their installations could not meet the criteria, operating at an average 39% PUC 216.6b efficiency and 50% AB 1685 efficiency. Finally, micro-turbine generators showed poor overall performance with efficiencies of 28% and 37%, respectively.

Table 90 shows the overall efficiencies for the units considered in this study calculated under PUC 216.6b and AB 1685 criteria (shown in Equation 25 and Equation 26). As in realistic scenarios, the values presented in Table 90 assume a CHP utilization factor of 50% and heat recovery factor of 60%.

$$\eta_{\text{PUC216.6b},\,i} = \eta_{elec\,i} \cdot \left(1 + 0.5 \cdot \left(\frac{Q_{HR}}{Q_{elec}}\right)_i\right) \tag{25}$$

$$\eta_{\text{AB1685},\,i} = \eta_{elec\,i} \cdot \left(1 + \left(\frac{Q_{HR}}{Q_{elec}}\right)_i\right) \tag{26}$$

With respect to PUC 216.6b requirements, Table 90 shows that only fuel cells and fuel cells-gas turbine hybrid systems can fully meet the minimum efficiency requirements. In addition, natural gas ICE larger than 250 kW would meet the minimum requirements according to calculations, even though current metered data shows otherwise. Finally, calculated efficiencies for micro-turbine generators would not meet the requirements by PUC 216.6b, even though they show significantly higher values than the overall 29% efficiencies reported by the California Public Utilities Commission.

With respect to AB 1685, only hybrid systems show overall efficiencies that exceed 60%. High-temperature fuel cells present 59% efficiencies, only one percentile point below the AB 1685 requirements. The rest of DG technologies present overall efficiencies that are far below the minimum requirements. These low values of efficiency are due in part to the values assumed for overall heat recovery and CHP utilization factors, which are $f_{HR}$=60% and $f_{CHP}$=50%, respectively. Assuming that the maximum heat that can be recovered stays at 60%, increasing $f_{CHP}$ to 55% would enable high-temperature fuel cells to comply with AB 1685 requirements. Increasing $f_{CHP}$ further to 87% and 91% would enable ICE and MTGs, respectively, to comply with the minimum requirements.

**Table 90. Overall efficiencies of DG units calculated under two regulatory frameworks: PUC 216.6b and AB 1685**

| | Efficiencies % - PUC 216.6b criteria (>42.5%) | | | | | |
|---|---|---|---|---|---|---|
| **Size** | **LTFC** | **HTFC** | **MTG** | **NGIC** | **TURB** | **HYBR** |
| <50 kW | 43.4 | 53.5 | 38.3 | 40.4 | | 72.3 |
| 50–250 kW | 43.4 | 53.5 | 39.5 | 40.4 | | 72.3 |
| 250 kW–1 MW | | 53.5 | 40.8 | 45.5 | 33.2 | 72.3 |
| 1–5 MW | | 53.6 | | 47.2 | 36.6 | 72.3 |
| 5–20 MW | | 53.6 | | 48.9 | 40.4 | 72.3 |
| 20–50 MW | | 53.6 | | | 45.9 | 72.3 |
| | **Efficiencies % - AB 1685 criteria (>60%)** | | | | | |
| **Size** | **LTFC** | **HTFC** | **MTG** | **NGIC** | **TURB** | **HYBR** |
| <50 kW | 50.7 | 59.0 | 46.5 | 48.3 | | 74.5 |
| 50–250 kW | 50.7 | 59.0 | 47.6 | 48.3 | | 74.5 |
| 250 kW–1 MW | | 59.0 | 48.6 | 52.5 | 42.3 | 74.5 |
| 1–5 MW | | 59.1 | | 53.9 | 45.1 | 74.5 |
| 5–20 MW | | 59.1 | | 55.3 | 48.3 | 74.5 |
| 20–50 MW | | 59.1 | | | 52.8 | 74.5 |

Overall, the efficiency parameters assumed for DG units in this study agree qualitatively well with the efficiencies reported by the CPUC (CPUC 2007). Compared to CPUC reported values, efficiency estimates in this report for fuel cells are slightly lower. For ICE, efficiency values are slightly higher than CPUC values. Finally, efficiency values assumed for MTG, based on literature data, are significantly higher than the CPUC-reported values. Even though there is a large discrepancy in terms of MTG performance, penetration of MTG in realistic scenarios is low. Consequently, comparison of $CO_2$ emissions displacement by DG in this study should not be too sensitive to MTG efficiencies.

It is interesting to note that the potential $CO_2$ emissions displacement due to CHP also agree qualitatively well with the values presented in the CPUC's sixth year impact report. Table 89 shows that fuel cells with CHP emit at 742–744 lb $CO_2$/MWh, which is significantly lower than the overall grid emissions of 1014 lb $CO_2$/MWh, resulting in a net decrease in $CO_2$ emissions. Net emissions from ICE with CHP are in the range of 821–1032 lb $CO_2$/MWh, which could result in a net increase or decrease in $CO_2$ emissions, depending on the size of the unit. Finally, net emissions from MTG with CHP are in the range of 1019–1107 lb $CO_2$/MWh, which is over the overall grid emissions factor, resulting in a net increase in $CO_2$ emissions with respect to the grid.

Similarly, the CPUC report indicates that fossil-fuel fuel cells reduced $CO_2$ emissions, installations of MTG increased $CO_2$ emissions, and ICE installations had a neutral effect with respect to the California grid. The CPUC report, however, shows quantitatively worse efficiency and emissions than the values presented here for ICE and MTG. Nonetheless, the CPUC report

is based on metered data from 2005–2006; whereas this project presents efficiency estimates for the year 2030, which should be better than the current DG performance.

Section 5.0 of this report presents the results of DG technology mix estimated for the South Coast and San Joaquin Valley Air Basins. Estimates based on DG market studies suggest that more than 95% of the DG installed capacity will be supplied by gas turbines and internal combustion engines, and only 2% will be supplied by high-temperature fuel cells. Assuming additional incentives for R&D in DG technologies, the penetration of high-temperature fuel cells could increase to up to 15% of the total DG installed capacity, lowering the contribution of gas turbines and internal combustion engines to the total installed capacity. Nevertheless, the DG market studies used to estimate DG penetration were conducted prior the approval of AB32. Including regulatory pressure and incentives as a result of AB32 could increase the penetration of fuel cells and hybrid technologies and reduce the penetration of gas turbines and internal combustion engines.

### 6.2.1. Contribution of DG Scenarios to $CO_2$ Emissions

The impacts of DG presented in Section 5.0 correspond to the effects on criteria pollutant concentrations. Similarly, impacts of DG on $CO_2$ emissions can be estimated using the resulting DG mix and the emission factors presented above. Realistic implementation suggests that DG could meet between 7% and 18% of the total increased peak demand between 2007 and 2030. In addition, DG has the capability to displace boiler emissions by using CHP units. Gas turbines and ICE are expected to be the predominant DG technologies. High-temperature fuel cells could contribute to 2%–15% of the total DG capacity and increasing the percentage of high-temperature fuel cells reduces the average $CO_2$ emissions from distributed generation technologies.

The DG technology distribution in scenarios SoCAB-R1 and SoCAB-R5 for the SoCAB, and in scenarios SJV-R1 and SJV-R4 for the SJV, are presented in Table 91 and Table 92, respectively. Scenario SoCAB-R1 is analogous to scenario SJV-R1, and the differences in the DG mix are due to the difference in land-use distribution between the SoCAB and the San Joaquin Valley. Similarly, scenario SoCAB-R5 is analogous to scenario SJV-R4. These two scenarios assume a higher penetration of fuel cells than in scenarios SoCAB-R1 and SJV-R1, due to environmental forcing to reduce $CO_2$ emissions. Scenarios SoCAB-R1, SJV-R1, SoCAB-R5 and SJV-R4 provide the bounds for $CO_2$ emissions amongst realistic DG scenarios. Namely, scenarios SoCAB-R1 and SJV-R1 correspond to the realistic scenarios with highest $CO_2$ emissions per MWh produced; whereas scenarios SoCAB-R5 and SJV-R4 correspond to the realistic scenarios with the lowest emissions.

Table 93 shows the total direct emissions of $CO_2$ from DG, the net $CO_2$ emissions from DG accounting for CHP emissions displacements, and the total emission reductions with respect to average California grid emissions. Direct $CO_2$ emissions from DG are higher than 1014 lb/MWh for all realistic scenarios, due to high penetration of gas turbines. However, if CHP emissions displacements are accounted for, net emissions from DG are less than 920 lb/MWh, approximately 9% lower than average California grid emissions. Average DG emissions in realistic scenarios in the SJV are slightly lower than in the SoCAB because the DG technology

mix estimated for the SJV includes a higher percentage of natural gas ICE and a lower percentage of gas turbines, compared to the realistic scenarios for the South Coast Air Basin. As mentioned above, ICE could be preferred over gas turbines if only $CO_2$ emissions are considered. However, criteria pollutant emissions from ICE are significantly higher than from gas turbines, which could offset the benefits of reducing $CO_2$ emissions. Results show that implementation of DG suggested by scenarios SoCAB-R1 and SJV-R1 could lead to reductions in $CO_2$ emissions from electricity generation of 9.3% in the SoCAB and 10.2% in the SJV, with respect to the same electricity produced by the average California grid. High deployment of high-temperature fuel cells suggested by scenarios SoCAB-R5 in the SoCAB and SJV-R4 in the SJV could lead to decreases in $CO_2$ of 11.2% in the SoCAB and 12.0% in the San Joaquin Valley.

**Table 91. Overall DG mix for realistic scenarios SoCAB-R1 and SoCAB-R5 in the South Coast Air Basin of California**

| | DG mix (%) – Scenario SoCAB-R1 | | | | | |
|---|---|---|---|---|---|---|
| **Size** | **LTFC** | **HTFC** | **MTGS** | **NGIC** | **TURB** | **HYBR** |
| <50 kW | 0.3 | 0.0 | 0.0 | 0.6 | | 0.0 |
| 50–250 kW | 0.1 | 0.3 | 0.4 | 3.4 | | 0.0 |
| 250 kW–1 MW | | 0.3 | 0.0 | 3.6 | 0.1 | 0.0 |
| 1–5 MW | | 0.6 | | 16.6 | 4.0 | 0.1 |
| 5–20 MW | | 0.8 | | 13.3 | 21.8 | 0.0 |
| 20–50 MW | | 0.2 | | | 33.4 | 0.1 |
| | **DG mix (%) – Scenario SoCAB-R5** | | | | | |
| **Size** | **LTFC** | **HTFC** | **MTGS** | **NGIC** | **TURB** | **HYBR** |
| <50 kW | 0.5 | 0.2 | 0.0 | 0.3 | | 0.0 |
| 50–250 kW | 0.1 | 1.5 | 0.3 | 2.2 | | 0.0 |
| 250 kW–1 MW | | 1.8 | 0.0 | 2.1 | 0.1 | 0.0 |
| 1–5 MW | | 4.0 | | 12.9 | 4.3 | |
| 5–20 MW | | 7.0 | | 8.9 | 20.0 | |
| 20–50 MW | | 0.8 | | | 32.9 | |

**Table 92. Overall DG mix for realistic scenarios SJV-R1 and SJV-R4 in the San Joaquin Valley**

| | DG mix (%) – Scenario SJV-R1 | | | | | |
|---|---|---|---|---|---|---|
| **Size** | **LTFC** | **HTFC** | **MTGS** | **NGIC** | **TURB** | **HYBR** |
| <50 kW | 0.3 | 0.0 | 0.0 | 0.7 | | |
| 50–250 kW | 0.1 | 0.3 | 0.4 | 4.3 | | |
| 250 kW–1 MW | | 0.3 | 0.0 | 4.5 | 0.1 | |
| 1–5 MW | | 0.6 | | 20.9 | 3.3 | |
| 5–20 MW | | 0.8 | | 16.8 | 18.3 | |
| 20–50 MW | | 0.2 | | | 28.1 | |
| | **DG mix (%) – Scenario SJV-R4** | | | | | |
| **Size** | **LTFC** | **HTFC** | **MTGS** | **NGIC** | **TURB** | **HYBR** |
| <50 kW | 0.5 | 0.2 | 0.0 | 0.3 | | |
| 50–250 kW | 0.1 | 1.6 | 0.3 | 2.8 | | |
| 250 kW–1 MW | | 1.9 | 0.0 | 2.7 | 0.1 | |
| 1–5 MW | | 4.1 | | 16.7 | 3.7 | |
| 5–20 MW | | 7.1 | | 11.5 | 17.3 | |
| 20–50 MW | | 0.8 | | | 28.4 | |

**Table 93. $CO_2$ emissions from DG and reductions in $CO_2$ emissions with respect to average California grid emissions in realistic DG scenarios for the South Coast Air Basin and the San Joaquin Valley of California in 2023**

| | **Total Electricity (MWh/day)** | **DG Direct Emissions (lb/MWh)** | **DG-CHP Net Emissions (lb/MWh)** | **DG-CHP Total Net Emissions (tons/day)** | **Emission Reductions with Respect to California Grid Emissions** | |
|---|---|---|---|---|---|---|
| | | | | | **(tons/day)** | **(%)** |
| *SoCAB* | | | | | | |
| SoCAB-R1 | 19528 | 1090 | 920 | 8979 | 922 | 9.3 |
| SoCAB-R5 | 34548 | 1065 | 900 | 15549 | 1967 | 11.2 |
| *SJV* | | | | | | |
| SJV-R1 | 4074 | 1079 | 910 | 1854 | 212 | 10.2 |
| SJV-R4 | 7207 | 1054 | 892 | 3216 | 439 | 12.0 |

# 7.0 Model Sensitivity

Air quality models (AQMs) are instrumental to assess the potential air quality impacts of DG within urban basins. Only through the use of a detailed AQM one can assess the effects of increased DG emissions on the complex, non-linear, and concurrent processes of transport, mixing, and heterogeneous and homogeneous chemistry that lead to criteria pollutant concentrations of interest. However, numerical predictions from mathematical models are subjected to various sources of uncertainty. For instance, emissions inventories usually represent the largest uncertainties associated with output concentrations in three-dimensional urban/regional models (Griffin et al. 2002a). A quantitative analysis of AQM responses to different input parameters is a prerequisite to characterize these sources of uncertainty. Additionally, such analysis also identifies those input parameters and simulation conditions responsible for most of the model output variation.

This section includes sensitivity analyses of model predictions for the SoCAB and for the SJV. The analyses are designed to reflect the uncertainties that DG implementation scenarios introduce in air quality simulations. During the preceding study by Samuelsen et al. (2005), a detailed sensitivity analysis was conducted for the air quality model for the SoCAB. The analyses presented in this section complement the findings acquired in the preceding study.

## 7.1. Air Quality Model Sensitivity for the SOCAB

### *7.1.1. Previous Sensitivity and Uncertainty Analyses*

A preceding study by Samuelsen et al. (2005) investigated the uncertainty and sensitivity of ozone and $PM_{2.5}$ aerosol to variations in selected input parameters using a Monte Carlo methodology. The selection of input parameters was based in their potential to affect the concentrations predicted by the model and also to reflect changes in emissions due to DG implementation in the South Coast Air Basin. Numerical simulations were performed with the CIT three-dimensional air quality model. Multiple model evaluations were completed, and statistical methods applied to identify those parameters with the largest effect on both the predicted concentrations of selected species and the uncertainty associated with their prediction.

The study provided a measure of the basinwide and time-dependent model error bounds for ozone mixing ratios and $PM_{2.5}$ aerosol concentrations. Detailed temporal evolution of Latin hypercube sampled statistics derived from the multiple AQM predictions were evaluated at selected SoCAB sites. Results indicated that normal probability density distributions best describe the variance of predicted concentrations. Furthermore, comparisons between basinwide distributions of base case and calculated mean values lead to the conclusion that normal probability density distributions are also adequate to characterize the uncertainty of modeled spatial maxima throughout the basin (not only for a limited number of sites). Domain-wide error bounds for species considered in the study were consistent with the normal distributions. The largest relative error for ozone is approximately 42% (76 ± 32 ppb); whereas maximum concentrations show an error of approximately 17% (221 ± 37 ppb). For $PM_{2.5}$, the

largest error is ~17% (48 ± 8 μg $m^{-3}$), but the largest domain-wide concentration (108 ± 11 μg $m^{-3}$) has a relative error of 10%.

The study also aimed to separate the potential air quality impacts of DG from the model uncertainty to various input parameters. Results showed that changes no greater than 70% to 80% in nominal values of input variables results in 18% to 40% variability of ozone mixing and $PM_{2.5}$ aerosol concentrations. Moreover, the sensitivity analyses performed in this work demonstrated that the variation in side boundary conditions imposed on VOC and $NO_X$ emissions are the major contributors to uncertainty and sensitivity of ozone predictions in most regions throughout the South Coast Air Basin. Ozone boundary conditions have a marginal contribution to uncertainty in most locations, except for sites located near the boundaries of the computational domain. Results showed that an increase in $NO_X$ emissions leads to reductions in ozone mixing ratios. In contrast, increasing the values of VOC-side boundary conditions results in higher ozone mixing ratios. This is due to ozone formation being VOC-limited over most of the South Coast Air Basin. Sensitivity analyses also showed that $PM_{2.5}$ aerosol is sensitive to changes in $NH_3$ and $NO_X$ emissions. Furthermore, increasing these emissions resulted in higher $PM_{2.5}$ aerosol concentrations throughout the basin.

### *7.1.2. Model Sensitivity to Baseline Emissions*

Distributed power generation introduces new sources of emissions in the air basin of interest, adding to the existing sources in that particular region. Consequently, the relative impacts of DG depend strongly on the baseline emissions to which emissions from DG are added. Baseline emissions provide the overall dynamics of the chemistry involved in a particular area. For instance, in areas with high $NO_X$ emissions, such as Los Angeles, moderate decreases in $NO_X$ emissions lead to increases in ozone concentration and moderate increases favor ozone termination reactions that reduce ozone concentrations. This phenomenon has been observed in Los Angeles during weekday-weekend transition, which is referred to as the "weekend effect." Weekday $NO_X$ emissions are higher than during weekends, but peak ozone concentrations over the weekends are typically higher than on weekdays (Qin et al. 2004; Blanchard and Tanenbaum 2003). On the other hand, in areas with low $NO_X$ emissions, such as the San Joaquin Valley, reductions in $NO_X$ emissions cause a decrease in ozone concentration (Vijayaraghavan et al. 2006). These two opposite behaviors are determined by the VOC/$NO_X$ ratio. Under high VOC-to-$NO_X$ ratios—termed as a *$NO_X$-limited regime*—ozone production increases by adding nitrogen oxides. Conversely, under low VOC-to-$NO_X$ ratios—termed as *VOC-limited*—ozone production is disfavored by increasing $NO_X$ emissions (Finlayson-Pitts and Pitts 2000).

The baseline emissions for the years 2023 and 2030 used in this study are based on the emissions presented in the 2007 Air Quality Management Plan developed by the South Coast Air Quality Management District (SCAQMD 2007). Currently, the SoCAB is not in compliance with ozone and particulate matter air quality standards, and state agencies are required to develop emission control strategies to help reduce criteria pollutant concentrations. These air pollution control strategies are included in future emission inventories, which are then used in air quality models to demonstrate that such strategies indeed achieve the desired reductions in pollutant concentrations. Generally, the emissions inventory that leads to compliance with air quality

standards after the required emission controls are implemented is often referred as the *attainment* emissions inventory. The attainment inventory has been modified continuously in successive air quality management plans. The inventory proposed in the 2007 AQMP includes detailed accountable emission reductions due to specific control measures. In addition, the inventory includes across-the-board reductions by 2023 that are needed to lower ozone levels, although developers still do not know how these additional reductions will be accomplished.

The total basinwide emissions in the 2007 AQMP attainment scenario include substantial reductions in emissions with respect to the proposed attainment scenario developed in the 2003 AQMP, which was designed to demonstrate compliance with ozone standards by the year 2010. In particular, the 2007 AQMP attainment inventory proposes a 55% reduction in $NO_X$ emissions with respect to the 2003 AQMP inventory. Table 94 presents the total basinwide emissions in the SoCAB proposed in the attainment inventories for the 2003 AQMP and the 2007 AQMP.

**Table 94. Estimated daily basinwide emissions for years 2010 (SoCAB-B1) and 2023 (SoCAB-B2) in the South Coast Air Basin of California**

| Species | Baseline 2010 based on 2003 AQMP (tons/day) | Baseline 2023 based on 2007 AQMP (tons/day) |
|---|---|---|
| | Scenario SoCAB-B1 | Scenario SoCAB-B2 |
| VOC | 453 | 420 |
| $NO_X$ | 251 | 114 |
| CO | 2064 | 1966 |
| $SO_X$ | 33 | 19 |
| $PM_{2.5}$ | 140 | 88 |

This section explores the air quality impacts of a selected number of DG scenarios using the two baseline inventories mentioned above. The goal is to understand how the same perturbation in emissions—due to DG implementation scenarios—affects the resulting air quality of two different baseline emissions inventories. First, simulation results of the two baseline emissions inventories are analyzed and compared. Secondly, three DG scenarios are simulated using the 2003 AQMP attainment inventory. Those scenarios are then compared to the same scenarios developed using the 2007 AQMP attainment inventory, which are presented in Section 5.1.

### *Baseline Air Quality as a Function of Baseline Emissions*

Simulations using the baseline emission inventories based on the 2003 AQMP and 2007 AQMP attainment emissions inventories were performed using the meteorological conditions of the August 27–29, 1987, episode. Table 95, Figure 82, and Figure 83 report the maximum concentrations of some criteria pollutants for both cases. Results show that ozone and $PM_{2.5}$ concentrations peak at locations downwind from Los Angeles, where the strongest focus of emissions is located. On the other hand, CO concentrations peak in Central Los Angeles. Ozone, $NO_2$, and $PM_{2.5}$ peaks occur downwind from main emissions because they are secondary

pollutants; whereas CO is a primary pollutant and its concentrations depend mainly on direct emissions.

Although baseline simulations for the 2003 and 2007 AQMP emissions use emission inventories that have been developed to demonstrate attainment of ozone and $PM_{2.5}$ air quality standards, ozone and $PM_{2.5}$ concentrations exceed the established air quality standards. This is because the CACM chemical mechanism predicts higher oxidative capacity that leads to higher concentrations of $O_3$ than the predicted by other chemical mechanisms, such as SAPRC-99, which has been used in the AQMP (Jimenez et al. 2003).

**Table 95. Maximum concentration of pollutants on August 29 in baseline cases for the 2003 and the 2007 AQMP attainment inventories**

| Pollutant | 2003 AQMP attainment | 2007 AQMP attainment |
|---|---|---|
| 1-hour $O_3$ | 181 ppb | 152 ppb |
| 8-hour $O_3$ | 151 ppb | 129 ppb |
| 1-hour CO | 2.5 ppm | 1.7 ppm |
| 1-hour $NO_2$ | 93 ppb | 77 ppb |
| 24-hour $PM_{2.5}$ | 94 μg/m$^3$ | 60 μg/m$^3$ |

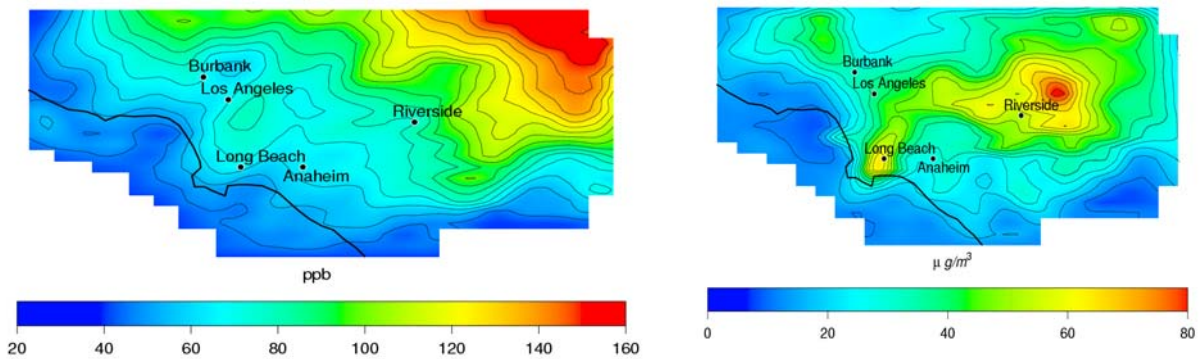


**Figure 82. Air pollutant concentrations in the South Coast Air Basin of California using the 2003 AQMP attainment inventory: (a) peak ozone concentrations, and (b) 24-hour $PM_{2.5}$ concentrations**

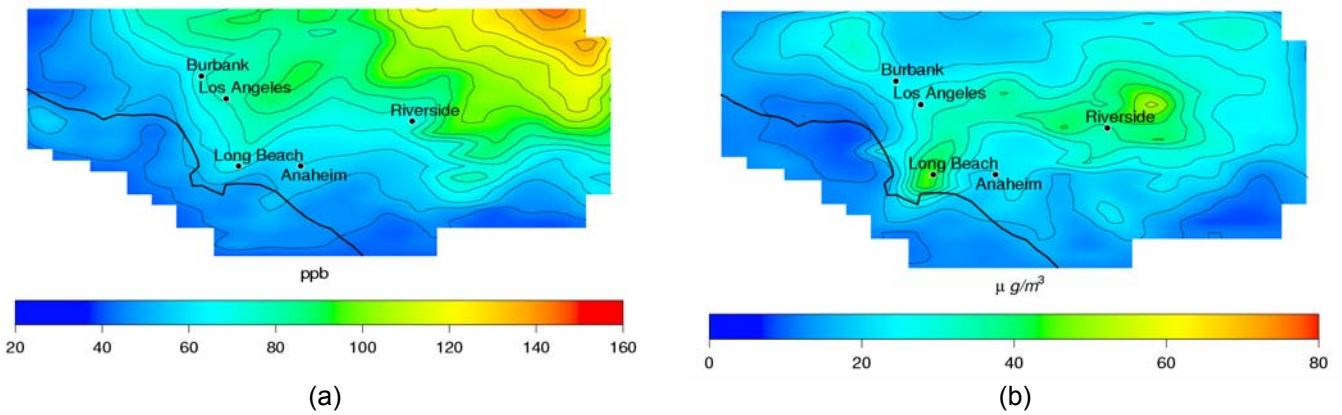


**Figure 83. Air pollutant concentrations in the South Coast Air Basin of California using the 2007 AQMP attainment inventory: (a) peak ozone concentrations, and (b) 24-hour $PM_{2.5}$ concentrations**

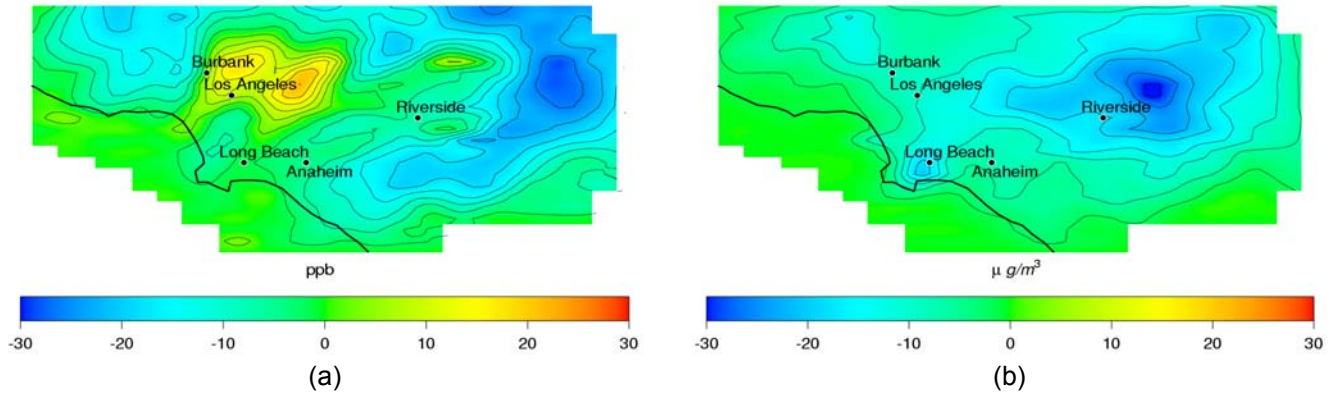


**Figure 84. Differences in air pollutant concentrations in the South Coast Air Basin of California between the 2007 and the 2003 AQMP attainment cases (values represent the 2007 case minus the 2003 case): (a) peak ozone concentrations, and (b) 24-hour $PM_{2.5}$ concentrations**

Figure 82 presents the peak ozone concentration and the 24-hour average concentration of $PM_{2.5}$ resulting from the simulation of the 2003 AQMP attainment inventory case. Figure 83 presents concentrations of the same pollutants, using the 2007 AQMP attainment inventory. Finally, Figure 84 shows the differences in peak ozone and 24-hour average $PM_{2.5}$ between the 2003 AQMP and 2007 AQMP cases.

Pollutant concentrations in the 2007 AQMP case are significantly lower than in the 2003 AQMP case. Peak ozone concentration decreases by 29 ppb, which represents a 16% decrease. This reduction is mainly due to the substantial reduction in $NO_X$ emissions from 251 tons/day in the 2003 AQMP inventory to 114 tons/day in the 2007 AQMP inventory. Although reducing $NO_X$ emissions leads to an overall decrease in the ozone peak in the basin, peak ozone concentrations near Los Angeles increases by 20 ppb, due to a VOC-limited regime present in that area. The overall maximum 24-hour $PM_{2.5}$ concentration in the basin, which occurs in the eastern part of the domain, declines by 34 $\mu g/m^3$ (~36% decrease). Additionally, particle concentrations near the port of Long Beach decrease by up to 20 $\mu g/m^3$. Decreases in $PM_{2.5}$ around Riverside are mainly

due to the reduction in nitrate particles resulting from the substantial decrease in $NO_X$ emissions (see Figure 85a).

On the other hand, decreases at the port are closely related to the reductions in $SO_X$ emissions, which reduce the concentration of sulfate aerosols (see Figure 85b). To a lesser extent, reductions in direct emissions of particles, comprised mainly by organic carbon and unresolved inorganic particles, contribute to the overall reduction in $PM_{2.5}$ concentrations (see Figure 85c and Figure 85d). In conclusion, maximum reductions in ozone and $PM_{2.5}$ concentrations from the 2003 AQMP case to the 2007 case are due to the important reductions in $NO_X$ emissions. Reductions in $SO_X$ and PM emissions contribute secondarily to the reduction in $PM_{2.5}$ concentrations.

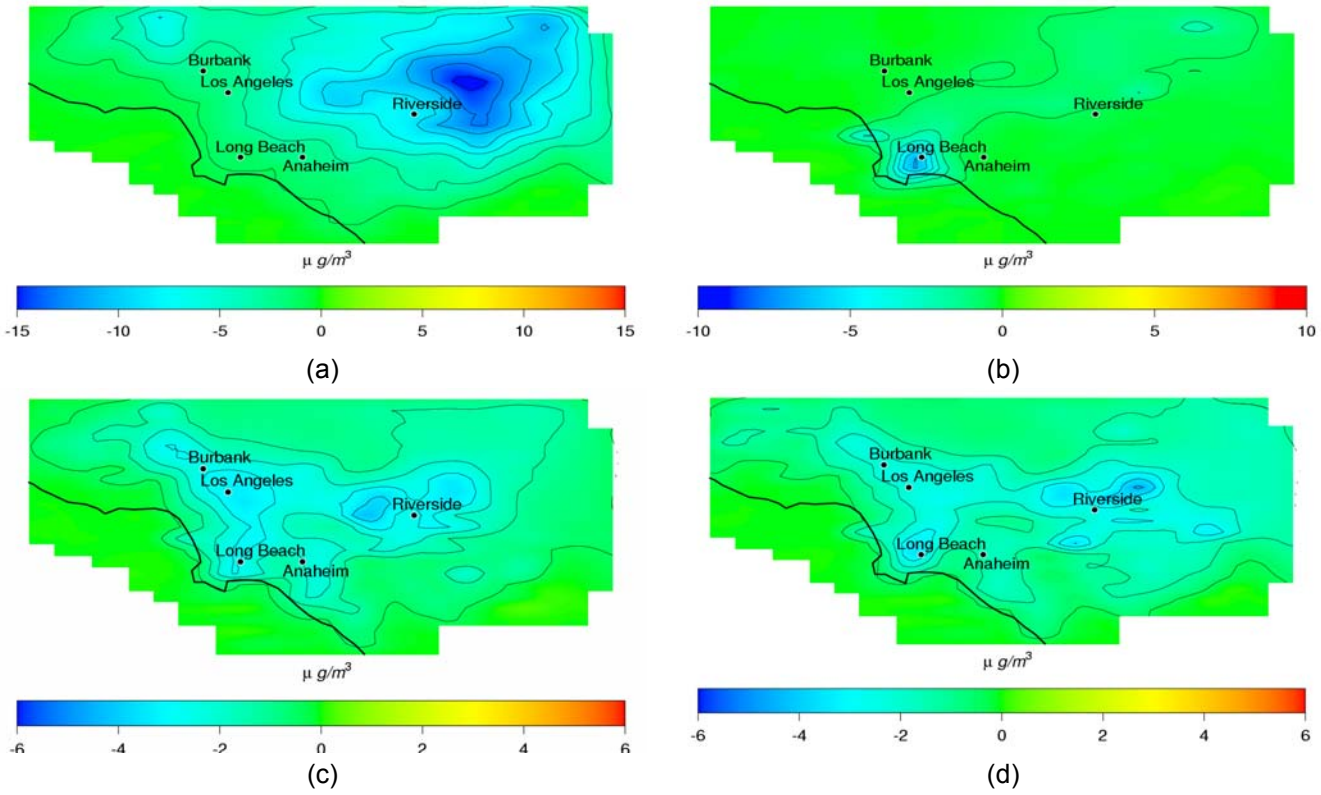


**Figure 85. Differences in 24-hour average $PM_{2.5}$ concentrations in the South Coast Air Basin of California between the 2007 and the 2003 AQMP attainment cases (values represent the 2007 case minus the 2003 case): (a) nitrate aerosol, NO3-; (b) sulfate aerosol, SO42-; (c) organic carbon; and (d) unresolved inorganic aerosol**

### *Air Quality Impacts of DG as a Function of Baseline Emissions*

As shown in the previous section, baseline air quality changes significantly with changes in the baseline emissions. These important changes affect also how small perturbations in emissions due to DG implementation influence air pollutant concentrations. Considering a particular DG scenario, its relative impact on 2003 AQMP baseline emissions will be smaller than the impact on 2007 AQMP emissions, just because the 2003 AQMP inventory includes higher emissions than the 2003 AQMP inventory. In particular, relative impacts of DG on $NO_X$ emissions vary

significantly because baseline $NO_X$ emissions are reduced by 55% from the 2003 AQMP to the 2007 AQMP. Table 96 presents the emissions from three different scenarios: realistic scenario SoCAB-R3 and spanning scenarios EHP and BACT. The emissions are expressed in absolute terms (in tons/day) and in relative terms (as a percentage of total basinwide emissions in the 2003 AQMP and the 2007 AQMP inventories).

The biggest changes in baseline emissions affect $NO_X$, in addition to $SO_X$ and particulate matter. As emissions of $NO_X$ decrease by more than half, the relative impacts in $NO_X$ emissions due to DG (namely, total emissions from DG divided by total basinwide emissions from all sources) augment by more than twice. For instance, in the realistic scenario SoCAB-R3, $NO_X$ emissions are reduced by 0.12 tons per day due to CHP utilization. This decrement corresponds to a decrease of 0.05% with respect to 2003 AQMP emissions and to a decrease of 0.11% with respect to 2007 AQMP emissions. On the other end, the spanning scenario BACT introduces 9.9 tons/day of $NO_X$, which corresponds to an increase of 3.94% and 8.68% with respect to the 2003 and 2007 AQMP emissions, respectively. Similarly, relative impacts of $SO_X$ and $PM_{2.5}$ emissions from DG on total 2007 AQMP emissions are nearly 40% bigger than the relative impacts of DG on the 2003 AQMP emissions, as the baseline 2007 AQMP emissions of $SO_X$ and $PM_{2.5}$ are approximately 40% lower than the emissions in the 2003 AQMP inventory.

**Table 96. Baseline emissions and emissions from three different DG scenarios in absolute terms (in tons/day) and relative terms (with respect to the 2003 AQMP emissions and the 2007 AQMP emissions)**

| | CO | $NO_X$ | VOC | $SO_X$ | $PM_{2.5}$ |
|---|---|---|---|---|---|
| *Baseline basinwide emissions (tons/day)* | | | | | |
| 2003 AQMP | 2064 | 251 | 453 | 33 | 140 |
| 2007 AQMP | 1966 | 114 | 420 | 19 | 88 |
| *Absolute basinwide emissions from DG (tons/day)* | | | | | |
| SoCAB-R3 | 0.74 | -0.12 | 0.06 | 0.08 | 0.58 |
| EHP | 4.38 | 2.40 | 0.40 | 0.30 | 2.43 |
| BACT | 39.66 | 9.90 | 4.26 | 0.19 | 1.57 |
| *Relative emissions from DG (%) with respect to 2003 AQMP attainment inventory* | | | | | |
| SoCAB-R3 | 0.04 | -0.05 | 0.01 | 0.24 | 0.41 |
| EHP | 0.21 | 0.96 | 0.09 | 0.91 | 1.74 |
| BACT | 1.92 | 3.94 | 0.94 | 0.58 | 1.12 |
| *Relative emissions from DG (%) with respect to 2007 AQMP attainment inventory* | | | | | |
| SoCAB-R3 | 0.04 | -0.11 | 0.01 | 0.42 | 0.66 |
| EHP | 0.22 | 2.11 | 0.10 | 1.58 | 2.76 |
| BACT | 2.02 | 8.68 | 1.01 | 1.00 | 1.78 |

The impacts of DG on ozone concentrations are generally stronger when the 2007 AQMP emissions are used. Figure 86 presents the impacts on peak ozone concentration of the three DG scenarios described above, using the two baseline emission inventories. In general, impacts of realistic scenarios are small. Using the 2007 AQMP emissions, reduction of $NO_X$ due to DG in scenario SoCAB-R3 leads to a decrease of half ppb in the peak ozone concentration. Impacts of scenario SoCAB-R3 on peak ozone concentration using 2003 AQMP emissions are mixed, leading to small decreases and increases in peak ozone. The addition of $NO_X$ emissions due to spanning scenarios EHP and BACT leads to increases in peak ozone concentrations throughout the domain with 2007 AQMP emissions.

On the other hand, the same increases in $NO_X$ emissions caused by those spanning scenarios using 2003 AQMP lead to a decrease in peak ozone concentrations in a large area of the center of the domain. This denotes that the 2003 AQMP emissions inventory provides a VOC-limited regime in the central part of the South Coast Air Basin. Additionally, these results suggest that the reduction in $NO_X$ emissions from the 2003 to the 2007 AQMP shifts the SoCAB atmospheric dynamics from a VOC-limited regime to a $NO_X$-limited regime. Table 97 shows the maximum increases and decreases on peak ozone concentrations due to the different DG scenarios using 2003 and 2007 AQMP baseline inventories.

As in the case with ozone concentrations, impacts of DG on $PM_{2.5}$ are stronger when the 2007 AQMP emissions are used. Figure 87 and Table 97 present the DG impacts on 24-hour average $PM_{2.5}$ concentrations. Impacts of DG realistic scenarios are small, and small differences are observed between the cases using the 2003 AQMP emissions and the ones using 2007 AQMP emissions. Emissions from DG spanning scenarios produce qualitatively similar impacts on $PM_{2.5}$ concentrations. Namely, increases in $NO_X$, $SO_X$, and PM emissions due to DG lead to increases in $PM_{2.5}$ concentration, regardless of the baseline emissions used. However, impacts of DG using the 2007 AQMP emissions are more widespread than in the cases where 2003 AQMP emissions are used.

In conclusion, 2007 AQMP emissions provide atmospheric conditions that are more sensitive to emission changes than the conditions created by the 2003 AQMP, and impacts of DG are stronger when using 2007 AQMP emissions. In addition, substantial reductions of $NO_X$ emissions adopted in the 2007 AQMP emissions shift the atmospheric chemistry of the SoCAB from VOC-limited[5] conditions to $NO_X$-limited[6] conditions.

[5] Typically, under VOC-limited conditions, an increase in $NO_X$ leads to a decrease in ozone concentrations
[6] Typically, Under $NO_X$-limited conditions, an increase in $NO_X$ leads to an increase in ozone concentrations

**Table 97. Impacts on peak $O_3$ and 24-hour $PM_{2.5}$ of selected DG scenarios, using two different baseline scenarios**

| | Δ peak $O_3$ | | Δ 24-hour $PM_{2.5}$ | |
|---|---|---|---|---|
| | Maximum increase | Maximum decrease | Maximum increase | Maximum decrease |
| | (ppb) | (ppb) | (ppb) | (ppb) |
| *2003 AQMP* | | | | |
| SoCAB-R3 | 0.5 | 0.5 | 1.1 | 0.5 |
| EHP | 1.0 | 1.5 | 1.4 | 0.8 |
| BACT | 2.1 | 3.2 | 1.9 | 0.4 |
| *2007 AQMP* | | | | |
| SoCAB-R3 | 0.7 | 0.9 | 0.9 | 0.6 |
| EHP | 1.2 | 0.7 | 1.4 | 0.6 |
| BACT | 4.6 | 3.6 | 2.6 | 1.0 |

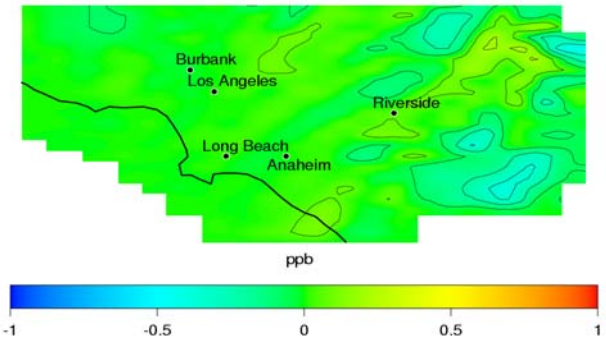


SoCAB-R3 with 2003 AQMP inventory

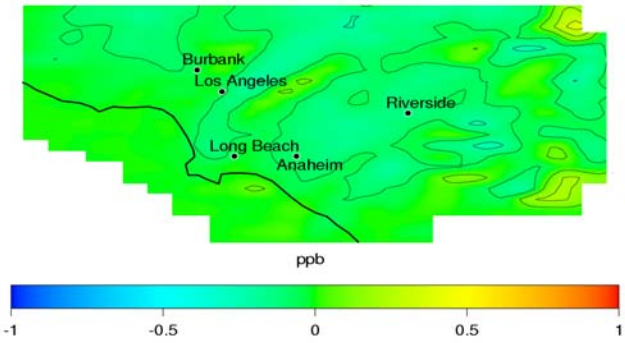


SoCAB-R3 with 2007 AQMP inventory

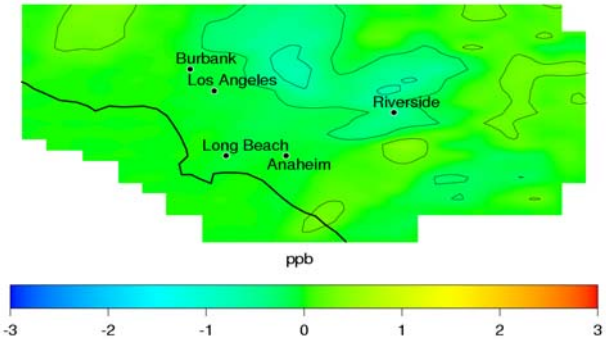


EHP with 2003 AQMP inventory

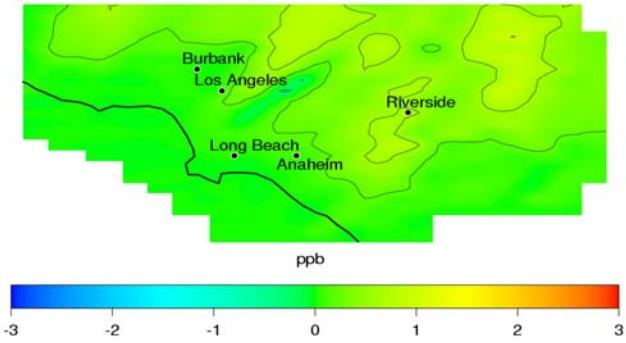


EHP with 2007 AQMP inventory

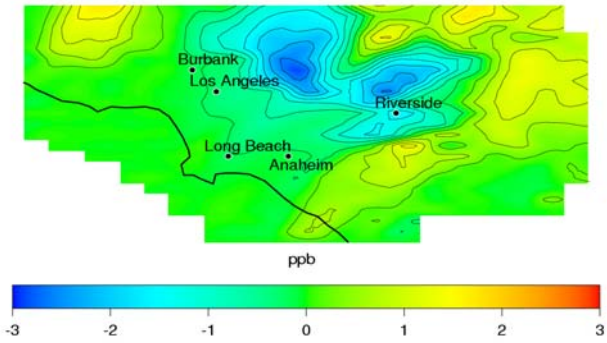


BACT with 2003 AQMP inventory

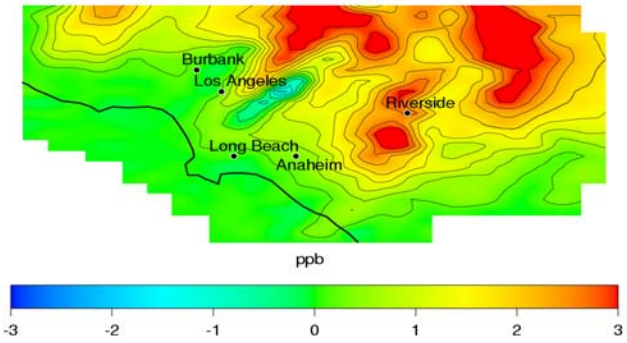


BACT with 2007 AQMP inventory

**Figure 86. Impacts of three different DG scenarios on peak ozone concentrations using the 2003 AQMP attainment inventory (plots on the left column) and the 2007 AQMP attainment inventory (plots on the right column)**

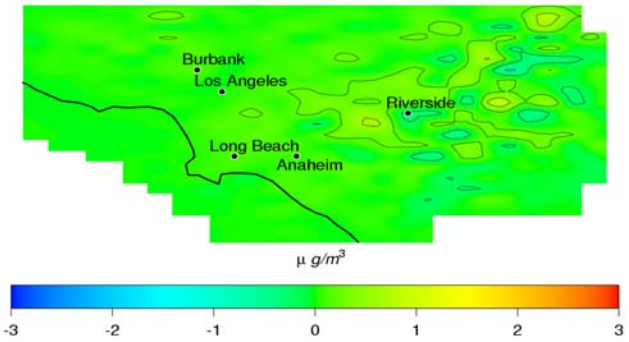


SoCAB-R3 with 2003 AQMP inventory

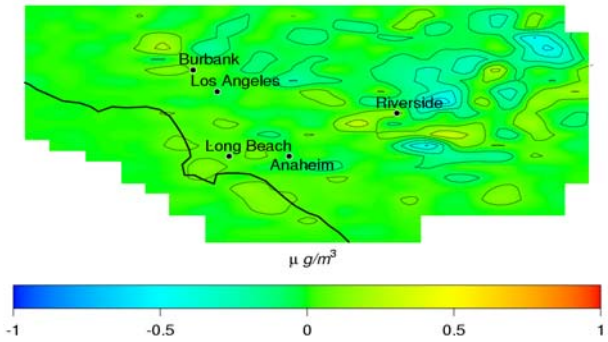


SoCAB-R3 with 2007 AQMP inventory

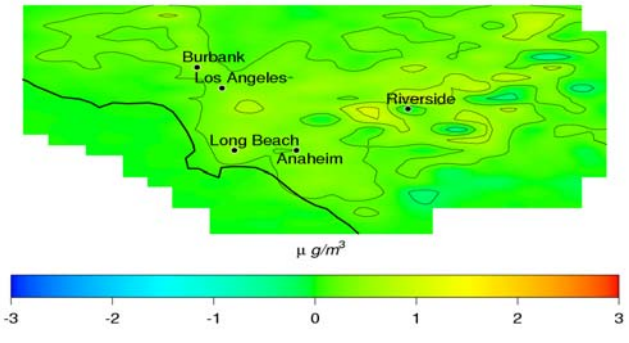


EHP with 2003 AQMP inventory

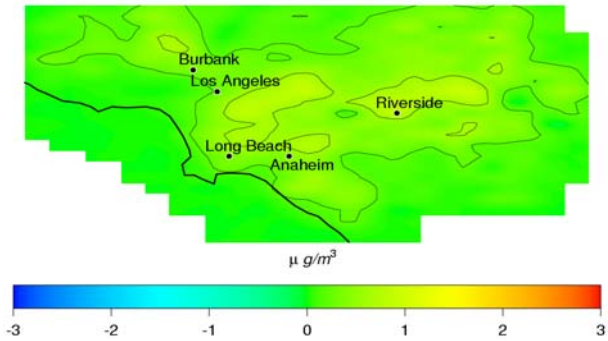


EHP with 2007 AQMP inventory

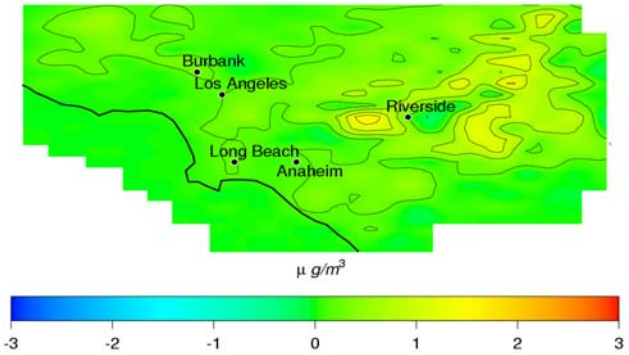


BACT with 2003 AQMP inventory

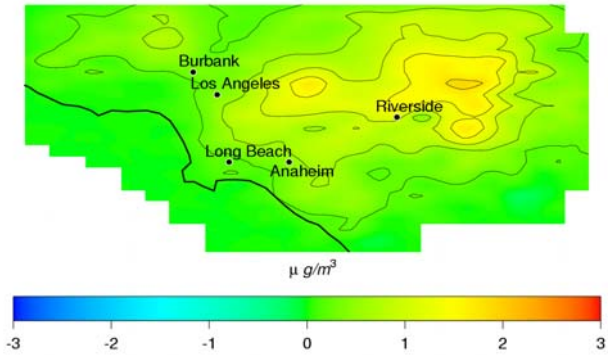


BACT with 2007 AQMP inventory

**Figure 87. Impacts of three different DG scenarios on 24-hour average $PM_{2.5}$ concentrations using the 2003 AQMP attainment inventory (plots on the left column) and the 2007 AQMP attainment inventory (plots on the right column)**

### 7.1.3. Model Sensitivity to Central Generation Versus Distributed Generation

A previous study (Ianucci et al. 2000) determined the total emissions produced by DG deployment for criteria pollutants during different years. Assessment of these emissions was obtained through estimates of DG market penetration, and then compared with those emissions from a case in which only central generation is considered. The conclusion reached by that study showed that no cost-effective DG technology will lower the net emissions of California's current central generation system. Fuel cells show promising benefits for air quality due to their significantly lower emissions with respect to both central and distributed sources, but high installation costs limits fuel cells to a marginal market penetration. Allison and Lents (2002) compared emissions impacts of different DG technologies and fuel types. They concluded that even the lowest-emitting DG technology is marginally competitive with combined cycle power generation. These studies, however, are limited to the evaluation of only increasing the total amount of emissions. Also, Heath et al. (2006) considered the potential for increased human inhalation exposure to air pollutants when power plants are replaced by distributed generation. Yet, Heath et al. (2006) restricted their work to pollutants emitted directly into the atmosphere using a simplified mass transport approach.

Rodriguez et al. (2006) studied the potential air quality impacts of DG in the SoCAB in the year 2010. Rodriguez et al. presented a series of possible DG implementation scenarios and estimated their air quality impacts with respect to a baseline 2010 scenario that included no DG or other additional in-basin generation. That paper assumed that if no DG was installed, electricity would be imported from outside the basin, and as a result, no emissions from central generation would be introduced in the SoCAB.

The present study considers that limitations in the transmission of electricity could require additional in-basin generation. In-basin generation could be met either by DG—as studied by Rodriguez et al.—or by central generation. This work analyzes the air quality impacts of in-basin central generation in the SoCAB in the year 2010 and compares them to the air quality impacts of DG that Rodriguez et al. reported in their previous study.

#### *Emissions*

Baseline emissions for the simulations are based on the emissions inventory developed by the SCAQMD for the 2003 AQMP to demonstrate attainment of the 1-hour ozone standard. This emissions inventory includes current emission controls planned for 2010 and other measures that would reduce baseline emissions to a level at which ozone concentration would not exceed the federal 1-hour air quality standard (120 ppb). Additionally, emissions from distributed or central generation are estimated and added to baseline emissions.

Sample Distributed Generation Scenarios

Rodriguez et al. (2006) simulated a series of DG scenarios that assumed a DG market penetration such that DG would meet a specific fraction of the total increased electricity demand from 2002 to 2010. Scenarios with low DG market penetration showed very small impacts on $O_3$ and $PM_{2.5}$. Only scenarios that assumed a penetration of 20% or more of the

increased electricity demand from 2002 to 2010 produced some discernable air quality impacts. This market penetration corresponds to a total newly installed capacity of 1062 MW.

**Table 98. Parameters for two sample distributed generation scenarios**

| Name | Description | Penetration (% of increased demand) | Technology mix[b] (%) | | | | | |
|---|---|---|---|---|---|---|---|---|
| | | | GT | ICE | MTG | FC | PV | Hybrid |
| R3[a] | GIS land-use distribution, technology mix depends on activity sector, realistic duty cycles, and CHP | 20 | 48 | 18 | 15 | 10 | 5 | 4 |
| PW2010[a] | Population-weighted spatial distribution, DG operated baseloaded | 20 | 30 | 30 | 25 | 7 | 8 | -- |

Source: from Rodriguez et al. 2006

[a] Terminology for DG scenarios follows the terminology used in Rodriguez et al. 2006

[b] GT: gas turbines; ICE: natural gas internal combustion engines; MTG: micro-turbine generators; FC: fuel cells; PV: photovoltaic; Hybrid: gas turbine + fuel cell hybrid systems

For the sake of comparison, this study selects two sample DG scenarios simulated by Rodriguez et al. (2006). The first DG scenario corresponds to a case in which DG market penetration is based upon a methodology developed to account for detailed land-use geographical information systems (GIS) data and market studies for DG implementation. In addition, it includes CHP applications, which use the excess heat from DG units and eliminate the need for boilers to provide heat. As a result, use of CHP leads to emission reductions due to displacement of emissions from boilers (Medrano et al. 2008). The second DG scenario assumes a particular DG technology mix, and that the spatial distribution of DG implementation is proportional to the distribution of population density in the SoCAB in 2010. Specific factors for these two scenarios are presented in Table 98.

Sample Central Power Plants

Fossil fuel-based power generation in California is mostly based on natural gas, although there are few coal-based power plants (California Energy Commission 2007b). In the case of the SoCAB, restrictive emission standards in the SCAQMD only allow for implementation of natural gas power plants amongst fossil-fuel based technologies. Therefore, this study analyzes the air quality impacts of a sample natural gas power plant.

Emission factors are obtained from the High Desert Power Plant Project, which was installed in the Mojave Desert, and has been on-line since April 2003 (California Energy Commission 2000). The power plant consists of three 240-MW combined cycle gas turbines with selective catalytic reduction systems. The application for certification submitted to the California Energy Commission identifies the emission limits for normal operation, as well as for start-up and shut-down events. The present study analyzes the air quality impacts of the operation of a plant

under two scenarios: (1) continued normal operation during 24 hours, and (2) discontinued operation that includes two start-up events (2 hours/event) and two shut-down events (1 hour/event) and a total of 18 hours of normal operation, which can be considered as a "worst-day" scenario in terms of pollutant emissions. To compare the same central capacity with the capacity installed in the DG scenarios, the sample plant considered in this study has five 240-MW combined cycle turbines, with a total capacity of 1200 MW.

Emission factors for the power plant are only reported as aggregate species VOC, $NO_X$, $SO_X$, and PM. For modeling purposes emissions must be speciated according to the CACM chemical mechanism. In addition, particle emissions need to be disaggregated in eight different size bins, as supported by the aerosol module in the UCI-CIT model. Gas-phase and aerosol phase chemical speciation of emissions is based upon speciation of a natural gas reciprocating internal combustion engine by ARB (see Table 99). In addition, size resolution of particles is based on measurements of particles emissions from a gas turbine combustor (Brundish et al. 2005; see Table 100).

**Table 99. Chemical speciation of emissions based on a natural gas internal combustion engine based on ARB speciation database**

| Species | | Fraction |
|---|---|---|
| $NO_X$ | | |
| | NO | 0.830 |
| | $NO_2$ | 0.170 |
| VOC | | |
| | Formaldehyde | 0.019 |
| | Short alkanes ($C_2$-$C_6$) | 0.812 |
| | Long alkanes ($C_7$-$C_{12}$) | 0.015 |
| | Ethene | 0.027 |
| | Small Olefins | 0.108 |
| | Large Olefins | 0.004 |
| | High SOA Yield Aromatics | 0.003 |
| | Low SOA Yield Aromatics | 0.009 |
| | Aldehydes | 0.002 |
| $SO_X$ | | |
| | $SO_2$ | 0.950 |
| | $SO_3$ | 0.050 |
| PM | | |
| | Elemental Carbon | 0.200 |
| | Chloride | 0.070 |
| | Sulfates | 0.450 |
| | Nitrates | 0.006 |
| | Unresolved inorganics | 0.264 |
| | Potassium | 0.006 |
| | Calcium | 0.006 |

Source: ARB 2006c. Speciation profiles used in ARB modeling, accessed in 2006, www.arb.ca.gov/ei/speciate/speciate.htm.

**Table 100. Size distribution of particle emissions of a gas turbine combustor**

| Bin # | PM size range | | Fraction |
|---|---|---|---|
| | lower (μm) | upper (μm) | |
| 1 | 0.039 | 0.078 | 0.0002 |
| 2 | 0.078 | 0.156 | 0.0067 |
| 3 | 0.156 | 0.313 | 0.1079 |
| 4 | 0.313 | 0.625 | 0.1726 |
| 5 | 0.625 | 1.250 | 0.6905 |
| 6 | 1.250 | 2.500 | 0.0552 |
| 7 | 2.500 | 5.000 | 0.0044 |
| 8 | 5.000 | 10.000 | 0.0004 |

Source: Brundish et al. 2005

Air quality impacts of a central power plant depend strongly on the location of the installation. To assess the effect of location on the potential air quality impacts of installing a power plant, two locations were selected for this study: (1) Huntington Beach, Orange County, and (2) Etiwanda, San Bernardino County. These locations were selected because they have already licensed the installation of a central power plant, and they could be susceptible for installing extra capacity in the future. Huntington Beach represents a location that is generally upwind from Riverside, which is typically under poor air quality conditions. On the other hand, Etiwanda represents a location that is far downwind from Los Angeles, the main focus of emissions in the SoCAB, and near the area with the poorest air quality conditions. Hence, these two locations are illustrative of a broad spectrum of air quality impacts that central generation could produce.

Comparison of Emissions From Central Power Plants and Distributed Generation

Resulting emissions from two sample distributed generation scenarios and from central generation are shown in Table 101. Total emissions from normal operation of a central power plant are significantly lower than emissions from DG, except for $NO_X$ and ammonia. The $NO_X$ emissions from DG in scenario R3 are lower than emissions from central generation due to emissions displacement by CHP applications assumed for DG installations. On the other hand, total emissions from central generation under "worst-day" conditions are comparable to emissions from DG emissions. However, emissions from DG are spread throughout the air basin; whereas emissions from central generation are concentrated in only one point. As a result, air quality impacts from DG are diluted due to the sparse distribution of emission focuses. On the contrary, emissions from central generation affect a reduced area, but the impact is significantly stronger than in the DG scenarios (see Figure 88 and Figure 89).

**Table 101. Daily emissions from selected distributed generation scenarios and from central generation under normal conditions of operation and under discontinued operation ("worst-day")**

| | Pollutant Emissions (tons/day) | | | | | |
|---|---|---|---|---|---|---|
| | VOC | CO | $NO_X$ | $NH_3$ | $SO_X$ | $PM_{10}$ |
| *Distributed Generation* | | | | | | |
| R3 | 0.64 | 9.06 | -0.35 | 0.80 | 0.12 | 0.97 |
| PW2010 | 0.80 | 8.19 | 2.54 | 0.25 | 0.10 | 0.61 |
| *Central Generation* | | | | | | |
| Normal Operation | 0.04 | 1.05 | 1.08 | 1.60 | 0.00 | 0.06 |
| Worst-day | 0.86 | 20.63 | 1.99 | 1.60 | 0.07 | 1.09 |

### *Air Quality Impacts*

Air quality impacts on ozone peak concentration produced by DG and central generation are presented in Figure 88. In general, impacts on peak ozone concentration are related to $NO_X$ emissions. In the SoCAB, $NO_X$ concentrations are typically high, leading to high $NO_X$/VOC ratios and VOC-limited conditions. Addition of $NO_X$ emissions under a VOC-limited regime leads to a decrease in ozone concentration. Hence, scenarios with increases in $NO_X$ emissions produce reductions in peak ozone concentration (Figure 88(b)–Figure 88(f)). On the contrary, DG scenario R3 reduces $NO_X$ emissions, and hence, produces small increases in peak ozone concentrations. The range of impacts on $O_3$ in the DG scenarios is ±1 ppb. Impacts on $O_3$ due to central generation depend on location and operation conditions. Impacts on $O_3$ due to the plant installed in Etiwanda are significantly smaller than the impacts produced by the plant located in Huntington Beach. Under normal conditions, the plant in Huntington Beach produces decreases in $O_3$ concentration of 11 ppb and increases of 2 ppb. Operation of the same plant under "worst-day" conditions leads to decreases in ozone concentration of 13 ppb and increases of 6 ppb. In addition, the area of increases in ozone concentration due to "worst-day" operating conditions is larger than the area affected by the same plant operated under normal conditions.

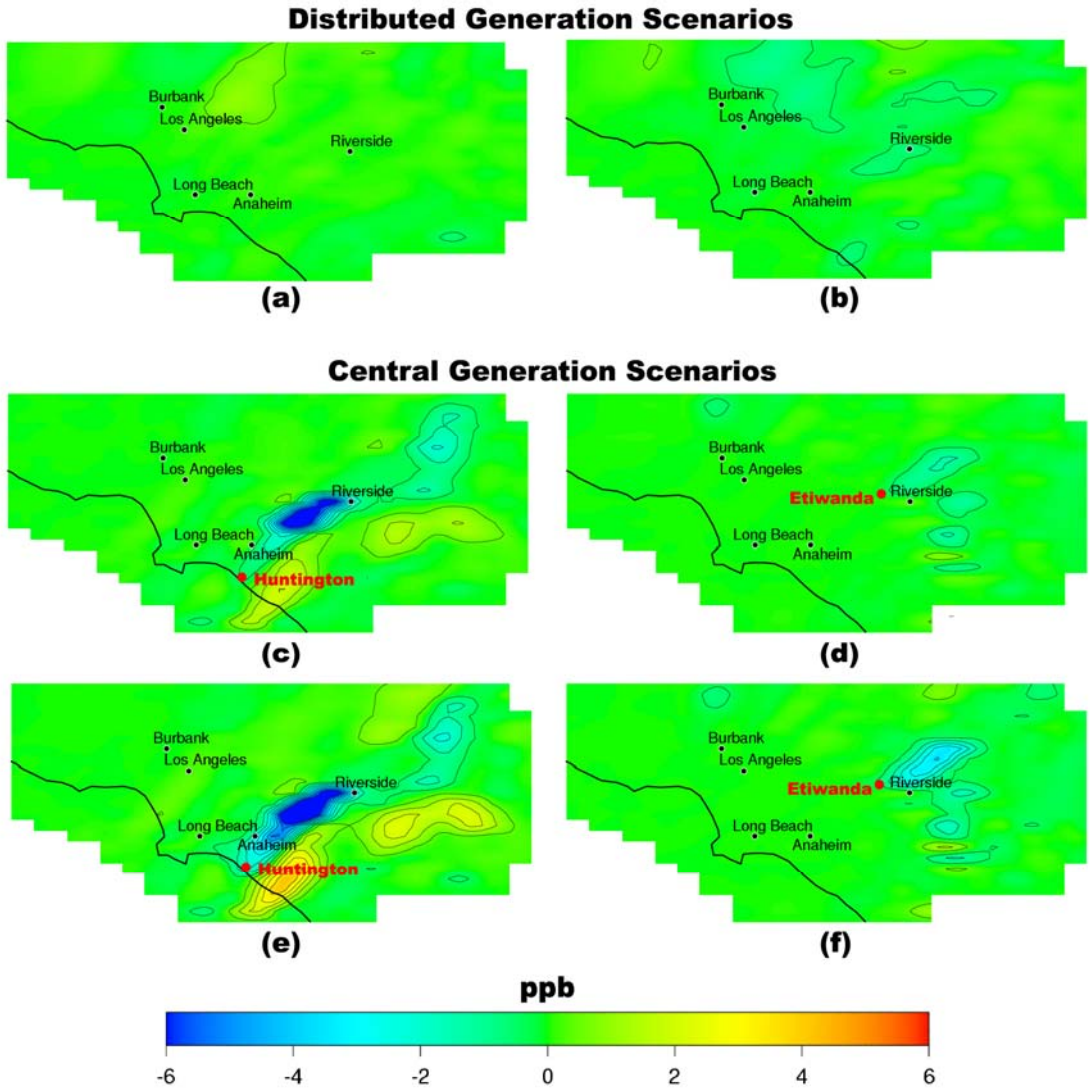


**Figure 88. Difference in peak $O_3$ concentration: (a) R3, (b) PW2010, (c) Normal operation of Huntington Beach power plant, (d) Normal operation of Etiwanda power plant, (e) "Worst-day" operation of Huntington Beach power plant, and (f) "Worst-day" operation of Etiwanda power plant**

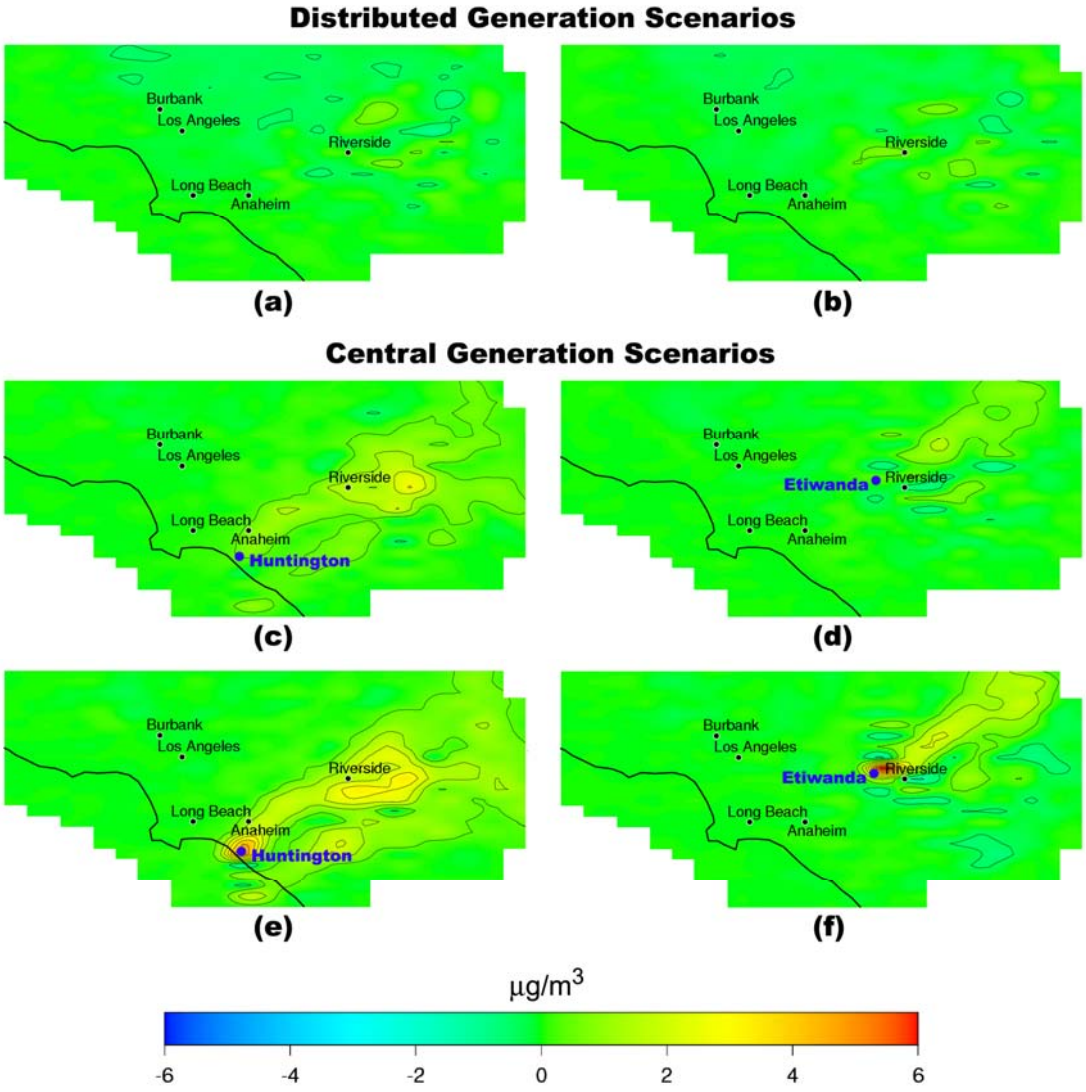


**Figure 89. Difference in 24-hour average $PM_{2.5}$ concentration: (a) R3, (b) PW2010, (c) Normal operation of Huntington Beach power plant, (d) Normal operation of Etiwanda power plant, (e) "Worst-day" operation of Huntington Beach power plant, and (f) "Worst-day" operation of Etiwanda power plant**

Air quality impacts on 24-hour average $PM_{2.5}$ concentration is presented in Figure 89. Changes in $PM_{2.5}$ are due to direct emissions of particles and to secondary formation of aerosol due to the addition of $NO_X$, $SO_X$, and VOC, which can react to form secondary aerosols. Impacts of DG on $PM_{2.5}$ are smaller than 1 $\mu g/m^3$; whereas central generation under normal conditions increases $PM_{2.5}$ concentrations by up to 4 $\mu g/m^3$. Operation of central generation under "worst-day" conditions produces increases in $PM_{2.5}$ concentrations of up to 15 $\mu g/m^3$ (note that the scale in Figure 89 has been truncated to 6 $\mu g/m^3$ to show better contrast). Impacts on $PM_{2.5}$ due to direct emissions of particles are localized near the location of the power plant and correspond to the highest impacts. On the other hand, impacts on secondary $PM_{2.5}$ occur far downwind from the

central plant, and lead to increases in $PM_{2.5}$ of 2 and 3 $\mu g/m^3$, due to the power plants in Etiwanda and Huntington Beach, respectively.

In conclusion, even though emissions from central generation are lower than emissions from the DG scenarios considered herein, central generation concentrates emissions in a small area; whereas DG spreads emissions throughout a large area of the air basin. As a result, air quality impacts from central generation are greater than the impacts from distributed generation. Effects of central generation are more concentrated in a small area, as opposed to being spread out in the cases with distributed generation. In addition, impacts of central generation depend strongly on the location of the power plant. Between the two locations explored in this study, the plant located in Huntington Beach (upwind from the areas with high ozone and $PM_{2.5}$ concentrations) has a greater impact than the plant located in Etiwanda (downwind of the main foci of direct emissions near Los Angeles).

## 7.2. Air Quality Model Sensitivity for SJV

Implementation of DG in the San Joaquin Valley was developed following a methodology analogous to the one developed for the South Coast Air Basin. As seen in the previous section, impacts of DG might be sensitive to baseline emissions. Also, location and distribution of DG determine in great extent the resulting air quality impacts of distributed generation technologies. As in the case of the SoCAB, the reactivity of the atmosphere may vary significantly within the SJV air basin. The following sections evaluate model sensitivity and the sensitivity of DG impacts in a similar fashion as performed for the South Coast Air Basin.

### *7.2.1. Model Sensitivity to Baseline Emissions*

The year 2023 is a landmark year for SJV, as the district needs to achieve compliance with the federal 8-hour ozone standard by that year. Accordingly, ARB and the SJVAPCD have conducted modeling studies for the year 2023. Recently, SJVAPCD released the plan as mandated by the U.S. EPA that outlines the path towards the attainment of 8-hour federal standard by 2023. Figure 90 shows expected $NO_X$ reductions from implementation of this plan. It is expected that total $NO_X$ emissions come down to 160 tons per day by the year 2023. Modeling studies conducted by SJVAPCD have shown that ozone concentration in the basin is more sensitive to $NO_X$ reductions than ozone. Hence, the plan calls for significant reduction in $NO_X$ emissions. The VOC reductions are shown to be important in early stages of the plan. Total VOC emissions per day in the valley by 2023 are expected to be at 355 tons per day. The future year base case for the current DG study is developed based on estimates presented in this air quality management plan (AQMP). Basinwide emissions from 2000 inventory are scaled such that total $NO_X$ emissions are 160 tons per day and VOC emissions are 355 tons per day. This methodology was endorsed by participants from DG workshop held in Fresno on April 24, 2007. Figure 91 shows 1-hour ozone maximum ground level concentrations that are predicted after these reductions in emissions are accounted for in the four days of simulation. As compared to results from the 2000 base case, major reductions are seen in maximum 1-hour ozone concentrations. Similarly, maximum 8-hour ozone concentrations decrease considerably as well.

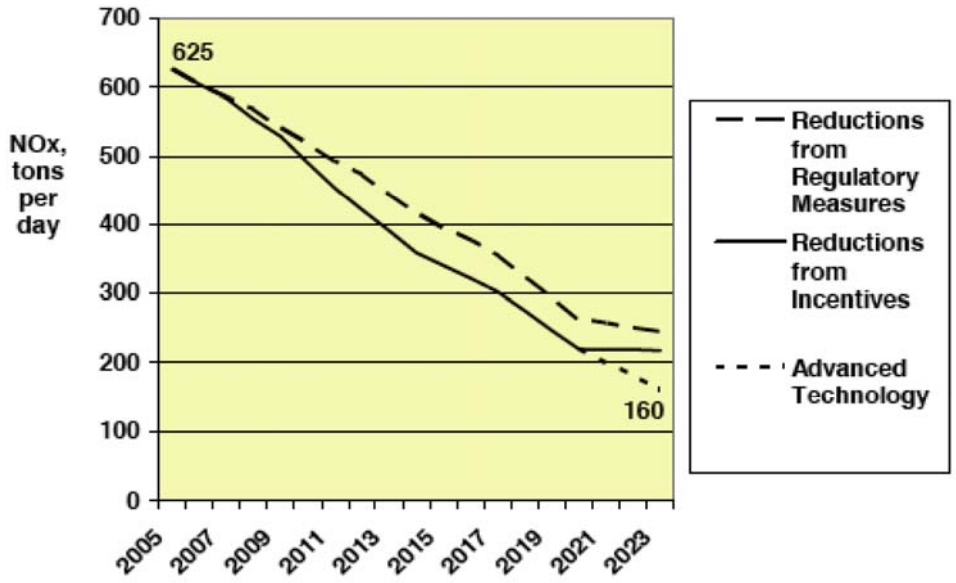


**Figure 90. Reduction in $NO_X$ emissions as proposed in the SJV 8-hour ozone attainment plan**

Source: SJVAPCD

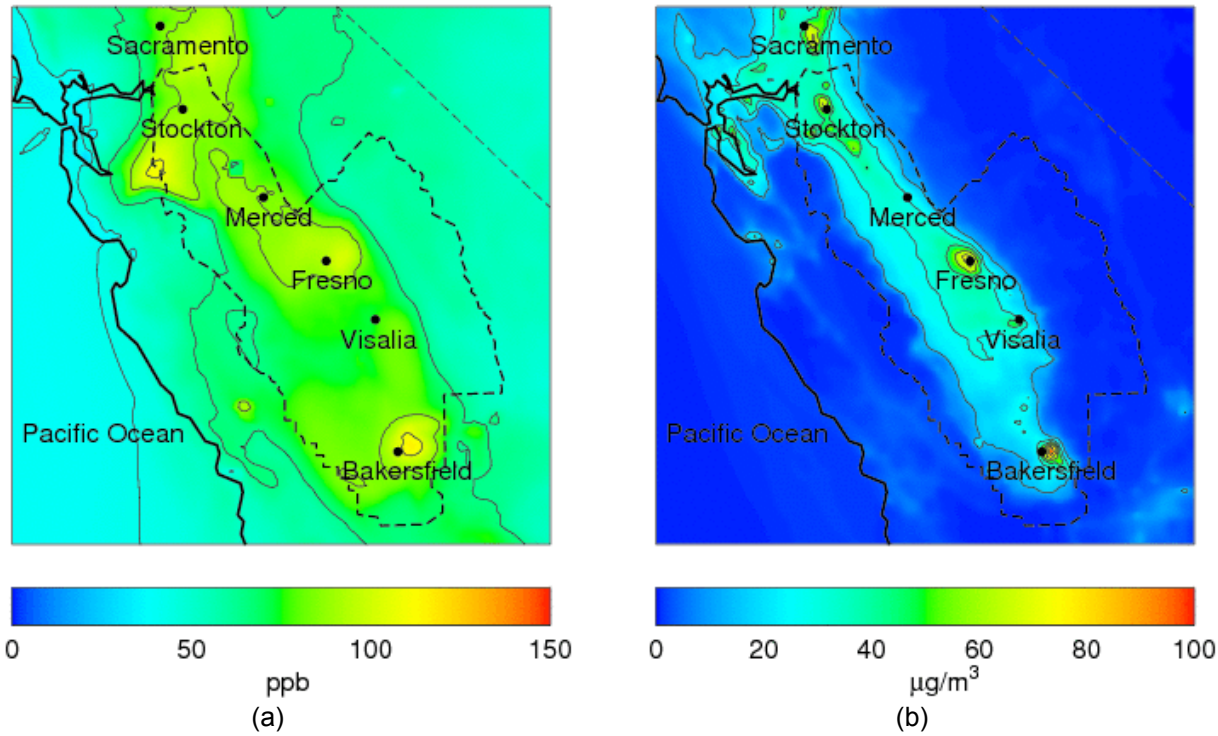


**Figure 91. Air pollutant concentrations in the San Joaquin Valley of California using the 2007 ozone attainment plan inventory: (a) peak 1-hour ozone concentrations, and (b) 24-hour $PM_{2.5}$ concentrations**

### *Baseline Air Quality as a Function of Baseline Emissions*

There are still some uncertainties regarding the strategies to accomplish the drastic reductions in emissions presented in Figure 90. The SJVAPCD estimated that those levels of emissions would be required to comply with the federal 8-hour ozone standard in effect in 2007 (80 ppb), but it is not clear yet how these reductions will be achieved. This study analyzes the sensitivity of model predictions with respect to an uncertainty bound of ±20% in total basinwide emissions. Namely, in addition to the 2023 baseline inventory, two additional cases are considered in which baseline emissions are scaled by 1.2 and 0.8 to analyze the sensitivity of peak ozone and 24-hour average $PM_{2.5}$ concentrations to total emissions in the SJV.

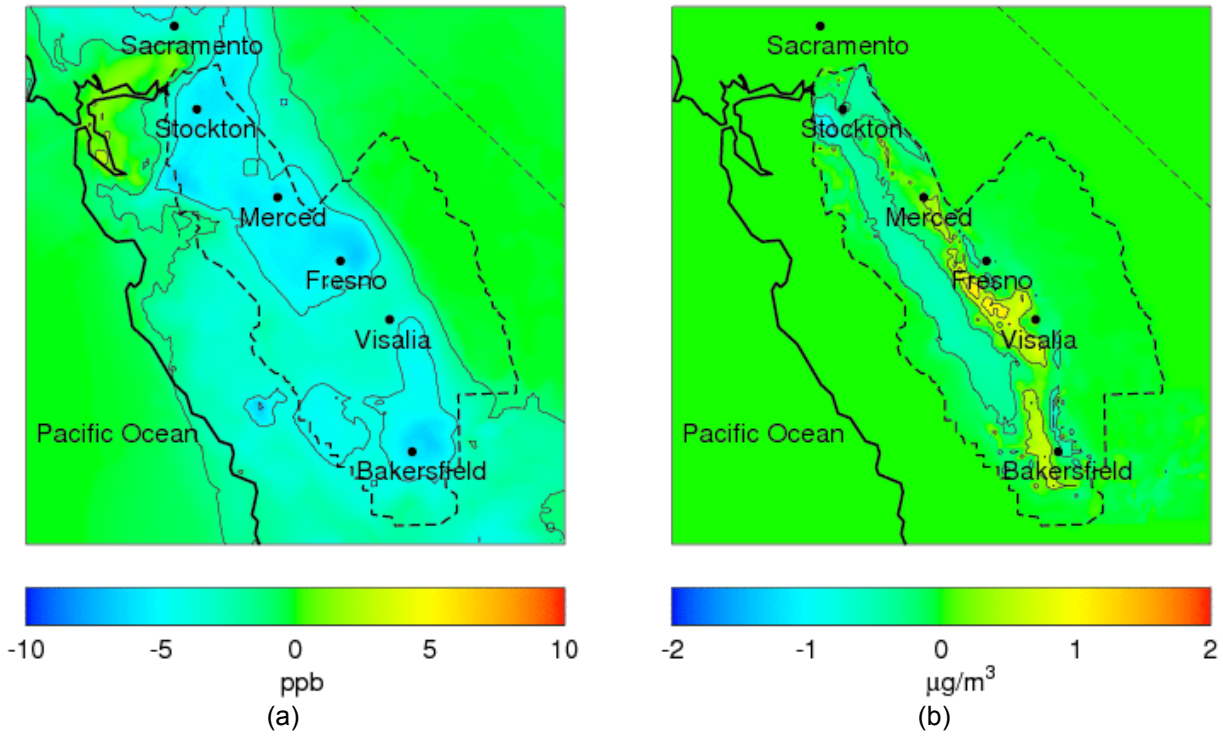


**Figure 92. Impacts on (a) peak 1-hour ozone and (b) 24-hour average $PM_{2.5}$ concentrations if baseline emissions are multiplied by 0.8. Concentration values represent 0.8 × baseline emissions case minus baseline emissions case.**

Figure 92 presents the differences in peak ozone and 24-hour $PM_{2.5}$ concentrations between the case in which emissions are scaled by 0.8 and the baseline case. Similarly, Figure 93 presents the differences in pollutant concentrations between the case with 1.2 times the baseline emissions and the baseline case. With respect to ozone concentration, a decrease in total basinwide emissions by 20% decreases peak ozone concentrations by 7 ppb. Conversely, increasing total emissions by 20% causes peak ozone concentrations to increase by 7 ppb. With respect to $PM_{2.5}$ concentrations, changes in baseline emissions lead to mixed trends. Reducing emissions by 20% produces decreases in $PM_{2.5}$ in the western part of the basin by approximately 1 µg/m³ but it increases $PM_{2.5}$ in areas near the major cities in the basin by over 1 µg/m³. Increasing emissions by 20% produces nearly the opposite trend on $PM_{2.5}$ concentrations.

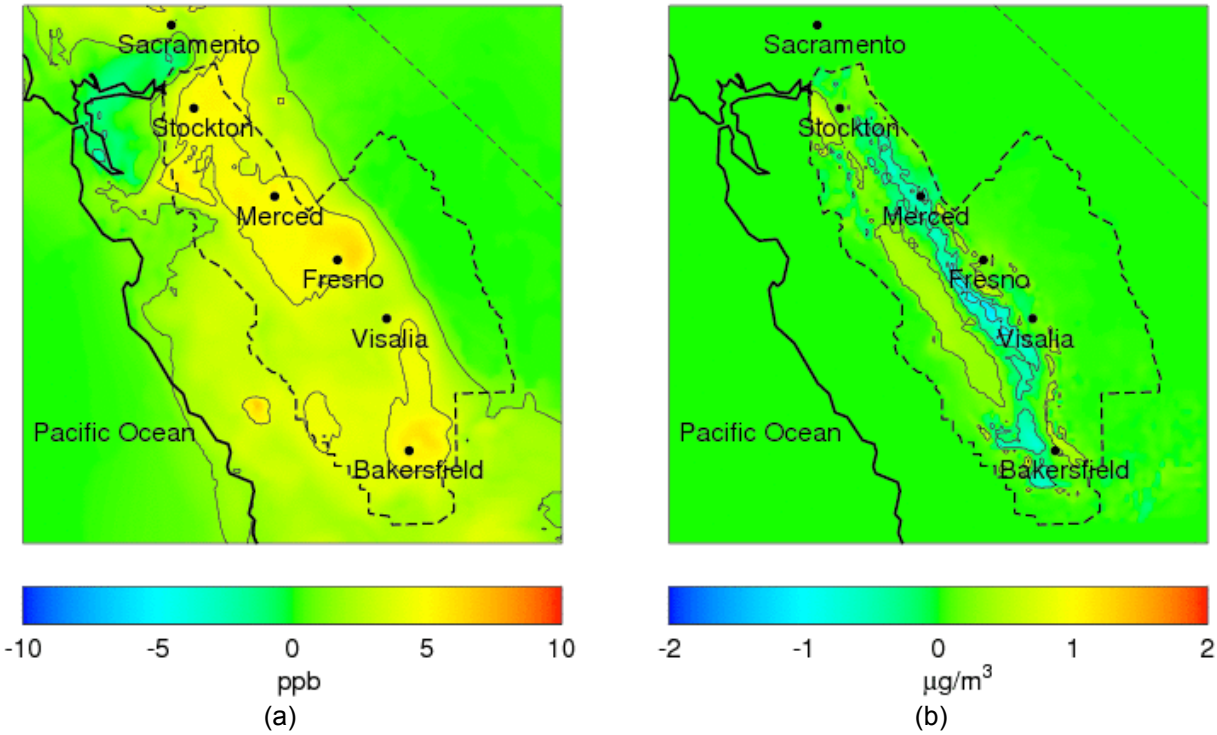


**Figure 93. Impacts on (a) peak ozone and (b) 24-hour average $PM_{2.5}$ concentrations if baseline emissions are multiplied by 1.2. Concentration values represent 1.2 × baseline emissions case minus baseline emissions case.**

### *Air Quality Impacts of DG as a Function of Baseline Emissions*

Impacts of DG are evaluated using the two additional baseline emission inventories presented above. The DG scenario selected for this analysis is the "No CHP" spanning scenario, which introduces 373 MW of DG installed capacity. The emissions from DG in this scenario correspond to an increase of 0.13% with respect to 2023 baseline emissions. At this level of DG penetration, the air quality impacts of DG on peak ozone concentration and 24-hour $PM_{2.5}$ concentrations are very similar within the ±20% uncertainty bound in the baseline emissions. As shown in Figure 94, impacts of DG on peak ozone concentration are of the same order—up to 0.1 ppb—in the cases with 0.8 and 1.2 times the baseline emissions. Only small differences are observed in the area affected by DG, and it appears that DG has a slightly more widespread impact on ozone in the case with 0.8 times the baseline emissions. This occurs mainly because the relative impacts of DG are larger as baseline emissions decrease, which is consistent with the trends observed for the SoCAB. Likewise, Figure 95 shows that the impacts of DG on 24-hour average $PM_{2.5}$ concentration are similar within the ±20% uncertainty bound in the baseline emissions. In general, air quality impacts of DG in the SJV appear to be less sensitive to changes in baseline emissions than in the case of the SoCAB. In part, this occurs because DG penetration in the SJV is expected to be far lower than the penetration in the South Coast Air Basin.

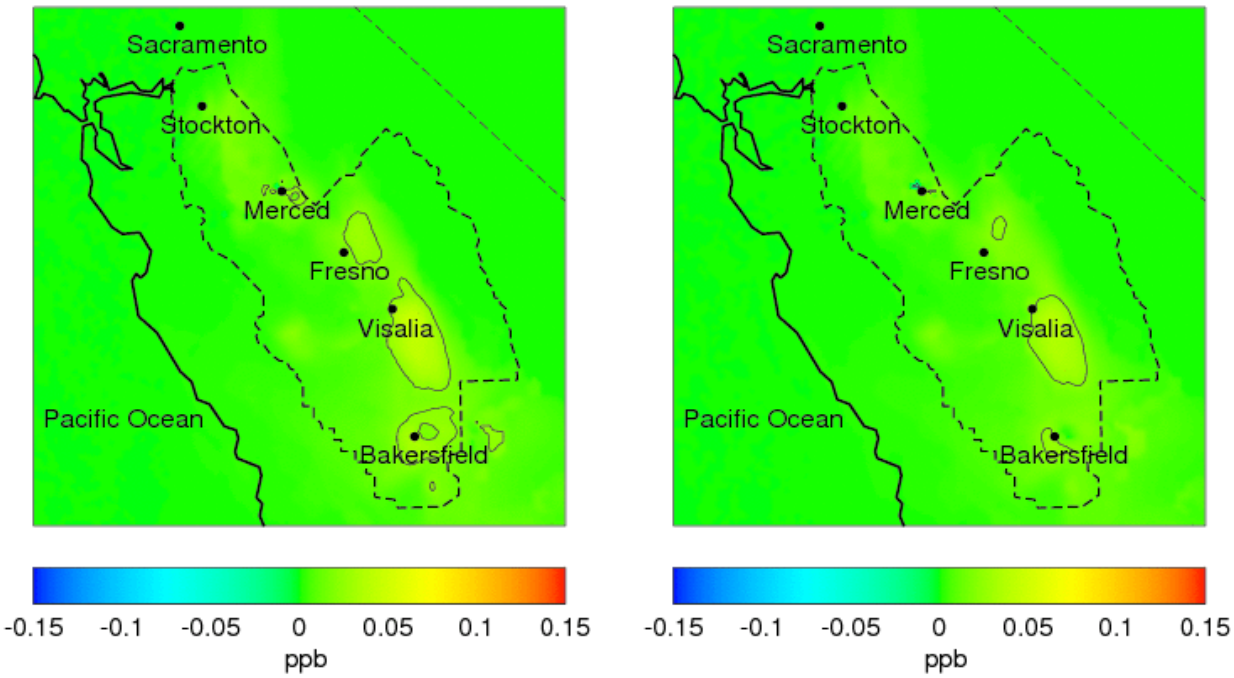


(a) DG case – 0.8×Baseline case (b) DG case – 1.2×Baseline case

**Figure 94. Impacts of DG on peak ozone concentration using two different baseline emissions inventories: (a) 0.8 × 2023 baseline emissions, and (b) 1.2 × 2023 baseline emissions**

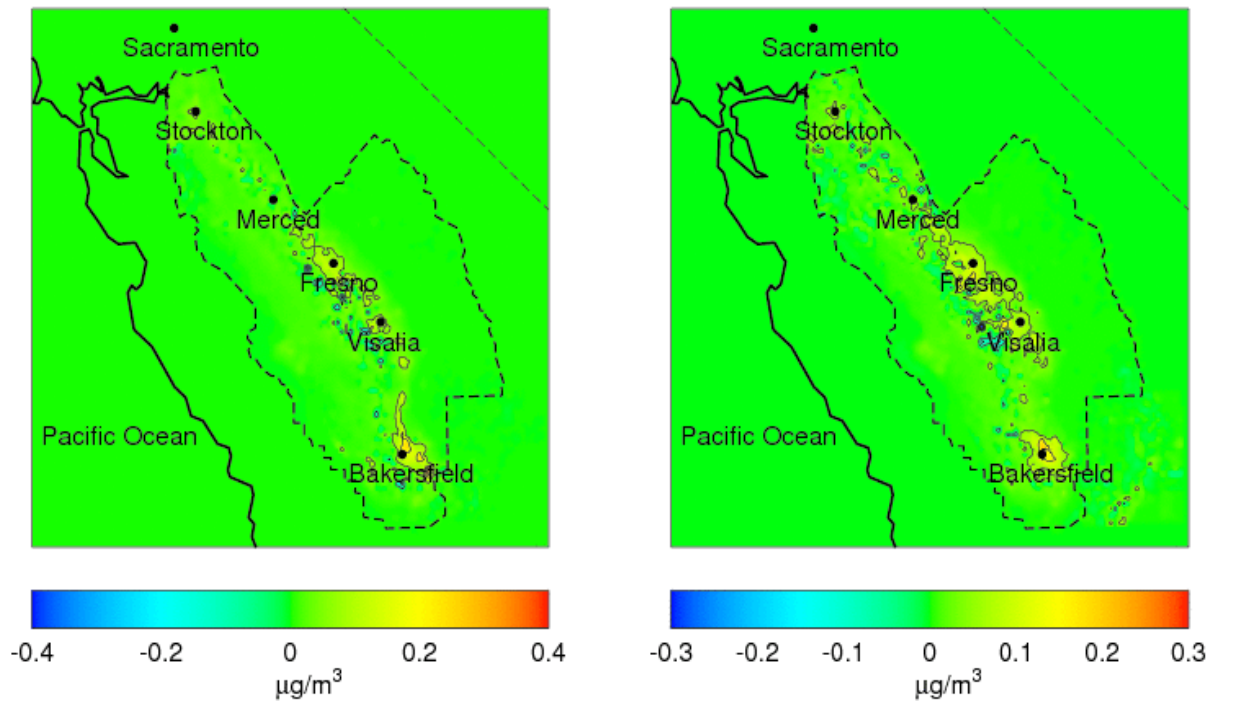


DG case – 0.8×Baseline case DG case – 1.2×Baseline case

**Figure 95. Impacts of DG on 24-hour average $PM_{2.5}$ concentration using two different baseline emissions inventories: (a) 0.8 × 2023 baseline emissions, and (b) 1.2 × 2023 baseline emissions**

### 7.2.2. Model Sensitivity to Spatial Distribution of Emissions

In this section, the sensitivity of DG impacts is studied for spatial dependence. Distributed generation emissions from one region of the SJV air basin may affect other regions because of atmospheric transport of emissions. Rodriguez et al. (2007) has shown that DG emissions from coastal areas of the SoCAB lead to increases in ozone and $PM_{2.5}$ concentrations in the eastern region of the SoCAB. Therefore, a sensitivity analysis was conducted to analyze if any such regional trends exist in the SJV basin.

As shown in Figure 96, the valley is divided in to three regions: the Northern region (San Joaquin, Stanislaus, and Merced counties), the Central region (Madera and Fresno counties), and the Southern region (Tulare and Kern counties). Distributed generation emissions are introduced in only one of these regions for each scenario. Distributed generation power and other parameters that are used in this study are same as spanning scenario NOCHP. In the NOCHP scenario, the total DG power installed is equivalent to 18% increase in peak demand from 2007 to 2023. No emissions displacement from CHP is considered in this scenario, leading to addition of $NO_X$ and VOC emissions to the basin.

Figure 97 shows increases in peak 1-hour ozone concentration from three scenarios that include DG emissions in either North, Central, or Southern regions of the valley. Ozone increases by about 0.1 ppb in each of these scenarios. In each of these cases, the impact is limited to only the region where DG is introduced. Temporal profiles of impacts from these scenarios show 1-hour peak ozone concentration due to DG emissions decreases in the night and increases during the day. Ozone decreases in the nighttime, due to the titration from $NO_X$ emissions, and it increases during the daytime due to photochemistry of additional $NO_X$ and VOCs from DG emissions. However, the impact at all times during the day is limited only to the region where DG is introduced. This is attributed to limited atmospheric transport in the basin due to stagnation and low wind speeds.

Figure 98 shows increases in 24-hour average $PM_{2.5}$ concentration from the three scenarios described above. For each of these scenarios, $PM_{2.5}$ increases up to 0.3 $\mu g/m^3$. However, a general trend of PM increases occurring north of locations with DG emissions is predicted in these scenarios. Observation of temporal profiles has shown that atmospheric transport of DG emissions and reaction products of those emissions are transported northward during the winter PM episode. However, the range of such transport is observed to be limited. Therefore, depending on meteorological conditions, it is possible for DG emissions from one region to impact other regions.

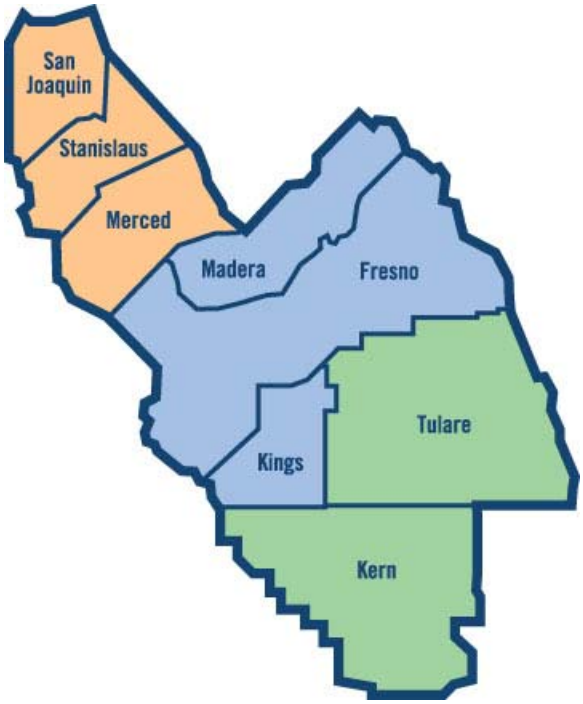


**Figure 96. SJV is divided in to three regions to evaluate spatial sensitivity of DG emissions**

Source: SJVAPCD 2007. (www.valleyair.org/general_info/aboutdist.htm)

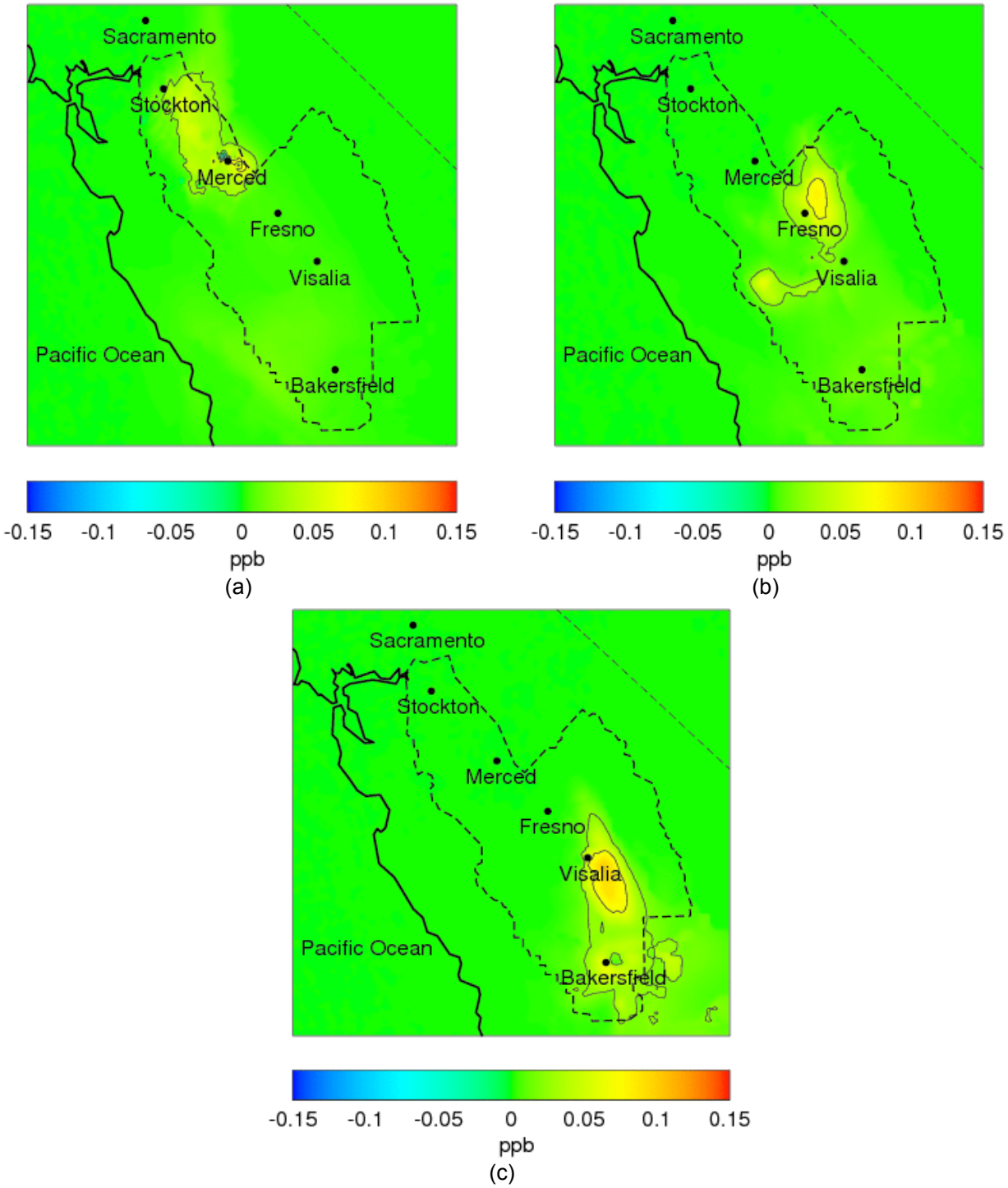


**Figure 97. Impacts of DG on peak ozone concentration when emissions are introduced in only the: (a) Northern region of SJV; (b) Central region of SJV; and (c) Southern region of SJV**

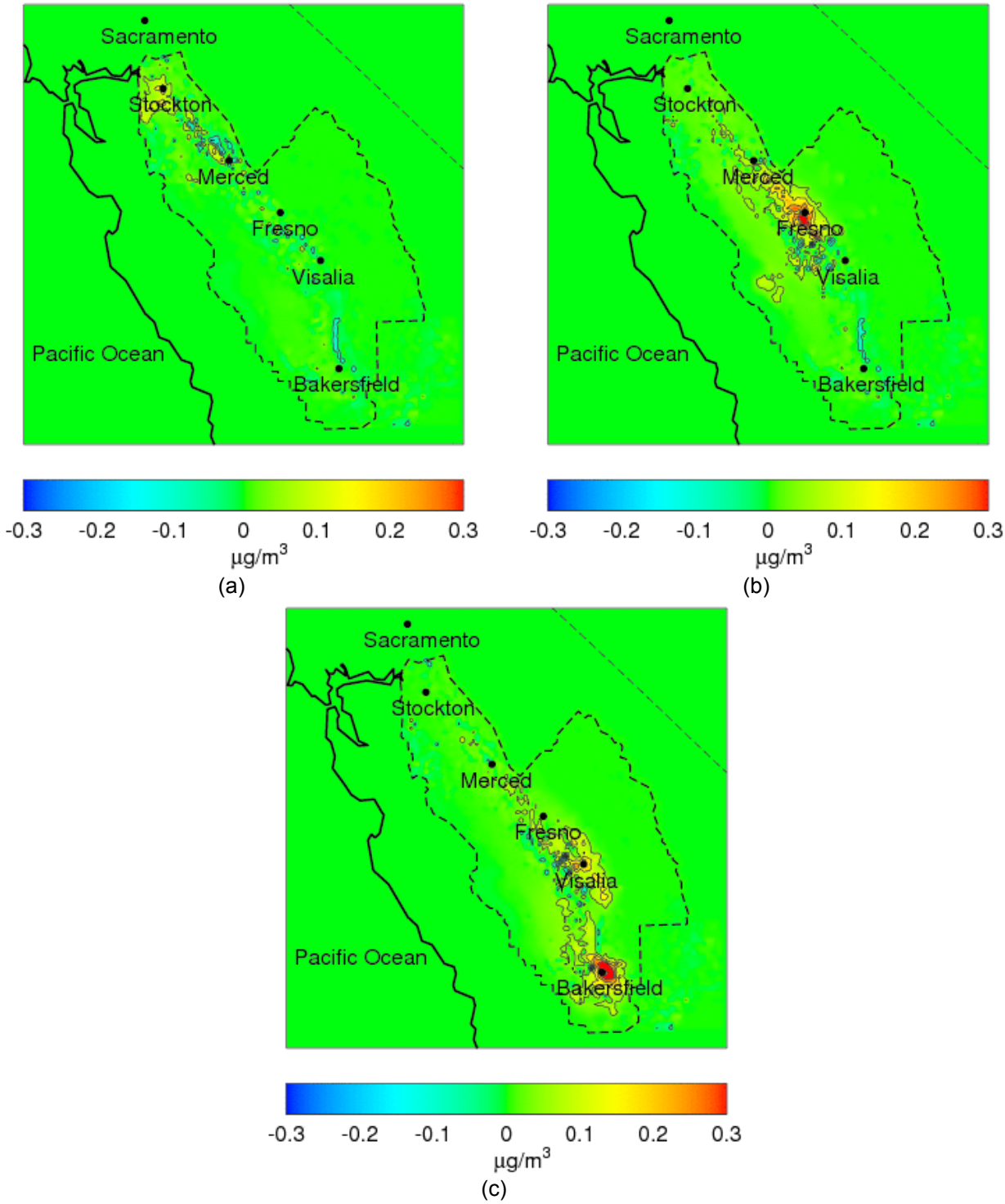


**Figure 98. Impacts of DG on 24-hour average PM concentration when emissions are introduced in only the: (a) Northern region of SJV; (b) Central region of SJV; and (c) Southern region of SJV**

### 7.2.3. Model Sensitivity to Central Generation Versus Distributed Generation

In this section, air quality impacts of central generation are compared to those from distributed generation systems with equivalent total power. Central generation is characterized by concentrated emissions of $NO_X$ which are usually located in remote areas. In contrast, distributed generation introduces emissions in urban areas that already have significant local emissions sources.

Two scenarios are developed to compare air quality impacts from central generation with those from distributed generation. In the first scenario, emissions from a 1200 MW central plant are introduced in the basin. The location of the central plant is determined based on plants that have recently become operational in the San Joaquin Valley. The information on location and capacities of all central plants in the SJV is obtained from the U.S. EPA database eGRID. Based on this information, emissions from a central power plant are introduced west of Bakersfield. Emission factors and speciation of VOC emissions are described in the earlier part of this section, Sample Central Power Plants.

In the second scenario, emissions from distributed generation of 1200 MW total capacity are introduced in the basin. The spatial distribution of these emissions corresponds to land-use distribution. The technology mix is determined using the methodology developed for realistic scenarios. It is assumed that 60% of DG power is implemented with CHP application, with 50% heat utilization efficiency.

Figure 99 shows increase in ozone and $PM_{2.5}$ concentrations from central and distributed generation of equivalent capacities. Central generation results in a 3 ppb increase of peak-ozone concentration. These increases are predicted to occur in the region surrounding the central plant location. In contrast, distributed generation results in a 0.5 ppb increase of peak-ozone concentration. However, ozone impacts from DG are observed throughout the basin. Maximum impacts are predicted to occur near Visalia, followed by Bakersfield and Fresno. Similar results are also predicted for $PM_{2.5}$ concentrations. Similar to ozone impacts, a highly localized PM increase of 1.5 $\mu g/m^3$ is predicted to occur in the model cells surrounding the central plant. Distributed generation of equivalent capacity results in $PM_{2.5}$ increase of about 0.4 $\mu g/m^3$. In conclusion, effects from central generation are greater in magnitude and localized. Impacts from DG are much lower and occur throughout the basin.

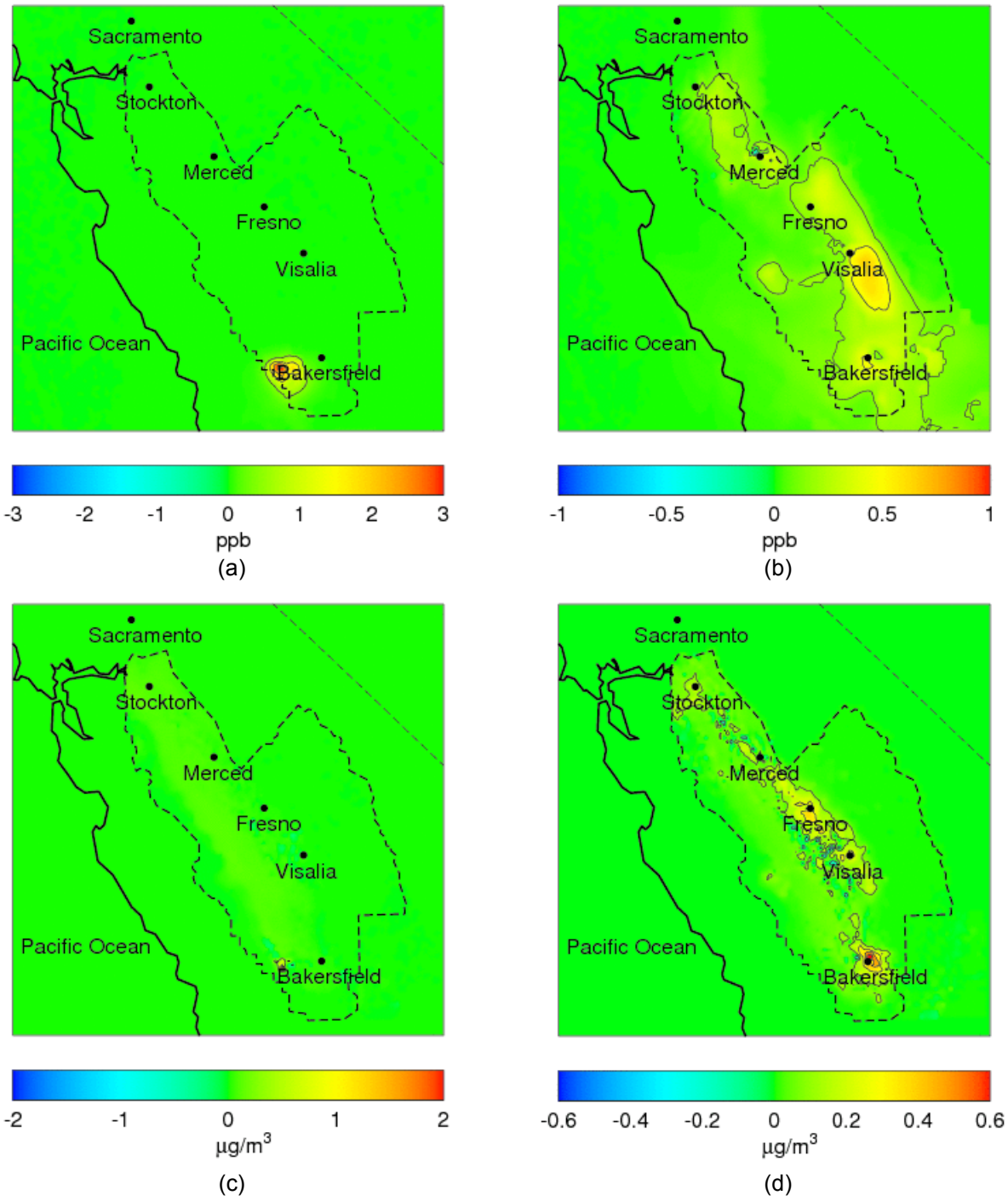


**Figure 99. Air quality impacts of central generation in SJV: (a) impact on maximum 1-hour ozone from a 1200 MW power plant located in the southern part of the SJV; (b) impact on maximum 1-hour ozone from DG penetration that provides a total power capacity of 1200 MW; (c) impact on 24-hour average PM from a 1200 MW power plant located in the southern part of the SJV; and (d) impact on 24-hour average PM from DG penetration that provides a total power capacity of 1200 MW**

# 8.0 Conclusions

## 8.1. Implementation of DG in the SoCAB

A series of temporally and spatially resolved implementation scenarios has been developed to determine the potential air quality impacts of distributed generation (DG) in the South Coast Air Basin (SoCAB). According to market studies, DG market penetration could supply over 2 GW of power capacity by the year 2030. Such penetration, considered for the realistic scenarios, would introduce new foci of emissions that would be distributed throughout the South Coast Air Basin. Assuming that all DG units would comply with ARB 2007 emissions standards as early as in 2023, the emissions associated to DG would contribute less than 1% to total basinwide emissions. In addition, the use of combined heating and power (CHP) technologies in DG systems has the potential to reduce $NO_x$ emissions. For realistic scenarios it is assumed that CHP units will recuperate on average 30% of the excess heat from DG units operation—assuming 60% of heat recovery and 50% of CHP utilization. This percentage of excess heat use, however, does not reduce emissions from boilers displaced by CHP to offset completely the emissions from distributed generation technologies. As a result, net emissions from DG are positive. The resulting air quality impacts of realistic DG scenarios are small. Maximum increases in peak ozone concentration are smaller than 1 ppb; whereas 24-hour average $PM_{2.5}$ concentrations increase by up to 1.1 $\mu g/m^3$.

To investigate some of the parameters that define a DG implementation scenario, a set of spanning scenarios was developed and simulated to analyze the potential effects of DG on air quality. The parameters studied include the spatial distribution of DG, the duty cycle of DG operation, the technology mix of DG, the potential for emissions displacement, the DG market penetration, and the DG emission factors. Based on the air quality modeling results of these spanning scenarios, the following conclusions of the study can be made:

- The application of ARB 2007 emissions standards for all DG units reduces the impacts of DG significantly. Even assuming high DG penetration of up to 5 GW, emissions from DG would increase peak ozone concentration and 24-hour average $PM_{2.5}$ concentrations by only 1.2 ppb and 1.4 $\mu g/m^3$, respectively, if the ARB 2007 limits are applied. Hence, DG could affect slightly the efforts to attain ozone air quality standards. Thus, application of ARB 2007 emissions standards to all DG units, including gas turbines and ICE is recommended to minimize the effect of DG on air quality.
- Distributed generation could preferentially be installed in areas where there is a more rapid growth in population, such as in Riverside and San Bernardino counties, compared to other areas such as Los Angeles or Orange County. Placing DG in Los Angeles and Orange County leads to the most significant air quality impacts in downwind locations (San Bernardino and Riverside). Placing DG farther inland near Riverside and San Bernardino reduces impacts in these regions, which currently suffer most from high pollutant concentrations, but displaces the air quality impacts towards the mountains near the borders of the South Coast Air Basin.

- Operation of DG following a duty cycle that peaks in the afternoon causes slightly smaller impacts on peak ozone concentrations than a case in which the same amount of electricity is produced in a baseload mode. However, the area affected by increased ozone in the duty cycle case (PeakTot) is slightly larger than the baseload case (LU) because ozone precursors in the PeakTot case are released at the time of maximum ozone production.
- Installation of DG permitted under the BACT standards valid in 2007 could significantly increase the air quality impacts of DG, and could increase peak ozone concentrations by up to 4.6 ppb and 24-hour average $PM_{2.5}$ concentrations by up to 2.6 $\mu g/m^3$ in the year 2030. This would hinder strongly the efforts to reduce ozone concentration to achieve compliance with ozone air quality standards.
- Violations of the BACT limits in internal combustion engine (ICE) installations have been reported by the AQMD, and they were found to sometimes comprise a tripling of emissions above the permitted levels. If these emissions levels were ever produced by future implementation of ICE in the SoCAB, air quality impacts of DG could be high.
- Large gas turbines and fuel cells introduce the lowest emissions of $NO_X$ amongst fuel-driven technologies (based on literature data), and fuel cells introduce the lowest particle emissions. As a result, future use of large gas turbine systems produced the smallest impacts on peak ozone concentration, and use of fuel cell systems did not produce noticeable impacts on $PM_{2.5}$ concentrations. The addition of photovoltaics in the DG mix in substitution of other DG technologies reduces the impact of DG emissions on air quality.
- Use of CHP could offset $NO_X$ emissions from DG if a high percentage of the heat is recuperated and used. Combined heating and power units recuperating 100% of the excess heat from DG could lead to maximum decreases in peak ozone concentrations of up to 0.6 ppb. In addition, reduction of $NO_X$ emissions due to DG could reduce the formation of secondary $PM_{2.5}$ and lead to a net reduction of $PM_{2.5}$ concentrations in some areas in the basin. However, CHP emission credits allows for DG particle emissions that are higher than the emissions from boilers. As a result, direct net PM emissions from DG are higher if CHP is included.
- Distributed generation could substitute for existing central power plants in the future, resulting in a change in the distribution of emissions from power generation. However, emissions from DG offset the emissions of the power plants that would be removed from the SoCAB. This type of future implementation scenario would reduce ozone concentrations and $PM_{2.5}$ near the power plants, but also could lead to increases in the basinwide maximum peak ozone and 24-hour average $PM_{2.5}$ concentrations of up to 2.8 ppb and 2 $\mu g/m^3$, respectively.
- Widespread use of electric vehicles supported by a DG infrastructure to generate the electricity could lead to significant reductions of ozone and particulate matter precursors. These emissions reductions could lead to reductions in ozone and $PM_{2.5}$ of 6 ppb and 4 $\mu g/m^3$, respectively. However, these pollutant reductions assume the use of low-emitting DG technologies, such as large gas turbines and fuel cells, or renewable

power systems. The use of technologies that emit at a higher rate could offset the benefits of removing vehicle emissions from the basin.

## 8.2. Implementation of DG in the SJV

This report presents future scenarios of DG technology deployment in the SJV basin, together with their potential air quality impacts. Four realistic scenarios were developed for the year 2023. These scenarios were developed using the same systematic framework employed for the SoCAB, but adapted to the characteristics of the San Joaquin Valley. The results from the DG implementation scenarios development showed that realistic scenarios do not add significant amounts of emissions to the basin. This is mainly because the DG technologies considered in the analyses have relatively low rates of pollutant emissions. In addition, the application of CHP would result in considerable displaced boiler emissions in the SJV, leading to low $NO_X$ emissions, although CHP does not completely offset emissions from DG. Nine spanning scenarios were also developed in order to provide further understanding of the potential air quality impacts of DG installation throughout the SJV basin. In addition, six DG scenarios that consider power generation from biomass resources were developed for the year 2023.

Air quality impacts from DG scenarios were quantified using two regional air quality models: CAMx and CMAQ. The CAMx model was used to simulate a summer ozone episode, and CMAQ was used to simulate a winter PM episode. Model simulations showed that realistic scenarios have no significant impacts on the regional air quality. There was no significant change in maximum 1-hour average ground-level ozone concentrations. On the other hand, 24-hour average ground-level PM concentrations increased by as much as 0.43 $\mu g/m^3$ at certain locations, for realistic scenarios. Some spanning scenarios showed higher impacts when a high level of DG deployment was considered or when less stringent emission standards or non-compliance with standards was considered. For instance, the assumption that internal combustion engines (ICE) would operate in the SJV at the levels permitted in 2007 by BACT emissions standards significantly increased DG air quality impacts on maximum ozone and 24-hour average PM concentrations. Similarly, assuming an extra high penetration of DG produced more significant overall impacts.

The following general trends were observed in this study:

- Ozone concentrations are predicted to mostly increase with the introduction of $NO_X$ emissions from DG deployment. This is because ozone formation in the SJV is $NO_X$ limited for the emission levels that are estimated to attain the 8-hour ozone standard.
- Particulate matter concentrations are predicted to increase with DG for most part of the domain. However, $NO_X$ emissions from DG during nighttime lead to reduction in $PM_{2.5}$ at some locations in the basin. This is attributed to the titration of ozone by $NO_X$ leading to a decrease in secondary PM formation. This effect was more evident in scenarios that included performance degradation or high emission levels from DG technologies.
- Ground-level 1-hour ozone and 24-hour average $PM_{2.5}$ impacts are predicted to be more concentrated in or near the urban areas of the basin (e.g., Stockton, Merced, Fresno, Visalia, and Bakersfield). The locales with the highest impacts were shown to occur close

to where DG emissions are released. Transport throughout the basin was shown to not significantly affect the locations where air quality impacts of DG occur.

- Air quality impacts from the operation of DG following a duty cycle that peaks in the afternoon do not differ significantly from the air quality impacts predicted from the operation of DG following a baseload duty cycle. This is due to the low level of emissions resulting from DG penetration that is assumed in this study.
- Although the predicted impacts are small, the air quality impacts consistently increased with an increase in total installed DG power in the San Joaquin Valley Air Basin. Scenarios with large-scale deployment of DG assumed the highest DG penetration amongst spanning DG scenarios in the air basin. Such a level of aggregate power, which is comparable to the capacity of a large central power plant, could increase ozone by 1 ppb and $PM_{2.5}$ by 1.1 $\mu g/m^3$.
- Air quality impacts from biomass scenarios predicted increases in maximum 1-hour ozone by 0.12 ppb and $PM_{2.5}$ by 0.63 $\mu g/m^3$. The application of CHP does not completely offset $NO_X$ emissions from biomass scenarios. Therefore, air quality impacts from biomass power are higher than those predicted for DG scenarios with comparable power, because direct emissions from biomass with direct combustion are higher than natural gas-based DG technologies.

## 8.3. Contribution of DG to Greenhouse Gas (GHG) Emissions

Direct $CO_2$ emissions from DG are higher than average grid emissions—1014 lb/MWh—for all realistic scenarios, due to high penetration of gas turbines. However, if CHP emissions displacements are accounted for, net emissions from DG are less than 920 lb/MWh—approximately 9% lower than average California grid emissions. Average DG emissions in realistic scenarios in the SJV are slightly lower than those in the SoCAB because the DG technology mix estimated for the SJV includes a higher percentage of natural gas ICE and a lower percentage of gas turbines, compared to the realistic scenarios for the South Coast Air Basin. As mentioned above, ICE could be preferred over gas turbines if only $CO_2$ emissions are considered. However, criteria pollutant emissions from ICE are significantly higher than from gas turbines, which could offset the benefits of reducing $CO_2$ emissions. Scenarios with high deployment of high-temperature fuel cells could lead to decreases in $CO_2$ of 11.2% in the SoCAB and 12.0% in the San Joaquin Valley. As suggested by actual heat recovery metered data obtained by the CPUC, findings in this report suggest that fuel cells have the highest potential for overall electricity and heat recovery efficiency and for $CO_2$ emission reductions with respect to current California grid emissions.

## 8.4. Model Sensitivity Analysis

Evaluation of model sensitivity to key parameters that may affect air quality impacts of DG is presented in this report. Evaluation is conducted for the SoCAB and the SJV. First, model sensitivity has been tested with respect to changes in baseline emissions. Changes in baseline emissions proposed in the air quality management plan for the SoCAB and in the attainment plan for the SJV have been evaluated using air quality models for those two particular areas.

Baseline emissions determine the chemical regimes that determine how small emission perturbation due to DG implementation can affect the air quality of a particular area. In addition, this report evaluates the effect of agglomeration of emissions in specific geographical areas in the domains of interest, and in particular, how the model predicts air quality impacts of central generation that is comparable to the estimated DG implementation. The main conclusions of this sensitivity study are as follows:

South Coast Air Basin:

- Emissions reductions from 2003 to 2007 AQMP shift the SoCAB air quality from VOC-limited to $NO_X$-limited conditions:
  - 2003 AQMP: increase in $NO_X$ emissions leads to a decrease in peak $O_3$
  - 2007 AQMP: increase in $NO_X$ emissions leads to an increase in peak $O_3$
- Distributed generation impacts using 2007 AQMP emissions are generally stronger than using the 2003 AQMP, because emissions from the 2007 AQMP provide a more reactive environment for atmospheric chemistry. Mainly, the lower reactivity in the 2003 AQMP is caused by the significantly higher $NO_X$ emissions, compared to the 2007 AQMP. Significantly higher $NO_X$ emissions provide a VOC-limited environment, which translates into less sensitivity of ozone concentration to changes in $NO_X$ emissions due to DG.
- Emissions from power plants operating under normal conditions are significantly lower than DG emissions. However, air quality impacts of central generation are more intense and localized than the impacts of DG. In particular, power plant locations that are near the coast, upwind from areas with typically high ozone and $PM_{2.5}$ concentrations, potentially lead to most intense air quality impacts.

San Joaquin Valley:

- Changes of 20% in baseline emissions do not strongly affect air quality impacts of distributed generation.
- Emissions from DG do not undergo significant atmospheric transport due to stagnation and low wind velocities during the summertime ozone episode. In contrast, emissions from DG are transported northward during the wintertime PM episode.
- Impacts from central generation are higher in magnitude compared to distributed generation. However, impacts are limited to the area around the central plant.

# 9.0 References


Allen, P. 2003. SoCAB emissions inventory. The California Air Resources Board.

Allison, J. E., and J. Lents. 2002. "Encouraging Distributed Generation of Power That Improves Air Quality: Can We Have Our Cake and Eat it Too?" *Energy Policy* 30 (9): 737–752.

ARB. 2006a. ARB emission information for facilities, available at: www.arb.ca.gov/app/emsinv/facinfo/facinfo.php.

ARB. 2006b. ARB California Air Quality Data. www.arb.ca.gov/aqd/aqdcd/aqdcddld.htm.

ARB. 2006c. Speciation Profiles Used in ARB Modeling. www.arb.ca.gov/ei/speciate/speciate.htm.

ARB. 2007a. EMFAC2007: Emission Factors Model. Available at: www.arb.ca.gov/msei/onroad/latest_version.htm.

ARB. 2007b. Emissions Inventory Data. www.arb.ca.gov/ei/emissiondata.htm.

Binkowski, F. S., and U. Shankar. 1995. "The Regional Particulate Model 1: Model Description and Preliminary Results." *J. Geophys. Res.* 100(D12): 26191–26209.

Biomass Collaborative. 2008. The California Biomass Collaborative Biomass Facilities Reporting System. http://biomass.ucdavis.edu/bfrs.html.

Blanchard, C. L., and S. J. Tanenbaum. 2003. "Differences Between Weekday and Weekend Air Pollutant Levels in Southern California." *J. Air & Waste Manage. Assoc*. 53:816–828.

Boedecker, E., J. Cymbalsky, and S. Wade. 2000. *Modeling Distributed Generation in the NEMS Building Models.* Energy Information Administration.

Brundish, K. D., M. N. Miller, C. W. Wilson, M. Jefferies, M. Hilton, and M. P. Johnson. 2005. "Measurement of Smoke Particle Size and Distribution Within a Gas Turbine Combustor." *Journal of Engineering for Gas Turbines and Power* 127:286–294

Carter, W. P. L. 2000. *Documentation of the SAPRC-99 Chemical Mechanism for VOC Reactivity Assessment.* Final report to the California Air Resources Board, Contracts 92-329 and 95-308. May. Available at www.cert.ucr.edu/~carter/absts.htmSaprc99.

California Energy Commission. 1999. *Market Assessment of CHP in the State of California.* Onsite Sycom Energy Corporation, prepared for California Energy Commission.

California Energy Commission. 2000. Commission Decision: Application for Certification for the High Desert Power Project, High Desert Power, LLC. Docket No 97-AFC-1, P800-00-003.

California Energy Commission. 2005a. California Energy Demand 2006–2016 Staff Energy Demand Forecast. CEC-400-2005-034-SF-ED2.

California Energy Commission. 2005b. California Power Plants Database, California Energy Commission. www.energy.ca.gov/database/index.html#powerplants.

California Energy Commission. 2005c. *Biomass in California: Challenges, Opportunities and Potentials for Sustainable Management and Development.* California Energy Commission. CEC-500-2005-160.

California Energy Commission. 2006. *An Assessment of Biomass Resources in California, 2006 Assessment.* CEC-500-2006-094-D.

California Energy Commission. 2007a. *California Energy Demand 2008–2018: Staff Revised Forecast.* FINAL Staff Forecast, 2nd Edition. CEC-200-2007-015-SF2. www.energy.ca.gov/2007publications/CEC-200-2007-015/CEC-200-2007-015-SF2.PDF.

California Energy Commission. 2007b. *2006 Net System Power Report.* CEC-300-2007-007.

CERTS. 2003. *California's Electricity Generation and Transmission Interconnection Needs Under Alternative Scenarios.* Consultant Report for the California Energy Commission. Contract No. 500-03-106.

Chin, G., H. Dixon, J. Kato, and A. Komorniczack. 2001. Guidance for the Permitting of Electrical Generation Technologies. California Air Resources Board.

CPUC. 2003. *California Self-Generation Incentive Program. Second Year Impacts Evaluation Report.* Itrón Inc., prepared for Southern California Edison.

CPUC. 2005. *California Self-Generation Incentive Program. Fourth Year Impacts Evaluation Report.* Itrón Inc., prepared for Southern California Edison.

CPUC. 2006. "PUC Creates Groundbreaking Solar Energy Program." Press release for the California Solar Initiative. Docket #: R.04-03-017.

CPUC. 2007. *California Self-Generation Incentive Program. Sixth Year Impact Evaluation Report.* Itrón Inc., Submitted to PG&E and the Self-Generation Incentive Program Working Group. Prepared by Itron, Inc. Vancouver, Washington. August.

E2I. 2004. *Distributed Energy Resources Emissions Survey and Technology Characterization.* Palo Alto, California.

EIA. 1999a. *1998 Manufacturing Energy Consumption Survey (MECS).* Energy Information Agency.

EIA. 1999b. *A Look at Residential Energy Consumption in 1997.* Energy Information Agency.

EIA. 2000. A Look at Building Activities in the 1999 Commercial Buildings Energy Consumption Survey (CBECS). Energy Information Agency.

EIA. 2003a. *2002 Manufacturing Energy Consumption Survey (MECS).* Energy Information Agency.

EIA. 2003b. *A Look at Residential Energy Consumption (RECS) in 2001.* Energy Information Agency.

EIA. 2004. *A Look at Building Activities in the 2003 Commercial Buildings Energy Consumption Survey (CBECS).* Energy Information Agency.

EIA. 2006. *2006 Annual Energy Outlook.* Energy Information Administration

EPRI. 2005. *Assessment of California Combined Heat and Power Market and Policy Options for Increased Penetration.* EPRI, Palo Alto, California. California Energy Commission, Sacramento, California. CEC-500-2005-173.

EPRI. 2007. Technical specifications for future DG technologies. Internal communication with Dr. E. M. Knipping.

Finlayson-Pitts B. J., and J. N. Pitts, Jr. 2000. *Chemistry of the upper and lower troposphere.* Academic Press.

Fuel Cell Energy. 2007. Results from emissions testing of a DFC-300® operating on anaerobic digester gas. Internal communication.

Gellins, C. W., and K. E. Yeager. 2004. Transforming the electric infrastructure. *Physics Today* 57 (12): 45–51.

Griffin, R. J., D. Dabdub, M. J. Kleeman, M. P. Fraser, G. R. Cass, and J. H. Seinfeld. 2002a. "Secondary Organic Aerosol - 3. Urban/Regional Scale Model of Size- and Composition-Resolved Aerosols." *Journal of Geophysical Research-Atmospheres* 107(D17): 4334.

Griffin, R. J., D. Dabdub, and J. H. Seinfeld. 2002b. "Secondary Organic Aerosol - 1. Atmospheric Chemical Mechanism for Production of Molecular Constituents." *Journal of Geophysical Research-Atmospheres* 107(D17): 4332.

Harley, R. A., A. F. Russell, G. J. McRae, and J. H. Seinfeld. 1993. "Photochemical Modeling of the Southern California Air Quality Study." *Environmental Science & Technology* 27:378–388.

Heath, A. G., A. S. Hoats, and W. W. Nazaroff. 2006. "Intake Fraction Assessment of the Air Pollutant Exposure Implications of a Shift Toward Distributed Electricity Generation." *Atmospheric Environment* 40: 7164–7177.

Ianucci, J., S. Horgan, J. Eyer, and L. Cibulka. 2000. *Air Pollution Emissions Impacts Associated with the Economic Market Potential of Distributed Generation in California.* Distributed Utility Associates, prepared for The California Air Resources Board.

Idaho National Laboratory. 2006. Full Size Electric Vehicles, Advanced Vehicle Testing Activity. Available at http://avt.inel.gov.

Jackson, B., D. Chau, K. Gurer, and A. Kaduwela. 2006. "Comparison of Ozone Simulations Using MM5 and CALMET/MM5 Hybrid Metrological Fields for the July/August 2000 CCOS Episode." *Atmospheric Environment* 40:2812–2822.

Jacobson, M. Z., W. G. Colella, and D. M. Golden. 2005. "Cleaning the Air and Improving Health With Hydrogen Fuel Cell Vehicles." *Science* 308:1901–1905.

Jenkin, M. E., S. M. Saunders, and M. J. Pilling. 1997. "The Tropospheric Degradation of Volatile Organic Compounds. A Protocol for Mechanism Development." *Atmos. Environ.* 31(1):81–104.

Jimenez P., J. M. Baldasano, and D. Dabdub. 2003. "Comparison of Photochemical Mechanisms for Air Quality Modeling." *Atmos. Environ.* 37:4179–4194.

Kay, M. 2003. Personal communication, SCAQMD.

Kay, M. 2006. Internal Combustion Engines Emissions Survey. Personal communication, SCAQMD.

Kaduwela, A. 2005. *Ozone and $PM_{2.5}$ Monitoring Data in the San Joaquin Valley During the California Regional Particulate Air Quality Study, December 1999 to December 2000.* The California Air Resources Board.

Kleeman, M. J., Q. Ying, and A. Kaduwela. 2005. "Control Strategies for the Reduction of Airborne Particulate Nitrate in California's San Joaquin Valley." *Atmospheric Environment* 39: 5325–5341.

Lenssen, N. 2001. "The California Power Crisis. The Role of Distributed Generation." *Cogeneration and On-Site Power Generation* 2(3).

Little, A. 2000. *Opportunities for Micropower and Fuel Cell Gas Turbine Hybrid Systems in Industrial Applications.* Arthur D Little, prepared for Lockheed Martin Energy Research Corporation and the U.S. DOE Office of Industrial Technologies.

Magliano, K. L, V. M. Hughes, L. R. Chinkin, D. L. Coe, T. L. Haste, N. Kumar, and F. W. Lurmann. 1999. "Spatial and Temporal Variations in $PM_{10}$ and $PM_{2.5}$ Source Contributions and Comparison to Emissions During the 1995 Integrated Monitoring Study." *Atmospheric Environment* 33(29): 4757–4773.

Marnay, C., J. S. Chard, K. S. Hamachi, T. Lipman, M. M. Moezzi, et al. 2001. Modeling of Customer Adoption of Distributed Energy Resources. Consortium for Electric Reliability Technology Solutions, Ernest Orlando Lawrence Berkeley National Laboratory. Prepared for the California Energy Commission.

Martin, J., and H. John. 2004. *A Comparison of Dairy Cattle Manure Management With and Without Anaerobic Digestion and Biogas Utilization.* Eastern Research Group, Inc. Boston, Mass.

Medrano, M., J. Brouwer, M. Carreras-Sospedra, M. A. Rodriguez, D. Dabdub, and G. S. Samuelsen. 2008. "A Methodology for Developing Distributed Generation Scenarios in Urban Areas Using Geographical Information Systems." *International Journal of Energy Technology and Policy* In press.

Meng, Z., J. H. Seinfeld, P. Saxena, and Y. P. Kim. 1995. "Atmospheric Gas-Aerosol Equilibrium, IV, Thermodynamics of Carbonates." *Aerosol Sci. Technol.* 23:131–154.

Meng, Z., D. Dabdub, and J. H. Seinfeld. 1998. "Size–Resolved and Chemically Resolved Model of Atmospheric Aerosol Dynamics." *J. Geophys. Res.* 103:3419–3435.

Moya, M., S. N. Pandis, and M. Z. Jacobson. 2002. "Is the Size Distribution of Urban Aerosols Determined by Thermodynamic Equilibrium? An Application to Southern California." *Atmospheric Environment* 36(14): 2349–2365.

Nexus. 2002. *Performance and Cost Trajectories of Clean Distributed Generation Technologies.* Energy Nexus Group, prepared for the Energy Foundation.

NREL. 2003a. *Gas Fired Distributed Generation Technology Characterization: Microturbines.* Energy and Environmental Analysis, Inc, prepared for National Renewable Energy Laboratory.

NREL. 2003b. *Biopower Technical Assessment: State of the Industry and Technology.* National Renewable Energy Laboratory. NREL/TP-510-33123.

ONSITE SYCOM Energy Corporation. 1999. *Market Assessment of Combined Heat and Power in the State of California.* Prepared for the California Energy Commission.

Qin, Y., G. S. Tonnesen , and Z. Wang. 2004. "Weekend/Weekday Differences of Ozone, $NO_x$, CO, VOCs, $PM_{10}$ and the Light Scatter During Ozone Season in Southern California." *Atmospheric Environment* 38 (19): 3069–3087.

Rodriguez, M. A., M. Carreras-Sospedra, M. Medrano, J. Brouwer, G. S. Samuelsen, and D. Dabdub. 2006. "Air Quality Impacts of Distributed Power Generation in the South Coast Air Basin of California 1: Scenario Development and Modeling Analysis." *Atmospheric Environment* 40:5508–5521.

Rodriguez, M. A., J. Brouwer, G. S. Samuelsen, and D. Dabdub. 2007. "Air Quality Impacts of Distributed Power Generation in the South Coast Air Basin of California 1: Model Uncertainty and Sensitivity Analysis." *Atmospheric Environment* 41:5618–5635.

Samuelsen, S., D. Dabdub, J. Brouwer, M. Medrano, M. Rodriguez, and M. Carreras-Sospedra. 2005. *Air Quality Impacts of Distributed Generation.* California Energy Commission, PIER Energy-Related Environmental Research. CEC-500-2005-069-F.

SCAQMD. 2000. Best Available Control Technology Guidelines, SCAQMD.

SCAQMD. 2003a. "Addendum to the Proposed Modification to the Draft 2003 Air Quality Management Plan and Additional Comments and Responses." South Coast Air Quality Management District.

SCAQMD. 2003b. 2003 Air Quality Management Plan (AQMP), approved by the South Coast Air Quality Management District (SCAQMD) Executive Board on August 1, 2003, www.aqmd.gov/aqmp/AQMD03AQMP.htm.

SCAQMD. 2007. 2007 Air Quality Management Plan (AQMP), available at: www.aqmd.gov/aqmp/07aqmp/07AQMP.html.

SCAQMD. 2008a. South Coast Air Quality Management District, Board Meeting Date: January 4, 2008, Agenda No. 20. www.aqmd.gov/hb/2008/January/080120a.htm.

SCAQMD. 2008b. "Amendment of Rule 1110.2, Emissions from Gaseous and Liquid-Fueled Engines, South Coast Air Quality Management District." February 1, 2008. Last access at: www.aqmd.gov/rules/reg/reg11/r1110-2.pdf.

SJVPCD. 2007. San Joaquin Valley Air Pollution Control District website. About the District. www.valleyair.org/general_info/aboutdist.htm.

SJVAPCD. 2005. San Joaquin Valley Air Pollution Control District Air Pollution Control Officer's Determination of VOC Emission Factors for Dairies. San Joaquin Valley Air Pollution Control District. Available at: www.valleyair.org/busind/pto/dpag/APCO%20Determination%20of%20EF_August%201_.pdf.

SJVAPCD. 2002a. San Joaquin Valley Unified Air Pollution Control District, Best Available Control Technology (BACT) Guideline 3.3.12: Fossil Fuel Fired IC Engine > 50 hp. Last Update: 10/1/2002.

SJVAPCD. 2002b. San Joaquin Valley Unified Air Pollution Control District, Best Available Control Technology (BACT) Guideline 1.3.2: Fluidized Bubbling Bed Combustor (biomass-fired). Last Update: 11/21/2002.

Stockwell, W. R., F. Kirchner, M. Kuhn, and S. Seefeld. 1997. "A New Mechanism for Regional Atmospheric Chemistry Modeling." *J. Geophys. Res. Atmos.* 102:25,847–25,879.

Tomashefsky, S., and M. Marks. 2002. Distributed Generation Strategic Plan. California Energy Commission.

U.S. DOE/U.S. EPA (U.S. Department of Energy and U.S. Environmental Protection Agency). 2000. *Carbon Dioxide Emissions for the Generation of Electric Power in the United States.* www.eia.doe.gov/cneaf/electricity/page/co2_report/co2emiss.pdf.

U.S. EPA. 2007. *Guidance on the Use of Models and Other Analyses in Attainment Demonstrations for the 8-Hour Ozone NAAQS.* U.S. Environmental Protection Agency. EPA-454/B-07-002.

U.S. EPA. 2008. Technology Transfer Network, Clearinghouse for Inventories & Emissions Factors: Emissions Factors and AP-42. Available at: www.epa.gov/ttn/chief/ap42/index.html (last accessed September 2008).

Vijayaraghavan, K., P. Karamchandani, and C. Seigneur. 2006. "Plume-in-Grid Modeling of Summer Air Pollution in Central California." *Atmospheric Environment* 40:5097–5109.

Whitby, E. R., P. H. McMurry, U. Shankar, and F. S. Binkowski. 1991. Modal Aerosol Dynamics Modeling. Rep. 600/3-91/020, Atmospheric Research and Exposure Assessment

Laboratory, U.S. Environmental Protection Agency, Research Triangle Park, North Carolina. (NTIS PB91- 161729/AS).

Whitby, E. R., and P. H. McMurry. 1997. "Modal Aerosol Dynamics Modeling." *Aerosol Sci. and Technol.* 27:673–688.

Yanenko, N. N. 1971. *The Method of Fractional Steps.* New York: Springer.

Zeldin, M. D., L. D. Bregman, and Y. Horie. 1990. *A Meteorological and Air Quality Assessment of the Representativeness of the 1987 SCAQS Intensive Days.* Final report to the South Coast Air Quality Management District.

# 10.0 Acronyms

| | |
|---|---|
| APEP | Advanced Power and Energy Program |
| AGL | Above ground level |
| AQM | Air quality model |
| AQMP | Air Quality Management Plan |
| BACT | Best Available Control Technology |
| CAAQS | California Ambient Air Quality Standard |
| ARB | California Air Resources Board |
| CACM | Caltech Atmospheric Chemistry Mechanism |
| CAMx | Comprehensive Air Quality Model with Extensions |
| CALMET | California Meteorological Model |
| CCOS | Central California Ozone Study |
| CEC | California Energy Commission |
| CG | Central generation |
| CIT | California Institute of Technology |
| CHP | Combined cooling, heating and power |
| CO | Carbon monoxide |
| $CO_2$ | Carbon dioxide |
| CTMS | Chemical transport modeling system |
| DER | Distributed energy resources |
| DVF | Future design value |
| DG | Distributed generation |
| EMFAC | Emission Factors Model |
| EMS | Emissions Modeling System |
| FC | Fuel cell(s) |
| GE | Gross error |
| GT | Gas turbine(s) |

| | |
|---|---|
| HHV | Higher heating value |
| HTFC | High-temperature fuel cell |
| HYBR | Gas turbine-fuel cell hybrid system |
| ICE | Internal combustion engine |
| IMS95 | Integrated Monitoring Study 95 |
| LADWP | Los Angeles Department of Water and Power |
| LTFC | Low-temperature fuel cell |
| MCFC | Molten carbonate fuel cell(s) |
| MM5 | Pennsylvania State University / National Center for Atmospheric Research Mesoscale Model |
| MPMPO | Model to Predict the Multiphase Partitioning of Organics |
| MSW | Municipal solid waste |
| MTG | Micro-turbine generator(s) |
| NB | Normalized bias |
| NE | Normalized error |
| NGIC | Natural gas internal combustion engine |
| $NH_3$ | Ammonia |
| $NO_X$ | Nitrogen oxides |
| NG | Natural gas |
| PEMFC | Proton exchange membrane fuel cell(s) |
| $PM_{2.5}$ | Particulate matter (less than 2.5 microns) |
| $PM_{10}$ | Particulate matter (less than 10 microns) |
| PV | Photovoltaic(s) |
| RPM | Regional particulate model |
| SAPRC | Statewide Air Pollution Research Center |
| SCAG | Southern California Association of Governments |
| SCAPE2 | Simulating Composition of Atmospheric Particles at Equilibrium 2 |
| SCAQMD | South Coast Air Quality Management District |

| | |
|---|---|
| SCAQS | Southern California Air Quality Study |
| SCE | Southern California Edison |
| SCR | Selective Catalytic Reduction |
| SGIP | Self-Generation Incentive Program |
| SIP | State Implementation Plan |
| SJV | San Joaquin Valley |
| SJVAB | San Joaquin Valley Air Basin |
| SJVAPCD | San Joaquin Valley Air Pollution Control District |
| SOA | Secondary Organic Aerosol |
| SoCAB | South Coast Air Basin |
| SOFC | Solid Oxide Fuel Cell(s) |
| $SO_x$ | Sulfur oxides |
| TURB | Gas turbine |
| UCI-CIT | University of California, Irvine – California Institute of Technology |
| UPR | Unpaired Peak Ratio |
| U.S. DOE | United States Department of Energy |
| U.S. EPA | United States Environmental Protection Agency |
| VOC | Volatile Organic Compounds |